Structure and function of the mammalian small heat shock protein Hsp25

Amie Michelle Morris
University of Wollongong

Structure and Function of the Mammalian Small Heat Shock Protein Hsp25

Amie Michelle Morris, B. Sc. (Hons)

A thesis submitted in fulfilment of the requirements
for the degree of Doctor of Philosophy

School of Biological Sciences
and Department of Chemistry
University of Wollongong
Wollongong, Australia

2007

Declaration

This thesis is submitted in accordance with the regulations of the University of Wollongong in fulfilment of the degree of Doctor of Philosophy. It does not include any material previously published by another person except where due reference is made in the text. The experimental work described in this thesis is original and has not been submitted for a degree to any other University.

Amie Morris

Acknowledgements

I would like to thank my supervisors Mark Walker, John Carver and Teresa Treweek for their expertise, insight and guidance.

I would also like to thank Madge and Wilford for their advice and help with obtaining results from complicated equipment.

Most sincere thanks to Teresa, who gave me so much support on so many levels. Tezza, I can always count on you for those important self-esteem boosts and constant reminders that life will return to "normal" at the end of all of this. You have always been there for me and have been an amazing guide throughout my entire time as a research student.

To all of the Walker labrats and the upstairs posse – Anna, Carola, Christine, Coley, Corky, Elise, Fay, Gill, Jake, Justin, Kara, Martina, Tam, Tracey and Vidiya – thankyou all for the fun times and support. Thankyou to my former office buddy Arezou for being there through the ups and downs of writing and to Yoke, Michael and Ana for being around for those vital distractions.

To Heather and Riley, thankyou both for understanding.

To Martin and Pauline, thankyou for accepting me into your family and for all your support and food.

My most heartfelt thanks to Mum and Dad who are always there for me. I couldn't have made it through any of this without you.

Finally, thankyou to Jesse for understanding and always believing in me.

Contents

List of Figures

List of Tables

List of Abbreviations

ADH	alcohol dehydrogenase
ANS	1-anilino-8-naphthalene sulphonate
Ap	ampicillin
ATP	adenosine triphosphate
BCA	bicinchoninic acid
BSA	bovine serum albumin
CD	circular dichroism
crys	crystallin
cvHsp	cardiovascular Hsp
D_2O	deuterium oxide
DEAE	diethylaminoethyl
DMPK	dystrophia myotonica-protein kinase
DMSO	dimethylsulphoxide
DNase I	deoxyribonuclease I
DRM	desmin-related myopathy
DTT	dithiothreitol
E. coli	*Escherichia coli*
EDTA	ethylenediaminetetraacetic acid
ESI	electrospray ionisation
FPLC	fast protein liquid chromatography
Hsp	heat shock protein
HSQC	heteronuclear single-quantum coherence
IPTG	isopropyl-β-D-thiogalactosidase
Km	kanamycin
LB medium	Luria-Bertani medium
MG	molten globule
MS	mass spectrometry
NanoESI	nanoscale electrospray ionisation

NMR	nuclear magnetic resonance
NOE	nuclear overhauser effect
NOESY	nuclear overhauser effect spectroscopy
ODPF	outer dense fibre protein
PAGE	polyacrylamide gel electrophoresis
PCR	polymerase chain reaction
PEI	polyethylenimine
PMSF	phenylmethylsulphonyl fluoride
SDS	sodium dodecyl sulphate
SEC	size-exclusion chromatography
sHsp	small heat shock protein
TEMED	N,N,N',N'-tetramethylethylenediamine
TOCSY	total correlation spectroscopy
Tris	tris(hydroxymethyl)aminomethane
WET	water suppression enhanced through T1 effects
X-gal	5-bromo-4-chloro-3-inodlyl-β-D-galactopyranoside

List of Publications and Presentations

A.M. Morris, T.M.Treweek, J.A. Carver and M.J. Walker (2007) "Glutamic acid residues in the C-terminal extension of Hsp25 are critical for structural and functional integrity". *Under revision*.

A.M. Morris, M.J. Walker and J.A. Carver (2006) "Structure/function studies on the mammalian small heat shock protein Hsp25: the role of the C-terminal extension". Poster presentation at *Molecular Chaperones & the Heat Shock Response meeting, Cold Spring Harbor Laboratory, New York*.

A.M. Morris, J.A. Carver and M.J. Walker (2005) "The role of the C-terminal extension of the mammalian small heat shock protein Hsp25". Poster presentation at *Higher Degree Research Student Conference, University of Wollongong*.

A.M. Morris, J.A. Carver and M.J. Walker (2005) "The role of the C-terminal extension of the mammalian small heat shock protein Hsp25". Poster presentation at *The Lorne Conference on Protein Structure and Function*.

A.M. Morris, J.A. Carver and M.J. Walker (2004) "Structure and function studies on the mammalian small heat shock protein Hsp25". Poster presentation at *The Lorne Conference on Protein Structure and Function*.

T.M. Treweek, A.M. Morris and J.A. Carver (2003) "Intracellular protein unfolding and aggregation: The role of small heat-shock chaperone proteins". *Aust. J. Chem.* 56(5): 357-367.

T.M. Treweek, M.J. Walker, A.M. Morris and J.A. Carver (2002) "Structure/function studies of small heat shock chaperone proteins". Poster presentation at *Molecular Chaperones & the Heat Shock Response meeting, Cold Spring Harbor Laboratory, New York*.

Abstract

Hsp25 is the murine equivalent of human Hsp27, both of which are members of the small heat shock protein (sHsp) family. sHsps are a group of intracellular molecular chaperones that protect unstable intermediates of cellular proteins from aggregation and precipitation. Hsp27 and other sHsps play a role in various neurodegenerative diseases such as Alzheimer's, Alexander's, Creutzfeld-Jakob and Parkinson's diseases. Crystallisation of mammalian sHsps has thus far not been achieved due to the polydisperse and dynamic nature of these proteins. As a result, the oligomeric structure of sHsps is unclear, hindering the elucidation of the functional mechanisms of these proteins.

In this study, a series of site-directed Hsp25 mutants was constructed, in which polar residues of the flexible region of the C-terminal extension were replaced with less polar residues. The C-terminal extension of sHsps is typically short and unstructured and is thought to play an important role in solubilising these proteins and the complexes they form with target proteins by counteracting the hydrophobicity of the remainder of the sHsp. The C-terminal extension is also implicated in interaction with target proteins.

Wildtype Hsp25 and various C-terminal extension mutants (E190A, R192A, Q194A, E199A, E204A, Q205A, K209L) were expressed and successfully purified. A truncation mutant, E190stop, was also constructed but became insoluble during the purification process, demonstrating the importance of the C-terminal extension in maintaining the stability of Hsp25. Wildtype and

mutant Hsp25 proteins were characterised structurally and functionally using a range of spectroscopic techniques, including far-UV circular dichroism spectroscopy, tryptophan and ANS binding fluorescence spectroscopy, size-exclusion fast protein liquid chromatography, nuclear magnetic resonance spectroscopy and chaperone assays under both reduction and heat stress conditions. These experiments enabled the identification of residues key to the chaperone ability of Hsp25.

The R192A and Q194A mutants were functionally indistinct from the wildtype protein and exhibited only minor alterations to their structure. It was therefore concluded that the R192 and Q194 residues are not vital for Hsp25 to function as a molecular chaperone.

Each of the glutamic acid residue mutants exhibited significant alterations in tertiary structure, with increases in exposure of hydrophobic regions compared with wildtype Hsp25, and a minor decrease in the oligomeric size of the E190A mutant was observed. Functionally, these mutants showed poor thermostability and disrupted chaperone function. Glutamic acid residues are abundantly present in proteins from thermophilic organisms and are implicated in the stability of these proteins at high temperatures. Replacement of each of the glutamic acid residues in the C-terminal extension of Hsp25 resulted in loss of solubility at elevated temperatures, indicating that these residues perform similar roles in both Hsp25 and thermophilic proteins. The increase in surface hydrophobicity may have contributed to the poor thermostability of these

mutants and also the inefficient capture of target proteins observed in the chaperone assays.

The tertiary and quaternary structures of the Q205A mutant were significantly perturbed and the function of this mutant was completely abolished under heat stress conditions. Alterations to the tertiary structure of the N-terminal domain were observed and oligomerisation was severely disrupted, with three distinct oligomeric forms being present: an oligomer larger than that of the wildtype protein and two smaller oligomers. The chaperone activity of this mutant was comparable to that of wildtype Hsp25 under reduction stress conditions, indicating that each of the oligomeric forms were functional. Under heat stress conditions, however, the Q205A mutant co-precipitated along with the target proteins. Flexibility of the mutated residue was considerably decreased, as assessed by NMR experiments, but the remainder of the C-terminal extension was not significantly altered. Together, these results lead to the conclusion that the Q205 residue is vital for the performance of Hsp25 as a molecular chaperone at elevated temperatures.

Mutation of the K209 residue also showed disruption to the oligomerisation of Hsp25, with the K209L mutant eluting as three peaks after size-exclusion chromatography. This mutant was functionally defective under reduction stress conditions but showed comparable chaperone activity to the wildtype at high temperature, suggesting that the smaller oligomeric species require temperature-induced structural alterations in order to acquire chaperone ability. Because full chaperone activity was observed under reduction stress conditions,

direct interactions between the C-terminal lysine residue of Hsp25 and target proteins is unlikely to be a requirement of chaperone activity.

The stabilisation of αB-crystallin by αA-crystallin is important for the maintenance of the structure and function of αB-crystallin in the eye lens, where these sHsps are present in a ~3:1 ratio. Outside the eye lens, however, αA-crystallin is found only in trace amounts in some tissues. Co-complexes between various sHsps have been observed *in vivo*, for example between αB-crystallin and Hsp27, and it has been proposed that one or more ubiquitous sHsps stabilise αB-crystallin in non-lenticular tissues. Whilst αB-crystallin was found to be unstable above ~69°C, Hsp25 remained almost completely in solution at 100°C. A 3:1 Hsp25:αB-crystallin mixture showed practically identical thermostability to the Hsp25 homo-oligomer and provides support for the role of this sHsp as a stabiliser of αB-crystallin. Chaperone activity assays of the 3:1 mixture show results closely resembling those of the Hsp25 homo-oligomer and demonstrate that interactions between the two sHsps result in an altered chaperone activity of αB-crystallin.

Significant insights into the structure and function of Hsp25 were gained in this study. Several residues in the C-terminal extension were identified as critical to the structural and functional integrity of this sHsp and analysis of the amino acid composition of the C-terminal extensions of sHsps from various organisms indicate that some of these residues may play similar roles in other sHsps.

Chapter 1

Introduction

1.1. Protein Folding

It has long since been established that the information required for a protein to fold into its correct conformation is contained entirely within its amino acid sequence [1]. A substantial number of small proteins, containing less than about 150 residues and able to rapidly bury hydrophobic residues, are capable of folding spontaneously into their native structure in isolation *in vitro* [2,3]. These smaller proteins can adopt their native conformation directly from the unfolded, linear state [4]. Larger and multi-domain proteins are also able to fold spontaneously but the efficiency of this process is very low [5,6].

With the exception of the small proteins capable of exhibiting "two-state kinetics", the folding of a linear polypeptide chain into its three-dimensional structure occurs sequentially through the formation of a limited number of intermediates termed "molten globule" (MG) states [7,8]. Molten globules are defined as partially-folded intermediates that contain elements of native secondary structure but lack significant tertiary structure [9]. They have a compact form which is slightly less tightly packed than the native state and lack specific side-chain interactions found in the native form [10]. Molten globules are highly dynamic, interconverting states, rather than a single conformation, that are in equilibrium with the unfolded state [11,12]

Formation of molten globule intermediates associated with protein folding is related to the relative kinetic energy of the states involved [13]. Although the

folding protein can adopt various intermediate conformations, a limited number of alternative pathways are followed that result in a reduction in the amount of free energy [14,15]. Protein folding occurs rapidly, with folding half-time within seconds for bacterial proteins or minutes for eukaryotic proteins *in vivo* and the intermediate states are present only transiently [16-18]. However, molten globules can be formed that are energetically favourable and do not continue along the protein folding pathway. These intermediates become "kinetically trapped" and are therefore long-lived, with the potential to form misfolded conformations [3,17]. This process can be visualised as a protein folding funnel [19,20] (Figure 1.1).

Please see print copy for figure

Figure 1.1: The protein folding funnel. Unfolded proteins undergo successive transitions to the lowest energy state via MG intermediates. The native state represents the conformation with the lowest energy. Proteins may be misfolded if they are caught in "kinetic traps" and their lowest energy conformation does not represent the native state. From [20].

1.1.1. The Off-Folding Pathway

Because of their partially-folded structure, molten globules contain significant surface-exposed hydrophobicity and are therefore prone to aggregation [21]. During protein folding, molten globules are typically transient intermediates. If the presence of the molten globule state is prolonged, folding proteins are able to associate with each other and enter the irreversible off-folding pathway [13] (Figure 1.2). In doing so, folding intermediates have the potential to aggregate with each other and subsequently become insoluble [22,23].

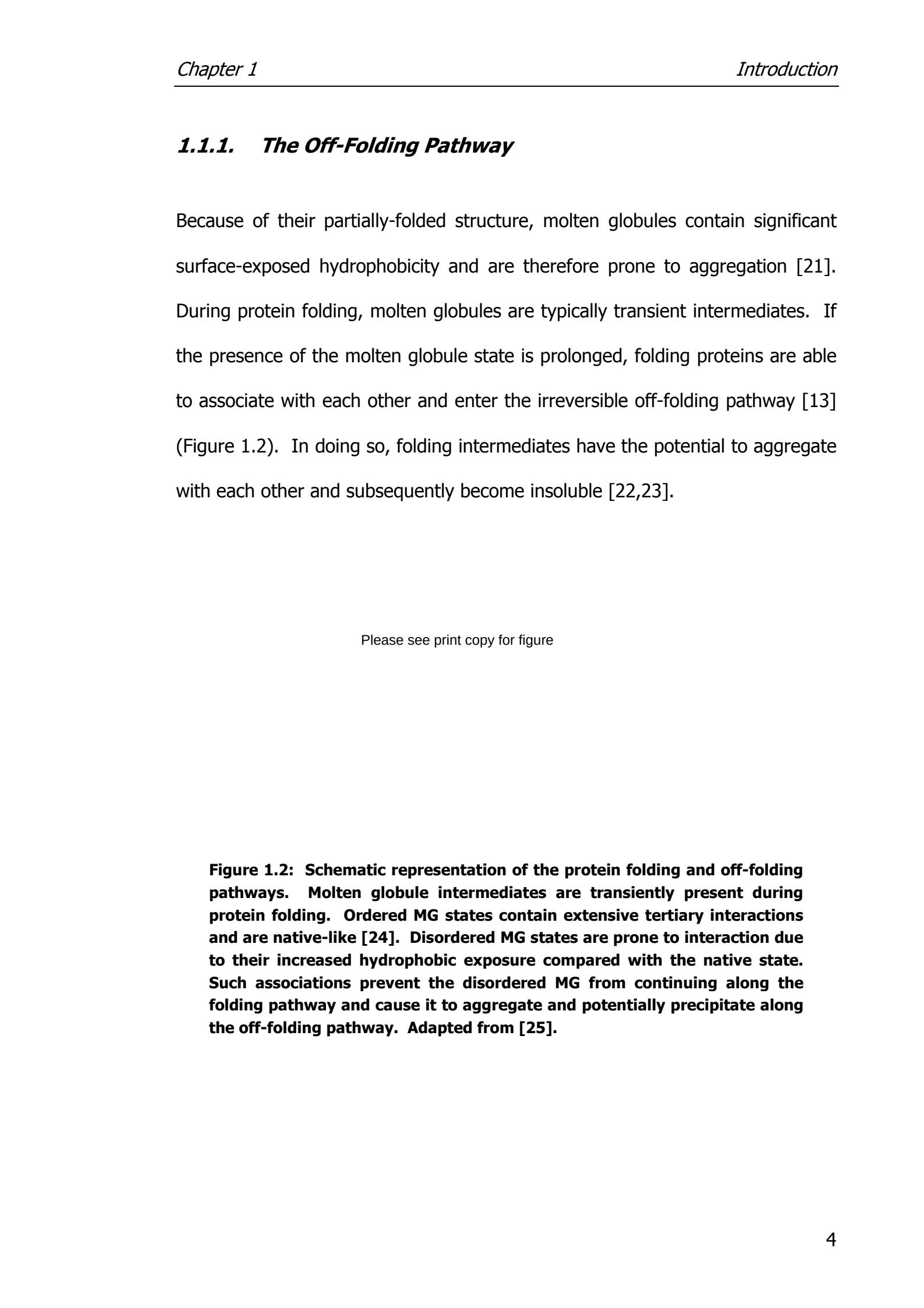

Figure 1.2: Schematic representation of the protein folding and off-folding pathways. Molten globule intermediates are transiently present during protein folding. Ordered MG states contain extensive tertiary interactions and are native-like [24]. Disordered MG states are prone to interaction due to their increased hydrophobic exposure compared with the native state. Such associations prevent the disordered MG from continuing along the folding pathway and cause it to aggregate and potentially precipitate along the off-folding pathway. Adapted from [25].

Protein folding studies are typically performed at dilute concentrations in a simple buffer [26,27]. Whilst valuable information regarding protein folding has been obtained through such experiments, the conditions under which protein folding occurs *in vivo* is much more complex. The cell is a crowded environment, with the concentration of protein and RNA in a typical *E. coli* cell being 300-400 g/L [28,29]. Because there is little available free space, intermolecular interactions are favoured and the potential for associations between enduring molten globules is great [30,31]. Compounded by the high local concentration of many nascent polypeptide chains due to the presence of polyribosomes, the dead-end molten globule states are forced into close proximity to each other, enhancing the potential for aggregation [32,33]. Aggregates of partially-folded proteins may become insoluble, resulting in an accumulation of inactive proteins which can no longer attain their native state and fulfil their function [34].

1.1.2. Protein Misfolding Diseases

The function of the majority of proteins is attributable to its unique three-dimensional structure [6]. Failure to fold into its correct structure limits or abrogates the protein's ability to perform the biological roles for which it was produced [35]. Not only does the aggregation of folding intermediates strip the cell of an important resource, the presence of the aggregates themselves can have dire consequences and result in a wide range of diseases, such as those described in Table 1.1.

Table 1.1: Representative human diseases associated with defective protein folding [36-39].

Please see print copy for table

"Conformational diseases" such as Alzheimer's, Parkinson's and Huntington's diseases are associated with proteins that do not attain or maintain their native structure, resulting in aggregation and insolubilisation [40]. The insoluble deposits in these diseases form either plaques or fibrillar tangles within tissues and their accumulation ultimately results in cell damage or death [35,41].

Protein misfolding does not necessarily result in the formation of aggregates but may involve the loss of important components of the cellular machinery. For example, cystic fibrosis transmembrane conductance regulator (CFTR) is normally co-translationally translocated into the ER with the assistance of transient interactions with Hsp70, processed by the Golgi apparatus and transported to the plasma membrane [42]. A deletion mutant of CFTR, responsible for 70% of cystic fibrosis cases, is improperly folded and remains bound to Hsp70 in the ER and is targeted for degradation [43,44]. CFTR is a cAMP-regulated chloride channel in epithelial cells and its absence results in improper electrolyte transport across epithelial membranes which in turn leads to the characteristic thick mucous secretions in the lungs and intestines of cystic fibrosis sufferers [45,46].

1.2. Molecular Chaperones

Because most proteins do not fold spontaneously and are prone to aggregation during folding, protein folding efficiency in the cell would be too low to meet biological requirements without intervention [33]. Protein folding *in vivo* is

facilitated by the presence of a large group of related proteins that interact with folding proteins throughout the folding process and beyond. These helper proteins have been termed "molecular chaperones".

Molecular chaperones are a diverse group of structurally unrelated proteins that assist in the formation of correct protein structure without becoming a part of the final structure [47]. Protein folding with the aid of molecular chaperones can be referred to as "assisted self-assembly" [48]. The principle that the requisite information for the achievement of the native structure is still upheld, as molecular chaperones do not guide folding or impart any information to facilitate folding. Rather, molecular chaperones prevent the association of partially-folded proteins by transiently interacting with regions of the folding intermediate and stabilising its non-native structure [49]. The folding protein is thereby intercepted before it commits to alternative, unproductive pathways. Molecular chaperones do not act as catalysts in protein folding and their assistance does not increase the rate of folding. Instead, the chaperoning role increases the yield of correctly folded proteins by preventing interactions between molten globule intermediates [50]. Typically, more than 95% of nascent polypeptides fold into their native state under normal cellular conditions thanks to the presence of molecular chaperones, or heat shock proteins (Hsps) [12].

The heat shock response was first noted in 1962 with the observation of chromosomal "puffs" corresponding to increased RNA synthesis under elevated

temperatures in *Drosophila* [51,52]. Some 10 years later, it was shown that these puffs coincided with the expression of a group of proteins which were later termed heat shock proteins [53]. Although functionally related, molecular chaperones are a structurally diverse group of proteins. The five main families of Hsps are defined by the apparent subunit mass, as determined by SDS-PAGE: Hsp100, Hsp90, Hsp70, Hsp60 and the small heat shock proteins (sHsps). Under physiological conditions, each of these Hsp families perform roles that contribute to the functional form of "target" proteins. Some of the Hsp groups also perform a range of diverse tasks. An overview of the Hsp100, Hsp90, Hsp70 and Hsp60 families is given in Table 1.2.

1.2.1. Hsp70

The Hsp70 and Hsp60 molecular chaperones families function as a co-operative team to facilitate the correct folding of cellular proteins. Hsp70 (bacterial DnaK) is the first molecular chaperone encountered by the folding protein. This chaperone functions as a monomer and recognises short, extended, hydrophobic-rich segments of the polypeptide chain, thus protecting unfolded polypeptides from interacting either with other regions on the extended chain or other non-native proteins in the cell [54-56].

Table 1.2: Representative members of the Hsp100, Hsp90, Hsp70 and Hsp60 families [50,57-60].

Please see print copy for tables

The chaperone action of Hsp70 is dependent on a co-chaperone of the Hsp40 (bacterial DnaJ) family and ATP hydrolysis. Hsp40 recognises and binds to the polypeptide as it emerges from the ribosome, targeting ATP-bound Hsp70 to the chain [61]. Because Hsp70 is able to bind co-translationally to the translating polypeptide, one nascent chain may be stabilised by many Hsp70 molecules [62]. Release of the polypeptide from Hsp70 is dependent on co-factors and ATP [63].

Binding and release of Hsp70 may undergo many cycles until a sufficient length of the chain has been translated to allow the nascent chain to fold. The polypeptide may then proceed to fold independently or be passed to the Hsp60 chaperone machinery for further stabilisation [64,65].

1.2.2. Hsp60

The Hsp60 (bacterial GroEL) family, also known as the chaperonin family, provides folding assistance for polypeptides that cannot achieve their native structure in the cellular environment, despite stabilisation by the Hsp70 chaperones. It is estimated that approximately 15% of all bacterial proteins require interaction with Hsp60 to fold correctly [66].

Hsp60 is arranged in two heptameric discs with seven-fold rotational symmetry [67,68], forming a large, open cavity that can accommodate folding proteins of up to approximately 75 kDa [69,70]. Molten globule intermediates bind to hydrophobic binding sites on the inner apical surface of one of the Hsp60 rings

[71-73]. Binding of ATP allows the association of the co-chaperone Hsp10 (bacterial GroES), a single heptameric ring of ~10 kDa subunits [74], which displaces the folding protein into the Hsp60 cylinder and acts as a lid [75]. Protein folding therefore proceeds in isolation, negating the danger of aggregation due to hydrophobic interactions with other folding intermediates [76]. Co-operative hydrolysis of ATP causes conformational changes in the Hsp60 subunits that lead to the interior becoming progressively more hydrophilic, thus encouraging the burial of hydrophobic regions of the target protein [77]. ATP hydrolysis in the opposite ring of GroEL triggers the bound Hsp10 to dissociate and the target protein to be released into the bulk solution [78].

The polypeptide may fold to its native state within the cage or complete its folding after release from Hsp60 [79]. Many proteins require several binding-release cycles to attain their native structure. Upon release, these proteins still expose extensive hydrophobicity and are recaptured by Hsp60 [78]. The possible interactions of a nascent polypeptide with the Hsp70 and Hsp60 systems *en route* to its native structure is shown in Figure 1.3. Hsp60 is also able to reduce the pool of aggregation-prone intermediates by unfolding kinetically-trapped molten globules and allowing them to re-enter the protein folding pathway [59].

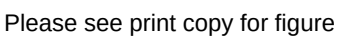

Figure 1.3: Protein folding by the Hsp70 and Hsp60 molecular chaperone systems. The nascent polypeptide is co-translationally stabilised by Hsp70 to prevent aggregation. On completion of translation, the polypeptide may fold spontaneously or be stabilised by Hsp70. On release from Hsp70, the polypeptide may proceed independently along its folding pathway or be captured by Hsp60. The polypeptide may also be passed directly from Hsp70 to Hsp60. Once inside the Hsp60 folding "cage", the polypeptide proceeds to fold in isolation, assisted by conformational changes in Hsp60. The polypeptide is released into the bulk solution either in its native state or as a molten globule (MG) folding intermediate, which may fold to its native state without further assistance or be recaptured by Hsp60. Adapted from [80].

1.2.3. Hsp100

The Hsp100 (bacterial Clp) family of chaperones is important for cellular thermotolerance [81] and functions on the off-folding pathway to prevent protein aggregation becoming a burden for the cell. Hsp100 exists as a six-membered ring [82] and is involved in the dissipation of protein aggregates, either by reactivating the constituent proteins or assisting in their proteolysis [50,83].

Disaggregation of protein aggregates is achieved by Hsp100 in concert with the Hsp70 system [84]. The Hsp100 hexamer binds to the protein aggregate and an ATP-induced conformational change drives the exposure of hydrophobic regions on the target protein, allowing it to be recognised by the Hsp70 folding system [85]. Hsp100 is not directly involved in the proteolysis of protein aggregates – this is achieved by the actions of the unrelated protease ClpP [86,87]. Rather, Hsp100 facilitates degradation by altering the conformation of the target protein to make it a more accessible substrate of ClpP [88].

1.2.4. Hsp90

The Hsp90 family is important for the regulation of a wide range of functional proteins associated with cell signalling and is one of the most abundant molecular chaperones [5,89]. Hsp90 functions as a dimer [90,91] and operates in association with various co-chaperones and ATP [92-94]. In eukaryotes, Hsp90 has been shown to be important for the activation of steroid receptors,

transcription factors, kinases and tumour suppressors [95,96] and can act co-operatively with Hsp70 in the late stages of folding of steroid hormone receptors [97]. Once folded, the receptor is inactive and only attains its hormone-binding conformation after interaction with Hsp90 [98,99].

1.3. Stress and the Heat Shock Response

The protein folding pathway is reversible, with the unfolding reactions being the reverse of the folding reactions [14] (Figure 1.2). Changes in the local environment of a protein can result in a conformational change which affects not only the function of the protein but also the balance between folding and unfolding [100]. Formation of the native state becomes disfavoured and correctly-folded proteins begin to unfold, potentially reducing the yield of the native state to zero [14,101]. A range of conditions place stress on the cell and promote protein unfolding, such as those listed in Table 1.3. The shift towards protein unfolding under these conditions results in an increased concentration of molten globule folding intermediates and therefore an increased risk of protein aggregation [5].

Table 1.3: Factors that induce the heat shock response [88,101-108].

Please see print copy for tables

1.4. Small Heat Shock Proteins

sHsps derive their name from their small monomeric size, ranging from 12 kDa in *Caenorhabditis elegans* to 43 kDa in *Saccharomyces cerevisiae* [109], although they exist under physiological conditions as oligomers of up to 50 subunits [110,111] and 1.2 MDa in mass [112,113]. With the exception of some pathogenic bacteria, sHsps are found in all organisms [102,114]. The number of sHsp family members differs with the organism, with bacteria, archaea and single-celled eukaryotes typically possessing one or two sHsps and higher, multi-cellular eukaryotes usually containing multiple sHsp genes [114]. Plants are particularly abundant with sHsps, with higher plants having up to 40

representatives [109]. Whilst plants contain organelle-localised sHsps, the sHsps in all other organisms, including mammals, are restricted to the cytoplasm and nucleus [115,116].

sHsps perform their chaperone function on the off-folding pathway. Long-lived molten globule intermediates in danger of aggregation are recognised through their hydrophobic exposure and sequestered into a large complex [117,118]. Whilst sHsps are unable to facilitate refolding or degradation, targets are held in a folding-competent conformation thus enabling further processing by ATP-dependent molecular chaperones, e.g. Hsp70, when cellular conditions return to normal [118,119].

sHsps are able to bind up to one target molecule per monomer present within the oligomer, making sHsps the most efficient family of molecular chaperones [104]. Members of the sHsp family are the most strongly induced molecular chaperones in response to stress, with their synthesis both during stress and subsequent recovery occurring over a longer period of time than members of other molecular chaperone families [120]. Expression of sHsps can be elevated up to 20 times that of constitutive levels and may comprise up to 1% of the total protein content in some cells under stress [100].

The human arsenal of sHsps consists of ten known members [121], which are listed in Table 1.4. Although traditionally defined as having increased expression under heat stress, not all sHsps are stress-inducible. In addition,

not all sHsps are expressed in all tissue types. Despite this, seven of the human sHsps are expressed in muscle tissue [121].

Table 1.4: The ten known human sHsps. MKBP, cvHsp and ODFP are the abbreviations for dystrophia myotonica-protein kinase (DMPK)-binding protein, cardiovascular Hsp and outer dense fibre protein, respectively. Accession numbers are given in Appendix A.

sHsp	Alternative Name	Class	Location
HspB1	Hsp27	I	Ubiquitous
HspB2	MKBP	II	Striated muscle
HspB3	HspL27	II	Striated muscle
HspB4	αA-crystallin, CRYAA	II	Eye lens
HspB5	αB-crystallin, CRYAB	I	Ubiquitous
HspB6	Hsp20, p20	I	Ubiquitous
HspB7	cvHsp	II	Striated muscle
HspB8	Hsp22, H11	I	Ubiquitous
HspB9	-	II	Testis
HspB10	ODFP, ODF1	II	Testis

Dividing the human sHsps into two groups based on their evolutionary divergence enables a distinction between the ubuiquitous, stress-induced sHsps (Class I) and those that are have restricted expression (Class II) [108]. The importance of Class I sHsps in the general stress response is obvious, considering their presence in almost every tissue type and their stress-inducibility. On the other hand, Class II sHsps have more specific roles that

correlate to their localisation. For example, αA-crystallin is primarily restricted to the eye lens whilst HspB9 and ODFP, the two most recent additions, are both found only in the testis and are important for spermatogenesis [122,123].

αA- and αB-Crystallin are closely related to each other, with their genes sharing 57% homology [124]. In the eye lens, they are found as subunits of α-crystallin in a ratio of 3:1 (αA:αB-crystallin), and comprise approximately one third of the total lenticular protein content [125]. α-Crystallin maintains the transparency of the lens by acting as a structural protein to ensure proper refraction of light and chaperoning other crystallins to prevent opacification as a result of aggregation [126,127]. This latter role is particularly important, as no protein turnover occurs in the lens, and is dicussed further in Chapter 7. Unlike αA-crystallin, αB-crystallin is found in most tissue types, most significantly the heart, skeletal muscle, skin, oesophagus, nervous system, kidney and placenta [120,128,129], and is stress-inducible. αB-Crystallin possesses chaperone activity independently of αA-crystallin and is thus an important participant in the general stress response.

Hsp27 is closely related to αB-crystallin and also shares a wide tissue distribution [120,130]. Studies on the mouse equivalent of Hsp27, Hsp25, have greatly contributed to the current knowledge of Hsp27. Hsp25 differs from Hsp27 by only four residues in length and minor residue changes. Henceforth, unless otherwise stated, Hsp27 will be used to denote the human sHsp and Hsp25 to refer to the mouse equivalent.

1.5. Structure of sHsps

1.5.1. Primary Structure

sHsps are characterised by a conserved region of 80-100 amino acid residues denoted the α-crystallin domain, also known as the putative C-terminal domain [131,132]. This region is flanked by an N-terminal domain and C-terminal extension, both of which are poorly conserved and display variability in sequence and length throughout the sHsp family. sHsps are the least conserved family of Hsps. In humans, for example, the homology ranges from 8 to 53% between individual members [108]. A sequence alignment of representative sHsps from various organisms highlighting key features is shown in Figure 1.4.

sHsps from plants, yeast and most invertebrates are encoded for by intronless genes, with some invertebrate examples containing one intron [133]. Mammalian sHsp genes typically contain either one or two introns. The genes of Hsp27 and αA- and αB-crystallin are comprised of three exons and two introns. Exon 1 corresponds approximately to the entire N-terminal domain (residues 1-67 in αB-crystallin) and represents an independent structural unit [134]. Exons 2 and 3 (residues 68-108 and 109-175 in αB-crystallin, respectively) together make up the C-terminal region comprised of the α-crystallin domain and C-terminal extension [135].

```
Hsp25        1 --MTERRVPFS--LLRSPSWEPFRDWYPAHSRLFDQAFGVPRLPDEWSQW  46
Hsp27        1 --MTERRVPFS--LLRGPSWDPFRDWYP-HSRLFDQAFGLPRLPEEWSQW  45
αA-crys.     1 ---MDVTIQHP--WFK-RTLGPFY-----PSRLFDQFFGEGLFEYDLLPF  39
αB-crys.     1 ---MDIAIHHP--WIR-RPFFPFHS----PSRLFDQFFGEHLLESDLFP-  39
Hsp20        1 -MEIPVPVQPS--WLR-RASAPLPGLSA-PGRLFDQRFGEGLLEAELAAL  45
HspB3        1 ---MAKIILRHLIEIPVRYQEEFEARGLEDCRLDHALYALPGPTIVDLRK  47
HspB7        1 --MSHRTSSTFRAERSFHSSSSSSSSSTSSSASRALPAQDPPMEKALSMF  48
MKBP         1 --MSGRSVPHA---HPATAEYEFAN----PSRLGEQRFGEGLLPEEILTP  41
Hsp12.6      1 ---------------------------------MEEKVVE--LTHNWSAE  15
Hsp16-2      1 ----------------MSLYHYFR-------PAQRSVFGDLMRDMALMER  27
Hsp16.9      1 --MSIV--------RRSNVFDPF-------ADLWADPFDT-FRSIVPAIS  32
Hsp18.1      1 --MSLIPSFFS--GRRSNVFDPFS------LDVWDPLKDFPFSNSSPSAS  40
Hsp26        1 SFNSPFFDFFDNINNEVDAFNRLLGEGGLRGYAPRRQLANTPAKDSTGKE  50
Hsp16.5      1 ----------------MFGRDPFDS---LFERMFKEFFATPMTGTTMIQS  31
IbpA         1 --------------MRNFDLSPL--------YRSAIGFDR-LFNHLENN-  26
IbpB         1 --------------MRNFDLSPL--------MRQWIGFDK-LANALQNAG  27

Hsp25       47 FS-------AAGWPGYVRPLPAATAEGPAAVTLAAPAFSRALNRQLSSGV  89
Hsp27       46 LG-------GSSWPGYVRPLPPAAIESPA---VAAPAYSRALSRQLSSGV  85
αA-crys.    40 LS-------STISPYYR------------------QSLFR--T-VLDSGI  61
αB-crys.    40 TS-------TSLSPFYLR------------P----PSFLRAPS-WFDTGL  65
Hsp20       46 CP-------TTLAPYYLR------------A----PSVALP--------V  64
HspB3       48 TR-------AAQSPPVD----------------------------SAAE  61
HspB7       49 SDDFGSFMRPHSEPLAFP--------------------------ARPGGA  72
MKBP        42 ---------TLYHGYYVR-----------------PRAAPAGE-GSRAGA  64
Hsp12.6     16 ---------QWDWPLQH-----------------------------NDEV  27
Hsp16-2     28 ----------QFAPVCR---------------------------ISPSES  40
Hsp16.9     33 GG-------SSETAAFA-------------------------------NARV  46
Hsp18.1     41 -F-------PRENPAFV-------------------------------STRV  53
Hsp26       51 VARPNNYAGALYDPRDETLDDWFDN-------DLSLFPSGFGFPRSVAVP  93
Hsp16.5     32 ---------STGIQISGK-----------------------------GFMP  44
IbpA        27 ----------QSQSNGG-------------------------------YPPY  37
IbpB        28 ----------ESQS----------------------------------FPPY  35

                          β1

Hsp25       90 SEIRQTADRWRVSLDVNHFA-PEELTVKTKE--GVVEITGKHEERQDEHG 136
Hsp27       86 SEIRHTADRWRVSLDVNHFA-PDELTVKTKD--GVVEITGKHEERQDEHG 132
αA-crys.    62 SEVRSDRDKFVIFLDVKHFS-PEDLTVKVQD--DFVEIHGKHNERQDDHG 108
αB-crys.    66 SEMRLEKDRFSVNLDVKHFS-PEELKVKVLG--DVIEVHGKHEERQDEHG 112
Hsp20       65 AQVPTDPGHFSVLLDVKHFS-PEEIAVKVVG--EHVEVHARHEERPDEHG 111
HspB3       62 TPPREGKSHFQILLDVVQFL-PEDIIIQTFE--GWLLIKAQHGTRMDEHG 108
HspB7       73 GNIKTLGDAYEFAVDVRDFS-PEDIIVTTSN--NHIEVRAE---KLAADG 116
MKBP        65 SELRLSEGKFQAFLDVSHFT-PDEVTVRTVD--NLLEVSARHPQRLDRHG 111
Hsp12.6     28 IKVTNTNDKFEVGLDASFFT-PKEIEVKVAG--DNLVIHCRHESRAEHYG  74
Hsp16-2     41 SEIVNNDQKFAINLNVSQFK-PEDLKINLDG--RTLSIQGE-QELKTDHG  86
Hsp16.9     47 DWKETPEAHV-FKVDLPGVK-KEEVKVEVEDG-NVLVVSGERSREKEDKN  93
Hsp18.1     54 DWKETPEAHV-FKADLPGLK-KEEVKVEVEDD-RVLQISGERSVEKEDKN 100
Hsp26       94 VDILDHDNNYELKVVVPGVKSKKDIDIEYHQNKNQILVSGEIPSTLNEES 143
Hsp16.5     45 ISIIEGDQHIKVIAWLPGVN-KEDIILNAVG--DTLEIRAKRSPLMITES  91
IbpA        38 NVELVDENHYRIAIAVAGFA-ESELEITAQD--NLLVVKGAHADEQKERT  84
IbpB        36 NIEKSDDNHYRITLALAGFR-QEDLEIQLEG--TRLSVKGTPEQPKEEKK  82

              β2    β3          β4      β5
```

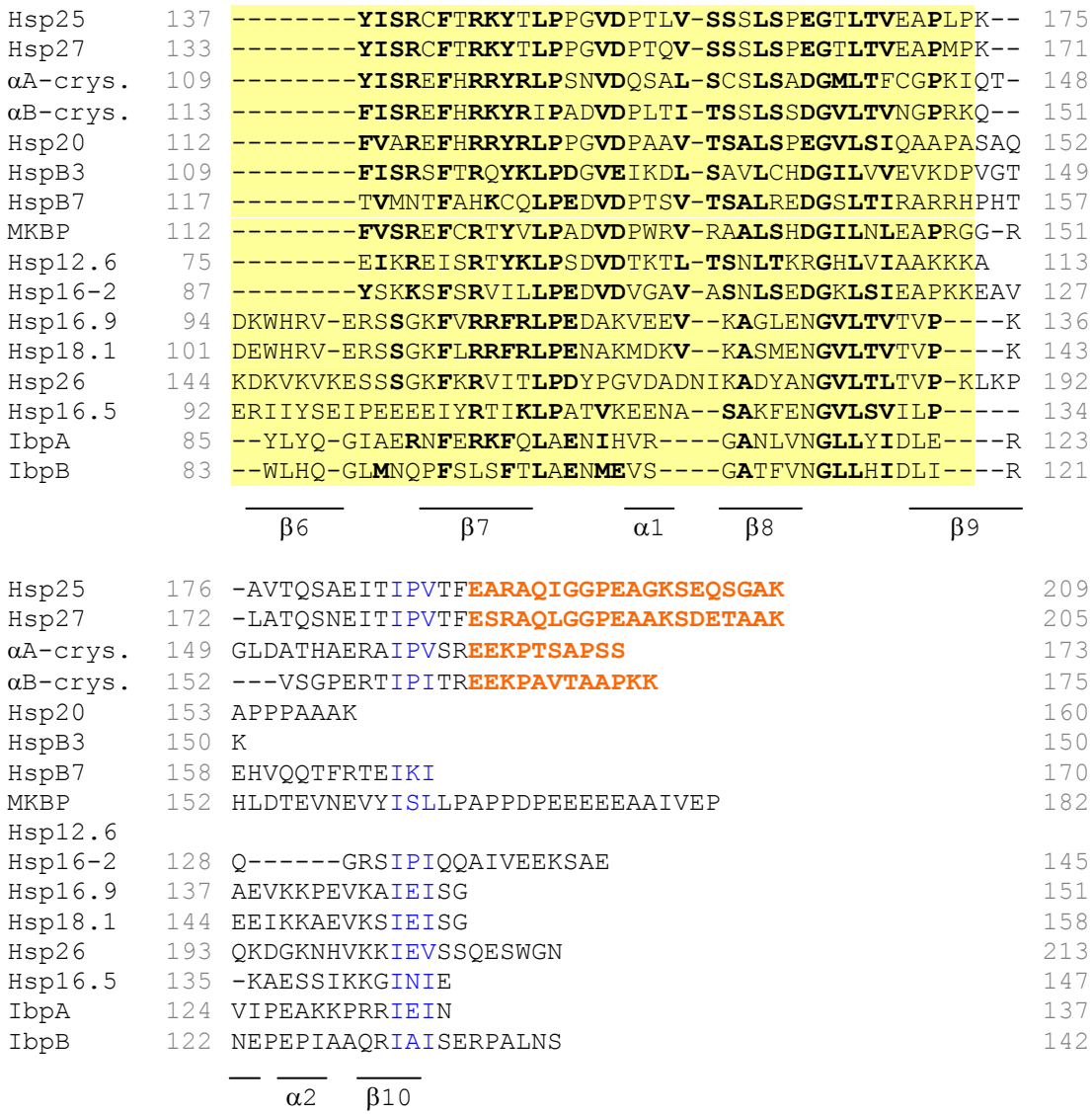

Figure 1.4: Sequence alignment of some major sHsps from various organisms. The approximate location of the α-crystallin domain is highlighted in yellow. Flexible residues of the C-terminal extensions of Hsp25, Hsp27, αA- and αB-crystallin are shown in orange and the IXI motifs of all sHsps, where present, are shown in blue. The PF-rich region of sequence similarity and consensus sequence for the paralogous sHsps Hsp27/25, Hsp20, αA- and αB-crystallin in the N-terminal domain are shown in brown. Identical or chemically similar residues (grouped as [FYW], [ILVM], [HRK], [DE], [GA], [TS] and [NQ] as based on the BoxShade programme in BioManager by ANGIS) in at least 8 sequences are shown in bold. The approximate positions of α-helices and β-strands, based on the crystal structure of Hsp16.5 [136], are indicated. Sequences were aligned in ClustalW and manually edited. Sequences are *Mus musculus* Hsp25, human Hsp27, αA- and αB-crystallin, Hsp20, HspB3, HspB7 and MKBP, *Brugia malayi* Hsp12.6, *Caenorhabditis elegans* Hsp16-2, *Tritium aestivum* Hsp16.9, *Pisum sativum* Hsp18.1, *Saccharomyces cerevisae* Hsp26, *Methanococcus jannaschii* Hsp16.5, *Escherichia coli* IbpA and *E. coli* IbpB. Accession numbers are given in Appendix A.

1.5.1.1. The α-Crystallin Domain

The α-crystallin domain is the characteristic feature of sHsps and forms a block of sequence similarity when sHsps are aligned, as highlighted in Figure 1.4. Despite some variability within this region, the hydrophobicity and flexibility profiles of this region are similar for all sHsps investigated and conserved residues, shown in bold in Figure 1.4, and consensus sequences have been identified even in distantly related sHsps [116,133,137]. The consensus regions F-X-R-polar-aromatic-X-L-P and polar-G-V-L-polar-aliphatic-polar-aliphatic-P-basic correspond to residues 142-149 and 164-177 in Hsp25, respectively [109,116]. Animal sHsps contain the additional consensus region KHEERXXDXXXXHG corresponding to residues 123-132 in Hsp25 [109].

1.5.1.2. The N-Terminal Domain

The N-terminal domain of sHsps is variable in length, ranging from 24 residues in Hsp12.3 of *C. elegans* to 246 residues in Hsp42p of *S. cerevisiae* [109]. There are no sequence similarities in the N-terminal domain that are observed throughout all, or even most, sHsps, although some minor similarities are often seen between quite distant sHsps. These are typically phenylalanine and proline rich regions [104,109]. Extensive gaps therefore appear in the alignment of the N-terminal domain [109]. Phylogenetic analyses have shown that the mammalian sHsps Hsp27, Hsp20 and αA- and αB-crystallin are paralogous proteins and that exon 1 may share a common origin [134]. These sHsps contain the consensus sequence RLFDQXFG at positions 28-35.

1.5.1.3. The C-Terminal Extension and IXI Motif

The C-terminal extension is a relatively short section that also varies in length, from two residues in Hsp16-2 of *C. elegans* to 49 residues in Hsp27 of *Drosophila* and a small number of sHsps lack a C-terminal extension altogether [109,138]. Despite low sequence similarity, a significant proportion of the C-terminal extension is comprised of polar residues. Where the extension is sufficiently long, the consensus sequence I/V-X-I/V, more commonly referred to as the IXI motif, is observed, as shown in Figure 1.4 [109]. Because of residue conservation in the paralogous sHsps mentioned above, this region can be expanded and referred to as the TIPIT-like motif for these proteins.

1.5.2. Higher Order Structure

The majority of sHsps, including all of those from mammals, exist as large oligomers which are polydisperse and dynamic, making the crystal structures unattainable and direct visualisation of the structure of these sHsps impossible. In the last several years, however, the crystal structures of two sHsps, Hsp16.5 from the thermophilic archaeon *Methanococcus jannaschii* and Hsp16.9 from wheat, have been solved [136,139]. Whilst these sHsps are from organisms distantly related to mammals, their crystal structures have been invaluable tools in the investigation of the otherwise elusive structure of mammalian sHsps. Together with indirect techniques contributing to structural information and a degree of caution, these crystal structures enable structural features of sHsps in general to be determined.

1.5.3. Secondary Structure

A common feature of all sHsps is the high proportion of β-sheet structure, typically 40-50% [140,141]. A summary of the secondary structure estimations from circular dichroism studies of Hsp25 and the α-crystallins is shown in Table 1.5. The β-sheet content has been shown to reside predominately in the α-crystallin domain of Hsp16.5 and form a compact, β-sheet sandwich [114,116]. The abundance of β-sheets in the α-crystallin domain can be seen in Figure 1.4, where the approximate locations of the β-sheets of Hsp16.5 are shown. Two antiparallel sheets are formed from strands β2, β3, β9 and β8 in one sheet and β7, β5 and β4 in the opposing sheet, with a loop containing β6 protruding [116]. There is some variation in the number of β-strands and their exact location throughout the sHsp family. For example, Hsp16.9 lacks the β1 equivalent of Hsp16.5 but all other β-strands are almost identically located [139]. Spin-labelling experiments suggest the absence of the β1-strand in the α-crystallin subunits, αA- and αB-crystallin [142]. The β6 loop is significantly shorter in animal sHsps, with some studies showing that the β-strand itself is missing [121,143]. The β6 loop is therefore also referred to as the β5-β7 loop. Although largely disordered, the N-terminal region contains the majority of the α-helical content of sHsps. Two helices have been located in the α-crystallin domain of Hsp16.5 and predicted for αA-crystallin [144].

Table 1.5: Secondary structure of Hsp25 and the α-crystallins.

sHsp	α-helix	β-sheet	β-turn	Random coil	References
Hsp25	2%	46%	18%	34%	[145]
α-crystallin	6-14%	35-40%	13-17%	30-36%	[146,147]
αA-crystallin	5-9%	40-54%	16-21%	22-39%	[148-150]
αB-crystallin	10-14%	33-44%	16-25%	26-35%	[148,151-153]

In the C-terminal extension, the IXI motif forms a short β-strand, preceded by a short α-helical region in Hsp16.5. The region following the IXI motif, shown in orange in Figure 1.4, is unstructured and flexible.

1.5.4. Tertiary Structure

Based on the exon pattern for mammalian α-crystallins and conserved residues, Wistow (1985) [154] hypothesised that αA-crystallin forms two distinct structural units, corresponding to the N-terminal domain (exon 1) and the α-crystallin domain and C-terminal extension (exons 2 and 3). These structural units are also distinct in their hydrophobic properties – hydrophilicity is mainly located in the conserved α-crystallin domain whilst the N-terminal domain is more hydrophobic [133,155]. NMR spectroscopy has since confirmed that both αA- and αB-crystallin exist as two-domain structures, with the hydrophobic N-terminal domain and hydrophilic C-terminal domain each forming a globular entity [156].

1.5.5. Quaternary Structure

Although sHsps have similar secondary and tertiary structures, the oligomeric structure is variable throughout the sHsp family. The number and arrangement of constituent monomers depends on the individual sHsp, resulting in oligomeric structures of an assortment of sizes and overall shapes.

For most sHsps, the oligomeric building block is a dimer, an exception being Hsp16.3 from *Myobacterium tuberculosis* which is composed of trimers [157]. Dimerisation of *Methanococcus* Hsp16.5 and wheat Hsp16.9 occurs through the formation of an intersubunit composite β-sheet in which the β6 loop of one monomer is incorporated into the β-sheet sandwich of its partner monomer, although the β-strands are arranged slightly differently within the β-sheet sandwich [116,158] (Figure 1.5). Modelling studies show that the β6 loop of animal sHsps is too small to interact in this way, although residues in this region (133-144 in Hsp27 and 110-113 in αA-crystallin) have been shown to be involved in interactions between subunits [159-161]. These regions have been found to adopt different conformations and orientations compared with Hsp16.5 [162].

Whilst vital for dimerisation, the α-crystallin domain is not sufficient for the formation of larger complexes – the N-terminal domain is also required for this process. This can be seen directly in Hsp16.9, where the double disk structure is stabilised by interdisk intertwining of N-terminal domains and is further

evidenced by the lack of larger complex formation for the isolated α-crystallin domain of αB-crystallin [116,139,163]. Hsp12.6 from *C. elegans* has a comparatively short N-terminal domain and is unable to form large complexes, suggesting that there is a minimal N-terminal domain structural requirement for oligomerisation [138]. Further, associations between monomers of various sHsps, including Hsp16-2 from *C. elegans*, Hsp26 from *S. cerevisiae* and mammalian Hsp27, Hsp25, αA-crystallin and αB-crystallin, in which the N-terminal domain has been removed or significantly truncated, are limited to dimers or tetramers [130,163-168].

Please see print copy for figure

Figure 1.5: Ribbon diagrams of the dimers of Hsp16.5 (left) and Hsp16.9 (right), with each monomer shown in a different colour and N- and C-termini indicated. The β6 loop is clearly shown to be incorporated into the β-sheet of its partner monomer. Red lines on the Hsp16.5 structure correspond to bis-ANS binding sites in Hsp18.1. From [136] (Hsp16.5) and [139] (Hsp16.9).

Given the diversity of sHsp oligomers and variability of N-terminal domains, it appears that the N-terminal domain also influences oligomeric properties. Hsp16.5 containing the N-terminal domain of αA-crystallin forms oligomers of similar size to intact αA-crystallin, indicating that the larger N-terminal domain of αA-crystallin is too bulky to pack inside an oligomer of Hsp16.5 proportions [161]. The reverse chimeric protein displays apparently uncontrolled oligomerisation, thought to be a result of different dimer formation due to the shortened β6 loop [161,169]. These studies highlight that the interactions involving N-terminal domains are largely based on steric properties and involve relatively non-specific interactions [161,169].

Oligomerisation of sHsps is also dependent on regions in the C-terminal extension, although the flexible region appears to be dispensable. As discussed above and in [119], Hsp16.5, Hsp16.9 and pea Hsp18.1 are able to form oligomers despite their extensions extending only one or two residues beyond the IXI motif (Figure 1.4). Although these sHsps form rigid structures with defined symmetry, sHsps with polydisperse, heterogeneous oligomers, including all mammalian sHsps, also do not appear to require this flexible region for the formation of their native quaternary structures. Removal of the flexible region of the extension of αA-crystallin, Hsp25 or bacterial sHsps has no effect on the oligomerisation of these sHsps [145,167,170]. Further truncation to eliminate the IXI motif results in smaller αA-crystallin oligomers being formed [171]. Hsp20 naturally lacks both the IXI motif and the following flexible region and is unable to form aggregates larger than dimers [172].

The crystal structures of Hsp16.5 and Hsp16.9 show that oligomerisation of these sHsps involves an interaction between the IXI motif and the hydrophobic groove formed by β4 and β8 on another monomer [139]. Both of these regions are located within the conserved α-crystallin domain and it is therefore probable that all sHsps utilise the same contacts. The angle between the α-crystallin domain and the C-terminal extension can vary by up to 30° due to a hinge region between β9 and β10, allowing flexibility in the orientation of the extension and supporting a common mechanism of oligomerisation which is capable of producing the oligomeric variability observed throughout the sHsp family [116,139]. A range of orientations of the extension within the same oligomer could also contribute to the polydispersity of sHsps [173].

As a result of their polydisperse and dynamic nature, attempts to crystallise the majority of sHsps have failed and these sHsps typically elute from size-exclusion columns as broad peaks [173]. Heterogeneous populations of mammalian sHsp oligomers are observed by electron microscopy, with diameter ranges of 8 to 18 nm for αB-crystallin [174], 12 to 17 nm for αA-crystallin [169], 15 to 18 nm for Hsp25 [175], and 9 to 22 nm for Hsp27 [173]. These oligomers, along with those from native α-crystallin, are irregular and roughly spherical with no apparent symmetry [173,174]. The diameters of αB-crystallin and Hsp27 oligomers fit to a Gaussian distribution, suggesting non-specific subunit packing and thus plasticity in oligomer size and shape [174,176,177].

αB-Crystallin contains a central cavity of similar size to that of Hsp16.5 and native α-crystallin and regions of lower density are seen in the centre of αB-crystallin particles bound to target proteins [173,174]. Interestingly, approximately 10% of Hsp16.5 oligomers are irregular despite the relative uniformity in size of particles of this sHsp, which range from 11 to 13 nm, indicating that there is a degree of variability in the formation of even these relatively rigid structures [173].

Estimation of the monomeric composition of mammalian sHsps is hampered by the heterogeneity of sHsp oligomers. The widely accepted view is that the native α-crystallin oligomer is approximately 800 kDa in mass and contains ~40 subunits but changes in solvent conditions can result in the presence of other species from 320 kDa to 1.5 MDa [178]. Hsp25 and Hsp27 form a hexadecamer of ~400 kDa which is comprised of a tetramer of tetramers, each of which is a dimer of dimers [179]. A 32-mer is observed under some conditions, suggesting that dimerisation of oligomers is possible [175].

1.5.5.1. Oligomeric Models

Within the sHsp oligomer, monomers are arranged in quasi-equivalent positions [130,180]. The C-terminal region is more susceptible to proteolysis and deamidation than the N-terminal domain and unfolds first in denaturation studies, demonstrating that this region is more highly accessible to solvent [156,181-184]. The C-terminal extension is flexible and solvent-exposed [185].

Any feasible model for the oligomeric structure of mammalian sHsps must consider these properties and also allow for a two-domain tertiary structure, as discussed above, and the accommodation of a variable number of subunits. Examples of sHsp models include the three-layered model [186], a rhombic dodecahedron model [187], a micellar model in which the N-terminal domains are buried in the centre of the oligomer with the α-crystallin domains forming a surrounding layer [178], which was later modified to include results of modelling studies [188], and a pore-like structure [189].

The pore-like structure for α-crystallin proposed by Carver *et al.* [189] is a GroEL-like structure, with two annuli of 20 monomers each. The hydrophobic N-terminal domains of each ring are oriented towards each other and are somewhat protected from the solvent by the bulkier α-crystallin domains. The C-terminal extensions protrude from the α-crystallin domain and form a gate over the hole. This model was the first to propose that the α-crystallin oligomer has a large, central cavity, which was subsequently visualised through cryoEM studies of αB-crystallin [174].

Serine residues in the N-terminal domain of αB-crystallin are phosphorylatable, which suggests that at least part of the N-terminal domain is accessible to the solvent [190]. This does not correlate with the micellar-like models, in which the N-terminal domains are completely buried within the structure. Whilst the N-terminal domain is significantly more hydrophobic than the C-terminal region,

it does contain hydrophilic regions [155]. The annular arrangement allows both the burial of the hydrophobic areas and exposure of hydrophilic residues [189].

1.5.5.2. Subunit Exchange

sHsp oligomers have the ability to acquire and release subunits, a feature that contributes to their polydispersity [167,173,174]. sHsps exist in a dynamic equilibrium between the oligomer and smaller species. The hexadecamer of Hsp25 is in a concentration-dependent equilibrium with tetramers, with some dimeric forms being present [179]. No monomers are observed, indicating that the tetramer is comprised of two dimers, rather than four monomers, and that the exchange unit is the dimer [191,192].

αA-Crystallin exchanges subunits with αB-crystallin at a rate identical to that of exchange amongst αA-crystallin homo-oligomers [167]. This free exchange is intuitive given that the native α-crystallin monomer is comprised of both αA- and αB-crystallin. Unrestricted subunit exchange also occurs between αA-crystallin and Hsp27 but αA-crystallin is not able to exchange with unrelated crystallin proteins present in the eye lens, β- and γ-crystallin, suggesting that the α-crystallins and Hsp27 share a common structural interface [167]. *Methanococcus* Hsp16.5 is capable of subunit exchange with other Hsp16.5 oligomers but is not capable of exchange with αA-crystallin whilst wheat Hsp16.9 is able to exchange with pea Hsp18.1, providing evidence that sHsps from distantly related organisms have different structural requirements that are

incompatible with each other [139,193]. N-terminally truncated αA-crystallin undergoes very slow subunit exchange with full-length αA- and αB-crystallin and N-terminally truncated Hsp14.0 from the crenarchaeon *Sulfolobus tokodaii* loses subunit exchange ability compared with the wildtype, indicating that the N-terminal domain is involved in subunit exchange [194,195]. This correlates with the role of the N-terminal region in the formation of oligomers.

1.5.6. Structural Transitions

sHsps undergo structural alterations with increasing temperatures. Exposure of hydrophobic surfaces and tryptophan residues occurs above 30°C and from about 50°C these changes in tertiary structure accelerate and are accompanied by a gradual loss in β-sheet structure [179,196-200]. At ~62°C, sHsps lose almost all of their tertiary structure and exist in a molten globule-like state [200]. Furthermore, a significant loss of β-sheet structure is observed above ~80°C [198,201].

The second structural transition, commencing at ~50°C, is accompanied by changes in quaternary structure, with an increase in oligomeric size being observed for mammalian sHsps [117,179,200-205]. This is also the case when *Methanococcus* Hsp16.5 is heated to above physiological temperatures for the thermophilic organism from which it comes. It is likely this increase in oligomeric size is a result of dynamic expansion of the oligomer rather than the addition of subunits to the complex [206]. Larger particles and elongated

structures for mammalian sHsp oligomers can be observed by electron microscopy from temperatures around 65°C, indicating possible interactions between oligomers [179,203,204].

The subunit exchange kinetics of sHsps are strongly affected by temperature [164]. A significant increase in the subunit exchange rate is observed for α- and αA-crystallin from 37°C, with the exchange rate at temperatures above 60°C being too fast to measure, whilst subunit exchange is undetectable at lower temperatures [164,207]. The rate-limiting step of subunit exchange is the dissociation of the exchange unit from the oligomer, with an activation energy of 60 kcal/mol [164,207]. With more energy available at higher temperatures, the energy requirements are more easily met and result in the increase in subunit exchange rate.

Similar increases in exchange rate occurs in wheat Hps16.9 and *Mycobacterium* Hsp16.3, indicating that, whilst their structures are more static than those of mammalian sHsps, dissociation and re-association are still able to occur [139,208]. Hsp16.5 does not appear to undergo subunit exchange until temperatures of above 50°C are reached [193]. Similarly, *S. tokodaii* Hsp14.0 requires higher temperatures for significant increases in subunit exchange rates to be observed [194]. These sHsps are from hyperthermophilic organisms, with optimal growth temperatures of 80°C or more, and show that increases in subunit exchange rate are relevant to the physiological conditions of the organism.

1.6. Chaperone Activity of sHsps

Whilst sHsps perform a diverse range of house-keeping roles, their characteristic function is that of a stress protein. Although interactions between sHsps and their targets are known to be largely hydrophobic in nature, the mechanism of chaperone action is poorly understood due to a lack of structural information.

Binding of target proteins in the central cavity, as in the case of GroEL, is unlikely for sHsps as such interactions would not support the stochiometry of binding [104]. Further, electron microscopy shows that the apparently empty cavity of *Methanococcus* Hsp16.5 contains the 32 residues of the N-terminal domain that are not resolved in the crystal structure of this sHsp and a cavity becomes apparent in oligomers of *S. tokodaii* Hsp14.0 after truncation of 21 residues from the N-terminus [173,194].

Hydrophobic regions in αA- and αB-crystallin corresponding to β3 and β4 of Hsp16.5, respectively, bind the target protein melittin and malate dehydrogenase binds to a stretch spanning from β3 to β5 in pea Hsp18.1 [209,210]. Corresponding regions are proposed to be the binding site for Hsp16.5 [206]. An isolated peptide of αA-crystallin corresponding to β3 and β4 in Hsp16.5 is capable of chaperone activity, implying that this region is indeed the chaperone binding site [210]. Other studies have suggested that this component is necessary for chaperone activity but that other regions of the

protein are also required [104,211]. Hydrophobic regions in the N-terminal domain of αA- and αB-crystallin have been shown to have temperature-dependent increases in hydrophobic exposure and it has been proposed that these regions are also involved in target binding [180]

These putative chaperone sites are buried within the oligomeric structure and are therefore inaccessible to target proteins [116,212]. However, the dimeric form of wheat Hsp16.9 and a dimer comprised of the α-crystallin domain of αB-crystallin are capable of target binding, indicating that the chaperone sites are exposed in the exchange unit [139,163]. Indeed, the dynamic exchange of subunits is necessary for the chaperone activity of sHsps and the dimer can be considered the active form of the sHsp, with the oligomer being the storage form [139,142,193]. A summary of this scheme is represented in Figure 1.6.

sHsps are promiscuous chaperones that interact with a wide range of target proteins, ranging from 4 to 100 kDa in mass, under various stress conditions *in vitro*, for example thermal or chemical stress [213]. However, they interact only with unstable, aggregation-prone intermediates and do not associate with stably unfolded hydrophobic proteins [104,214]. Efficiency of sHsp chaperone action differs depending on properties of the target protein and assay conditions. The overall shape and size of the target protein and the amount of hydrophobicity it exposes are suggested to be factors affecting the efficiency of sHsp binding [197,215]. Stoichiometry of target binding is dependent, at least in part, on target size. sHsps appear to have a maximum binding capacity of

one target molecule per monomer, with efficiency decreasing with increasing target size [209,213,216].

sHsps display little chaperone activity below physiological temperatures [208,217]. Chaperone activity is enhanced from ~30°C, the temperature at which hydrophobic surfaces begin to become exposed [200,217]. This first structural transition can therefore be seen as an "activation" of sHsp function and may serve to minimise the self-association of sHsps and prevent chaperone activity under non-stress conditions [194,209].

Full-length sHsps remain soluble at temperatures well above physiological conditions, whilst C-terminally truncated Hsp25, αA-crystallin, frog Hsp30C and *C. elegans* Hsp16-2 precipitate much more readily, demonstrating that the C-terminal extension is important for sHsp stability [145,165,218,219]. Where present, the flexible region of the C-terminal extension is relatively short and contains a high proportion of polar residues, as shown for Hsp25 and three human sHsps in Figure 1.7. Replacement of a polar serine residue in the C-terminal extension of αA-crystallin with a hydrophobic tryptophan residue results in impaired thermostability, with the protein precipitating at ~55°C [220]. This corresponds to the second structural transition which results in increased hydrophobicity, as discussed above. Together, these observations lend strong support to the role of the C-terminal extension as a solubiliser, a function which requires both polarity and flexibility.

Figure 1.6: Schematic representation of the off-folding pathway and the chaperone action of sHsps. The reversible and fast folding pathway is represented by orange arrows and the irreversible and slow off-folding pathway by red arrows. Persistent disordered molten globules may aggregate via exposed hydrophobic regions, potentially resulting in insolubilisation. sHsps, with monomers represented as green circles, recognise these regions of hydrophobicity and interact with aggregation-prone molten globules via a dimeric form. sHsps act in an ATP-independent manner and maintain the bound target proteins in a folding-competent state. The C-terminal extension of sHsps, represented in brown, protrude from the sHsp oligomer and dimer even when associated with target proteins. The interaction of Hsp70 with the sHsp-target protein complex may allow the sequestered proteins to re-enter the folding pathway and be refolded to their native state. The target proteins may also be degraded via ubiquination and the proteasome system, also with the assistance of Hsp70. Scheme adapted from [18,221].

Hsp25	**E** A **R** A **Q** I G G P **E** A G **K S E Q S** G A **K**^{209}
Hsp27	**E S R** A **Q** L G G P **E** A A **K S D E T** A A **K**^{205}
αA-crys.	**E E K** P **T S** A P **S S**^{173}
αB-crys.	**E E K** P A V **T** A A **P K K**^{175}

Figure 1.7: Amino acid sequences of the flexible regions of the C-terminal extension of Hsp25, Hsp27 and the α-crystallins. Polar residues are shown in green.

The polarity of the flexible region of the C-terminal extension is also important in the function of sHsps. The effect of mutations in the C-terminal extension on the chaperone activity of sHsps is shown in Table 1.6. With the exception of a minor decrease in chaperone activity for the αA-crystallin mutant P-S-S → L-R-K-G, the mutants that involve either no change to or an increase in charge show similar activity to the corresponding wildtype protein. Reduction in polarity and increase in hydrophobicity leads to a decrease in chaperone activity under at least one experimental condition. The P-S-S → L-W-K-G mutant of αA-crystallin demonstrates function comparable to the wildtype protein towards luciferase under fructation stress at physiological temperatures, suggesting that the mode of action of sHsps may vary according to the target protein, type of stress or temperature.

An evolutionarily conserved lysine residue at the C-terminus of Hsp25, Hsp27 and αB-crystallin provides a strong electropositive region preceded by an electronegative region, although the importance of this residue is unclear. Cross-linking studies indicate that the C-terminal lysine of αB-crystallin serves

as an amine donor in transglutaminase reactions and is therefore important for interactions with target proteins [130,222]. Indeed, flexibility of the C-terminal extension of αB-crystallin is reduced in the presence of target proteins [214]. These data suggest that the C-terminal lysine directly interacts with target proteins, possibly as an electropositive "hook" which is capable of initially capturing the target proteins for further stabilisation via hydrophobic interactions [151].

Mutations of both lysine residues at the C-terminus of αB-crystallin to non-polar residues decreases the ability of this sHsp to protect against precipitation of target proteins and ischaemia, although truncation of these residues enhances the stability of this sHsp at high temperatures [151,223,224]. Mutations of the lysine residues may result in the extension folding back on itself and losing flexibility, thus sterically hindering target binding, whilst their removal may decrease interactions between the extension and other parts of the sHsp, thereby increasing the potential for association with targets [151,223]. Whilst there is evidence that the C-terminal lysine has a functional role, it is not a strict requirement for chaperone activity, as many sHsps do not have a lysine residue at the C-terminus. The C-terminal residue of αA-crystallin is a serine residue which, although polar, is not capable of the same interactions as the lysine of αB-crystallin. Indeed, flexibility of the extension of αA-crystallin is maintained upon target binding, suggesting that the extension of αA-crystallin is not involved in target capture or that interactions between the extension of this sHsp and target proteins are not maintained [214].

Table 1.6: The effect of C-terminal extension mutations on the chaperone activity of sHsps compared with wildtype protein, as measured by the prevention of precipitation or reactivation of target proteins. CS, Luc. and MDH are abbreviations for citrate synthase, luciferase and MDH, respectively. Residues are labelled as hydrophobic (red), non-polar (brown), polar (blue) and charged (green). ‡These mutants have an overall increase in length.

sHsp	Mutant	Target	Stress	Temp.	Activity	Ref.
αA-crys.	S173K	insulin	reduction	40°C	no change	[220]
αA-crys.	S173K	MDH	fructation	37°C	no change	[225]
αA-crys.	S173K	β_L-crys.	heat	55°C	no change	[225]
αA-crys.	P^{171}-S-S → L-G-K-G‡	insulin	reduction	40°C	no change	[220]
αA-crys.	P^{171}-S-S → L-G-K-G‡	MDH	fructation	37°C	no change	[225]
αA-crys.	P^{171}-S-S → L-G-K-G‡	β_L-crys.	heat	55°C	no change	[225]
αA-crys.	P^{171}-S-S → L-R-K-G‡	insulin	reduction	40°C	small dec.	[220]
αA-crys.	P^{171}-S-S → L-D-K-G‡	insulin	reduction	40°C	no change	[220]
αA-crys.	P^{171}-S-S → L-D-K-G‡	MDH	fructation	37°C	no change	[225]
αA-crys.	P^{171}-S-S → L-D-K-G‡	β_L-crys.	heat	55°C	no change	[225]
αA-crys.	P^{171}-S-S → L-W-K-G‡	insulin	reduction	40°C	decreased	[220]
αA-crys.	P^{171}-S-S → L-W-K-G‡	MDH	fructation	37°C	no change	[225]
αA-crys.	P^{171}-S-S → L-W-K-G‡	β_L-crys.	heat	55°C	decreased	[225]
αB-crys.	K174/175L	γ-crys.	heat	66°C	decreased	[151]
αB-crys.	K174/175L	Insulin	reduction	25°C	decreased	[151]
Hsp30C	D209G	CS	heat	40°C	decreased	[226]
Hsp30C	D209G	Luc.	reactivation	42°C	decreased	[226]
Hsp30C	D209/213G	CS	heat	40°C	decreased	[226]
Hsp30C	D209/213G	Luc.	reactivation	42°C	decreased	[226]

1.6.1. In Vivo *Chaperone Activity of sHsps*

Homo-oligomers of αB-crystallin are more effective chaperones than those of αA-crystallin at physiological temperatures, with the chaperone activity of αA-crystallin being highly temperature-dependent [148,227]. However, in the absence of αA-crystallin, lenticular αB-crystallin complexes are mostly insoluble, indicating that αA-crystallin is required for the stabilisation of αB-crystallin, at least in the high concentrations found in the lens: up to 450 mg/mL in humans [125,228]. The 3:1 αA:αB-crystallin stoichiometry found in the lens, therefore, appears to be a compromise between function and stability as a result of a balance in charge and hydrophobicity [202].

Of the ten known human sHsps, seven are expressed either ubiquitously or are distributed throughout striated muscle tissue (Table 1.4). It is hardly surprising, therefore, that the formation of hetero-complexes is not restricted to the α-crystallins, nor is it a lens-specific phenomenon. Where expression overlaps, Hsp27 and αB-crystallin can form co-complexes, both as newly synthesised proteins or through re-association of exchange units [229]. In contrast to sHsp homo-oligomers, the Hsp27-αB-crystallin hetero-complex dissociates upon heat shock, suggesting that the co-complex performs a different function than each of the homo-oligomers [229]. Although the stoichiometry of the hetero-oligomer is not known, it is possible that the combination of the two sHsps results in stabilisation, similar to the situation in the α-crystallin oligomer. *In vitro*, mixed oligomers containing Hsp27 and

αA-crystallin are capable of subunit exchange, even though they do not co-localise *in vivo* [167].

Class I and class II sHsps (Table 1.4) appear to form mutually exclusive oligomers, indicating that two independent sHsp systems operate in muscle tissue and perform distinct roles, with the possibility that the non-inducible class II sHsps are dominant under non-stressed conditions [230]. Mixed dimers can be formed for all combinations of the human class I sHsps (Hsp27, αB-crystallin, Hsp20 and Hsp22) and there is evidence that Hsp22 can co-dimerise with all of the other muscle-localised sHsps [231]. A summary of the possible co-dimerisation interactions known is given in Figure 1.8, although limited data are available concerning the class II sHsps [231].

Please see print copy for figure

Figure 1.8: Known interactions between sHsps that are found in muscle tissue. The dotted line between Hsp22 and HspB3 indicates that interaction between these sHsps is not certain. Reproduced from [231].

In addition to their role as chaperones as part of the stress response, sHsps are expressed constitutively, with basal levels of expression varying with cell type and the development, growth cycle, differentiation, proliferation and oncogenic status of the cell but typically comprising up to 0.1% of the total protein content of non-lenticular tissues [100,104,105]. Under normal physiological conditions, sHsps perform an extensive range of housekeeping roles, including those listed in Table 1.7.

Table 1.7: Housekeeping roles of the sHsp family

Housekeeping roles of sHsps
actin binding and microfilament dynamics [100,105]
RNA stabilisation [104,105]
elastase inhibition [104,105]
modulation of the cytoskeleton [104,105]
regulation of platelet factor XIII [104]
involvement in apoptosis [104]

1.7. sHsps and Disease

1.7.1. sHsps in Conformational Diseases

Neurodegenerative diseases such as the conformational diseases mentioned in section 1.1.2 are characterised by the formation of structured accumulations which are deposited in brain tissue, either within or surrounding the cell [35,40]. The composite proteins are normally soluble and typically expressed

systemically. For reasons that are unclear, conversion of these proteins into insoluble masses occurs significantly only within the nervous system, resulting in the formation of brain lesions [39,232,233].

αB-Crystallin and Hsp27 are expressed at elevated levels in the brains of patients suffering from Alzheimer's, Alexander's, Creutzfeld-Jakob and Parkinson's diseases [234-236]. Abnormally high levels of αB-crystallin are also observed in Huntington's disease, multiple sclerosis, glial tumours, benign tumours associated with tuberous sclerosis and many other disorders, making this sHsp a useful marker for the pathogenesis of these conditions [125,234,236].

Alzheimer's disease is one of the most prevalent neurodegenerative diseases and the most common cause of dementia [237]. The slow deposition of misfolding proteins over decades results in symptoms appearing later in life [40]. Cleavage of amyloid precursor protein produces the 42 residue β-amyloid peptide, which is thought to be degraded under normal conditions when produced in small amounts [238]. Most mutations in the amyloid precursor protein result in increased concentration of the β-amyloid peptide, through effects on the precursor protein itself or the secretase enzymes that cleave the precursor into β-amyloid [233,239]. The β-amyloid peptides accumulate, leading to the extracellular fibrillar plaques and intracellular neurofibrillary tangles that are characteristic of Alzheimer's disease.

The increase in αB-crystallin and Hsp27 levels in this disease is thought to be a defensive mechanism, increasing the potential for chaperone activity in an attempt to prevent accumulation of the aggregation-prone proteins [240,241]. Whilst the hallmark features of Alzheimer's Disease are the insoluble deposits, they may be inactive end-products of the pathogenic cascade or the result of the body's attempts to deal with the presence of the misfolded precursors [238,242]. There is strong evidence that the soluble precursors of the fibrillar deposits are responsible for the manifestation of disease symptoms [238]. The precursors are toxic and the interaction of sHsps may promote conformational changes and promote the formation of non-toxic, amorphous aggregates [40,243]. However, interaction between αB-crystallin and β-amyloid peptides induces the formation of highly neurotoxic complexes and thus the presence of elevated sHsp levels may contribute to the progression of Alzheimer's Disease [244].

Whilst elevated expression of αB-crystallin and Hsp27 is associated with an array of neurodegenerative diseases, these sHsps are also involved in a wide range of cancers outside the nervous system [125,234,245]. HspB9 has been found in tumours in several tissues, an interesting observation given its restricted localisation [246]. Whilst there is an association between cancer and elevated sHsp levels, the use of sHsps in prognosis predictions is unreliable [104,246].

1.7.2. Diseases Caused by sHsps

Several diseases are a direct result of modifications or mutations of the sHsps themselves. α-Crystallin undergoes many post-translational modifications, including truncation, acetylation, carbamylation, cross-linking, deamidation, glycation, oxidation, phosphorylation and racemisation/isomerisation [113,141]. Since there is no protein turnover in the lens, α-crystallins lose solubility with age [247]. Combined with age-related modifications and unfolding of other crystallin proteins, this results in the inability of α-crystallin to effectively maintain its chaperone ability and ultimately leads to reduced lens transparency [113,247,248].

Naturally-occurring missense mutations of either of the α-crystallin subunits is responsible for congenital cataract. R116C and R120G mutations in αA- and αB-crystallin, respectively, are structurally compromised with inhibited chaperone activity, resulting in lens opacification [249-251]. The mutated residues involved are in equivalent positions within the α-crystallin domain and are highly conserved, indicating that they make a significant contribution to sHsp structure and function [252].

fBecause αB-crystallin is widely distributed throughout the body, the R120G mutation of this sHsp also has systemic effects. Desmin-related myopathy (DRM) is an inherited neuromuscular disorder characterised by the accumulation of the intermediate filament desmin in the sarcoplasma of skeletal

and cardiac muscle cells [253]. Whilst αB-crystallin chaperones abnormal desmin, maintaining its solubility and allowing it to be removed over time, the R120G mutant is structurally and functionally compromised and therefore unable to prevent desmin aggregation [152,254-256]. The interaction between αB-crystallin and desmin is enhanced by the mutation, resulting in the inclusion of R120G in the intracellular aggregates [250,257]. The accumulation of desmin results in derangement of myofibrils and compromised muscle action. Because of the effects of this mutant in the eye lens, patients with desmin-related myopathy also suffer from cataracts [125].

Several mutations of Hsp27 have been identified as the cause of diseases affecting the nervous system. R127W, S135F, T151I and P182L mutants are associated with distal hereditary motor neuropathies and S135F and R136W are linked to Charcot-Marie-Tooth Disease, a hereditary neuropathy characterised by degeneration of peripheral nerves [258]. Maintenance of the axonal cytoskeleton and transport through organisation of the neurofilament network are disrupted as a result of these mutations [258,259]. With the exception of P182L, these residues are located in the α-crystallin domain and are conserved. Three of these mutations are in close proximity to R140, the equivalent of R120G in αB-crystallin, indicating that residues in this region are especially important for normal activity of sHsps. This region forms part of a β-strand involved in subunit-subunit interactions, as discussed above [260].

Mutations of Hsp22, K141N and K141E, are also linked to distal hereditary motor neuropathies and Charot-Marie-Tooth Disease [261,262]. Residue K141 also corresponds to position 120 in αB-crystallin.

sHsps clearly play an essential role under both physiological and stress conditions. The diverse housekeeping functions of sHsps are fundamental to a range of cellular processes and the chaperone activity under stress conditions is essential for the cell to survive various insults. This latter role is highlighted by the myriad of diseases that manifest upon failure of the sHsp as a chaperone, both as a result of abnormal cellular proteins or defective sHsps.

Preconditioning of cells with a brief, mild cellular stress provides a transient state of resistance to subsequent severe stresses [263,264]. The elevated levels of sHsps as a result of the initial insult allows the cell to survive normally lethal temperatures, an effect which has been observed for all organisms studied [264]. For example, increased levels of Hsp27 as a result of hyperthermia and other stresses has a protective effect against the toxicity of tumour necrosis factor-α in some cell lines [265]. Because of these protective effects, sHsps have the potential to be used as therapeutic targets. Of particular relevance is the protection against ischaemic damage to the heart, brain and kidney conferred by induced levels of sHsps [113]. Increasing the levels of expression of sHsps by various means such as mild heat stress, preventing protein degradation with the introduction of proteasome inhibitors, administration of drugs to stimulate sHsp expression or even the development

and introduction of small proteins or peptides to act as sHsp analogues are potential pharmacological strategies to invoke transient protection from ischaemia [103,264,266]. Increased expression of sHsps may also help to prevent the formation of toxic precursors or assist in their conversion into non-toxic, amorphous aggregates in conformational diseases [243].

Our current understanding of sHsps is far from complete. Despite the invaluable information gleaned from the crystal structures of plant and archaeon sHsps, investigation into the structure of mammalian sHsps is hindered by the heterogeneity and dynamic nature of these proteins, features that are vital for their function but render them resistant to crystallisation. A much greater appreciation of the mechanism of action of sHsps is needed if these proteins are to implemented as diagnostic or therapeutic tools. This study aims to enhance the knowledge of the structure of sHsps and how they function as molecular chaperones.

Chapter 2

Materials and Methods

2.1. Materials

Unless otherwise stated, all reagents used were of analytical grade. Acrylamide, agarose, ampicillin sulphate, dithiothreitol (DTT) and lysozyme were obtained from Amresco Inc. (Solon, Ohio, USA). Insulin, kanamycin sulphate, phenylmethylsulphonyl fluoride (PMSF), polyethylenimine (PEI) and yeast alcohol dehydrogenase (ADH) were obtained from Sigma-Aldrich (St Louis, Missouri, USA). Agar, tryptone and yeast extract were obtained from Oxoid Australia (West Heidelberg, Vic, Australia). IPTG and X-Gal were obtained from Progen Industries Ltd (Darra, Qld, Australia). ^{15}N-labelled ammonium chloride and D_20 were obtained from Cambridge Isotope Laboratories, Inc. (Andover, Massachusetts, USA). SnakeSkin™ pleated dialysis tubing was obtained from Pierce (Rockford, Illoinois, USA). DNase I was obtained from Roche Diagnostics (Basel, Switzerland). Restriction enzymes were obtained from Fermentas International (Burlington, Ontario, Canada).

The composition of various buffers and solutions referred to in this chapter are given in Appendix B.

2.2. General Molecular Techniques

2.2.1. Preparation of Electrocompetent Cells

A single colony of *E. coli* BL21(DE3) from a freshly-streaked agar plate was used to inoculate a 200 mL culture of LB medium. The culture was incubated

at 37°C with shaking until a cell density (A_{600}) of approximately 0.8 was reached. After being chilled on ice, the culture was centrifuged at 4,000×*g* for 15 min at 4°C. The cell pellet was thoroughly washed by a series of resuspension and re-centrifugation steps in 200 mL of cold dH_20, 100 mL of cold dH_20 and 4 mL of cold 10% glycerol. Finally, the cells were resuspended in 600 μL of cold 10% glycerol, divided into 40 μL aliquots and stored at –80°C.

2.2.2. Electrotransformation of Electrocompetent E. coli

Electrotransformation was performed on a GenePulser II (Bio-Rad, Hercules, California, USA) set to deliver a pulse of 2.5 kV with capacitance and resistance values of 25 μF and 200 Ω, respectively. An aliquot of electrocompetent *E. coli* BL21(DE3) cells was thawed on ice and placed in a cold electroporation cuvette along with 2 μL of plasmid DNA (section 2.3.1). The cuvette was flicked to ensure contact of the cells with the cuvette plates, placed in the GenePulser and pulsed once at the above settings. Cells were kept briefly on ice, suspended in 500 μL of SOC medium and incubated at 37°C with shaking for 1 h. Various volumes of the suspension were spread onto agar plates containing 100 μg/mL ampicillin (Ap) and incubated at 37°C for approximately 16 h.

2.2.3. Preparation of Bacterial Stocks

Glycerol stocks of *E. coli* BL21(DE3) transformed with wildtype and mutant pAK3038-Hsp25 were prepared for long-term storage. A single colony arising

from the plating of the electrotransformation suspension was plated onto a fresh agar plate containing 100 μg/mL Ap and incubated at 37°C for approximately 16 h. An inoculation loopful of colonies was taken from the freshly incubated plate and suspended in 2 mL of sterile 10% (v/v) glycerol containing 1% (w/v) casamino acids in a cryogenic sample tube and stored at –80°C.

2.2.4. Sodium Dodecyl Sulphate Polyacrylamide Gel Electrophoresis

Sodium dodecyl sulphate polyacrylamide gel electrophoresis (SDS-PAGE) was used to visualise the protein composition of samples at various stages of purification. Samples were mixed in a 1:1 ratio with 2× reducing buffer and boiled for 10 min. For bacterial whole cell culture samples, a 1 mL aliquot was centrifuged at 16,000×*g* for 5 min and the pellet resuspended in 100 μL of 0.7% sodium chloride before an equivalent volume of reducing buffer was added.

Proteins were separated on a 15% resolving gel and 4% stacking gel of 0.75 mm thickness in a MiniProtean 3 system (Bio-Rad, Hercules, California, USA) with a Bio-Rad Power Pac 300 power supply. The gels were immersed in SDS-PAGE running buffer and run at 100-250 V until the dye front had barely run off the gel. Protein bands were visualised by soaking the gels in rapid stain overnight and then destaining with several washes of rapid destain until the

background of the gels became clear. Gels were then stored in final destain before being scanned.

2.3. DNA Manipulation Techniques

2.3.1. Extraction of Plasmid DNA

Plasmid DNA was extracted from bacterial cells using a Wizard®*Plus* SV Miniprep DNA Purification System (Promega, Madison, Wisconsin, USA) as per manufacturer's instructions. All reagents used were supplied with the kit. A single colony of plasmid-containing bacteria from a freshly-streaked agar plate was used to inoculate a 5 mL LB culture containing 100 mg/mL Ap. The culture was incubated at 37°C with shaking for approximately 16 h and pelleted by centrifugation at 16,000×*g* for 5 min at room temperature. The pellet was thoroughly resuspended in 250 μL of resuspension solution. Cell lysis solution (250 μL) was added, and the suspension was gently mixed by inversion before the addition of 10 μL of alkaline protease solution and gently mixing as above. The sample was incubated at room temperature for 5 min before the addition of 350 μL of neutralisation solution. After gently mixing as above, the sample was centrifuged as above for 10 min. A spin column was inserted into a collection tube, and the cleared lysate resulting from the centrifugation step was decanted into the spin column. The lysate was centrifuged as before for 1 min and the flowthrough was discarded. Wash solution (750 μL) was added to the sample before centrifuging as above for 1 min. The flowthrough was

again discarded, and 250 μL of wash solution was added to the sample before centrifuging as above for 2 min. The spin column was transferred into a sterile 1.5 mL Eppendorf tube. Plasmid DNA was released from the spin column by the addition of 100 μL of nuclease-free water and centrifuging as before for 1 min. Extracted plasmid DNA was stored at –20°C.

2.3.2. Restriction Enzyme Digestions

The presence of the Hsp25 gene insert in the plasmid pAK3038 was confirmed by restriction enzyme digestions. Extracted plasmid DNA (5 μL) was placed in a 1.5 mL Eppendorf tube along with 1 μL each of *Bam*H1 and *Nde*I restriction enzymes, 2 μL of restriction enzyme buffer and MilliQ water to 10 μL. Digestions were centrifuged briefly and then incubated at 37°C for 2 h. DNA bands were visualised after agarose gel electrophoresis.

2.3.3. Agarose Gel Electrophoresis

Agarose gel electrophoresis was used to visualise the DNA composition of samples. Samples were mixed with loading dye before being loaded onto a 0.85% agarose gel. The gel was immersed in TAE buffer and run at 50-100 V with a Bio-Rad Power Pac 300 power supply until the dye front had travelled approximately two-thirds of the gel length. The gel was then stained by immersion in ethidium bromide solution for 15-30 min and then similarly destained in water. The stained DNA bands were visualised on a Gel Documentation System (NovaLine, Sydney, NSW, Australia).

2.4. DNA Sequence Analysis

2.4.1. Sequencing Primers

Sequencing primers designed to allow sequencing of the C-terminal extension of the Hsp25 gene and flanking regions are shown in Table 2.1, and approximate primer locations are outlined in Figure 2.1. Primers were synthesised by Sigma-Genosys (The Woodlands, Texas, USA). Storage stock solutions were prepared by resuspending the primer DNA in TE buffer (pH 8.0) to a final concentration of 80 μM. Working stock solutions of 1.6 μM were made by diluting the storage stocks in MilliQ water.

Table 2.1: Sequencing primers for the C-terminal region of *Hsp25*.

Primer Direction	Primer Sequence
Forward	5'-TCTCGGAGATCCGACAGA-3'
Reverse	5'-CTTTCGGGCTTTGTTAGCAG-3'

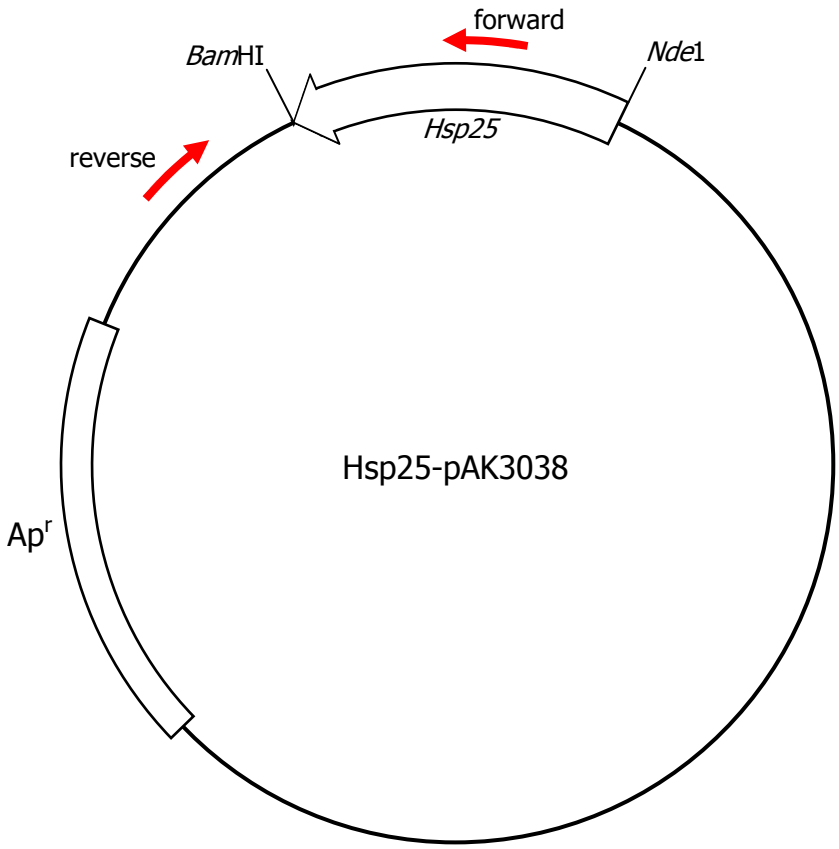

Figure 2.1: Plasmid map of pAK3038-Hsp25 showing the approximate positions of sequencing primers.

2.4.2. Sequencing Polymerase Chain Reaction

Prior to performing sequencing polymerase chain reaction (PCR), the template DNA was assessed by agarose gel electrophoresis (section 2.3.3). The concentration of the template DNA was estimated by visually comparing the intensity of the band to those of λ/Hind*III* markers. The optimal amount of DNA for sequencing is 200-500 ng, which corresponded to approximately 4 μL of extracted plasmid DNA (section 2.3.1).

Sequencing reactions were made up in 0.2 mL Thermo-Tubes (ABgene, Epsom, Surrey, UK) and comprised 4 μL of template DNA, 2 μL of 1.6 μM sequencing primer, 2 μL of 5× sequencing buffer, ABI Prism® BigDye™ Terminator Ready Reaction Mix (Applied Biosystems, Foster City, California, USA) (either 4 μL of v2.0 or 0.5 μL of v3.1) and made up to 10 μL with MilliQ water.

Template DNA was amplified on a Cool Palm 96 (Corbett Research, Mortlake, NSW, Australia) with 25 cycles of 96°C for 10 s for denaturation, 50°C for 5 s for annealing and 60°C for 4 min for polymerisation, with rapid thermal ramping. Reactions were then held at 4°C.

2.4.3. Precipitation of Amplified DNA

The amplified DNA was transferred to a 1.5 mL Eppendorf containing 2 μL of 1.5 M sodium acetate, 250 mM EDTA (pH 8.0) and 10 μL of MilliQ water. After the sample was vortexed thoroughly and briefly centrifuged, 75 μL of ice-cold 100% ethanol was added. The sample was kept on ice for 5 min before being centrifuged at 16,000×*g* for 15 min. The supernatant was carefully aspirated, and the pellet was washed with 200 μL of cold 70% ethanol and centrifuged as above for 5 min. The ethanol was carefully aspirated and the pellet was left to air-dry for 1-2 h in a fume hood. The precipitated DNA pellet was stored at –20°C.

2.4.4. Sequencing Electrophoresis

Sequencing was performed on an ABI Prism 377 DNA Sequencer (Applied Biosystems, Foster City, California, USA) with a 4% polyacrylamide sequencing gel. Immediately prior to loading onto the gel, precipitated DNA pellets were resuspended in 6 μL of sequencing loading dye, vortexed thoroughly and centrifuged briefly. The samples were heated at 90°C for 2 min and then centrifuged briefly before being placed on ice. A 2 μL sample was loaded onto the sequencing gel, which was run at 37 W for 10 h. Sequences were analysed using AutoAssembler software (Applied Biosystems, Foster City, California, USA).

2.5. Site-Directed Mutagenesis

Site-directed mutagenesis was performed using a QuikChange® Site-Directed Mutagenesis Kit (Stratagene, La Jolla, California, USA). A summary of the mutagenesis procedure is outlined in Figure 2.2. Control reactions were carried out alongside the mutagenic reactions according to the manufacturer's instructions. The concentration of extracted plasmid DNA was estimated as previously described (section 2.4.2).

2.5.1. Mutagenic Primers

Mutagenic primers were designed with the codon targeted for mutation flanked by 15 bases of homologous sequence on either side. Each mutation required a forward and a reverse primer, each containing the desired base changes.

Primers were synthesised by Sigma-Genosys (The Woodlands, Texas, USA). Storage stock solutions were prepared by resuspending the primer DNA in TE buffer (pH 8.0) to a final concentration of 200 μM. Working stock solutions of 2 μM were made by diluting the storage stocks in MilliQ water.

2.5.2. Mutagenic Polymerase Chain Reaction

Mutagenesis reactions were made up in 0.2 mL Thermo-Tubes and comprised of 1.7 μL (approximately 50 ng) of template DNA, 6 μL of 2 μM forward mutagenic primer, 6 μL of 2 μM reverse mutagenic primer, 5 μL of 10× reaction buffer and 1 μL of dNTP mix. Dimethyl sulphoxide (DMSO) was added to a final concentration of 5% to those reactions containing mutagenic primers capable of forming secondary structures, as advised by the supplier. A mutagenesis control reaction was performed with 2 μL (10 ng) of pWhitescript™ 4.5 kb control plasmid, 1.25 μL (125 ng) of control forward primer, 1.25 μL (125 ng) of control reverse primer, 5 μL of 10× reaction buffer and 1 μL dNTP mix. All reactions were made up to 50 μL with MilliQ water.

Please see print copy for figures

Figure 2.2: Overview of the mutagenic procedure (adapted from QuickChange® Site-Directed Mutagenesis manual (Stratagene, La Jolla, California, USA).

Immediately prior to commencing the PCR, 1 μL of *PfuTurbo*® DNA Polymerase (2.5 U/μL) was added to each reaction, which were then cycled on a Cooled Palm 96 (Corbett Research, Mortlake, NSW, Australia) at 95°C for 30 s followed by 14 cycles of 95°C for 30 s, 55°C for 1 min and 68°C for 10 min with rapid thermal ramping. The reactions were then held at 4°C.

To digest non-mutated template DNA, 1 μL of *Dpn*I (10 U/μL) was added to the reactions, which were mixed thoroughly by pipetting and briefly centrifuged. Reactions were then incubated at 37°C for 1 h and stored at –20°C.

2.5.3. Transformation into XL1-Blue Supercompetent Cells

XL1-Blue supercompetent cells were thawed on ice and distributed in 50 μL aliquots into pre-chilled 15 mL Falcon® tubes (Applied Biosystems, Foster City, California, USA). For each mutagenic reaction and mutagenesis control, 1 μL of the digested PCR product was added to an aliquot of cells. A transformation control was also performed, using 1 μL of the control plasmid pUC18. The cells and DNA were mixed by gentle swirling and kept on ice for 30 min before being heat pulsed in 42°C water for 45 s and immediately placed on ice for a further 2 min. The cells were suspended in 500 μL of pre-warmed NZY^+ medium and incubated at 37°C with shaking for 1 h. Various volumes of each mutagenic transformation were spread onto agar plates containing 100 μg/mL Ap to select for bacterial cells containing the plasmid. Mutagenesis and transformation

controls (250 μL and 5 μL[1], respectively) were spread onto agar plates containing 100 μg/mL Ap, 80 μg/mL X-gal and 20 mM IPTG. All plates were incubated at 37°C for approximately 16 h.

The efficiencies of the mutagenesis and transformation reactions were monitored by the control reactions. Blue colonies that grew on the control plates indicated successful mutagenesis and transformation of the mutagenesis control and successful transformation of the transformation control. The efficiency was calculated as the ratio of blue colonies to total colonies on either control plate.

2.5.4. Screening for Mutants

Random colonies growing on the mutagenic reaction plates were re-plated onto fresh agar plates containing 100 μg/mL Ap and incubated at 37°C for approximately 16 h. Plasmid DNA was extracted from each of the freshly-streaked plates, as described in section 2.3.1, and the presence of the Hsp25 gene was confirmed by double restriction enzyme digestions, as described in section 2.3.2. Samples that released the Hsp25 gene insert were subjected to forward and reverse sequencing (section 2.4). Those samples that displayed the correct mutation in both the forward and reverse DNA strand were confirmed as mutants. The plasmid DNA of these mutants was transformed

[1] a 200 μL pool of SOC medium was first put on the plate, then 5 μL of the control was added to this pool and the mixture was spread over the plate.

into *E. coli* BL21(DE3) and glycerol stocks prepared, as described in sections 2.2.2 and 2.2.3, respectively.

2.6. Expression Vectors for Hsp25 and αB-Crystallin

The pAK3038 plasmid containing the mouse Hsp25 gene under the control of a T7 promoter and an ampicillin resistance gene (Figure 2.3) was a gift from Prof. Matthias Gaestel (Institute of Biochemistry, Hannover, Germany). A 5 μg plasmid DNA pellet was resuspended in 50 μL of MilliQ water and transformed into *E. coli* BL21(DE3). Plasmid DNA was extracted and a double digest with restriction enzymes *Bam*H1 and *Nde*I was performed to confirm the presence of a gene insert. DNA sequencing was performed using a forward sequencing primer designed from within the Hsp25 gene sequence published by Gaestel *et al.* (1993) [267]. A reverse sequencing primer was designed from the results of sequencing with the forward primer to allow the complimentary strand to be sequenced.

2.7. Expression and Purification of Wildtype and Mutant Hsp25

The following procedure outlines the expression and purification of wildtype Hsp25. Mutant Hsp25 was expressed and purified using the same procedure as for wildtype Hsp25 unless otherwise stated.

Figure 2.3: Plasmid map of pAK3038 showing major features. pAK3038 is a modification of the pET3a plasmid (Novagen, San Diego, California, USA) [268-272].

2.7.1. Expression of Wildtype and Mutant Hsp25

A single colony of *E. coli* BL21(DE3) containing pAK3038-Hsp25 from a freshly-streaked agar plate was used to inoculate a 100 mL culture of LB medium containing 0.4% glucose and 100 μg/mL Ap. This starter culture was incubated at 37°C with shaking for approximately 16 h and then used to inoculate 2× 950 mL LB media containing 0.4% glucose and 100 μg/mL Ap. These 1 L cultures were incubated at 37°C with shaking until a cell density (A_{600}) of 0.7-0.9 was reached (approximately 2 h). Protein expression was induced by the addition of IPTG to a final concentration of 0.4 mM, and the culture was

incubated for a further 3 or 4 h. Cells were harvested by centrifugation at 4,000×*g* for 10 min at 4°C and stored at –20°C overnight if necessary.

2.7.2. Purification of Wildtype and Mutant Hsp25

Hsp25 was purified using a method modified from Horwitz *et al.* (1998) [273].

2.7.2.1. Cell Lysis

Cell pellets were resuspended in 12 mL of cold lysis buffer (pH 8.0). Pellets larger than approximately 8 g were halved and processed separately. Lysozyme (80 μL/g of pellet of a 10 mg/mL solution) and PMSF (4 μL/g of pellet of a 100 mM solution) were added to the lysate, which was then kept on ice for 20 min. After the addition of deoxycholic acid (4 mg/g of pellet), the lysate was incubated at 37°C with shaking for 30 min. DNase I (10 μL/g of pellet of a 2 mg/mL solution) was added to the lysate, which was kept at room temperature until the suspension was no longer viscous (approximately 30 min). The lysate was centrifuged at 17,000×*g* for 15 min at 4°C, and the resulting supernatant was ultracentrifuged at 100,000×*g* for 30 min at 4°C. The supernatant was decanted and stored at –20°C if necessary.

2.7.2.2. Anion-Exchange Chromatography

Immediately prior to anion-exchange chromatography, DTT, PEI and EDTA were added to the lysate to final concentrations of 10 mM, 0.12% and 1 mM, respectively. The lysate was kept at room temperature for 10 min, and then

centrifuged at 17,000×*g* for 10 min at 4°C. The supernatant was filtered through a 0.22 μm membrane.

Anion-exchange chromatography was carried out at 4°C. The filtered supernatant was loaded onto a DEAE-Sephacel (Sigma-Aldrich, St Louis, Missouri, USA) anion-exchange column (total volume ~90 mL, internal diameter 2.5 cm) equilibrated with 20 mM Tris-HCl (pH 8.5) containing 1 mM EDTA and 0.02% NaN_3. Hsp25 was eluted at a flow rate of 0.5 mL/min with a step-wise ionic gradient in the above buffer. Hsp25 and all mutants, with the exception of Hsp25-K209L, eluted at 100 mM NaCl; Hsp25-K209L eluted at 200 mM NaCl. Fractions of 6 mL were collected in a Model 2110 fraction collector (Bio-Rad, Hercules, California, USA). The column was washed with the above buffer containing 1 M NaCl to elute strongly-bound contaminating proteins.

Protein was detected by either measuring the absorbance at 280 nm of or performing a bicinchoninic acid (BCA) assay (Sigma-Aldrich, St Louis, Missouri, USA) on each of the fractions. Fractions containing Hsp25, as assessed by SDS-PAGE, were pooled and concentrated to approximately 3 mL in an Ultrafree-15 Centrifugal Filter Device (Millipore, Billerica, Massachusetts, USA). The concentrate was stored at 4°C for up to several days if necessary.

2.7.2.3. Size-Exclusion Chromatography

Size-exclusion chromatography was carried out at 4°C. Solid DTT was added to the concentrated anion-exchange peak to a final concentration of 50 mM. The

sample was kept at room temperature for up to 30 min, and then loaded onto a Sephacryl S-300HR (Pharmacia, Uppsala, Sweden) size-exclusion column (total volume ~470 mL; internal diameter 2.6 cm) equilibrated with 50 mM Tris-HCl (pH 8.0) containing 1 mM EDTA and 0.02% NaN_3. Protein was eluted at a flow rate of 0.33 mL/min and collected in 6 mL fractions.

Protein was detected and analysed as above. Hsp25-containing fractions were pooled and concentrated to approximately 1 mL in an Ultrafree-15 Centrifugal Filter Device. Buffer exchange was performed either by washing the Centrifugal Filter Device with 3× 15 mL volumes of MilliQ water or by dialysing against at least 3× 2 L volumes of MilliQ water at 4°C over 24 h. The concentrate or dialysate was then lyophilised and stored at –20°C.

2.7.3. Nanoscale Electrospray Ionisation Mass Spectrometry

Desalting and mass spectrometric analyses of wildtype and mutant Hsp25 samples were kindly performed by Dr Andrew Aquilina (University of Wollongong).

Desalting and denaturation of samples was performed using ZipTip®C18 pipette tips (Millipore, Billerica, Massachusetts, USA). Lyophilised protein samples were dissolved in 40% acetonitrile containing 1% formic acid to a final concentration of approximately 5 μM and 10 μL of this solution was applied to the tip and aspirated five times. Salts were removed by five aspirations with 10 μL of 1%

formic acid. Protein was eluted with 3 μL of 80% acetonitrile containing 1% formic acid.

Nanoscale Electrospray Ionisation Mass Spectrometry (nanoESI MS) was performed on a Q-Tof™ 2 mass spectrometer (Micromass UK Ltd, Simonsway, Manchester, UK) calibrated with sodium iodide. The desalted protein sample was electrosprayed from a gold-coated borosilicate capillary prepared in-house. The capillary, cone and collision cell voltages were set to 1.3 kV, 100 V and 4 V, respectively. Spectra were processed with MassLynx™ software (Waters, Milford, Massachusetts, USA).

2.7.3.1. Peptide Sequencing

Tandem MS of tryptic digestions of Hsp25 was performed as above with a collision voltage of 20 V.

2.8. Expression and Purification of Wildtype αB-Crystallin

E. coli BL21(DE3) transformed with pET24d(+)-αB-crystallin was a gift from Dr Teresa Treweek (University of Wollongong).

αB-Crystallin was expressed and purified using the same methods as for Hsp25 as outlined in section 0, with 50 μg/mL kanamycin being used instead of 100 μg/mL ampicillin.

2.9. Characterisation of Wildtype and Mutant Hsp25

Unless otherwise stated, concentrations of Hsp25 samples and target proteins used in this section were determined from the absorbance values at 280 nm measured on a UV-1601 UV-Visible spectrophotometer (Shimadzu, Rydalmere, NSW, Australia). An extinction co-efficient of 1.87 for a 1 mg/mL solution of Hsp25 [274] was used for both wildtype and mutant Hsp25 species, as aromatic residues were not affected by the mutations. A molecular mass of 23,014 Da was used for wildtype Hsp25, and masses of mutants were calculated according to the masses of substituted residues (Table 2.2).

Table 2.2: Molecular masses of Hsp25 and mutants used for the determination of protein concentration.

Mutant	Molecular Mass (Da)
wildtype	23,014
E190stop	21,061
E190A	22,956
R192A	22,929
Q194A	22,957
E199A	22,956
E204A	22,956
Q205A	22,957
K209L	22,999

All stock solutions were prepared in 50 mM sodium phosphate buffer (pH 7.3) containing 0.02% NaN_3 and assay samples were made up to volume with this buffer unless otherwise stated.

2.9.1. Far-UV Circular Dichroism Spectroscopy with Temperature Studies

Circular Dichroism (CD) measurements were performed on a J-810 spectropolarimeter (Jasco, Tokyo, Japan) connected to a Peltier temperature controlled water circulator (Jasco, Tokyo, Japan) with an external probe. A bandwidth of 1 nm and response time of 4 s were used and scanning was set to continuous at 100 nm/min. Ellipticity was recorded from 190 to 250 nm, with a data pitch of 0.1 nm.

Wildtype and mutant Hsp25 samples were prepared in 10 mM phosphate buffer (pH 7.5) to a final concentration of 10-15 μM and filtered through a 0.22 μm membrane. The samples were placed in quartz fluorescence cuvettes with a pathlength of 1 mm, placed in the spectropolarimeter and equilibrated until the temperature of the solution remained constant for at least 5 min.

A single scan was performed, and samples were diluted until the high tension voltage remained below 600 V for the 200-250 nm region and 800 V in the 190-200 nm region to achieve optimal signal to noise ratio. Spectra were acquired for each sample at 25°C, 37°C and 55°C and represent the accumulation of 16 scans. Sample concentration was determined by

performing a bicinchoninic acid (BCA) assay (Sigma-Aldrich, St Louis, Missouri, USA)

Circular dichroism spectra for the comparison of unmodified and modified wildtype Hsp25 proteins were acquired as above except that a 1 cm pathlength was used, spectra represent the accumulation of 6 scans and sample concentrations were approximately 1 μM, as determined by performing a Bradford Protein Microassay with BSA as a standard (Bio-Rad, Hercules, California, USA).

Units were converted to the mean residue ellipticity according to the equation in Figure 2.4 using the calculated concentration, number of residues and molecular weight of the respective protein samples (Table 2.2).

Please see print copy for figure

Figure 2.4: Equation for calculating mean residue ellipticity ($[\Theta]_{MRW}$) with units of deg.cm^2.dmol^{-1} where Θ is measured ellipticity in mdeg, M is the molar concentration of the protein sample, n is the number of residues per molecule and l is the pathlength in cm [275].

Deconvolution of the spectra to estimate secondary structure was achieved using the CDSSTR program [276-279] in the DICHROWEB Online Circular Dichroism Analysis suite [280,281]. Data from the 240-190 nm region with a data interval of 1 nm were used with Reference Set 4 optimised for this region.

2.9.2. Fluorescence Studies

Fluorescence studies were performed at 25°C on a F-4500 Fluorescence Spectrophotometer (Hitachi High-Technologies, Tokyo, Japan) with a Thermomix temperature controlled water circulator (B. Braun, Melsungen, Germany). The instrument was set to 700 V with scan speed of 240 nm/min. Slit widths were 5.0 nm and 10.0 nm for excitation and emission, respectively. Spectra correction and shutter control functions were disabled.

Wildtype and mutant Hsp25 samples were prepared in 3 mL quartz fluorescence cuvettes fitted with a magnetic stirrer to a final concentration of 5 μM and final volume of 1.5 mL. Samples were kept on ice and equilibrated in the fluorescence spectrophotometer for 10 min prior to reading.

2.9.2.1. Intrinsic Tryptophan Fluorescence

Intrinsic tryptophan fluorescence was performed using an excitation wavelength of 295.0 nm, with emission spectra being recorded from 300 to 450 nm. Preliminary experiments confirmed that differences observed between the wildtype and mutant proteins were reproducible (data not shown).

2.9.2.2. ANS Binding Fluorescence

1-Anilino-8-naphthalene sulphonate (ANS) binding fluorescence was performed with an excitation wavelength of 387.0 nm. Sequential 1.5 μL aliquots of freshly prepared 5 mM ANS were added to the samples and stirred for 1 min to

ensure thorough mixing prior to recording the maximum ANS binding fluorescence at 479.0 nm. Emission spectra were recorded from 400 to 650 nm at a final concentration of 85 μM ANS.

2.9.3. Size-Exclusion Fast Protein Liquid Chromatography

Size-exclusion fast protein liquid chromatography (FPLC) was performed at room temperature on a BioSep-SEC-S 4000 column (Phenomenex®, Torrance, California, USA) connected to an ÄKTA™FPLC™ system (Amersham Biosciences, Little Chalfont, Buckinghamshire, UK). Standards and Hsp25 samples were prepared to final concentrations of 2 mg/mL and 30 μM, respectively. The molecular weight standards used were blue dextran, thyroglobulin, apoferritin and catalase with respective molecular masses of 2 MDa, 669 kDa, 443 kDa and 250 kDa, as given by the suppliers. The standards and samples were centrifuged at 16,000×*g* for 5 min before 100 μL of the supernatants were loaded onto the column. Elution was performed at a flow rate of 0.5 mL/min and protein was detected at 280 nm by an in-built UV detector. Preliminary experiments confirmed that differences observed between the wildtype and mutant proteins were reproducible (data not shown).

2.9.4. Thermostability Studies

Thermostability studies were performed on a Cary-500 Scan UV-Vis-NIR spectrophotometer (Varian Inc., Palo Alto, California, USA) with a Cary temperature controller. Wildtype and mutant Hsp25 solutions were prepared to

a final concentration of 0.2 mg/mL. The solutions were heated in 1 mL quartz cuvettes with a 1 cm path length from 25°C to 100°C with thermal ramping of 1°C/min. Protein precipitation was monitored by light scattering at 360 nm, measured every minute.

2.9.5. Chaperone Activity Assays

2.9.5.1. Thermal Stress Assays

Thermal stress assays were performed at 55°C using yeast alcohol dehydrogenase (ADH) as the target protein. The concentration of freshly prepared ADH stock solution was determined using the extinction co-efficient of 14.6 for a 1% solution and the molecular mass of 141 kDa [282].

Assays were performed in a Hewlett Packard Diode Array UV-Vis spectrophotomer (Agilent Technologies, Forest Hill, Vic, Australia) connected to a Thermomix temperature controlled water circulator (B. Braun, Melsungen, Germany). Samples were prepared by the addition of all reagents except ADH in 1 mL acrylic cuvettes with a 1 cm path length and equilibrated at 55°C for at least 10 min. The assays were started by the addition of ADH to a final concentration of 2 μM to give a final cuvette volume of 800 μL. A range of chaperone concentrations were used to give a range of suppression levels of ADH precipitation, from a Hsp25 monomer:ADH subunit ratio of 0:1, corresponding to an absence of chaperone, to 1.4:1, which was found to give full suppression of ADH precipitation for wildtype Hsp25. Protein precipitation

was monitored by light scattering at 360 nm for 1 h with measurements taken every 30 s. Data presented are the averages of duplicates performed within the same experiment. Precipitation was plotted as a percentage of maximum precipitation (i.e. maximal light scatter for the samples with an absence of chaperone gave 100% precipitation).

2.9.5.2. Reduction Stress Assays

Reduction stress assays were performed using insulin from bovine pancreas as the target protein with dithiothreitol (DTT) as the reducing agent. A stock solution of insulin was prepared by adding 500 µL of buffer to approximately 8 mg of insulin and adjusting the pH with addition of 0.1 M NaOH until the insulin dissolved. Buffer was added to a final volume of 5 mL. The exact concentration of the insulin stock was determined using the molar extinction co-efficient of 6,080 [283].

Assays were performed in a 96 well plate in a FLUOstar OPTIMA platereader (BMG LABTECH GmbH, Offenburg, Germany). All reagents except DTT were added to the wells, with a final insulin concentration of 45 µM in each well. Various concentrations of Hsp25 were used, to give a range of Hsp25 monomer:target protein ratios from 0:1, corresponding to an absence of chaperone, to 0.5:1, which was found to give full suppression of insulin precipitation for wildtype Hsp25. The plate was incubated at 37°C for 10 min, and the assays were initiated by the addition of freshly prepared DTT to give a final DTT concentration of 20 mM and total well volume of 200 µL. Protein

precipitation was monitored by light scattering at 360 nm for 2 h with measurements every 2 min. Data presented are the averages of triplicates performed within the same experiment.

2.10. Uniform ^{15}N-Labelling of Wildtype and Mutant Hsp25

All glassware used for the expression of ^{15}N-labelled protein was washed by hand with 10% Decon-90 detergent and rinsed thoroughly with distilled water to ensure no traces of nitrogen-containing media were present. A 100 mL ^{15}N-M9 starter culture containing 100 μg/mL Ap was prepared by inoculation with colonies either from a glycerol storage stock or from a fresh transformation. Glycerol stocks were plated onto M9 minimal media plates containing 100 μg/mL Ap and incubated for approximately 24 h. A single colony was re-plated onto a fresh M9 minimal media plate containing 100 μg/mL and incubated for approximately 24 h. A single colony from this plate was used to inoculate the starter culture. Transformation was performed as outlined in section 2.2.2. The transformation mixture was resuspended in 500 μL of LB media and incubated at 37°C with shaking for 1 h. The cells were pelleted by centrifugation at maximum speed for 5 min and resuspended in cold sterile 0.7% NaCl. This was repeated and the resuspended pellets were used to inoculate the starter culture. The starter culture was incubated at 37°C with shaking for approximately 16 h and then used to inoculate 2× 950 mL ^{15}N-M9 media containing 100 μg/mL Ap. These 1 L cultures were incubated at 37°C with shaking until a cell density (A_{600}) of approximately 0.8 was reached

(3-6 h). Protein expression was induced by the addition of IPTG to a final concentration of 0.4 mM and the culture was incubated for a further 24 h. Cells were harvested by centrifugation at 4,000×*g* for 10 min at 4°C and stored at –20°C overnight if necessary.

Purification of ^{15}N-labelled proteins was performed in the same manner as for unlabelled proteins (section 2.7.2), with the exception of the size-exclusion chromatography step, where a pre-packed HiPrep 26/60 Sephacryl S-300 HR (GE Healthcare Bio-Sciences, Uppsala, Sweden) column was used for some purifications. Both chromatography steps were performed at either 4°C or room temperature. Purity and labelling efficiency was confirmed by mass spectrometry, as described in section 2.7.3.

2.11. Nuclear Magnetic Resonance Spectroscopy of Wildtype and Mutant Hsp25

^{15}N-labelled samples for nuclear magnetic resonance (NMR) studies were expressed and purified at the University of Wollongong. Freeze-dried ^{15}N-labelled samples were reconstituted in 600 μL of 10 mM phosphate, 10% D_2O buffer (pH 6.5 and 6.0 for wildtype and mutant Hsp25, respectively) containing 0.02% NaN_3, to in a final concentration of approximately 1 mM at the University of Adelaide, Australia. Acquisition of NMR spectra was performed at 25°C on a Varian Inova 600 NMR spectrometer (Varian Inc., Palo Alto,

California, USA) by Mr Phil Clements (University of Adelaide, Australia). Spectra were analysed at the University of Wollongong by the candidate.

2.11.1. ^{1}H-^{1}H Nuclear Magnetic Resonance Spectroscopy

Through-bond and through-space connectivities were determined from total correlation spectroscopy (TOCSY) [284] and nuclear Overhauser effect spectroscopy (NOESY) [285], respectively. Experiments were performed in the phase-sensitive mode using hypercomplex conjugation [286] with spin-lock periods of 30 ms and 100 ms for TOCSY and NOESY, respectively. Spectra were acquired with 256 t_1 increments over 2048 t_2 data points at a spectral width of 6000.2 Hz, with 32 and 64 scans for each t_1 increment for TOCSY and NOESY, respectively. ^{1}H-^{15}N couplings were removed by the application of globally-optimised alternating-phase rectangular pulse (GARP) decoupling [287] during acquisition. The solvent peak was suppressed using WET methods [288]. A line broadening of 3 Hz was applied prior to Fourier transformation of 1D spectra and 2D spectra were processed using a shifted Gaussian function in both directions. Chemical shifts were referenced to the residual water resonance at 4.81 ppm in each dimension.

2.11.2. ^{1}H-^{15}N Nuclear Magnetic Resonance Spectroscopy

^{1}H-^{15}N single-bond correlations were determined from heteonuclear single-quantum coherence (HSQC) spectroscopy [289]. Spectra were acquired with 16 scans for each of the 256 t_1 increments over 2048 t_2 data points at ^{1}H and

^{15}N spectral widths of 8000.0 and 2200.0 Hz, respectively. For all HSQC spectra, chemical shifts in the ^{1}H dimension were referenced to the residual water resonance at 4.81 ppm.

Longitudinal and transverse (T_1 and T_2, respectively) relaxation time constants were determined from series of HSQC spectra with delay durations of 0, 20, 70, 140, 240, 260, 520, 750 and 1140 ms for T_1 and 10, 30, 50, 70, 90, 110, 150 and 190 ms for T_2. Cross-relaxations between ^{1}H-^{15}N dipolar and ^{15}N chemical shift anisotropy (CSA) relaxations were eliminated by the application of ^{1}H 180° pulses during delay times [290,291].

The volume (integral) of each resonance was obtained using VNMR interactive peak picking functions and plotted as a function of delay time. The data were fitted to a two-parameter exponential decay function using SigmaPlot software and the relaxation time constant calculated from the equation in Figure 2.5 [292]. Errors were presented as the standard error of the time constant as given by SigmaPlot regression statistics for T_1 and T_2 values and the calculated standard error of a ratio (Figure 2.6) for T_1/T_2 and τ_m values.

2.12. Interactions between Hsp25 and αB-crystallin

Functional studies on mixtures of Hsp25 and αB-crystallin were undertaken as above except that reduction stress assays were performed on a SpectraMax 250 platereader (Molecular Devices, Sunnyvale, California, USA). For the chaperone

assays, a chaperone:target protein ratio resulting in comparable levels of precipitation for each of the sHsps was used.

Please see print copy for figure

Figure 2.5: Equation for calculating longitudinal (T_1) and transverse (T_2) ^{15}N relaxation constants from plots of peak integral versus delay time obtained through interactive peak picking of HSQC spectra where I(t) is the intensity after a delay of time t and I_0 is the intensity at t=0 [292].

$$s_{x/y} = \frac{x}{y}\sqrt{\left(\frac{s_x}{x}\right)^2 + \left(\frac{s_y}{y}\right)^2}$$

Figure 2.6: Equation for calculating the standard error of a ratio where x is the numerator, y is the denominator and s_x and s_y are the standard errors of x and y, respectively.

Chapter 3

Site-Directed Mutagenesis of Hsp25

3.1. Sequence Analysis of the C-Terminal Extension of sHsps

Flexibility and lack of structure in the C-terminal extension are important features in the proper functioning of sHsp oligomers. Since all structural information is contained within the amino acid sequence of a protein, valuable information can be obtained from identifying the determinants of the flexible nature of the C-terminal extension of sHsps. Because of the variability of the sequence of the C-terminal extension throughout the sHsp family, the conserved lack of structure in this region cannot be attributed to any specific feature/s in the primary structure.

A vast number of proteins have been shown to have intrinsically disordered regions that are necessary for their function [293-295]. Particular amino acid residues have been found to have a significantly increased abundance in such regions [296,297]. By analysing the sequence of the disordered C-terminal domain of linker histones, Lu and Hansen (2004) [298] determined that the amino acid composition of these regions is similar despite a lack of sequence conservation. Similar studies on the C-terminal extension of sHsps may help to highlight residues important for the flexibility and unstructured nature of this region.

The relative abundance of order- and disorder-promoting residues in the C-terminal extensions of the human sHsps and representative sHsps from

various organisms was investigated in a similar manner to studies performed by Lu and Hansen (2004) [298]. The C-terminal extensions were aligned at their IXI motifs (Figure 3.1) and residues aligning with the known flexible regions of αA- and αB-crystallin [299] were tallied (Table 3.1).

Eight of the 20 amino acids found in proteins tend to be present in greater proportions in regions of intrinsic disorder in proteins and have accordingly been termed disorder-promoting residues [300]. Approximately 70% of the residues in the flexible region of the C-terminal extension of sHsps are those that promote disorder and the five most abundant residues comprise a significant 58% of the total residues in the flexible regions of the extensions of sHsps from various organisms. The residue composition of these regions of mammals and other organisms is compared in Table 3.2. The high abundance of proline is not surprising as this residue is particularly associated with highly flexible regions of proteins [301]. Thus, whilst there is no sequence similarity amongst the flexible regions of the C-terminal extensions of sHsps, assessment of the amino acids of these regions demonstrate a conserved composition of residues that promote disorder.

human αA-crystallin	IPVSR**EEKPTSAPSS**
human αB-crystallin	IPITR**EEKPAVTAAPKK**
human MKBP	VYISLLPAPPDPEEEEEAAIVEP
human HspB3	–
human Hsp20	APASAQAPPPAAAK
human HspB7	IKI
human Hsp22	LPQDSQEVTCT
human HspB9	GSKASNLTR
human ODFP	CNPCSPYDPCNPCYPCGSRFSCRKMIL
human Hsp27	IPVTFESRAQLGGPEAAKSDETAAK
mouse Hsp25	IPVTFEARAQIGGPEAGKSEQSGAK
mouse αA-crystallin	IPVSREEKPSSAPSS
mouse αB-crystallin	IPITREEKPAVAAAPKK
bovine αA-crystallin	IPVSREEKPSSAPSS
bovine αB-crystallin	IPITREEKPAVTAAPKK
frog Hsp30C	IPISMDTAPRDAQELPPDAQTSNAEGDQKVD
Caenorhabditis Hsp16-2	IPIQQAIVEEKSAE
Drosophila Hsp26	IQIQQVGPAHLNVKANESEVKGKENGAPNGKDK
Drosophila Hsp27	VQIQQTGPAHLSVKAPAPEAGDGKAENGSGEKMETSK
soybean Hsp14	IEISG
wheat Hsp16.9	IEISG
pea Hsp18.1	IEISG
soybean Hsp21	IQVKVA
tomato Hsp21	ISIPKTEVEKKVIDVQIN
maize hsp22	IEVKVA
maize hsp23	IEIKVA
yeast Hsp26	IEVSSQESWGN
yeast Hsp42	IAIEEIPDEELEFEENPNPTVEN
Neurospora Hsp30	IAIN
Methanococcus Hsp16.5	INIE
Bradyrhizobium HspA	IPIDNLAASDVQQIEREAA
Bradyrhizobium HspB	ISISGSSASNVRQIDGKAA
Escherichia IbpA	IEIN
Escherichia IbpB	IAISERPALNS
Mycobacterium Hsp14	IQIRSTN
Mycobacterium Hsp18	ISVDRGNNGHQTINKTAHEIIDA

Figure 3.1: C-terminal extension sequences of sHsps from various organisms aligned at their IXI motif (shown in blue). Residues aligned to the flexible region of αA- and αB-crystallin are underlined. Sequences are from the ten human sHsps, *Mus musculus* Hsp25, *M. musculus* αA-crystallin, *M. musculus* αB-crystallin, *Bos taurus* αA-crystallin, *B. taurus* αB-crystallin, *Xenopus laevis* Hsp30C, *Caenorhabditis elegans* Hsp16-2, *Drosophila melanogaster* Hsp26, *D. melanogaster* Hsp27, *Glycine max* Hsp14, *Tritium aestivum* Hsp16.9, *Pisum sativum* Hsp18.1, *G. max* Hsp21, *Lycoperscon esculentum* Hsp21, *Zea mays* Hsp22, *Z. mays* Hsp23, *Saccharomyces cerevisae* Hsp26, *S. cerevisae* Hsp42, *Neurospora crassa* Hsp30, *Methanococcus jannaschii* Hsp16.5, *Bradyrhizobium japonicum* HspA, *B. japonicum* HspB, *Escherichia coli* IbpA, *E. coli* IbpB, *Mycobacterium tuberculosis* Hsp14 and *Mycobacterium leprae* Hsp18. Accession numbers are given in Appendix A.

Table 3.1: Frequency of residues in the flexible region of the C-terminal extension of sHsps from various organisms. sHsps lacking a flexible region are not shown. Residues that promote disorder are shaded in blue and those that promote order are shown in brown [300]. Superscript text indicates the organism from which the sHsps were derived: [B] bovine; [D] *Drosophila*; [H] human; [M] mouse; [S] soybean; [T] tomato; [Y] yeast.

	A	E	P	K	S	G	N	V	T	D	Q	I	L	R	C	H	M	F	Y	W
αA-crys[H]	1	2	2	1	3				1											
αB-crys[H]	3	2	2	3				1	1											
HspB2[H]	3	6	5	0				1		1		1	1							
Hsp20[H]	4		3	1							1									
Hsp22[H]		1						1	2		1				1					
HspB9[H]							1		1				1	1						
ODFP[H]			4	1	2	1	1			1		1	1	2	4		1	1	2	
Hsp27[H]	5	3	1	2	2	2			1	1	1		1	1						
Hsp25[M]	4	3	1	2	2	2					2	1		1						
αA-crys[M]	1	2	2	1	4															
αB-crys[M]	4	2	2	3				1												
αA-crys[B]	1	2	2	1	4															
αB-crys[B]	3	2	2	3				1	1											
Hsp30C	4	2	3	1	1	1	1	1	2	5	3		1	1						
Hsp16-2	4	3		1	1			1				1								
Hsp26[D]	3	3	2	5	1	4	4	3		1			1			1				
Hsp27[D]	4	4	2	4	3	5	1	1	2	1			1			1	1			
Hsp21[S]	1																			
Hsp21[T]		2		2			1	3	1	1	1	2								
Hsp22	1																			
Hsp23	1																			
Hsp26[Y]		1			1	1	1				1									
Hsp42		6	3				3	1	1	1		1	1					1		
HspA	4	2			1			1		1	2	1	1	1						
HspB	3			1	3	1	1	1		1	1	1		1						
IbpB	1		1		1		1						1	1						
Hsp14							1		1											
Hsp18	2	1		1		2	3		2	1	1	3				2				
Total	*57*	*49*	*37*	*33*	*29*	*19*	*19*	*17*	*16*	*15*	*14*	*12*	*10*	*9*	*5*	*4*	*2*	*2*	*2*	*1*

For comparison, the residue composition of representative intrinsically-disordered and globular proteins was also determined (Table 3.3). Surprisingly, there is little difference in the abundance of disorder-promoting residues between these two groups. However, an intrinsically-disordered protein is defined as a protein that contains a stretch of disorder within its sequence [302,303] and is not necessarily completely devoid of order. In contrast, the abundance of order-promoting residues is significantly lower in intrinsically-disordered proteins compared with globular proteins. The flexible region of the C-terminal extension of sHsps have a higher abundance of disorder-promoting and lower abundance of order-promoting residues compared with full-length intrinsically-disordered proteins.

In addition to being an important contributing factor to regions of protein structure, such as flexibility, the types of constituent amino acids can also influence functional aspects of a protein. The thermostability of a protein is related to the presence of charged groups, enabling electrostatic interactions, as well as hydrophobic and packing effects [304,305]. Proteins from thermophilic organisms have a higher proportion of polar and charged residues than their mesophilic counterparts and thus contain more stabilising ion pairs [306-308]. Lysine and glutamic acid residues are particularly increased at the expense of polar, uncharged residues in proteins from thermophilic organisms [306].

Table 3.2: Summary of the amino acid composition of the flexible regions of the C-terminal extension of sHsps from mammals and other organisms.

	Mammalian	Other
Disorder-promoting	80%	62%
Charged	31%	31%
Polar	22%	25%
Glutamic acid + lysine	26%	21%
Non-polar	47%	44%
Order-promoting	13%	24%

Table 3.3: Summary of the amino acid composition of representative globular and intrinsically-disordered proteins. Residue tallies are given in Appendix A.

	Globular	Disordered
Disorder-promoting	51%	57%
Charged	20%	27%
Polar	19%	28%
Glutamic acid + lysine	10%	14%
Non-polar	61%	45%
Order-promoting	37%	24%

These characteristics of thermostable proteins are reflected in the amino acid composition of the flexible regions of the C-terminal extensions of sHsps. Charged and polar residues comprise over half of the total residues in these regions (53% and 56% for mammals and other organisms, respectively), with a third of these residues being either glutamic or lysine residues (33% for both mammals and other organisms). These flexible regions therefore have the potential to form stabilising ion pairs with other regions of the sHsp and the solvent, contributing to the stability at super-physiological temperatures observed for αA-crystallin [220], as well as αB-crystallin up to ~63°C [309].

Design of Hsp25 Mutants

The importance of the C-terminal extension, and in particular its polarity, has been discussed previously (section 1.6). Mutants were designed to either remove the C-terminal extension of Hsp25 or reduce its polarity (Table 3.4). This study focussed on single residue substitution mutants and a truncation mutant, although multiple substitutions could also be considered in future studies.

A truncation mutant of Hsp25 was prepared in order to investigate the importance of an intact C-terminal extension. This was achieved through introduction of a stop codon. Of the eight mammalian sHsps with a C-terminal extension long enough to contain a flexible region, six contain a charged or polar residue at the C-terminus. This is also the case for a vast number of sHsps from various organisms (for example, see sequence alignment in [109]),

suggesting that the polarity of this residue is of particular importance. Additionally, three of the eight mammalian sHsps with flexible regions have lysine as the C-terminal residue. The importance of a lysine residue at the C-terminus of these sHsps is worthy of investigation given the abundance of lysine residues in proteins from thermophilic organisms, as discussed above. Due to the putative function of this residue in directly interacting with target proteins, the C-terminal lysine residue of Hsp25 was substituted with a non-polar leucine residue. This substitution resulted in a major alteration in the charge at the C-terminus whilst maintaining a similar side-chain structure of the C-terminal residue.

Glutamic acid is the second most abundant residue in the flexible region of the C-terminal extension of sHsps and a residue particularly implicated in the stability of proteins from thermophilic organisms. The flexible region of the C-terminal extension of Hsp25 contains three glutamic acid residues. In order to ascertain whether any of these residues are important for the chaperone activity of Hsp25, each of the glutamic acid residues in the C-terminal extension of Hsp25 were targeted for substitution.

Arginine and glutamine residues are polar, disorder-promoting residues that are do not have a conserved abundance throughout the sHsp family (Table 3.1) but are present in the flexible region of the C-terminal extension of Hsp25 and other sHsps. Regardless of residue composition, the overall polarity of the C-terminal extension of sHsps is also a conserved phenomenon. The arginine

and glutamine residues of the C-terminal extension of Hsp25 were targeted for substitution to investigate whether these less abundant residues in the C-terminal extensions of sHsps are important for Hsp25 as a molecular chaperone.

Table 3.4: Amino acid sequences of Hsp25 C-terminal extension mutants. The underlined region represents the C-terminal extension and residues in blue are mutated residues.

Mutation	Amino Acid Sequence
wildtype	-FEARAQIGGPEAGKSEQSGAK^{209}
E190stop	-F
E190A	-F**A**ARAQIGGPEAGKSEQSGAK
R192A	-FEA**A**AQIGGPEAGKSEQSGAK
Q194A	-FEARA**A**IGGPEAGKSEQSGAK
E199A	-FEARAQIGGP**A**AGKSEQSGAK
E204A	-FEARAAIGGPEAGKS**A**QSGAK
Q205A	-FEARAQIGGPAAGKSE**A**SGAK
K209L	-FEARAQIGGPEAGKSEQSGA**L**

3.2. Design of Mutagenic Primers

Mutagenic primers were designed according to each individual mutation. The codon containing the desired base changes was flanked by 15 bases of

unchanged sequence on either side. Two primers were required, one forward primer and one reverse compliment, to allow incorporation of the mutation into both strands of the gene. The forward and reverse mutagenic primers are shown in Table 3.5. Melting temperatures and GC contents of all primers fell within the recommended ranges 79-94°C and 51-70%, respectively.

3.3. Site-Directed Mutagenesis Reactions

Some mutagenic primers were susceptible to self-interaction and the formation of secondary structures, inhibiting binding to the template DNA strands. This was prevented by the addition of DMSO to reactions involving these primers. Control reactions were carried out alongside sample reactions to determine the efficiency of mutagenesis and transformation. The mutagenic efficiency was determined to be greater than 80% for each PCR performed.

3.4. Screening for Mutants

Transformation of the mutagenic PCR products into XL1-Blue supercompetent cells, re-plating of individual colonies and subsequent extraction of plasmid DNA allowed screening for plasmids containing the desired mutation. The double digestion of the extracted wildtype and mutant plasmids with restriction enzymes *Bam*H1 and *Nde*I produced an additional band of approximately 600 bp on the agarose gel, corresponding to the size of the Hsp25 gene (Figure 3.2).

Table 3.5: Sequences of oligonucleotide primers for site-directed mutagenesis of the C-terminal extension of Hsp25. The mutated codon is shown in blue and mutated residues in red. F and R indicate forward and reverse mutagenic primers, respectively.

Mutation	Primer
E190stop	5'-…TTC **GAG** GCC…-3'
F	5'-ATT CCG GTT ACT TTC **T**AG GCC CGC GCC CAA ATT-3'
R	5'-AAT TTG GGC GCG GGC CT**A** GAA AGT AAC CGG AAT-3'
E190A	5'-…TTC **GAG** GCC…-3'
F	5'-ATT CCG GTT ACT TTC G**C**G GCC CGC GCC CAA ATT-3'
R	5'-AAT TTG GGC GCG GGC C**G**C GAA AGT AAC CGG AAT-3'
R192A	5'-…GCC **CGC** GCC…-3'
F	5'-GTT ACT TTC GAG GCC **GC**C GCC CAA ATT GGG GGC-3'
R	5'-GCC CCC AAT TTG GGC G**GC** GGC CTC GAA AGT AAC-3'
Q194A	5'-…GCC **CAA** ATT…-3'
F	5'-TTC GAG GCC CGC GCC **GC**A ATT GGG GGC CCA GAA-3'
R	5'-TTC TGG GCC CCC AAT T**GC** GGC GCG GGC CTC GAA-3'
E199A	5'-…CCA **GAA** GCT…-3'
F	5'-CAA ATT GGG GGC CCA G**C**A GCT GGG AAG TCT GAA-3'
R	5'-TTC AGA CTT CCC AGC T**G**C TGG GCC CCC AAT TTG-3'
E204A	5'-…TCT **GAA** CAG…-3'
F	5'-GAA GCT GGG AAG TCT G**C**A CAG TCT GGA GCC AAG-3'
R	5'-CTT GGC TCC AGA CTG T**G**C AGA CTT CCC AGC TTC-3'
Q205A	5'-…GAA **CAG** TCT…-3'
F	5'-GCT GGG AAG TCT GCA **GC**G TCT GGA GCC AAG TAG-3'
R	5'-CTA CTT GGC TCC AGA C**GC** TTC AGA CTT CCC AGC-3'
K209L	5'-…GCC **AAG** TAG…-3'
F	5'-GAA CAG TCT GGA GCC **CT**G TAG AAG CCA TCA GCC-3'
R	5'-GGC TGA TGG CTT CTA C**AG** GGC TCC AGA CTG TTC-3'

Extracted plasmid DNA samples that released the Hsp25 gene insert after digestion were sequenced using the forward sequencing primer. The sequence of the reverse DNA strand of samples that contained the desired forward DNA sequence for the C-terminal extension was obtained using the reverse sequencing primer. Samples displaying the correct sequence in both strands were confirmed as mutants. The results of the DNA sequence analysis of Hsp25 are shown in Figure 3.3. The plasmid DNA of confirmed mutants was transformed into *E. coli* BL21(DE3) by electroporation and glycerol stocks were prepared.

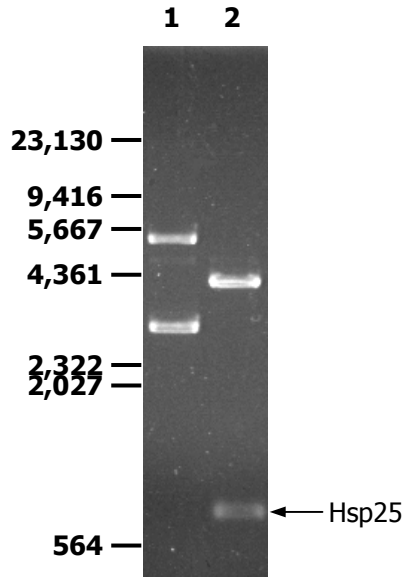

Figure 3.2: Agarose gel of restriction enzyme pAK3038-Hsp25 (lane 1) and pAK3038-Hsp25 digested with *Bam*H1and *Nde*I (lane 2). The band representing the Hsp25 gene insert is indicated. Marker sizes are given in base pairs.

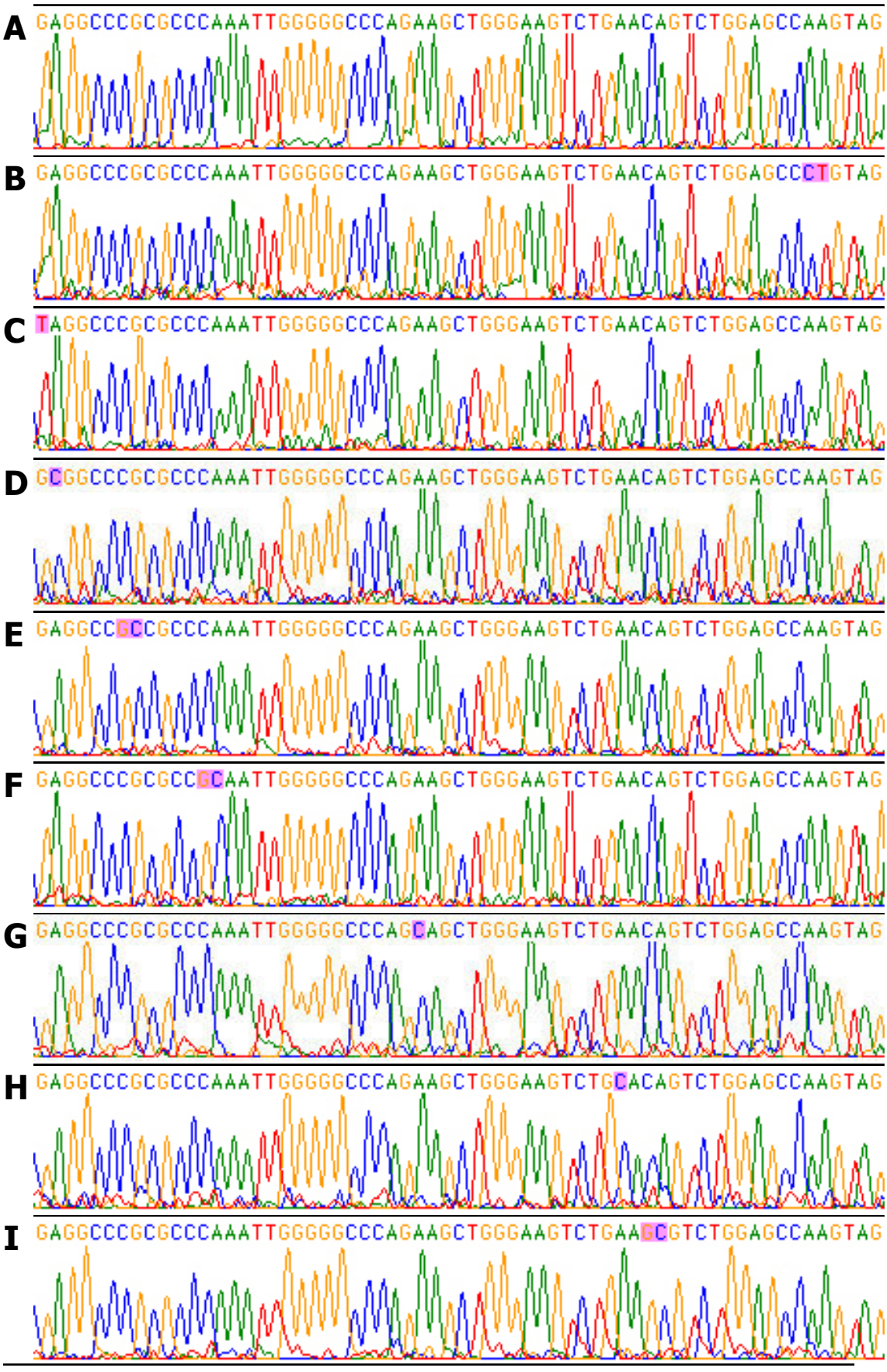

Figure 3.3: DNA sequence analysis of Hsp25 and mutants. Mutated bases are highlighted.

Chapter 4

Expression and Purification of Hsp25 and αB-Crystallin

4.1. Expression of Wildtype and Mutant Hsp25 and Wildtype αB-Crystallin

Overexpression of Hsp25 and αB-crystallin was induced by the addition of IPTG to a final concentration of 0.4 mM at the mid-log phase of *E. coli* BL21(DE3) growth. Whole cell lysate samples were taken at induction and 3 h after induction and analysed by SDS-PAGE.

The induced sample of *E. coli* BL21(DE3) (pAK3038-Hsp25) produced an intense band of 25 kDa which corresponds to Hsp25 (Figure 4.1A, lane 1). Overexpression of mutant Hsp25 proteins gave similar protein composition profiles with the exception of the truncation mutant (E186stop), which migrated further through the gel because of its smaller size (Figure 4.1A, lane 2). Overexpression of *E. coli* BL21(DE3) (pET24d(+)-αB-crystallin) produced a similar protein composition, with an intense band of 20 kDa corresponding to αB-crystallin (Figure 4.1B).

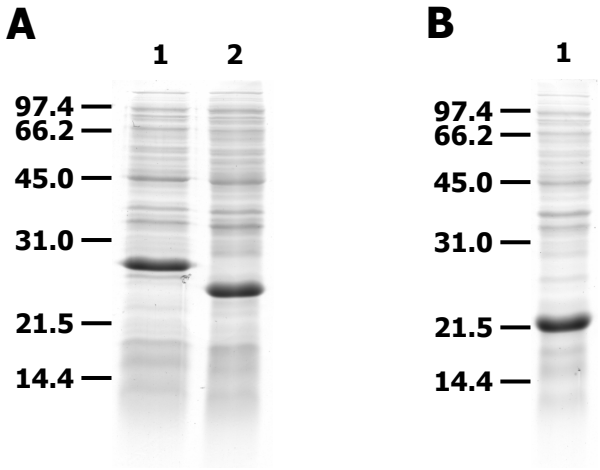

Figure 4.1: SDS-PAGE gel showing overexpression of *E. coli* BL21(DE3) (pAK3038-Hsp25) (A) and *E. coli* BL21(DE3) (pET24d(+)-αB-crystallin) (B). A: culture overexpressing wildtype Hsp25 3 h after induction (lane 1); culture overexpressing Hsp25-E190stop 3 h after induction (lane 2). B: culture overexpressing αB-crystallin 4 h after induction. Low range molecular weight standards are indicated, with masses given in kDa.

4.2. Purification of Wildtype and Mutant Hsp25 and Wildtype αB-Crystallin

Purification of wildtype and mutant Hsp25 and wildtype αB-crystallin was performed as per section 2.7.2. The Hsp25 truncation mutant (Hsp25-E190stop) precipitated out of solution during the preparation of the cell lysate for anion-exchange chromatography and could not be purified. This mutant protein was found to be in the insoluble fraction after centrifugation, as determined by SDS-PAGE. Attempts to purify this mutant by a method devised by Buchner *et al.* [272] were also unsuccessful. αA-Crystallin lacking the C-terminal extension has also been found to become insoluble during preparation of the cell extract for chromatography [218,221]. Treatment with

denaturant and subsequent dialysis to remove the denaturant enabled this mutant to remain soluble, although precipitate was formed during FPLC [218]. Precipitation of truncation mutants of Hsp25 and αA-crystallin during the purification process demonstrates that these sHsps lacking a C-terminal extension are inherently unstable, emphasising even at this early stage of the study the importance of the C-terminal extension as a solubilising feature of this protein. Further attempts at purifying the truncation mutant have not been made as yet.

With the exception of the K209L mutant, Hsp25 and mutants eluted from the DEAE-sephacel anion-exchange column at a sodium chloride concentration of 100 mM, as did αB-crystallin. Representative elution profiles are shown in Figure 4.2, and corresponding SDS-PAGE analysis of the fractions from the 100 mM peaks in Figure 4.5. The Hsp25-K209L mutant bound more strongly to the column than the wildtype and other mutants and required a salt concentration of 200 mM for elution, consistent with the substitution of the C-terminal lysine for leucine resulting in an overall increase in negative charge of the protein.

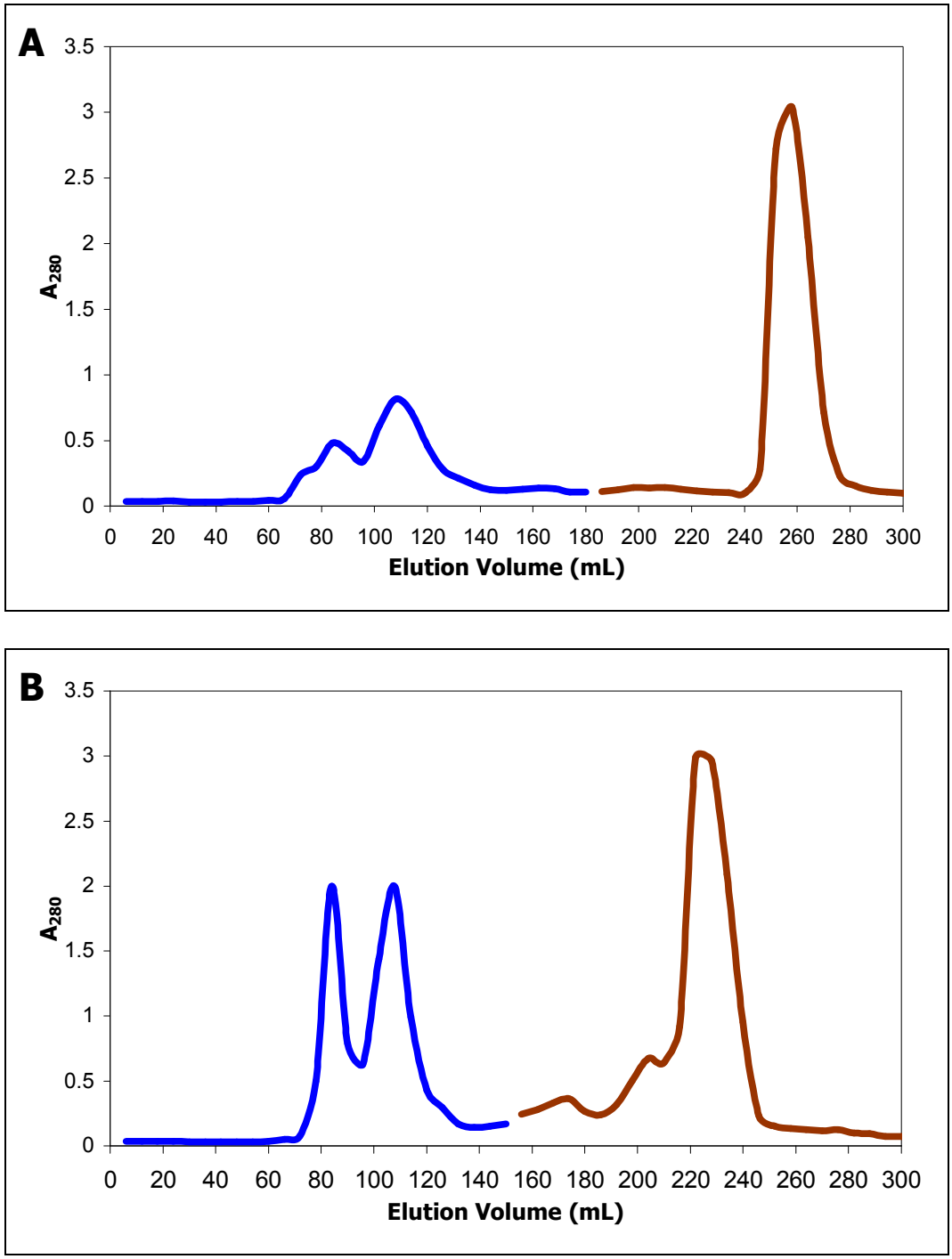

Figure 4.2: Elution profiles of anion-exchange chromatography of Hsp25 (A) and αB-crystallin (B). Protein was detected by measuring A_{280} of each fraction. Each sHsp eluted from the DEAE-sephacel column in both peaks at 100 mM NaCl in 20 mM Tris-HCl (pH 8.5) buffer containing 1 mM EDTA and 0.02% NaN_3 (blue trace). Contaminating protein was washed off the column with 1 M NaCl in the above buffer (brown trace).

Because they exist under native conditions as large oligomers, Hsp25 and αB-crystallin both eluted from the S-300 size-exclusion column in the first peak (Figure 4.3 and Figure 4.4). All Hsp25 mutants displayed a similar elution profile to that of wildtype Hsp25.

It should be noted that the BCA assay appeared to be less sensitive to the detection of Hsp25 compared with the contaminating *E. coli* proteins overall. The sample loaded onto the size-exclusion column contained primarily Hsp25, as shown by SDS-PAGE of anion-exchange chromatography elutions (Figure 4.5, lanes 3 and 4), and it would therefore be expected that the Hsp25-containing peak eluting from the size-exclusion chromatography (SEC) column would be significantly larger than the contaminating peak. The presence of proteins larger in mass than Hsp25 means that more peptide bonds are present in the contaminating proteins than in Hsp25 and therefore a greater reduction of copper occurs in the contaminating fractions. It is likely that these proteins also contain more reducing residues to contribute to this higher absorbance, but this cannot be confirmed without the amino acid sequence of the contaminating proteins. Indeed, members of other chaperone families (Hsp70 and Hsp60) have been shown to have a lower concentration of tryptophan and tryrosine residues compared with other globular proteins [310].

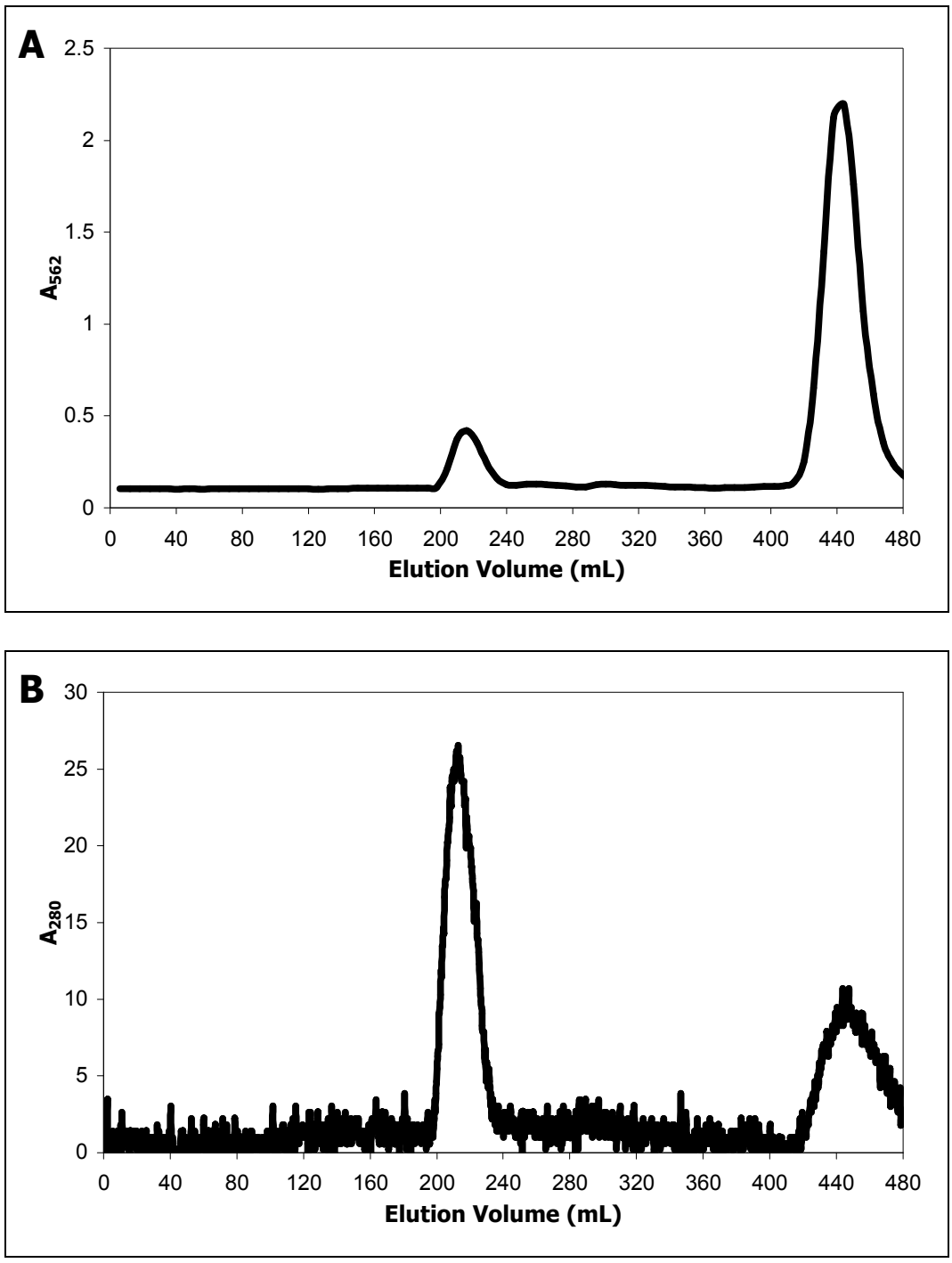

Figure 4.3: Elution profile of size-exclusion chromatography of Hsp25. Protein was detected by performing a BCA assay (A) or measuring A_{280} inline (B). Hsp25 eluted from the S-300 column in the first peak with 50 mM Tris-HCl (pH 8.0) buffer containing 1 mM EDTA and 0.02% NaN_3. Contaminating proteins eluted in the second peak.

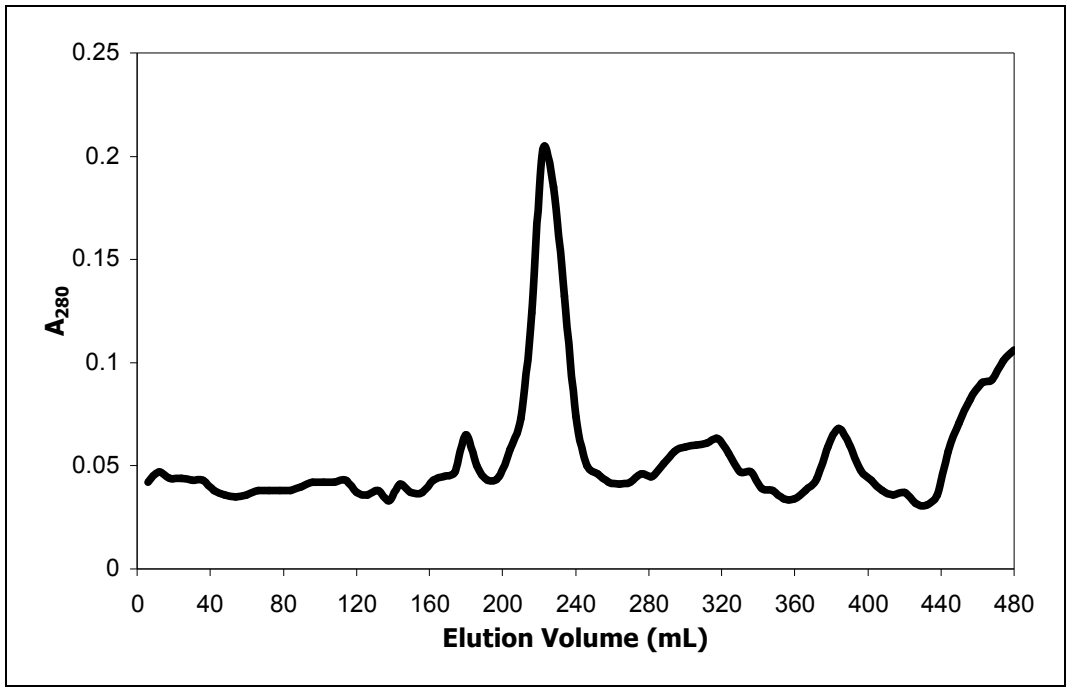

Figure 4.4: Elution profile of size-exclusion chromatography of αB-crystallin. Protein was detected by measuring A_{280} of each fraction. αB-Crystallin eluted from the S-300 column in the first significant peak with 50 mM Tris-HCl (pH 8.0) buffer containing 1 mM EDTA and 0.02% NaN_3. Contaminating proteins eluted in subsequent peaks.

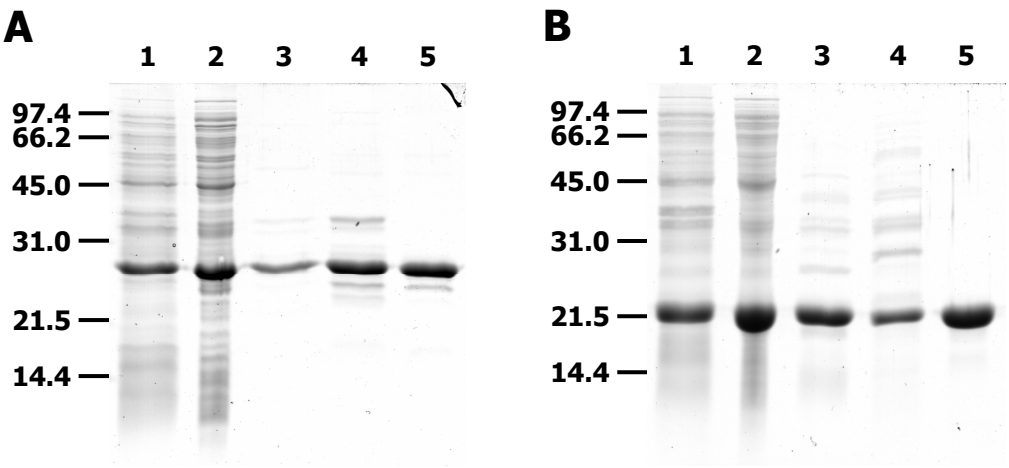

Figure 4.5: SDS-PAGE gel of the purification of Hsp25 (A) and αB-crystallin (B). Both gels show bacterial whole cell cultures containing the overexpressed protein (lane 1), lysate prior to chromatography (lane 2), 100 mM DEAE fractions containing the overexpressed protein (lanes 3 and 4), S-300 fraction containing the overexpressed protein (lane 5). Low range molecular weight standards are indicated, with masses given in kDa.

In order to ensure that the peak sizes were a result of the detection method rather than the loss of Hsp25 during SEC, a UV detector was used inline with the column. As can be seen in Figure 4.3B, the peak sizes are more representative of the relative concentrations of the proteins. Although there is a discrepancy between the BCA assay and the A_{280} values, use of the inline UV detector for every purification was not feasible. Whilst the BCA assay appears to underestimate the concentration of Hsp25, the chromatograms were used only qualitatively as an indicator of the presence of protein and not as a determination of concentration.

The composition of each of the peaks eluting from the anion-exchange and size-exclusion columns were analysed by SDS-PAGE (Figure 4.5). With the exception of the truncation mutant, as discussed previously, wildtype and all Hsp25 mutants and wildtype αB-crystallin were successfully purified, as indicated by the presence of only one band in the first size-exclusion peak.

4.2.1. Nanoscale Electrospray Ionisation Mass Spectrometry

Mass spectrometry was performed on the purified wildtype and mutant Hsp25 and wildtype αB-crystallin proteins to indicate the level of purity and give an accurate mass of each sample. The mass was also used to indicate that the correct amino acid substitution was made as a result of site-directed mutagenesis.

Representative mass spectra of wildtype Hsp25 and αB-crystallin are shown in Figure 4.6 and Figure 4.7, respectively. Full-length wildtype Hsp25 is shown by the predominant peak with mass of 23,014 Da in Figure 4.6A. The peak representing a smaller mass species (less 131 Da) was found to be Hsp25 with the N-terminal methionine residue cleaved. αB-crystallin was purified as a full-length protein (Figure 4.7). Masses of wildtype and mutant Hsp25 and wildtype αB-crystallin were within 1 kDa of expected values. Peaks arising from contaminating proteins were minor for both sHsps.

Removal of the N-terminal methionine is catalysed by the enzyme methionyl-aminopeptidase (MAP). The specificity of this enzyme is correlated to the length of the side chain of the second residue – shorter side chains result in a higher specificity for MAP and therefore a greater proportion of cleaved products [311,312]. Hsp25 was purified predominantly in the N-terminally excised form, a result of the high efficiency of removal of the N-terminal methionine when followed by a threonine residue [311]. The rules and mechanisms by which N-terminal methioinine excision occurs is thought to be convserved throughout all organisms [313,314]. It is therefore more than likely that Hsp25 expressed in mammalian cells is also processed to remove the N-terminal methioinine residue. MAP has a low efficiency when the N-terminal methionine is followed by an asparagine residue, as is the case for αA- and αB-crystallin, and N-terminal methionine excision of α-crystallin proteins is not reported.

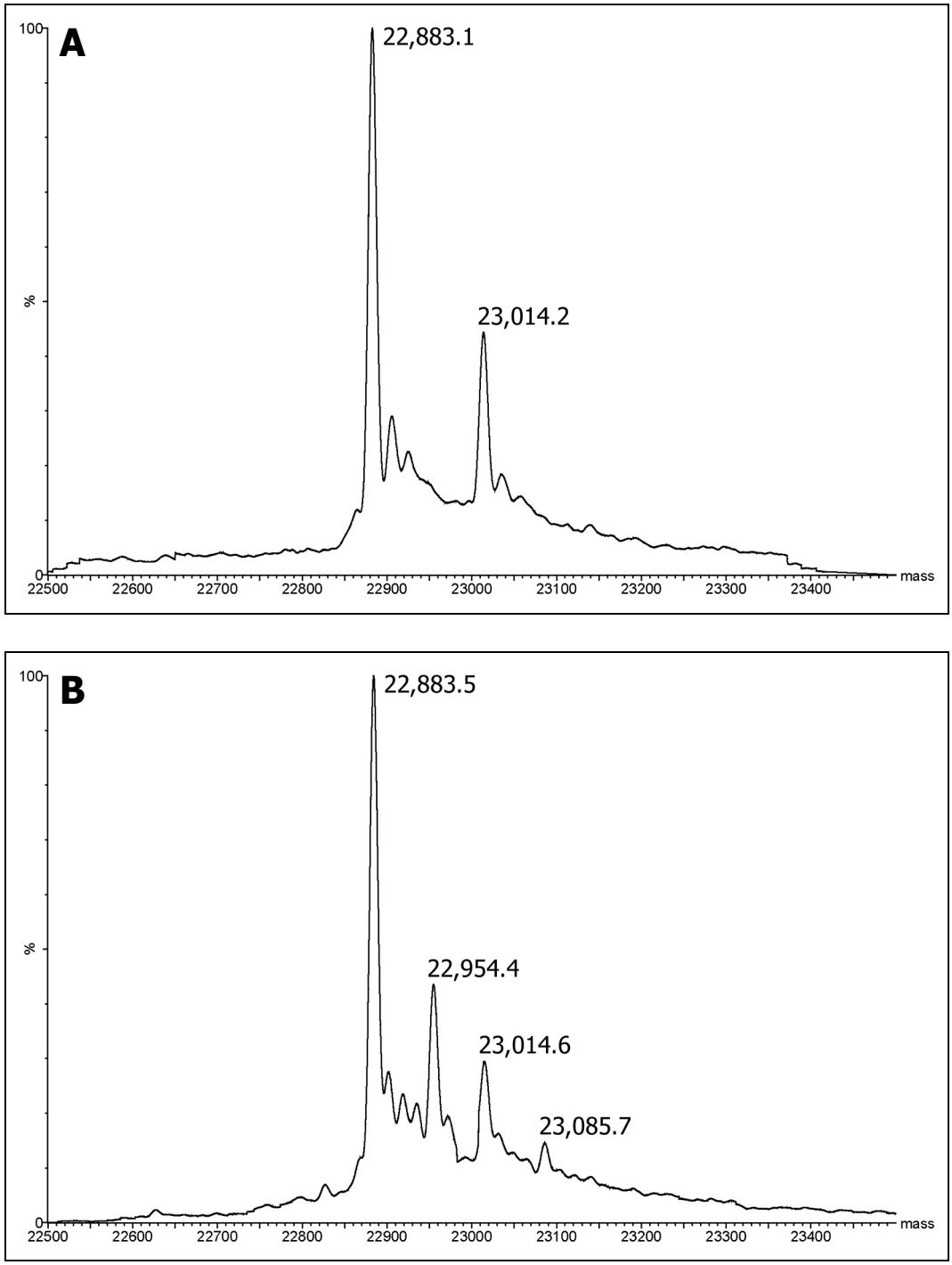

Figure 4.6: Mass spectra of purified wildtype Hsp25 (A) and wildtype Hsp25 with a modification attached to the cysteine residue (B) obtained by nanoscale electrospray ionisation mass spectrometry.

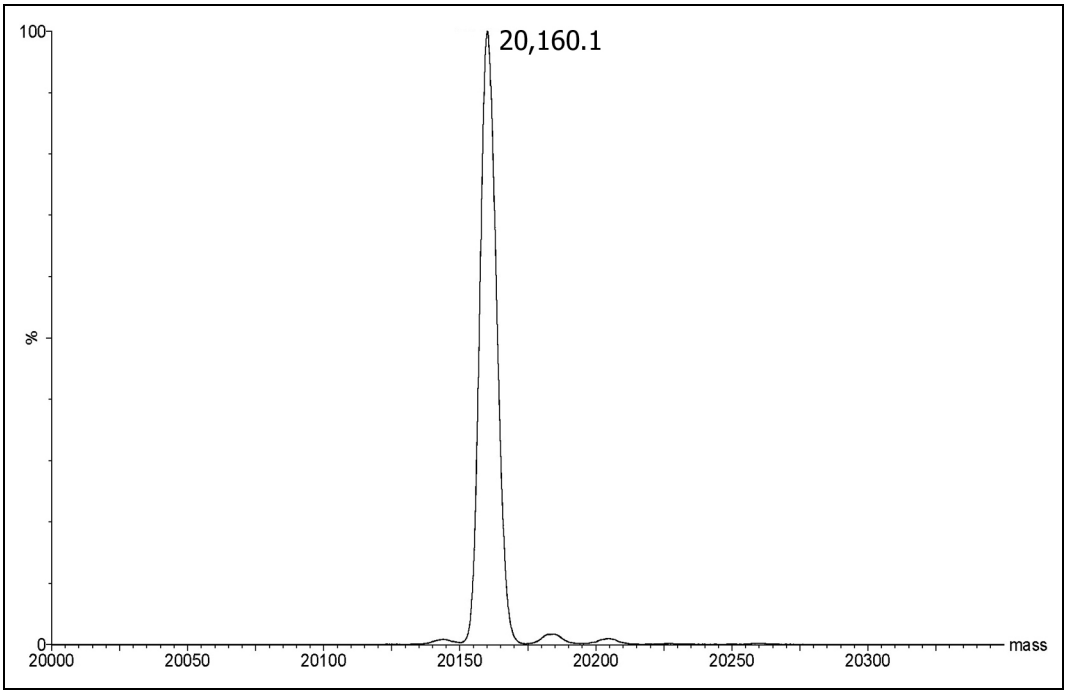

Figure 4.7: Mass spectrum of purified wildtype αB-crystallin obtained by nanoscale electrospray ionisation mass spectrometry.

Since the N-terminal domain of sHsps is variable in length and sequence, the removal of a single residue at the N-terminus is unlikely to affect the structure or function sHsps. Indeed, the addition of four residues to the N-terminus of αB-crystallin has no effect on the structure or chaperone ability of this sHsp and a fusion protein of αB-crystallin with a large protein (~43 kDa) attached to its N-terminus exhibites chaperone activity [315]. Further, no functional impact is observed when 33 residues are removed from the N-terminus of Hsp25 or an N-terminal 6-His tag is attached to Hsp25 [316].

Since the ratio of truncated to full-length Hsp25 is consistent for all Hsp25 purification batches, the molecular mass for Hsp25 used henceforth will be that of the full-length protein. Further, molecular mass is not a factor when

calculating concentrations from absorbance values as a molar extinction co-efficient is used.

As discussed above, purification of Hsp25 resulted in full-length protein and Hsp25 lacking the N-terminal methionine. In some purification batches, two additional peaks, with masses of 22,954.4 and 23,085.7 Da, were observed, corresponding to the expected two peaks with a mass addition of 71 Da (Figure 4.6B). This also occurred for mutant Hsp25 proteins. The relative abundance of +71 Da peaks varied between individual purification batches and the presence of these peaks was unable to be correlated with the order of purification of the various batches, the time taken for specific stages to be processed or the use of stored versus fresh reagents. The bacterial storage stock was also not a factor, as the same stock produced purified protein both with and without the additional peaks.

Tryptic digestion and subsequent mass spectrometry of a modified Hsp25 sample yielded the peptide CFTR[44], which was present in its expected mass and also with an additional 71 Da. Tandem mass spectrometry of the peptide containing the modification yielded peaks that were identified as a, b and y fragmentation ions. Both the a1 and b1 ions of the peptide contained the additional mass, demonstrating that the modification was attached to the cysteine residue at position 41.

No peak corresponding to 71 Da was observed in the tandem mass spectrum, indicating that the modification was uncharged and therefore excluding the

possibility of an additional alanine residue being incorporated into the protein. Modifications of 71 Da include an acetamidomethyl group, a DEAE group and acrylamide. The expression and purification of Hsp25 does not involve any reagents with an acetamidomethyl structure, ruling this possibility out. The DEAE group and acrylamide are components of the anion-exchange and size-exclusion resins, respectively. Modification by either of these possibilities would indicate degradation of the column resin, which would seem unlikely as these structures are very stable. Furthermore, if degradation was occurring, it would be expected that the extent of modification would increase with time. This was not observed and unmodified protein was able to be obtained subsequent to a highly modified batch.

Whilst modification of the cysteine residue with a DEAE or acrylamide group is a possibility, the identity of the modification was unable to be ascertained. Given the source of the modification was undeterminable, it was impractical to attempt to obtain a complete set of unmodified Hsp25 mutants. The effect of the modification of the cysteine residue is discussed in Chapter 5.

Chapter 5

Characterisation of Wildtype and Mutant Hsp25

5.1. Comparison of Unmodified and Modified Hsp25

Although wildtype and mutant Hsp25 proteins were purified successfully, modification of the cysteine residue of Hsp25 was unable to be controlled, as discussed previously. It was therefore necessary to ensure that the structural and functional properties of Hsp25 proteins investigated in this study were not influenced by the presence of the modification.

Hsp25 and Hsp27 each contain a single cysteine residue, through which an intersubunit disulphide bond can be formed. The function of these sHsps is not affected by the presence of covalently-linked dimeric forms [274,317]. Labelling with fluorescent probes attached to a cysteine residue does not produce a significant change in the conformation of Hsp27 [167] or αA-crystallin [159,318]. It is therefore unlikely that the modification of the cysteine residue of Hsp25 will result in any significant structural or functional changes. In order to confirm this, a preliminary study was performed in which an unmodified sample of Hsp25 was compared to a modified sample for each biophysical technique employed for the characterisation of mutant Hsp25 proteins.

Far-UV CD spectra of unmodified and modified wildtype Hsp25 are shown in Figure 5.1. Studies on αA-crystallin have concluded that the 210-220 nm region is susceptible to variation of up to 10% [159]. Thus, the minor differences observed in the shape of the spectra were deemed to be insignificant. Estimation of secondary structure using the CDSSTR

deconvolution program indicated maximum differences of 1% for all secondary structure types between the samples (Table 5.1). These spectra were similar to previously published far-UV CD spectra of Hsp25 [130,145,146], i.e. both unmodified and modified Hsp25 proteins were folded correctly after purification. No significant difference was thus observed between the structure of unmodified and modified Hsp25, as determined by far-UV CD.

Tryptophan fluorescence and ANS binding fluorescence spectra (Figure 5.2 and Figure 5.3) were virtually identical for unmodified and modified Hsp25. Modification of the cysteine residue therefore did not affect the overall environment of the tryptophan residues or ANS binding properties of Hsp25.

Chromatograms for the elution of unmodified and modified wildtype Hsp25 from the size-exclusion chromatography fast protein liquid chromatography (SEC FPLC) column are shown in Figure 5.4. The elution volume was the same for both unmodified and modified wildtype proteins, indicating that the oligomers have the same molecular weight and that the modification of the cysteine residue did not affect the quaternary structure of Hsp25.

The thermostability profiles of unmodified and modified wildtype Hsp25 are shown in Figure 5.5. Whilst the traces are not identical, there is a difference of less than 0.15 absorbance units between the two profiles. No precipitate was observed and, given this scale, it was concluded that the thermostability of Hsp25 was unaffected by modification of the cysteine residue.

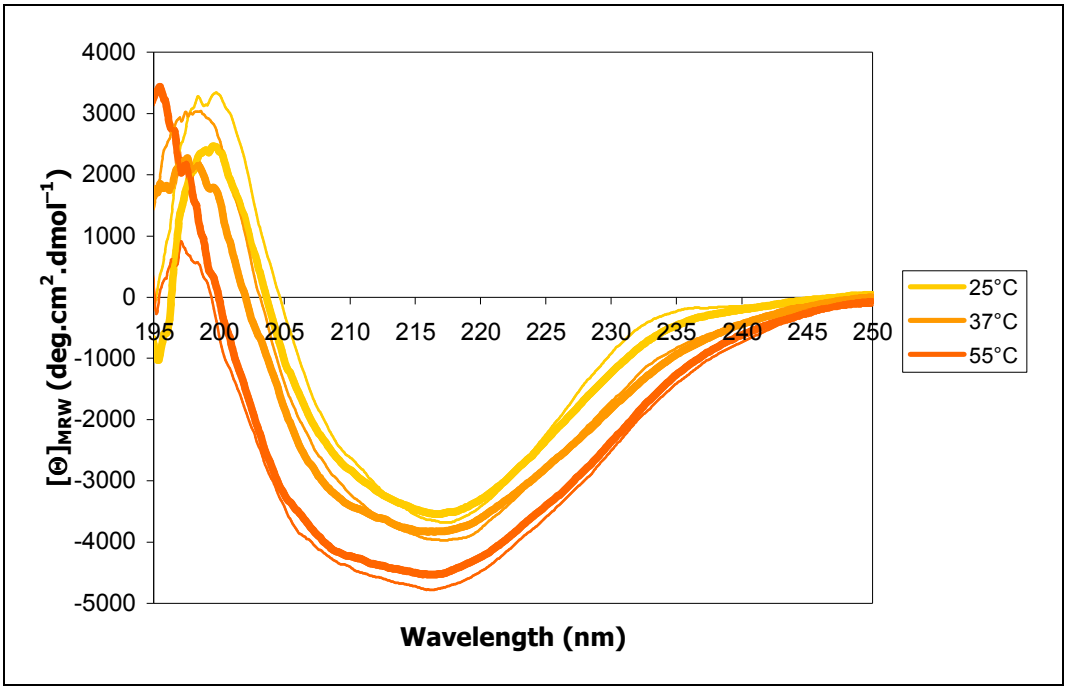

Figure 5.1: Circular dichroism spectra of unmodified (thick lines) and modified (thin lines) wildtype Hsp25 at 25°C, 37°C and 55°C. Samples were prepared in 10 mM sodium phosphate (pH 7.5). A pathlength of 1 cm was used and spectra presented are accumulations of six scans.

Table 5.1: Secondary structure comparison of unmodified and modified wildtype Hsp25 as estimated by the deconvolution program CDSSTR using data measured to 190 nm.

Hsp25	Temp. (°C)	α-helix	β-sheet	β-turn	Random coil
unmodified	25°C	5%	40%	23%	31%
	37°C	8%	38%	23%	30%
	55°C	9%	36%	23%	32%
modified	25°C	4%	41%	22%	32%
	37°C	7%	39%	22%	32%
	55°C	9%	36%	23%	31%

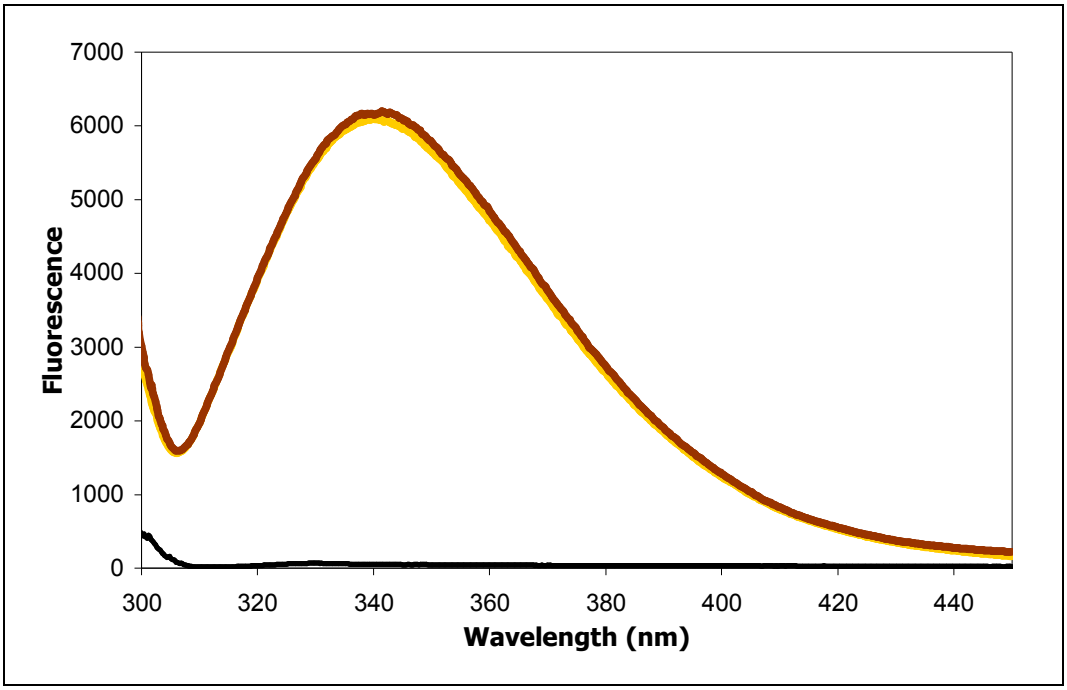

Figure 5.2: Tryptophan fluorescence spectra of unmodified (gold) and modified (brown) wildtype Hsp25, with buffer shown in black. Samples were prepared in 50 mM sodium phosphate buffer (pH 7.3) containing 0.02% NaN_3 to a final protein concentration of 5 μM. Excitation wavelength was 295 nm.

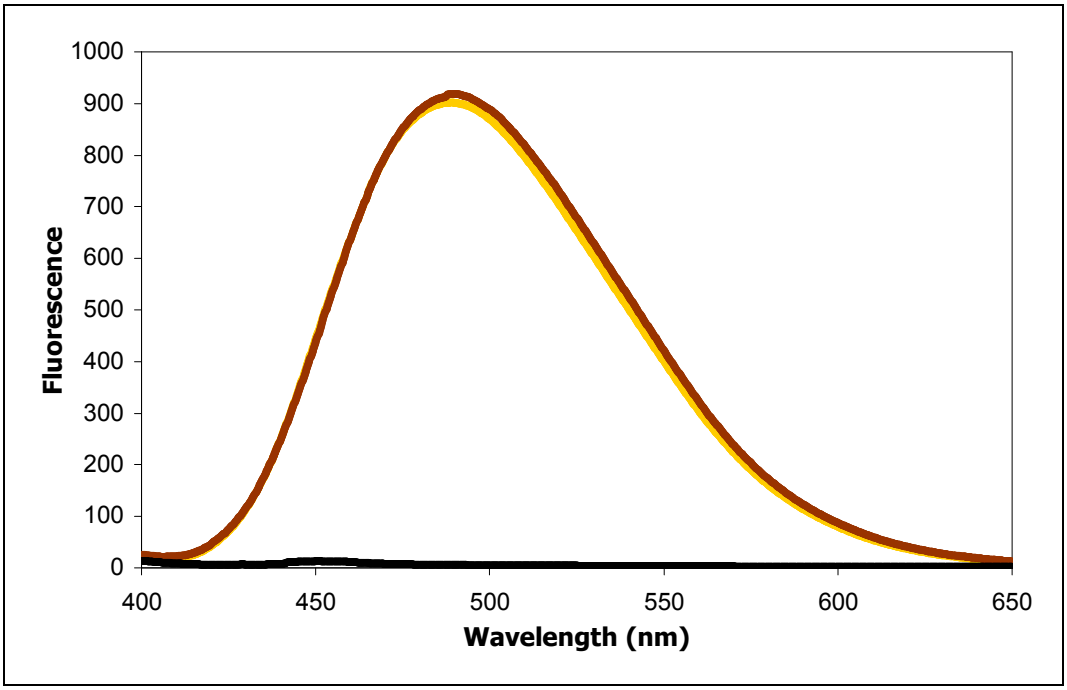

Figure 5.3: Emission spectra of ANS binding fluorescence of unmodified (gold) and modified (brown) wildtype Hsp25 at 60 μM ANS. Samples were prepared in 50 mM sodium phosphate buffer (pH 7.3) containing 0.02% NaN_3 to a final protein concentration of 5 μM. Excitation wavelength was 387 nm.

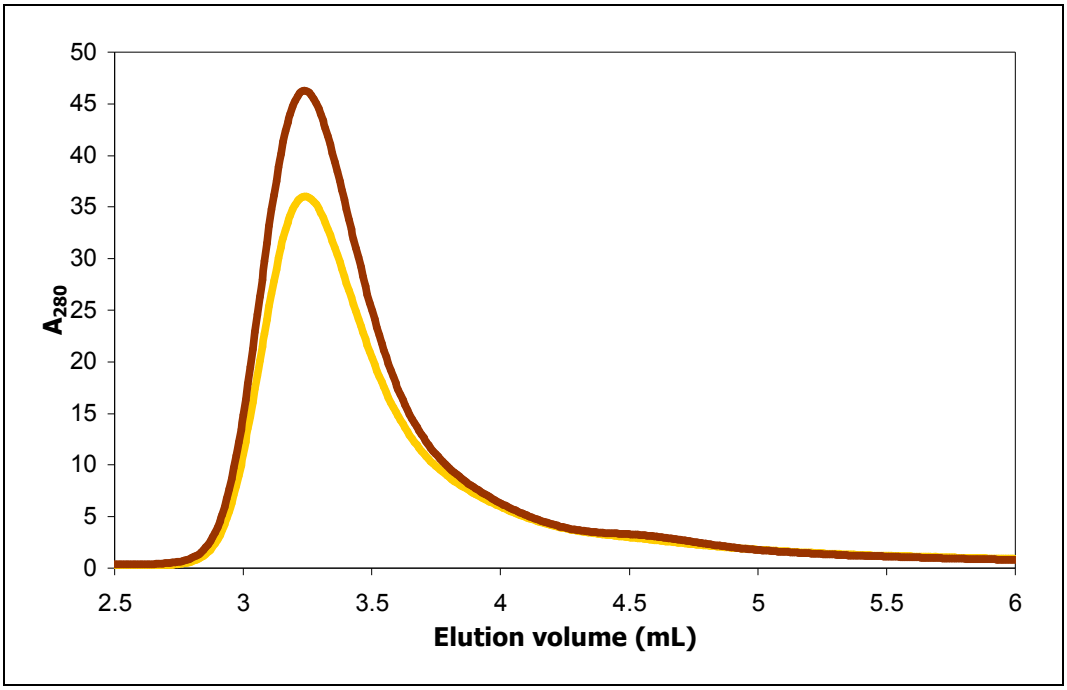

Figure 5.4: SEC FPLC chromatograms of unmodified (gold) and modified (brown) wildtype Hsp25. Samples were prepared in 50 mM sodium phosphate buffer (pH 7.3) containing 0.02% NaN_3 to a final protein concentration of 30 μM.

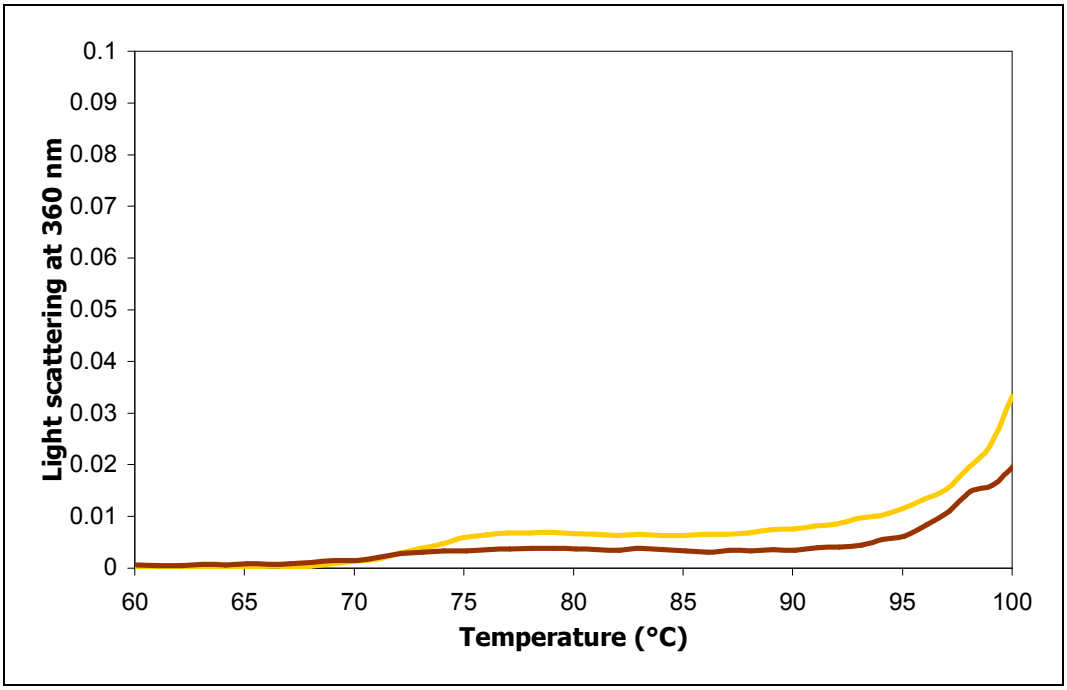

Figure 5.5: Thermostability profiles of unmodified (gold) and modified (brown) wildtype Hsp25. Samples were prepared in 50 mM sodium phosphate buffer (pH 7.3) containing 0.02% NaN_3 to a final protein concentration of 0.2 mg/mL. Temperature was increased at a rate of 1°C/min.

The precipitation of insulin under reduction stress and of ADH under thermal stress was comparable for unmodified and modified Hsp25 at each ratio (Figure 5.6 and Figure 5.7). Under these conditions, therefore, the modification of the cysteine residue did not significantly affect the chaperone activity of Hsp25.

The above results demonstrate that each property of Hsp25 assessed was highly comparable for both unmodified and modified Hsp25 samples. It was therefore concluded that the structure and function of Hsp25, at least as determined by these techniques, are not affected by the modification of the cysteine residue. Thus, it is appropriate to use either unmodified or modified samples of each Hsp25 protein for the characterisation of the structure and function of Hsp25 mutants.

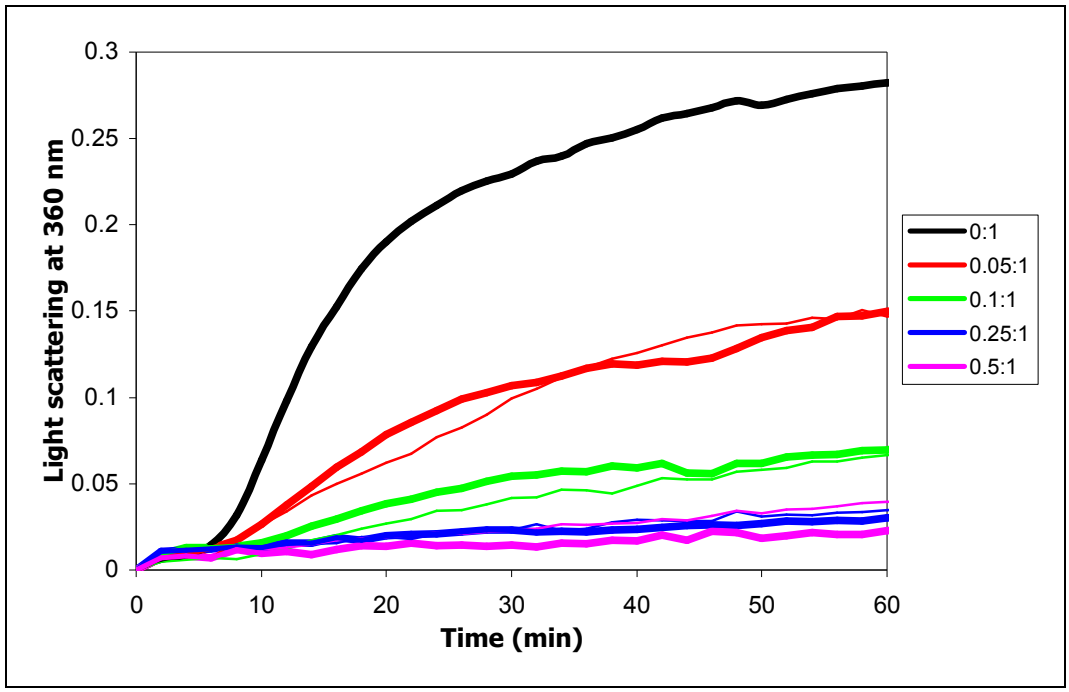

Figure 5.6: Chaperone activity of unmodified (thick lines) and modified (thin lines) wildtype Hsp25 as measured by the suppression of aggregation of insulin under reduction stress. Assays were performed at 37°C in 50 mM sodium phosphate buffer (pH 7.3) containing 0.02% NaN_3. The reduction of insulin was initiated by the addition of DTT to a final concentration of 20 mM. Ratios represent the molar concentration of Hsp25 monomers to insulin molecules. Traces are the average of triplicates.

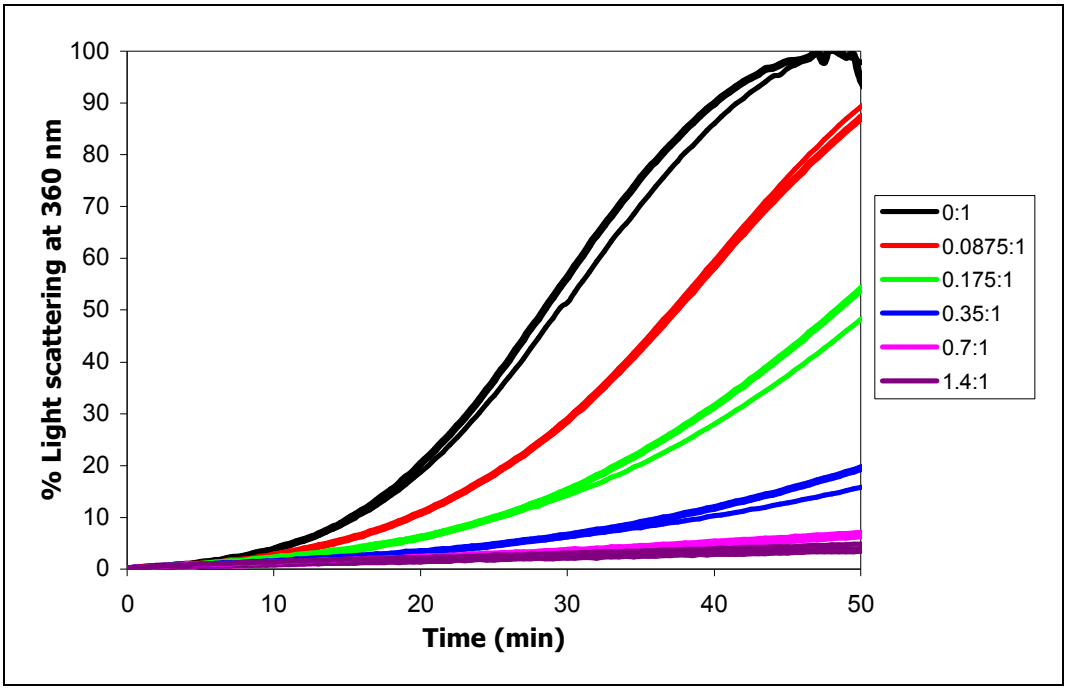

Figure 5.7: Chaperone activity of unmodified (thick lines) and modified (thin lines) wildtype Hsp25 as measured by the suppression of aggregation of ADH under thermal stress. Assays were performed at 55°C in 50 mM sodium phosphate buffer (pH 7.3) containing 0.02% NaN_3. Ratios represent the molar concentration of Hsp25 monomers to ADH subunits. Traces are the average of duplicates.

5.2. Far-UV Circular Dichroism Spectroscopy with Temperature Studies

Far-UV CD spectroscopy was carried out at 25°C, 37°C and 55°C. These temperatures were selected to correspond with the temperatures at which subsequent structural characterisation techniques and chaperone activity assays were undertaken.

Circular dichroism spectroscopy in the far-UV region can determine the average content of secondary structure in a protein [319]. A minimum at 217 nm is observed for wildtype Hsp25 and all mutants at each temperature (Figure 5.8).

This is indicative of a primarily β-sheet structure [159,320], a feature common to all sHsps. Hsp25 has been shown to have a secondary structure very similar to that of mammalian α-, αA- and αB-crystallin (as summarised in Table 1.5) and also the more distantly-related bacterial IpbB [321].

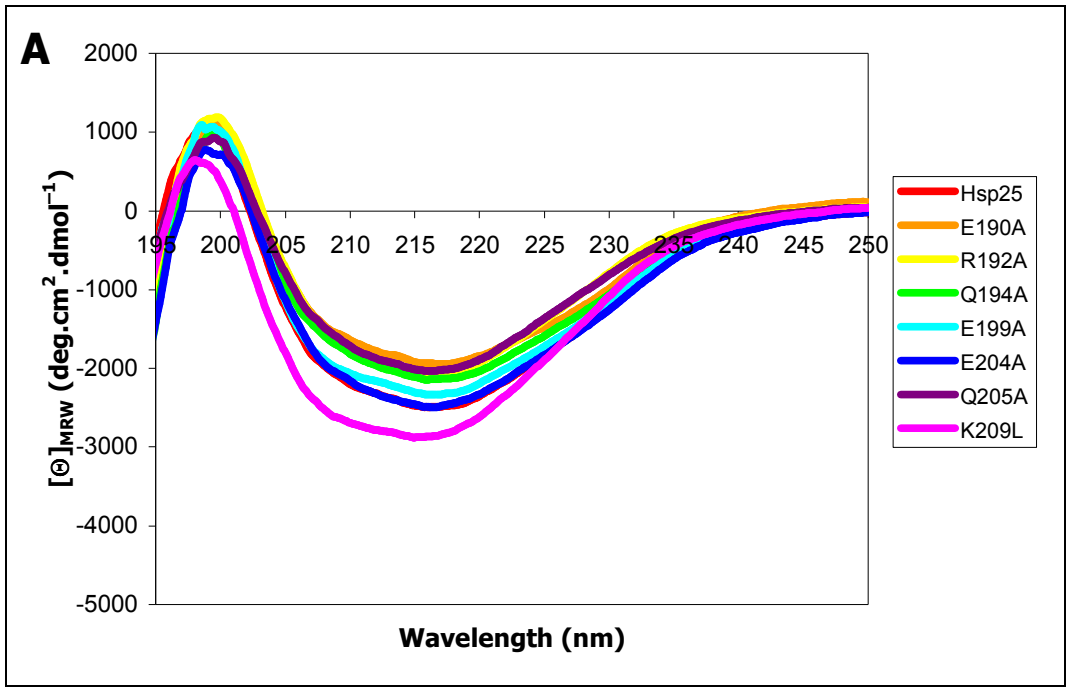

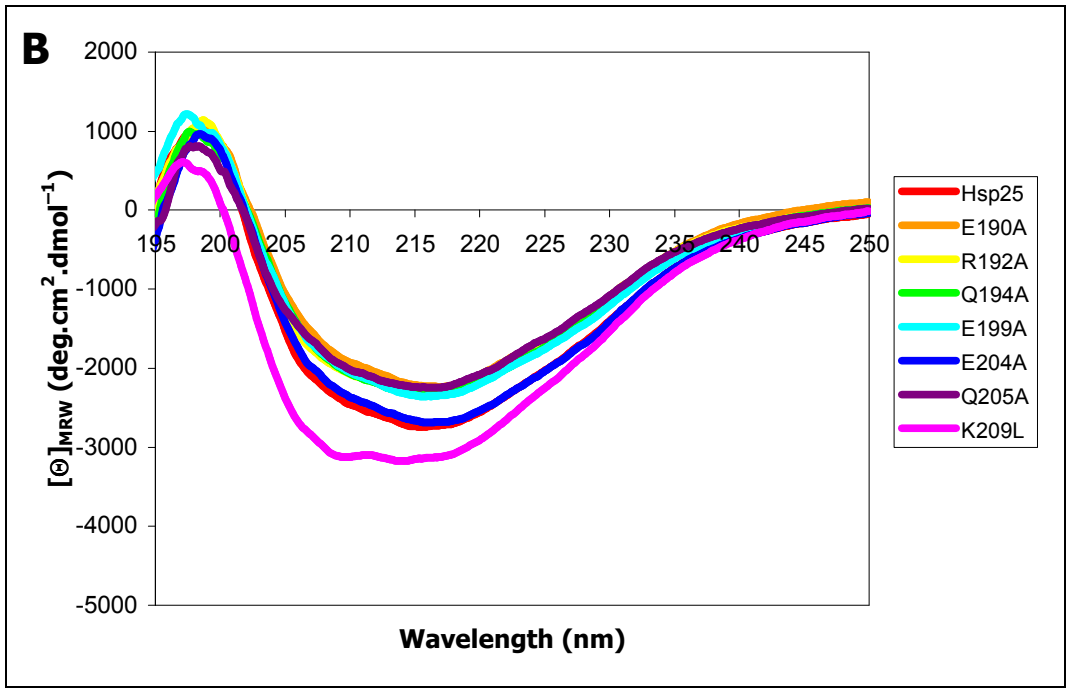

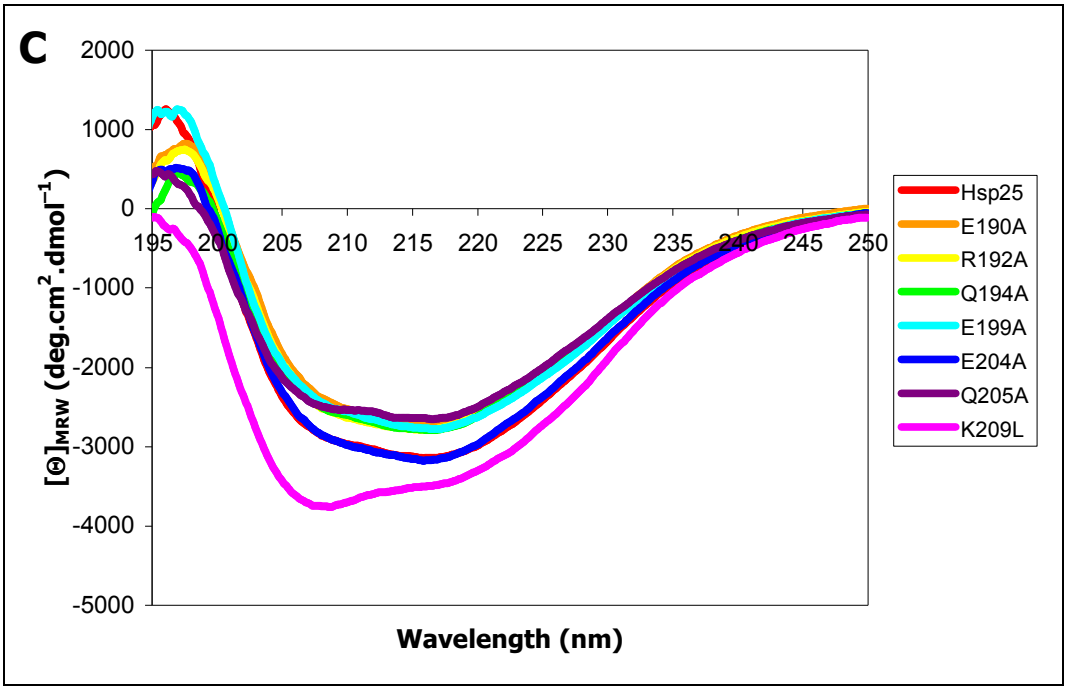

Figure 5.8: Circular dichroism spectra of wildtype and mutant Hsp25 at 25°C (A), 37°C (B) and 55°C (C). Samples were prepared in 10 mM sodium phosphate buffer (pH 7.5). A pathlength of 1 mm was used and spectra presented are accumulations of 16 scans.

An overall increase in the negative ellipticity and flattening of the spectra were observed with increasing temperature. The increase in negative ellipticity represents either an increase in or stabilisation of secondary structure [322] whilst flattening of the spectra associated with an increase in the negative ellipticity at or around 210 nm is indicative of an increase in α-helical content [320]. However, comparable differences between spectra in a range of previous studies have been deemed to be insignificant [150,191,201,204,323-325]. Furthermore, an error of ~10% is inherent in ellipticity measurements in the far-UV region [159].

Table 5.2: Secondary structure of wildtype and mutant Hsp25 as estimated by the deconvolution program CDSSTR using data measured to 190 nm.

Hsp25	Temp. (°C)	α-helix	β-sheet	β-turn	Random coil
wildtype	25°C	6%	38%	25%	30%
	37°C	6%	39%	25%	30%
	55°C	7%	39%	23%	31%
E190A	25°C	6%	41%	23%	30%
	37°C	6%	39%	24%	30%
	55°C	7%	38%	23%	31%
R192A	25°C	6%	41%	23%	29%
	37°C	6%	40%	23%	30%
	55°C	7%	38%	24%	31%
Q194A	25°C	6%	40%	23%	30%
	37°C	6%	41%	23%	30%
	55°C	7%	39%	23%	31%
E199A	25°C	6%	41%	23%	30%
	37°C	7%	38%	24%	31%
	55°C	7%	39%	22%	32%
E204A	25°C	8%	40%	22%	31%
	37°C	6%	39%	24%	31%
	55°C	7%	38%	24%	30%
Q205A	25°C	6%	41%	23%	29%
	37°C	7%	39%	23%	30%
	55°C	7%	38%	23%	31%
K209L	25°C	6%	40%	23%	31%
	37°C	8%	39%	24%	29%
	55°C	7%	36%	24%	31%

The relative proportions of secondary structure of wildtype and mutant Hsp25 as estimated by deconvolution are summarised in Table 5.2. The values determined for wildtype Hsp25 at 25°C are similar to those reported previously [145]. Maximum variations of 3% between mutants at each temperature and for each mutant over the temperature range investigated were observed, differences which fall within the expected margin of error associated with far-UV CD. Differences between wildtype Hsp25 and the K209L mutant appear to become more pronounced at elevated temperatures, with the negative ellipticity at ~208 nm increasing more noticeably than for the wildtype and other mutant proteins. Although deconvolution provides an estimation of the secondary structure of a protein and cannot be exclusively relied upon to represent structural details, differences of less than 2% between wildtype Hps25 and the K209L mutant at 55°C (Table 5.2) support the stabilisation of α-helical secondary structure in the K209L mutant at higher temperatures [322] rather than significant alterations to the structure itself. Thus, the secondary structure of Hsp25 was concluded to be not significantly affected by any of the mutations or an increase in temperature up to 55°C.

The reduction in the polarity of the C-terminal extension as a result of the mutations was not sufficient to alter the secondary structure of Hsp25, indicating that individual residues are not crucial for the determination of this level of structure. Indeed, a mutant of αB-crystallin in which the two C-terminal polar lysine residues were substituted with glycine was shown to have comparable secondary structure to the wildtype [151]. Similarly, mutants

of αA- and αB-crystallin in which the C-terminal extensions were swapped also have secondary structures similar to each other and their wildtype equivalents [326]. Even the removal of the C-terminal extensions of αA- and αB-crystallin and bacterial Hsp16.3 does not significantly affect the secondary structure of these proteins [218,223,327], further suggesting that the C-terminal extension of sHsps is not associated with the formation of secondary structure.

The secondary structure of Hsp25 did not change significantly with an increase in temperature from 25 to 55°C. This is consistent with previous far-UV CD studies on Hsp25 [179,191], α-crystallin [200,328] and IpbB [321,329] which show that these sHsps resist changes in secondary structure up to temperatures of approximately 60°C.

Thus, the secondary structure of the C-terminal mutants of Hsp25 prepared here do not have significantly different secondary structures to the wildtype protein, nor does the secondary structure change significantly with temperatures up to 55°C. Any differences in the higher levels of structure and functional properties of these mutants are therefore not a result of alterations to the secondary structure.

5.3. Intrinsic Tryptophan Fluorescence

Intrinsic tryptophan fluorescence depends strongly on the local environment of the tryptophan residues, including the buffer used, pH and the presence of other molecules or neighbouring groups [223,330]. A shift in the wavelength at

maximum fluorescence (λ_{max}) is indicative of a change in the polarity of the tryptophan environment [331]. In a polar solvent, a shift in λ_{max} to longer wavelengths represents an increase in polarity of the tryptophan environment [216,330]. Tryptophan fluorescence can therefore be used as a sensitive probe for the conformational stability of the local tertiary structure of proteins [332,333].

Hsp25 contains six tryptophan residues, five of which are localised to approximately the first half of the N-terminal domain (positions 16, 22, 43, 46 and 52) and one towards the beginning of the α-crystallin domain (position 99) (see Figure 1.4). Thus, the tryptophan fluorescence of Hsp25 is almost exclusively attributable to the first half of the N-terminal domain. The tryptophan fluorescence studies performed here on Hsp25 can therefore be used to provide information about the conformation of the N-terminal domain [334].

Wildtype and mutant Hsp25 proteins all gave peaks with fluorescence emission maxima located at around 340 nm (Figure 5.9, Table 5.3). A maximum at 332 nm indicates a tryptophan residue in a largely apolar environment whilst a tryptophan residue fully exposed to water would exhibit a maximum at 352 nm [333]. The overall environment of the tryptophan residues in Hsp25 is intermediate to these two extremes, although no information can be given regarding individual tryptophan residues. A further limitation of this technique is that it cannot be used to determine whether a change in tryptophan

fluorescence is a result of altered solvent exposure or adjustment of distances between tryptophan and charged residues.

A reduction in the λ_{max} value of the Q205A mutant was observed, indicating that the tryptophan residues in this mutant are in a less polar environment than in the wildtype. Whilst the overall tryptophan environment is still of a partially-exposed nature, this change suggests that the C-terminal extension plays a role in the determination of tertiary structure to some degree. This has previously been indicated by less subtle alterations to the C-terminal extension of mammalian sHsps: C-terminal chimeric proteins of αA- and αB-crystallin showed altered tertiary structure, as assessed by tryptophan fluorescence spectroscopy and near-UV CD studies [326]. That the substitution of this single residue in the C-terminal extension produced effects of similar extent to the replacement of the entire extension suggests that the Q205 residue of Hsp25 is fundamental in the formation of the structure of this sHsp.

No significant differences were observed in the λ_{max} values of the lysine, glutamic acid, arginine or proximal glutamine residue mutants, suggesting that these residues are not singularly disruptive to the solvent accessibility of the tryptophan residues. However, substitution of these residues produced significantly different maximum fluorescence (F_{max}) values compared to the wildtype protein. Changes in the fluorescence intensity can indicate an alteration in the rigidity of the environment around the tryptophan residues, with an increase in F_{max} correlating with a decrease in tryptophan flexibility, and

vice versa [251,335]. Thus, while the overall polarity of the tryptophan residues of each of these mutants was comparable to that of the wildtype, a decrease in flexibility of the tryptophan residues was observed for R192A, Q194A and each of the glutamic acid residue mutants. These decreases were similar for R192A and Q194A, with each of the glutamic acid residue mutants displaying progressive decreases in flexibility with the proximity of the mutation towards the C-terminus. The K209L mutant was seen to have an increase in tryptophan flexibility of a similar magnitude to the decrease observed for the E204A mutant.

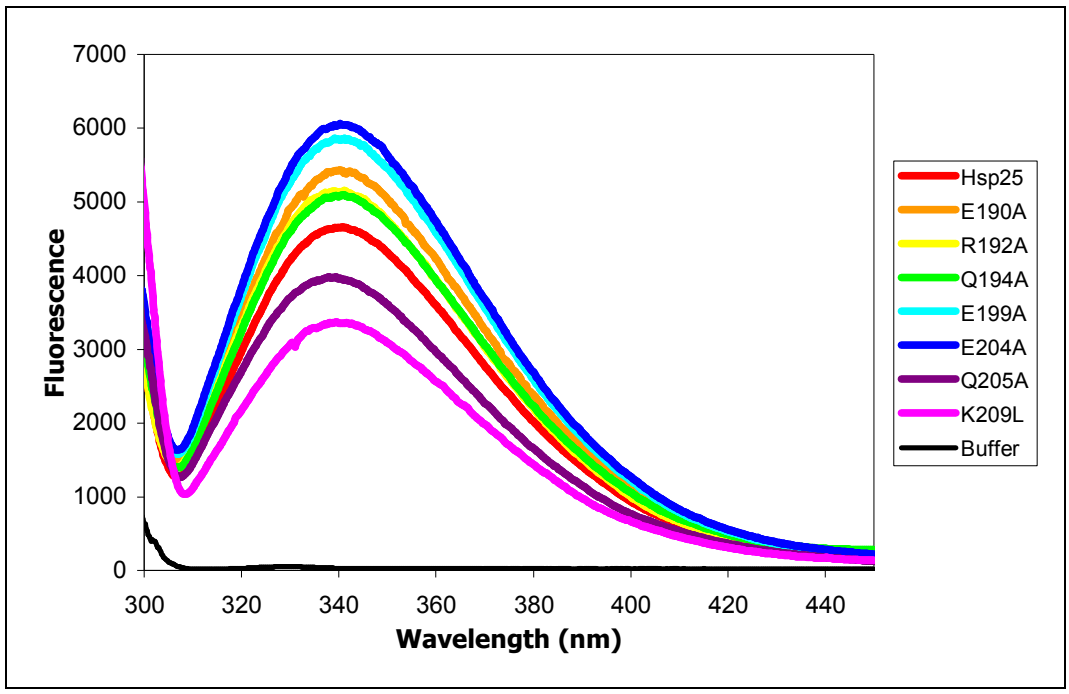

Figure 5.9: Tryptophan fluorescence spectra of wildtype and mutant Hsp25. Samples were prepared in 50 mM sodium phosphate buffer (pH 7.3) containing 0.02% NaN_3 to a final protein concentration of 5 μM. Excitation wavelength was 295 nm.

Table 5.3: Fluorescence maxima (F_{max}) and wavelength at maximum fluorescence (λ_{max}) for tryptophan fluorescence spectroscopy of wildtype and mutant Hsp25.

	F_{max}	λ_{max} (nm)
wildtype	4652	340.2
E190A	5417	340.3
R192A	5147	339.8
Q194A	5083	340.2
E199A	5856	340.3
E204A	6049	340.3
Q205A	3973	338.6
K209L	3361	339.8

With the exception of the Q205A mutant, which was shown to have reduced polarity of the tryptophan residues, substitution of these residues with non-polar alanine appeared to result in changes to the micro-environment of the tryptophan residues sufficient to affect the flexibility of the tryptophan residues but not to produce a structural effect to alter the overall proximity of the tryptophan residues in relation to the solvent or nearby polar groups. However, it must be emphasised that tryptophan fluorescence spectroscopy represents the overall tryptophan environment and the environment around any particular tryptophan residue cannot be determined: a change in the environment of one tryptophan residue may be masked by contrary changes to the other tryptophan residues such that the changes are cancelled out.

As far as can be determined, the tryptophan polarity of most of the mutants was unchanged compared with wildtype Hsp25, indicating that the tertiary structure of the first half of the N-terminal domain was unaltered. However, the apparent changes in the flexibility of the tryptophan residues do not seem feasible unless some movement in relation to the solvent or nearby groups has occurred. The conclusion that polarity of the tryptophan environment of all mutants except Q205A was unchanged must therefore be adopted with caution.

5.4. ANS Binding Fluorescence

The binding of ANS and other hydrophobic probes gives an indication of the exposed hydrophobicity of a protein. Such probes fluoresce weakly in aqueous solutions but display enhanced fluorescence associated with a shift to shorter wavelengths when bound to proteins and other macromolecules [223,336]. Binding occurs non-covalently in regions on the protein that have exposed clusters of hydrophobic aminoacyl residues [337]. Thus, λ_{max} is blue-shifted and fluorescence intensity is increased with the extent of binding and this technique provides a measure of the available hydrophobic surface on the protein [150,216].

sHsps exhibit significant ANS binding, which is consistent with their role as molecular chaperones in stabilising partially-folded states of proteins which expose significant hydrophobicity to solution. The ANS binding fluorescence at 479 nm of wildtype and mutant Hsp25 proteins increased with the addition of

ANS and reached a plateau centred around 85 μM (Figure 5.10A). The emission spectra at this concentration of ANS are shown in Figure 5.10B.

Whilst it is possible that the binding of any hydrophobic molecule to Hsp25 may alter the structure of the sHsp, ANS is a very small molecule (672 Da) compared with target proteins, particularly those investigated in this study. It is therefore unlikely that the binding of ANS affected the structure of Hsp25 to the same extent as binding of target proteins. Increased ANS binding fluorescence and a corresponding decrease in λ_{max} was observed for all of the glutamic acid residue mutants as well as for R192A and Q194A, indicating that these mutants have undergone conformational changes resulting in the exposure of hydrophobic regions that are inaccessible to the solvent in the wildtype protein. Conversely, the Q205A and K209L mutants exhibited a decrease in ANS binding fluorescence, indicating the internalisation of previously exposed clustered hydrophobic regions. These effects are likely a result of different spatial arrangements of elements of secondary structure, given that the secondary structure of the mutants was unaltered. Such is also the case for αA- and αB-crystallin [324].

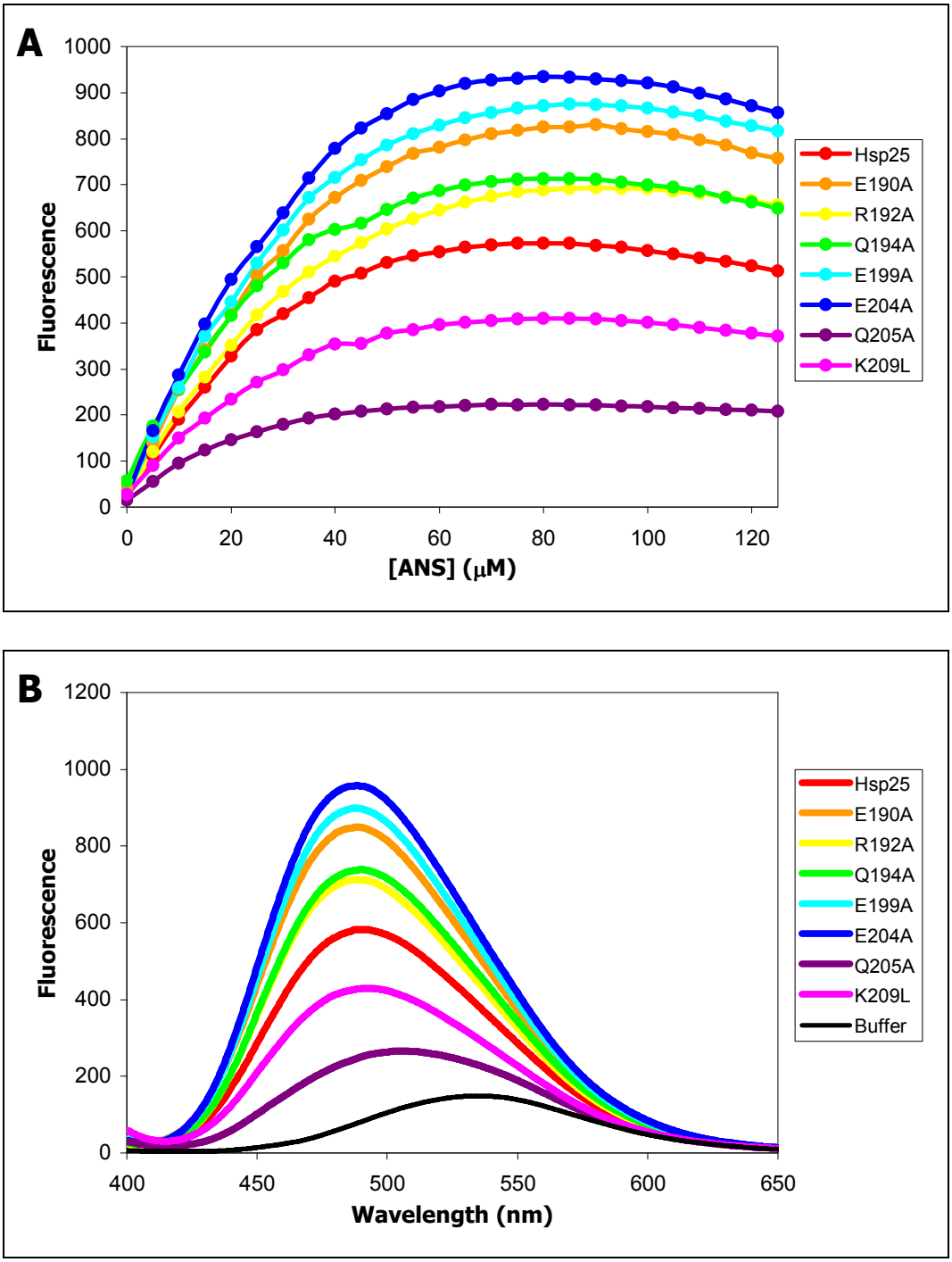

Figure 5.10: ANS binding fluorescence spectroscopy of wildtype and mutant Hsp25. (A) Fluorescence at 479 nm after the sequential addition of ANS; (B) Emission spectra at 85 μM ANS. Samples were prepared in 50 mM sodium phosphate buffer (pH 7.3) containing 0.02% NaN_3 to a final protein concentration of 5 μM. Excitation wavelength was 387 nm.

The increase in exposed clustered hydrophobicity observed for the R192A, Q194A and glutamic acid residue mutants indicates greater accessibility of the protein core as a result of less rigid packing [338]. This appears to contradict the apparent reduction in flexibility of the tryptophan residues. However, it must be remembered that the tryptophan environment represents the structure of the first half of the N-terminal domain only. Whilst the mutations resulted in increased rigidity of the first half of the N-terminal domain, at least in the immediate vicinity of the tryptophan residues, the remainder of the protein was less tightly packed, resulting in a loosening of the structure of the mutants overall. The opposite case is apparent for K209L, i.e. increased flexibility of the tryptophan environment with an overall tightening of tertiary structure.

Whilst the magnitudes of change for the ANS binding fluorescence intensity of the other mutants correlate approximately to the changes observed in tryptophan fluorescence intensity, the Q205A mutant shows a disproportionate decrease. This mutant is unique in this study in that it was the only mutant to show an alteration in the polarity of the tryptophan environment. The large decrease in hydrophobic exposure is consistent with an overall burial of regions on the surface of Hsp25, as was the case for the K209L mutant, also with some involvement by the N-terminal domain.

That the tertiary structure of Hsp25 is affected by some of the relatively modest alterations that have been made to the C-terminal extension in this study shows that the extension does indeed play a role in the folding of this sHsp after the

secondary structure has been established. Perturbations in the tertiary structure of these mutants suggests that interactions between the C-terminal extension and other regions of the protein made during the folding process are disrupted by the individual residue substitutions. Substitution of the Q205 residue resulted in a drastic change in overall conformation with evidence of alteration of the structure of the N-terminal domain. It is therefore likely that this residue is fundamental in the establishment or maintenance of contacts involving the C-terminal extension of Hsp25 in the folding of this sHsp.

Whilst fluorescence spectroscopic studies give an indication of the nature of changes to the tertiary structure of Hsp25 as a result of the mutations in the C-terminal extension, these methods are limited to overall structural information and cannot be used to investigate localised effects on structure. Near-UV CD could be used in conjunction with the above results to further elucidate the effects of the mutations on the overall tertiary structure of Hsp25, particularly around the aromatic residues.

5.5. Size-Exclusion Fast Protein Liquid Chromatography

Because sHsps exist in an oligomeric state under native conditions, size-exclusion chromatography with appropriate standards can be used to determine the size of the oligomer. A BioSep-SEC-S 4000 column was chosen for the determination of oligomeric sizes of wildtype and mutant Hsp25 as it gives good separation over two orders of magnitude. Standards ranging from 250 kDa to

2 MDa show a good linear relationship with a high correlation co-efficient (R^2 value) (Figure 5.11), indicating effective separation of protein in this molecular mass range.

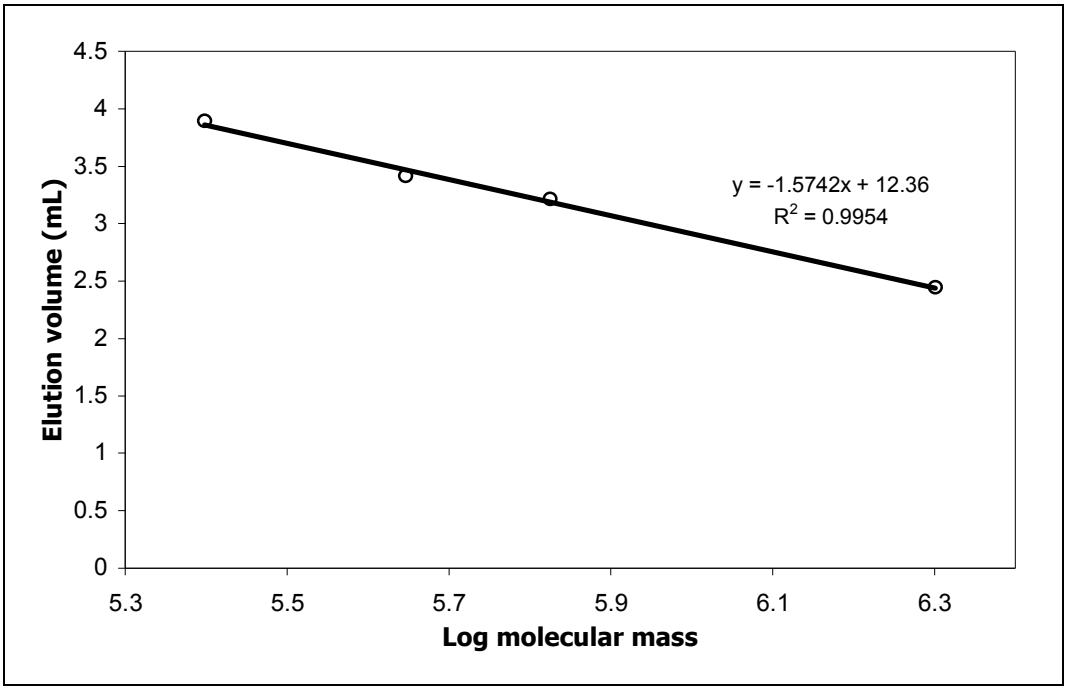

Figure 5.11: Standard curve for the elution of protein from a BioSep-SEC-S 4000 column. Standards used were blue dextran (2 MDa), thyroglobulin (669 kDa), apoferritin (443 kDa) and catalase (250 kDa).

Studies on the crystal structures of *Methanococcus* Hsp16.5 and wheat Hsp16.9 [136,139] show that the IXI motif within the C-terminal extension directly interacts with a hydrophobic groove formed by two β-sheets in the α-crystallin domain of another monomer [116]. For sHsps with sufficiently long C-terminal extensions to contain an IXI motif, this region is conserved [109] and vital for oligomerisation, as discussed previously (section 1.5.5). Because of the proximity between the IXI motif and the beginning of the flexible region of the

C-terminal extension, it is likely that the charged residues of the extension are also capable of interactions, perhaps with regions on other monomers, facilitating oligomerisation.

Although the C-terminal extension is a freely flexing protrusion from the surface of the oligomer and the flexible region is not a strict requirement for oligomerisation, as discussed previously, alterations to this region can influence the final oligomeric structure. For example, an αB-crystallin mutant in which the C-terminal extension was swapped for the C-terminal extension of αA-crystallin resulted in an increase in oligomeric size compared to wildtype αB-crystallin [326], suggesting that the nature of the C-terminal extension has a direct role in the determination of the final oligomeric structure of this sHsp.

Size-exclusion elution profiles of wildtype and mutant Hsp25 proteins are shown in Figure 5.12 and their calculated molecular masses are summarised in Table 5.4. Examination of the crystal structure of Hsp16.9 and Hsp16.5 shows that the angle between the α-crystallin domain and C-terminal extension can vary by up to 30° [139], giving rise to flexibility in the formation of oligomers and thus resulting in polydisperse populations of sHsp quaternary structures [116,173]. The elution peaks for sHsps from size-exclusion columns are therefore relatively broad [173,273]. To reflect this property, an average mass corresponding to the maximum of each peak is given, as well as the masses at half peak height [273].

Because the concentrations and volumes of each sample loaded were the same, as determined by A_{280} values, it was expected that the total area under the elution curve would be the same for each sample. However, this was not the case. Differences in peak heights are likely a result of the delivery of inconsistent sample volumes by the injection system, largely due to inexperience in using the system. Centrifugation of the samples prior to loading to remove any dust and other small particles may also have resulted in the loss of any aggregated or precipitated protein that may have been present in small amounts in the samples, resulting in the concentration of the loaded samples being slightly less than calculated and also inconsistent between samples. However, size determinations are made from the elution volume, not peak height, so this does not affect the results given by this technique [339,340].

The calculated average molecular mass of wildtype Hsp25 was approximately 613 kDa. This is consistent with the 680 kDa oligomer observed by Bova *et al.* (2000) [167] for Hsp27. However, widely differing values have also been reported, including approximate oligomeric sizes of 400 kDa [118,215], 570 kDa [160] and 740 kDa [175,316]. These inconsistencies can be ascribed to differences in buffer conditions between the analyses as variations in properties such as pH, ionic strength and temperature influence the oligomeric size of the sHsp [186,341].

The R192A, Q194A, E199A and E204A mutants eluted from the SEC column at similar volumes to wildtype Hsp25 with calculated oligomeric masses being

comparable to the wildtype protein. The overall oligomeric properties were therefore not affected by the disrupted tertiary structure observed for these mutants, particularly the glutamic acid residue mutants, suggesting that the native quaternary structure of Hsp25 is resistant to structural changes at the monomeric level. Indeed, selected mutations in the N-terminal domain of αB-crystallin (F28S), the α-crystallin domain of bacterial Hsp16.3 (L122V and L122A) or truncation of up to four residues from the C-terminus of αA-crystallin also results in comparable oligomeric sizes despite significant differences in tertiary structure compared with their respective wildtype proteins [153,171,342].

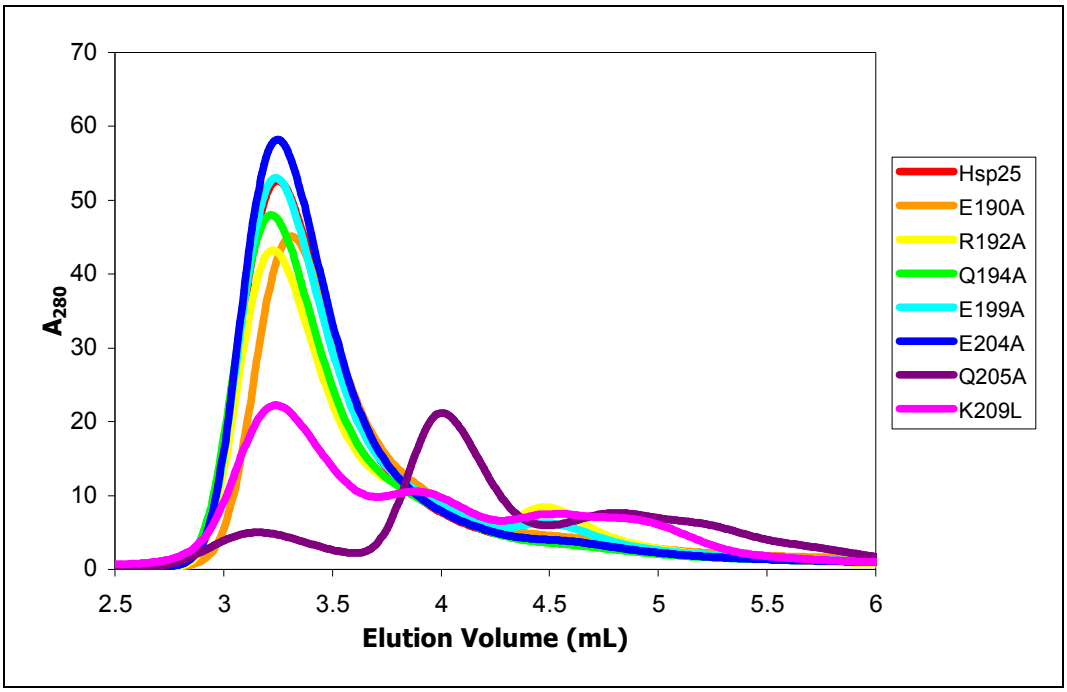

Figure 5.12: SEC FPLC chromatograms of wildtype and mutant Hsp25. Samples were prepared in 50 mM sodium phosphate buffer (pH 7.3) containing 0.02% NaN_3 to a final protein concentration of 30 μM.

Table 5.4: Approximate masses of wildtype and mutant Hsp25 as determined by SEC FPLC (Figure 5.12). Average mass is the mass at peak height and maximum and minimum values are the oligomeric sizes calculated from elution times at half peak height [273]. Dashes represent maximum and minimum peak height positions that could not be determined due to overlapping peaks.

Please see print copy for table

An overall loosening of the tertiary structure of the these mutants, as indicated by the increased exposure of clustered hydrophobic regions, was not sufficient to interfere with important monomer-monomer interactions required for correct oligomerisation. However, a similar but less intense increase in overall exposed clustered hydrophobicity elicited quaternary structural changes to the E190A mutant, resulting in a reduced oligomeric size. These differences are likely due to differing changes in the local tertiary structure at particular sites of the

mutant proteins that cannot be determined by the properties of the overall protein as detected by fluorescence spectroscopy.

Changes in the tertiary structure of various sHsp mutants comparable to those in the examples given above have lead to perturbation of the oligomeric structure of these proteins. For example, the N-terminal domain mutant F71G of αA-crystallin, C-terminal extension chimera proteins of αA- and αB-crystallin, truncation mutants of αA-crystallin in which 10-22 residues have been removed from the C-terminus and R116C and R120G mutants of αA- and αB-crystallin, respectively, all show significant variations in their quaternary structure compared with the respective wildtype proteins [149,152,171,326,341]. These observations indicate that a change in tertiary structure *per se* does not contribute to variations in oligomeric structure. Rather, specific changes in tertiary structure appear to be required for this to occur. This appears to also be the case for the E190A mutant of Hsp25 – different alterations in tertiary structure to the other mutants have combined to give similar cumulative effects. The E190 residue therefore appears to be important for the correct formation of the quaternary structure.

Given the proximity of this residue to the IXI motif, it is possible that the substitution of the E190 residue disrupts the binding of the IXI motif to other regions of the protein. The IXI motifs of Hsp16.9 and Hsp16.5 form hydrophobic contacts with a groove between β-sheets in the α-crystallin domain of another monomer, an interaction essential for the oligomerisation of

sHsps [136]. Although the C-terminal extensions of these sHsps lack flexible C-terminal regions, truncation of the C-terminal extension to remove the IXI motif results in the inability of αA-crystallin to form oligomers [171], indicating that interactions involving the IXI motif are also essential for the oligomerisation of mammalian sHsps containing flexible regions. Altering the polarity of residue 190, which is separated from the IXI motif of Hsp25 (at residues 185-187) by only two residues, appears to have interfered with the role of the IXI motif, resulting in altered oligomeric size.

Both the Q205A and K209L mutants eluted as three peaks, indicating that three distinct oligomeric structures were present. The most abundant K209L oligomer was of comparable size to the wildtype, indicating that the majority of monomer-monomer interactions were not perturbed, whilst an increase in size was seen for the Q205A mutant, although this was not the major peak in the SEC profile for this mutant (Figure 5.12). Changes in the overall surface properties of these mutants, as evidenced by the decrease in available hydrophobic regions, could allow contacts between monomers to occur at sites not normally involved in the interaction between subunits. This could lead to multiple monomer configurations within the oligomer and thus different packing arrangements, resulting in the formation of oligomers with different numbers of constituent monomers to the wildtype. Abnormal orientations of monomers within the oligomer in relation to the solvent may also prevent the binding of other subunits through steric hindrance.

The changes to the oligomeric size of the Q205A and K209L mutants of Hsp25 could also be directly contributed to by the altered properties of the C-terminal extension. Flexibility of the C-terminal extension is an important feature in the maintenance of correctly sized oligomers of sHsps. Introduction of hydrophobicity into the C-terminal extension of αA-crystallin has been shown to reduce the flexibility of the C-terminal extension and have significant effects on the overall structure of αA-crystallin [220]. It has been proposed that this flexibility is important for the role of the protruding C-terminal extension as a "spacer" to prevent interactions between adjacent sHsps oligomers and sHsp-target protein complexes [145,299]. Removal of the flexible region of the C-terminal extension of αB-crystallin results in randomly-sized oligomers, suggesting that disruption of the spacing mechanism has significant effects on the oligomeric structure [221]. In order to determine if the flexibility of the C-terminal extension of Hsp25 was indeed affected as a result of mutations of the Q205 and K209 residues, NMR studies would need to be performed.

Interestingly, the K175 mutant of αB-crystallin, corresponding to Hsp25-K209L, had comparable tertiary structures and oligomeric sizes to wildtype αB-crystallin, with no smaller oligomers being detected [221]. Clearly, substitution of the C-terminal lysine residue to leucine affects the structure of these sHsps differently. The overall structures of Hsp25 and αB-crystallin are significantly different: the length and sequence of the N-terminal domain and C-terminal extension, monomeric size and number of monomers in the oligomer are all disparate between these two proteins. In addition, the C-terminal lysine

residue of αB-crystallin is preceded by another lysine. The proximity of this lysine to the C-terminus may serve to partially counteract the effects of the mutation and override structural effects caused [222]. Such mitigation is not possible in Hsp25, as the C-terminal lysine is located next to two non-polar alanine residues.

Thus, whilst most of the Hsp25 mutants prepared were found to have similar oligomeric sizes to the wildtype protein, variations were observed for the E190A, Q205A and K209L mutants. A reduction in size of the E190A oligomer indicates that the basic overall structure of wildtype Hsp25 is preserved, with some variations in monomer packing. The Q205A and K209L mutants were present in three distinct oligomeric forms, indicating that the Q205 and K209 residues are particularly important for the arrangement of monomers within the oligomer of Hsp25.

5.6. Thermostability Studies

The importance of the presence of a C-terminal extension in the maintenance of sHsp solubility is highlighted by studies on truncation mutants. Removal of the C-terminal extension has been shown to reduce the solubility of sHsps from a range of organisms, from nematodes (Hsp16-2 [165]) to amphibians (Hsp30C [219]) through to mammals (αA-crystallin [171] and Hsp25 [145]). Apart from being relatively short and unstructured, the C-terminal extensions of sHsps have an abundance of polar residues. It is widely believed that that the polarity

allows the extension to interact with the solvent and counteract the hydrophobicity associated with the remainder of the protein, thus keeping the sHsp in solution [264,299].

Thermostability profiles of wildtype and mutant Hsp25 are shown in Figure 5.13. All proteins remained completely thermostable in solution until approximately 68°C. No precipitate was observed for wildtype Hsp25 at any temperature tested (up to 100°C). The arginine, glutamine and C-terminal lysine mutants also remained mostly in solution up to 100°C, whilst all of the glutamic acid residue mutants showed markedly reduced thermostability.

The structural transitions of mammalian sHsps with increasing temperature have been most extensively studied in α-crystallin. α-Crystallin undergoes two structural transitions with increased temperature: gradual increases in hydrophobic exposure from approximately 30°C and more rapid and distinct changes in tertiary structure, accompanied by alterations to secondary and quaternary structure, commencing at approximately 50°C, with a molten globule state being achieved at ~62°C [200], as discussed previously (section 1.5.6). The formation of the molten globule state corresponds approximately with the onset of aggregation of Hsp25 at around 69°C and is consistent with the increase in particle size of Hsp25 commencing from 65°C observed previously [179]. Loss of secondary structure of Hsp25 at this temperature has also been reported [179,191].

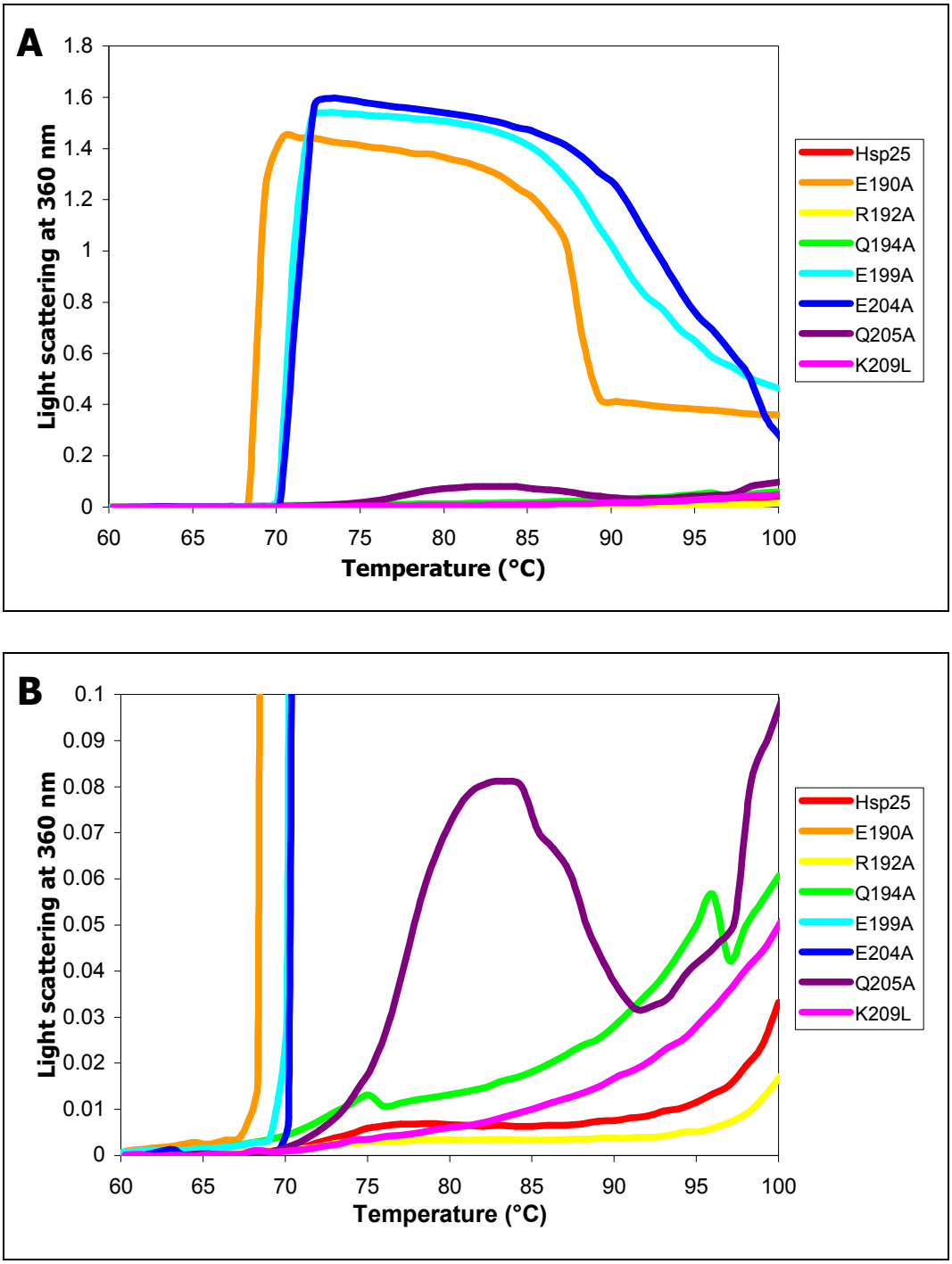

Figure 5.13: Thermostability profiles of wildtype and mutant Hsp25 showing full scale (A) and enlargement of the 0-0.1 A_{360} region (B). Samples were prepared in 50 mM sodium phosphate buffer (pH 7.3) containing 0.02% NaN_3 to a final protein concentration of 0.2 mg/mL. Temperature was increased at a rate of 1°C/min.

A slight but steady increase in the aggregate size of wildtype Hsp25 was observed until approximately 77°C, where a plateau was reached, again consistent with previous studies on this sHsp [179]. No further increases in light scattering occurred for ~10°C, suggesting that the molten globule state was stable in this temperature range. From 87°C, aggregation re-commenced gradually and then occurred more rapidly from approximately 95°C (Figure 5.13B).

The R192A mutant showed a similar thermostability profile to wildtype Hsp25, although the aggregation was less distinct, largely a result of slower aggregation prior to the plateau region. NMR studies show that R192 is the first residue in the flexible region of the C-terminal extension of Hsp25 [343]. Because this residue is adjacent to the anchor point for the flexible region, the flexibility and solvent-exposure of this residue is limited and the positive charge at this site would is not likely to contribute greatly to the solubilising effect of Hsp25. Therefore, substitution of this residue did not detrimentally affect the stability of Hsp25 and may have indeed increased the flexibility of the anchor region through reduction of steric hindrance associated with the long side-chain of the arginine residue compared with that of alanine. Further mutagenesis studies would be required to test this hypothesis.

The increase in hydrophobic exposure accompanying the second temperature-induced structural transition [201] resulted in aggregation and subsequent precipitation of the glutamine and lysine mutants, with precipitation being

visually evident at the conclusion of the assay of both glutamine mutants. The decrease in absorbance values observed was a result of the precipitate sinking to the bottom of the cuvette and therefore no longer obscuring the light path [344]. The traces of these three mutants display no plateau regions, indicating that the molten globule states are less thermostable than that of the wildtype, allowing precipitation to continue unabated.

The perturbation of oligomeric structure is likely the major contributing factor to the slightly reduced thermostability of the Q205A and K209L mutants compared to the wildtype protein. The K209L mutant did not show visible signs of precipitation, indicating that at least the oligomers of comparable size to the wildtype were stable at elevated temperatures. The Q205A mutant was not as stable, most likely a result of a combination of factors: this mutant primarily existed as smaller oligomers and the oligomeric size of the largest species was altered.

Marginally reduced thermostability was observed for Hsp25-Q194A despite this mutant having similar overall structural properties to the R192A mutant. The flexibility of the R192 residue is limited, as discussed above, whilst the Q194 residue has greater flexibility and solvent accessibility as a result of it being further from the anchor point [345]. The ability of the C-terminal extension to act as a solubiliser was therefore inhibited to a larger extent for the Q194A mutant but these effects were still comparatively minor.

Each of the glutamic acid mutants showed very poor thermostability, with maximal precipitation being reached within 2°C of the onset temperature (~68°C for the E190A mutant and ~70°C for the E199A and E204A mutants) (Figure 5.13A). All three glutamic acid residue mutants were much less thermostable than the wildtype protein and all of the other mutants. A similar result has been described for the replacement of adjacent glutamic acid residues with alanine (E164/165A) in the C-terminal extension of αB-crystallin [221]. Precipitation of these mutants corresponds with the formation of the molten globule state by wildtype Hsp25.

At 25°C, the glutamic acid residue mutants all had significantly increased surface hydrophobicity compared with wildtype Hsp25 and the other mutants. Greater exposure of hydrophobicity of sHsps occurs with increasing temperatures, as discussed above. Tertiary structure is gradually perturbed from 30°C, with the exposure of hydrophobic regions accelerating and being accompanied by gradual losses in β-sheet secondary structure from ~50°C and most tertiary structure being lost by ~62°C. These hydrophobic effects increase with increasing temperature, which leads to a greater propensity for mutual association. This phenomenon did not result in the precipitation of wildtype Hsp25, the glutamic acid residue mutants were not able to withstand equivalent changes on top of the already increased levels of surface hydrophobicity. Indeed, hydrophobic regions are more effectively buried in proteins that are thermostable [304].

The additional hydrophobicity presented to the solvent by the glutamic acid residue mutants is unlikely to be the only contributing factor to their poor thermostability, as the R192A and Q194A mutants also displayed significantly increased exposed hydrophobicity. The thermostability of proteins from thermophilic organisms has been shown to be related to electrostatic interactions through the presence of surface-exposed polar and charged groups, as well as hydrophobic and packing effects [304,305]. In comparison to mesophilic organisms, whose optimal growth temperature is 20-50°C [346], such as mammals, proteins from thermophilic organisms have a higher proportion of polar and charged residues, primarily glutamic acid and lysine [306,347]. Interactions between αB-crystallin subunits can be inhibited by the replacement of glutamic acid residues in the α-crystallin domain with other residue types, possibly through decreased electrostatic interactions and increased electrostatic repulsion [166]. Similarly, it is likely that the glutamic acid residues in the C-terminal extension of Hsp25 are important for electrostatic interactions with the solvent and potentially with other regions of the sHsp. The replacement of the glutamic acid residues with alanine resulted in a reduction in the potential for hydrogen bonding and electrostatic interactions and thus indicates that the glutamic acid residues are vital for the solubilising role of the C-terminal extension.

Whilst all of the Hsp25 mutants showed perturbed tertiary structure, and also oligomeric structure in the case of the E190A, Q205A and K209L mutants, only substitution of the glutamic acid residues resulted in dramatically reduced

thermostability. Similar results were obtained for each of the glutamic acid residue mutants despite varying degrees of disruption of tertiary structure being observed, suggesting that the gross structural changes were not solely responsible for their decrease in thermostability. The solubility of Hsp25 as a whole appears to be inherently linked to the presence of each of these glutamic acid residues.

5.7. Chaperone Activity Assays

The ability of wildtype and mutant Hsp25 to prevent the amorphous aggregation and precipitation of target proteins was assessed by chaperone activity assays. These assays were performed by placing a target protein under an appropriate stress *in vitro* in the presence of various concentrations of Hsp25 and monitoring protein precipitation over time.

Truncation of the flexible region of the C-terminal extensions of Hsp25 and αA-crystallin results in a proteins that retain significant chaperone ability despite changes to their tertiary structure [145,171]. Additionally, truncation of ten residues from nematode Hsp16-2 or up to 15 residues from bacterial HspH has little effect on the chaperone activity of these sHsps [165,170]. These studies suggest that the C-terminal extension is not directly involved in interactions with target proteins and its role in the formed oligomer is that of a solubiliser and is therefore required for the chaperone function of sHsps [145].

5.7.1. Reduction Stress Assays

Under reduction stress, the disulphide bonds between the A and B chains of insulin are broken. This results in the aggregation and precipitation of the B chain [273], which can be monitored by light scattering at 360 nm, while the A chain remains in solution. A final insulin concentration of 45 μM was used in all reactions, with increasing concentrations of Hsp25 up to a ratio of 0.5 Hsp25 monomers per insulin molecule. Precipitation was measured as light scattering at 360 nm.

Hsp25 contains a single cysteine residue that is capable of forming intersubunit disulphide bonds. As discussed previously (section 5.1), the removal of the ability of Hsp25 to form such bonds by various modifications of the cysteine residue does not affect the structure or function of this sHsp. The stability of C-terminally truncated Hsp25 and αB-crystallin, which lacks a cysteine residue, is not affected by the presence of DTT [145,339], indicating that the use of reduction stress to initiate insulin precipitation does not affect the stability of these proteins.

Full suppression of the precipitation of insulin under reducing stress was achieved at a ratio of 0.5:1 for wildtype Hsp25 (Figure 5.14A). The precipitation curves of insulin under reduction stress in the presence of mutant Hsp25 proteins are shown in Figure 5.14B-H and a summary of the relative levels of precipitation for the 0.1:1 ratio of each of the mutants are represented in Table 5.5. This ratio was selected as large differences were seen between

the mutants and the lines tended to be smoother than those of the other ratios. Wobbly lines are due to the use of a 96 well plate, which was read from below. Since aggregates and precipitates were free to move in solution, the light path was periodically obscured. The precipitation at 40 min was therefore used for the summary calculations as this point preceded any major "wobbles" in the traces.

The R192A (Figure 5.14C), Q194A (Figure 5.14D) and Q205A (Figure 5.14G) mutants displayed chaperone activity comparable to the wildtype. This is not surprising for the R192A and Q194A mutants, given the modest alterations to gross tertiary structure and similar quaternary structure and thermostability compared with wildtype Hsp25. Interestingly, the significant alterations to oligomeric structure of the Q205A mutant compared with the wildtype protein, in particular the presence of smaller species, had no effect on the chaperone activity of this mutant under these conditions.

A C-terminal truncation mutant of bacterial HspH retains chaperone activity at 43°C despite producing a larger oligomer [170]. This suggests that the significantly larger Q205A oligomer was capable of chaperone activity, although it was not the predominant species present. Indeed, since the chaperone activity of Hsp25-Q205A was similar to that of the wildtype protein, it is likely that all oligomeric species were capable of chaperone activity.

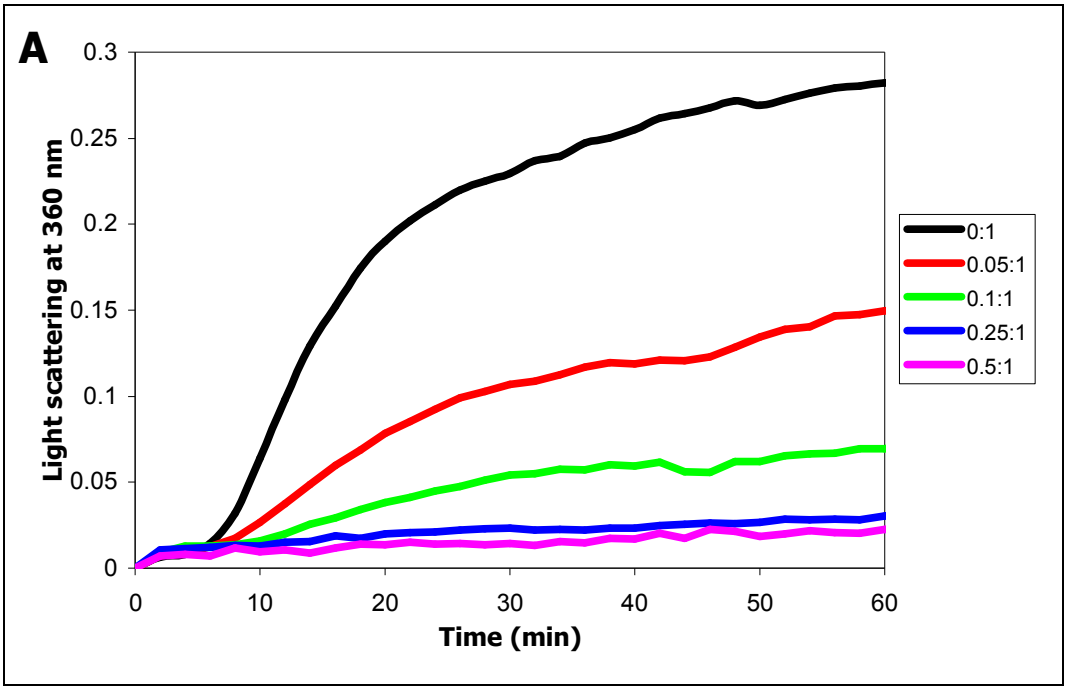
A
Light scattering at 360 nm
0.3
0.25
0.2
0.15
0.1
0.05
0
0
10
20
30
40
50
60
Time (min)
0:1
0.05:1
0.1:1
0.25:1
0.5:1

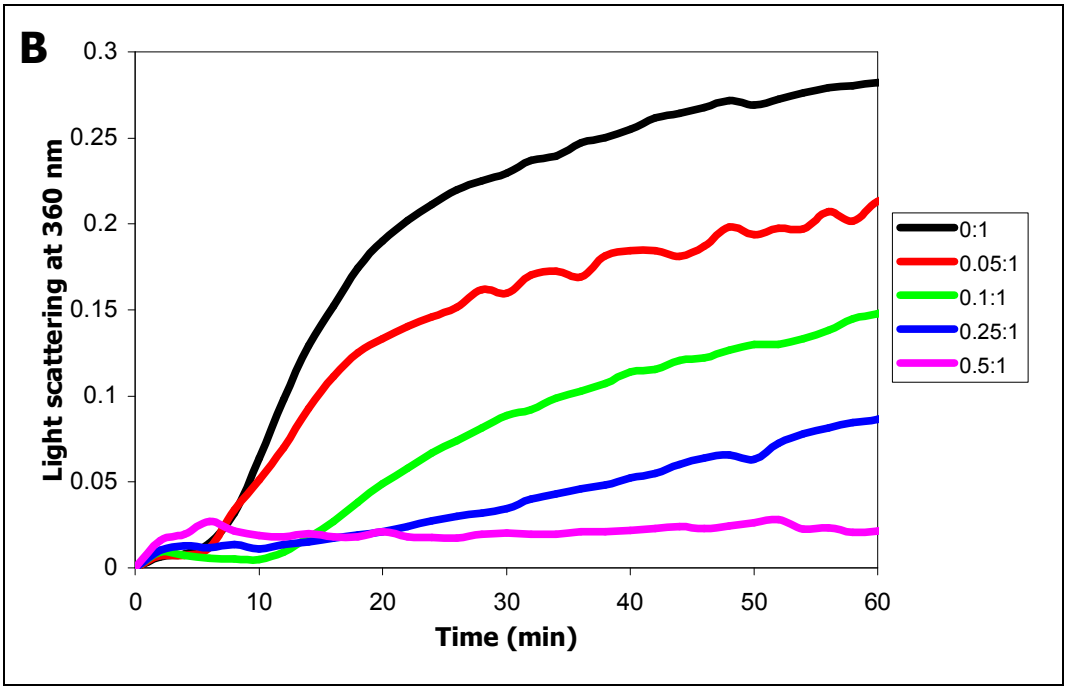
B
Light scattering at 360 nm
0.3
0.25
0.2
0.15
0.1
0.05
0
0
10
20
30
40
50
60
Time (min)
0:1
0.05:1
0.1:1
0.25:1
0.5:1

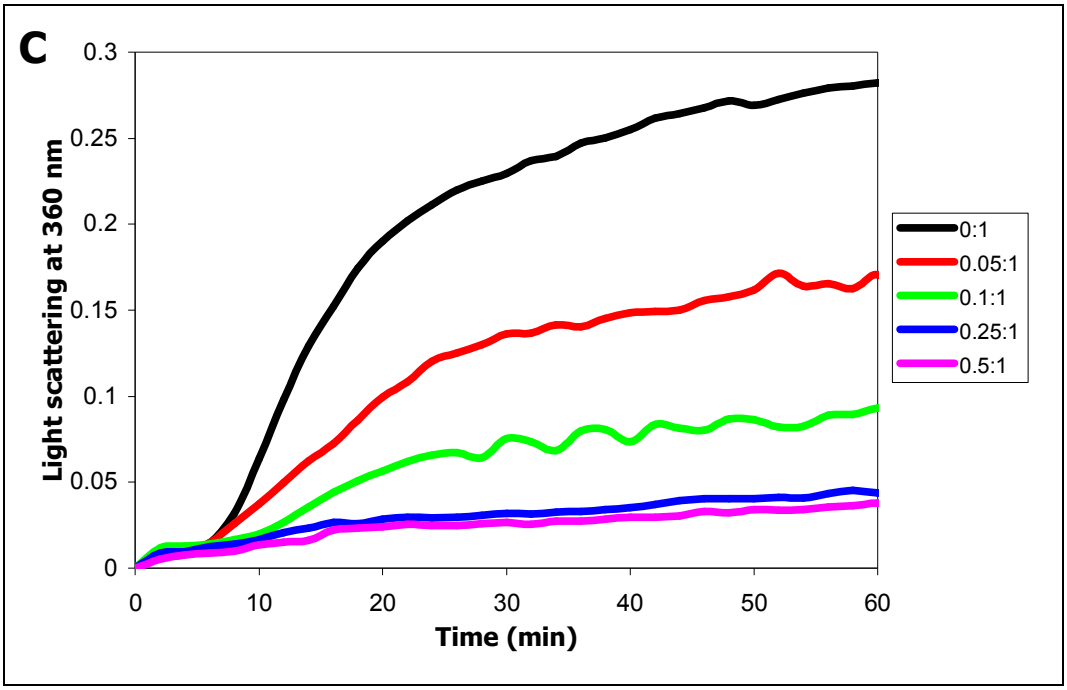
C
Light scattering at 360 nm
0.3
0.25
0.2
0.15
0.1
0.05
0
0
10
20
30
40
50
60
Time (min)
0:1
0.05:1
0.1:1
0.25:1
0.5:1

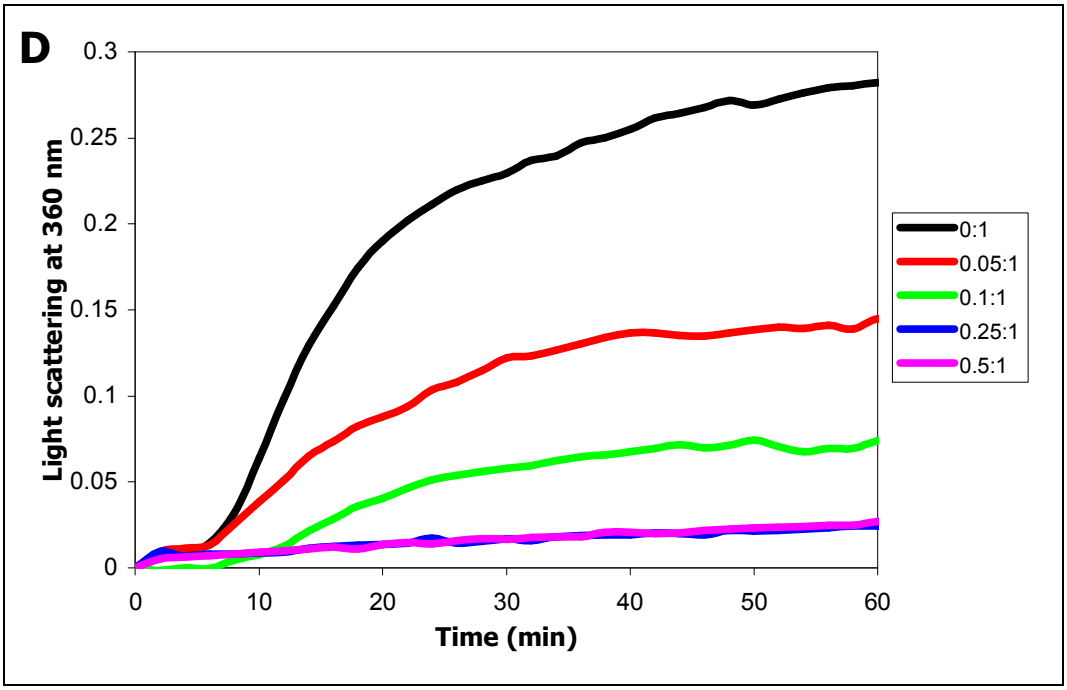
D
Light scattering at 360 nm
0.3
0.25
0.2
0.15
0.1
0.05
0
0
10
20
30
40
50
60
Time (min)
0:1
0.05:1
0.1:1
0.25:1
0.5:1

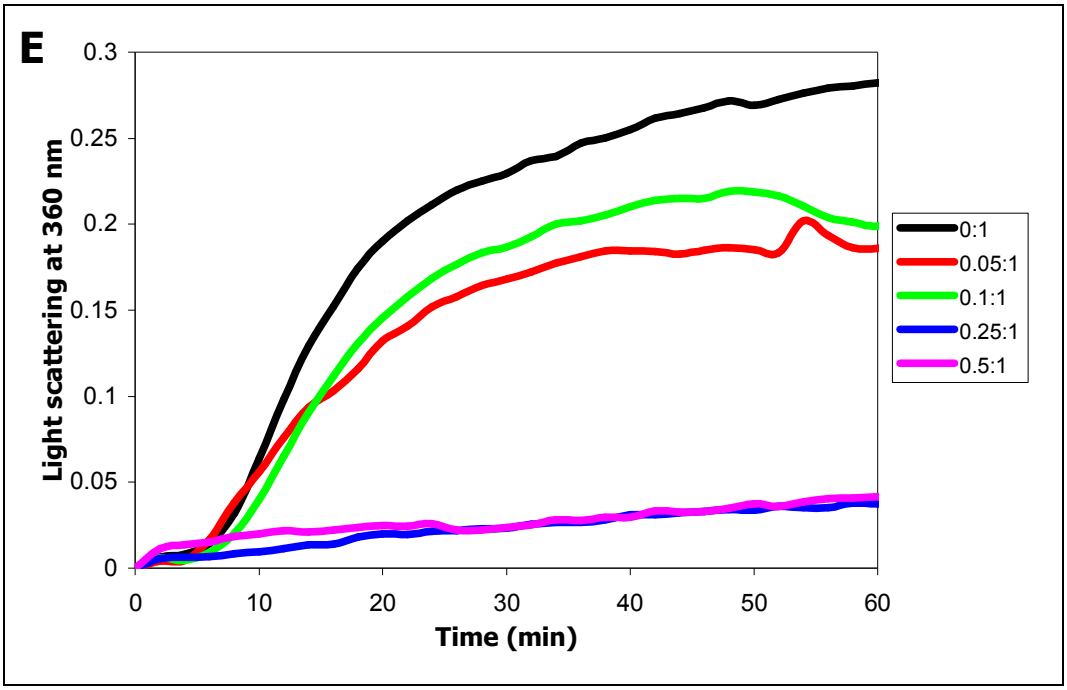
E
Light scattering at 360 nm
0.3
0.25
0.2
0.15
0.1
0.05
0
0
10
20
30
40
50
60
Time (min)
0:1
0.05:1
0.1:1
0.25:1
0.5:1

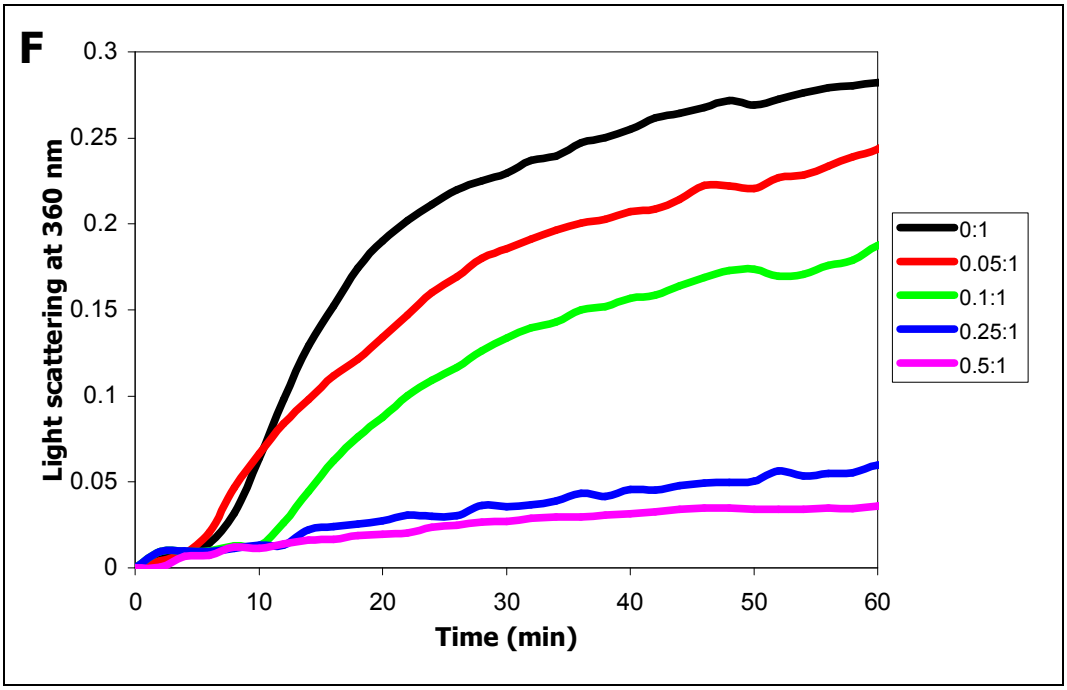
F
Light scattering at 360 nm
0.3
0.25
0.2
0.15
0.1
0.05
0
0
10
20
30
40
50
60
Time (min)
0:1
0.05:1
0.1:1
0.25:1
0.5:1

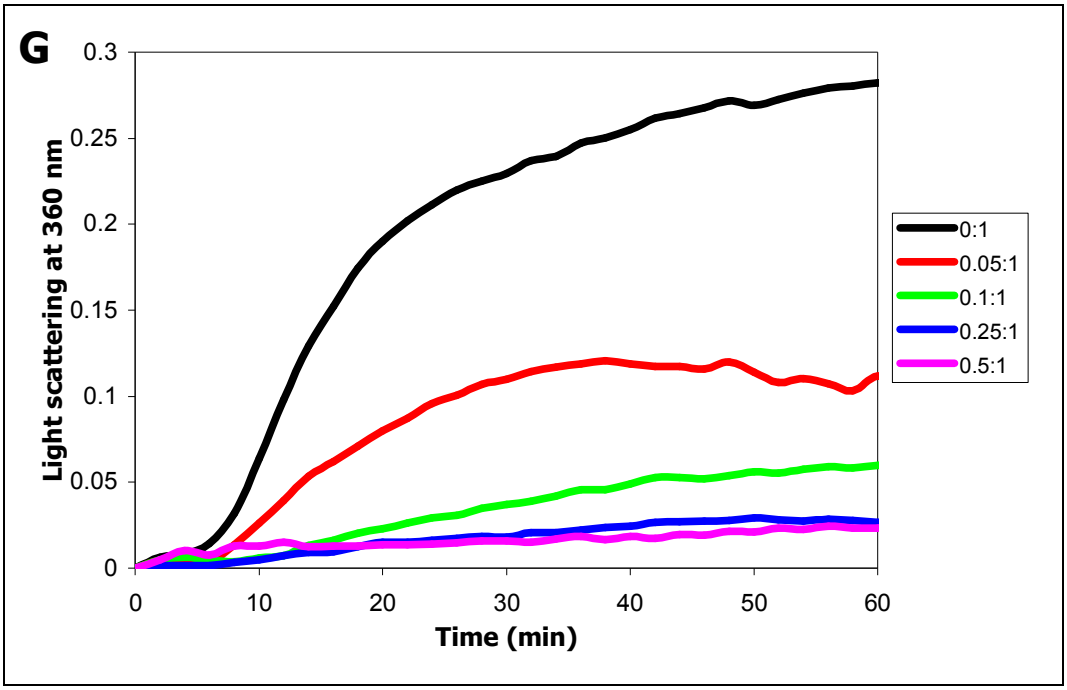

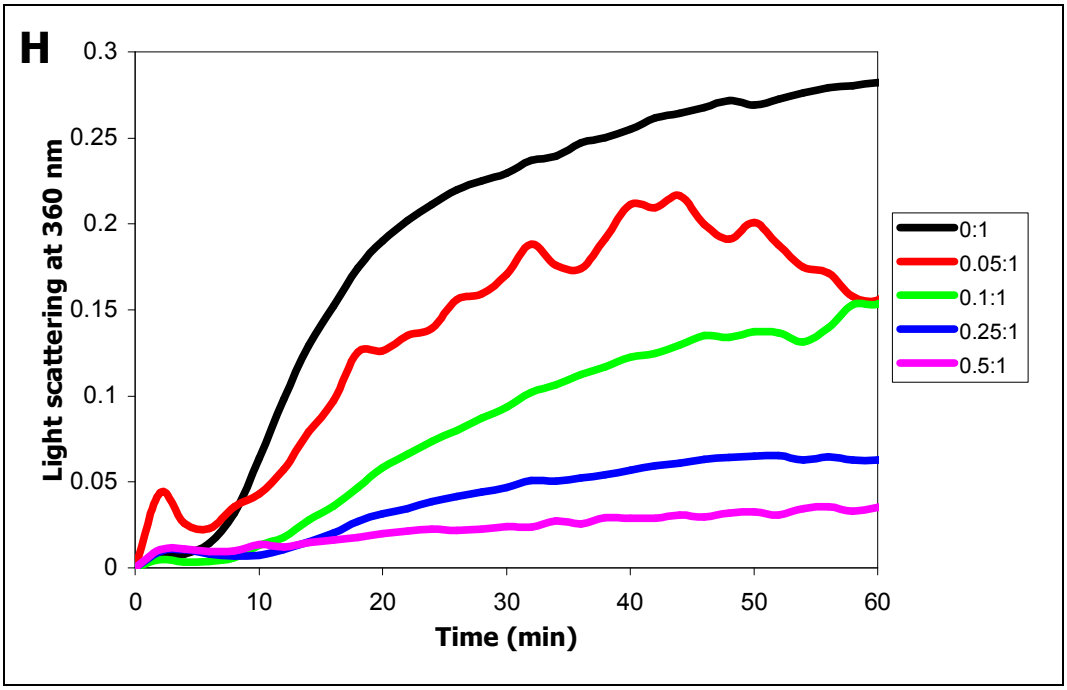

Figure 5.14: Chaperone activity of wildtype Hsp25 (A), Hsp25-E190A (B), Hsp25-R192A (C), Hsp25-Q194A (D), Hsp25-E199A (E), Hsp25-E204A (F), Hsp25-Q205A (G) and Hsp25-K209L (H) as measured by the suppression of aggregation of insulin under reduction stress. Assays were performed at 37°C in 50 mM sodium phosphate buffer (pH 7.3) containing 0.02% NaN_3. The reduction of insulin was initiated by the addition of DTT to a final concentration of 20 mM. Ratios represent the molar concentration of Hsp25 monomers to complete insulin molecules. Traces are the average of triplicates.

Table 5.5: Suppression of aggregation for insulin under reduction stress in the presence of Hsp25. Values shown are the relative suppression of precipitation at 40 min for the 0.1:1 ratio compared with the 0:1 ratio, which represented full precipitation.

Hsp25	Suppression of Precipitation (%)
wildtype	77
E190A	55
R192A	71
Q194A	73
E199A	18
E204A	57
Q205A	81
K209L	52

Recognition and sequestration of target proteins by sHsps is largely hydrophobic in nature. The chaperone activity of sHsps is therefore enhanced by increases in exposed hydrophobicity [196]. From this evidence, it would be expected that the glutamic acid residue mutants, with increased surface hydrophobicity (Figure 5.10), would display improved chaperone ability compared with wildtype Hsp25 [148]. This was not the case, however, with all three glutamic acid residue mutants exhibiting reduced chaperone activity towards insulin under reducing conditions.

It is evident that specific subtle structural changes, which cannot be detected with the techniques used in this study, have a greater influence on the

chaperone properties of Hsp25 than the overall surface features. Indeed, a lack of correlation between the amount of exposed clustered hydrophobicity as detected by hydrophobic dyes such as ANS and chaperone activity has been observed for αA- and αB-crystallin [348].

Whilst the chaperone binding site of sHsps remains elusive, there is evidence to suggest that binding of target proteins occurs in the groove between monomers and involves β-sheets located at the beginning of the α-crystallin domain corresponding to residues 70-88 in αA-crystallin [209,210]. It is likely that the altered structures of the glutamic acid residue mutants result in the disruption of binding sites and hindered recognition and sequestration of target proteins. Increased exposed hydrophobicity also promotes interactions among sHsp molecules and encourages incorrect aggregation of sHsp monomers and interaction between adjacent sHsp oligomers [349]. The formation of correctly-sized and slightly smaller oligomers suggests that, as best as can be determined, interactions between monomers within the oligomer are not significantly disrupted in these mutants. However, it is probable that the increased surface hydrophobicity facilitates association between oligomers, as discussed previously and illustrated by the poor thermostability of these mutants. The chaperone binding sites would therefore be less accessible to the target proteins, resulting in a decreased efficiency of target sequestration and thus the observed reduction in chaperone activity. The decrease in polarity of the C-terminal extension may also facilitate interaction between the extension

and other regions on the sHsp, potentially blocking chaperone binding sites and therefore resulting in less efficient binding of target proteins [299].

The K209L mutant displayed decreased chaperone activity towards insulin under reduction stress compared with wildtype Hsp25, suggesting that the positive charge at the C-terminus of Hsp25 is important for chaperone activity. Studies on αA-crystallin, which has a polar but uncharged serine residue at its C-terminus, demonstrate that introduction of positivity at or near the C-terminus does not detrimentally affect the chaperone activity of this sHsp at 37°C [220,225]. Conversely, substitution of the two C-terminal lysines of αB-crystallin lysine with leucine results in decreased ability to protect against target protein precipitation at 25°C [151]. Despite a loss of flexibility in the C-terminal extension of αB-crystallin upon interaction with γ-crystallin, truncation of five residues from the C-terminus does not affect the chaperone activity of this sHsp [214]. It appears, therefore, that the C-terminal residues are not directly involved in the capture of target proteins.

The truncation of 35 residues from the N-terminus of Hsp16.3 results in the inability of this sHsp to form large oligomers or display chaperone activity towards reduced target proteins [350], indicating that the larger oligomeric species is required for chaperone function. Similarly, the presence of smaller Hsp25-K209L species lacking chaperone activity could result in the overall reduction in chaperone activity observed for this mutant, despite the oligomers

being of comparable size to the wildtype protein potentially possessing full chaperone activity.

5.7.2. Thermal Stress Assays

Yeast ADH is a tetramer of four equal subunits, with a total mass of 141,000 Da. Each ADH subunit contains a zinc atom that is essential for its enzymatic activity [351]. Inactivation of yeast ADH results in the precipitation of the subunits and therefore can be achieved by the addition of a chelation agent, such as EDTA, in the presence of mild heat (commonly 37°C) or incubation under higher temperatures in the absence of EDTA. As such, ADH is a common target protein for both chelation and thermal aggregation assays. This study utilises the higher temperature inactivation of yeast ADH to assess the effectiveness of wildtype and mutant Hsp25 as molecular chaperones at elevated temperatures.

Thermal stress assays using yeast ADH are commonly performed at temperatures of 48 to 60°C. The inactivation and precipitation of yeast ADH at 55°C has been studied previously [282] and this temperature was found to produce the optimal rate of precipitation under the conditions used in this study (data not shown). This temperature was also well below the onset of observable aggregation and precipitation for all Hsp25 mutants, as shown by thermostability studies (section 5.6). Thus, any precipitation observed cannot be attributed to instability of Hsp25 proteins.

Because yeast ADH dissociates into its subunits and the number of monomers comprising an Hsp25 oligomer is unknown, subunit concentrations are used in this section. In all reactions, a final concentration of 8 μM yeast ADH subunits was used, with increasing concentrations of Hsp25 up to a ratio of 1.4 Hsp25 monomers per ADH subunit. Precipitation was measured as light scattering at 360 nm and the resulting precipitation curves were then converted into percentage precipitation of the 0:1 control ratio.

Wildtype Hsp25 was able to protect ADH from thermally-induced precipitation at all chaperone concentrations used, with complete suppression [315] being observed at a ratio of 1.4:1 and only minimal precipitation occurring for the 0.7:1 ratio (Figure 5.15A). This is consistent with the ability of sHsps to bind target proteins at around a 1:1 ratio. Complete suppression of yeast ADH precipitation was only achievable with approximately three times the relative concentration required for that of insulin under reduction stress, an apparent discrepancy explained by the efficiency of the chaperone activity of sHsps being at least partially dependent on the size of the target protein [216]. This is highlighted by preliminary assays in which the precipitation of catalase (subunit mass 62.5 kDa compared with a subunit mass of 35.3 kDa for yeast ADH) was not able to be fully suppressed at the higher ratio of 2:1 Hsp25 monomers:catalase subunits (data not shown).

Precipitation curves of mutants Hsp25 proteins are shown in Figure 5.15B-I. These results are summarised in Table 5.6 as the relative level of precipitation

for the 0.175:1 ratio of each mutant. This ratio was selected as the level of suppression by wildtype Hsp25 was intermediate and showed the greatest difference between the mutants.

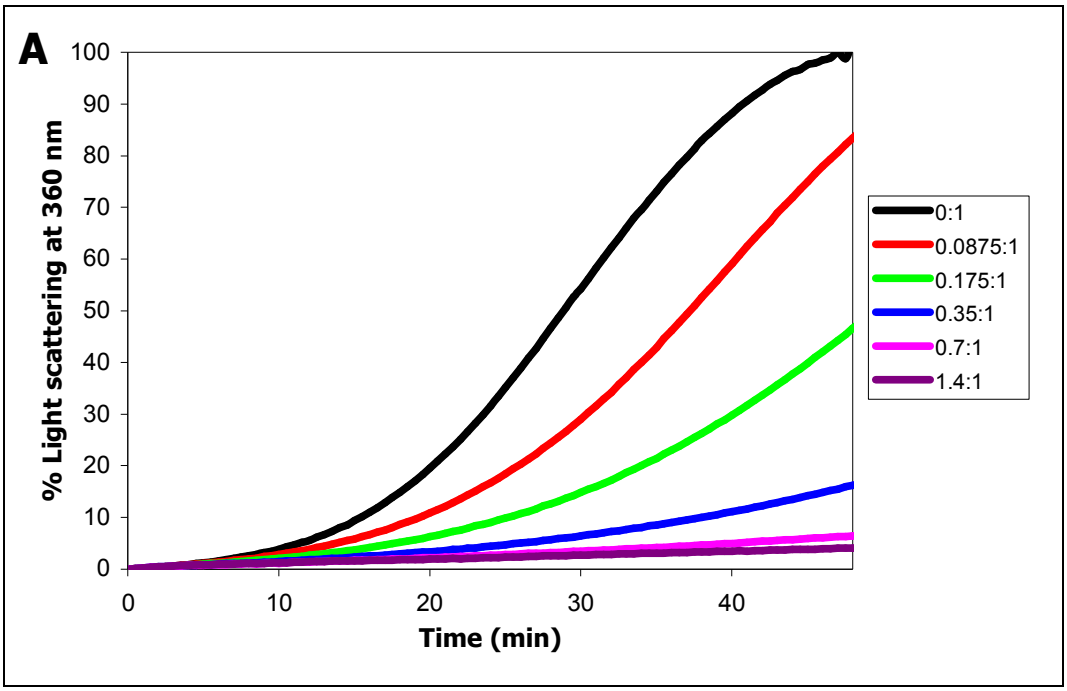

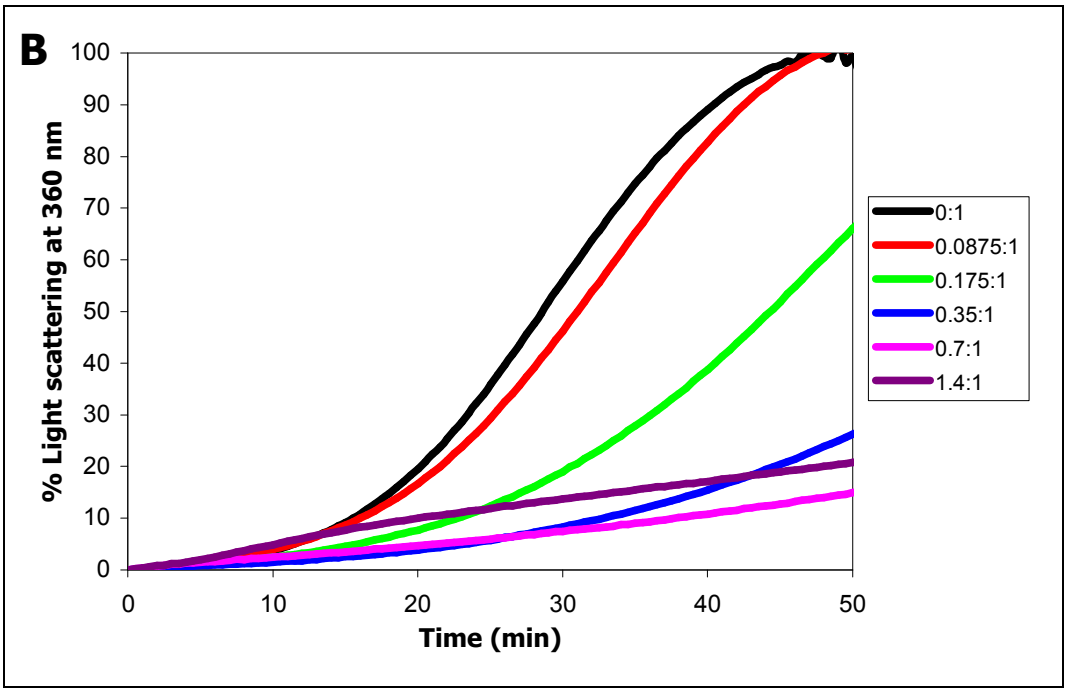

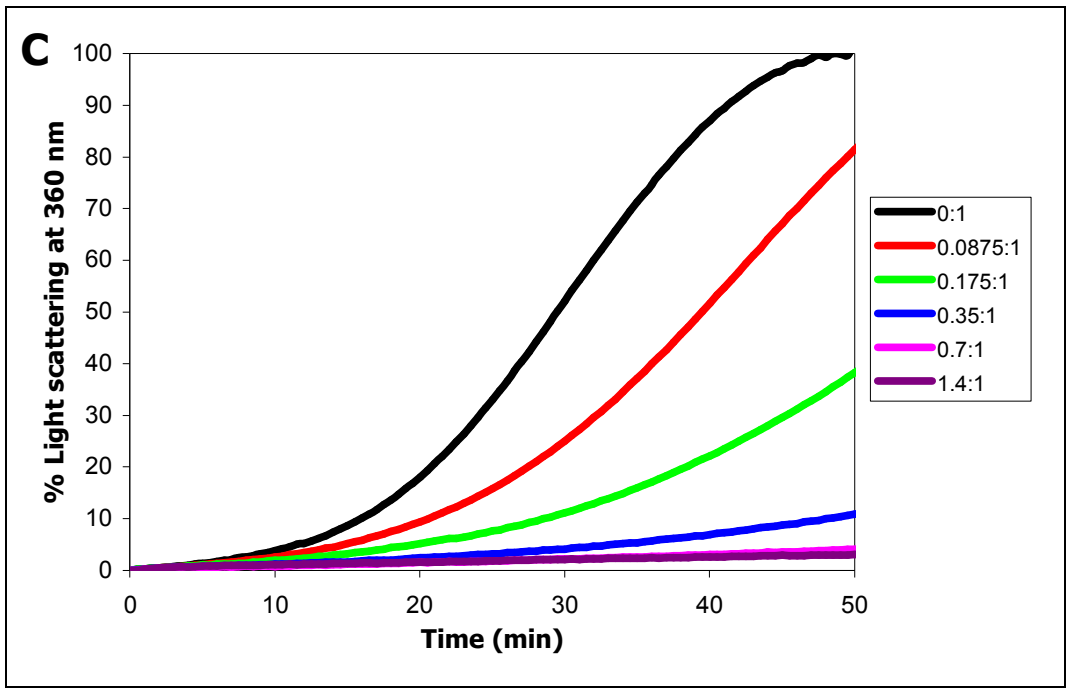
C
% Light scattering at 360 nm
Time (min)
0:1
0.0875:1
0.175:1
0.35:1
0.7:1
1.4:1

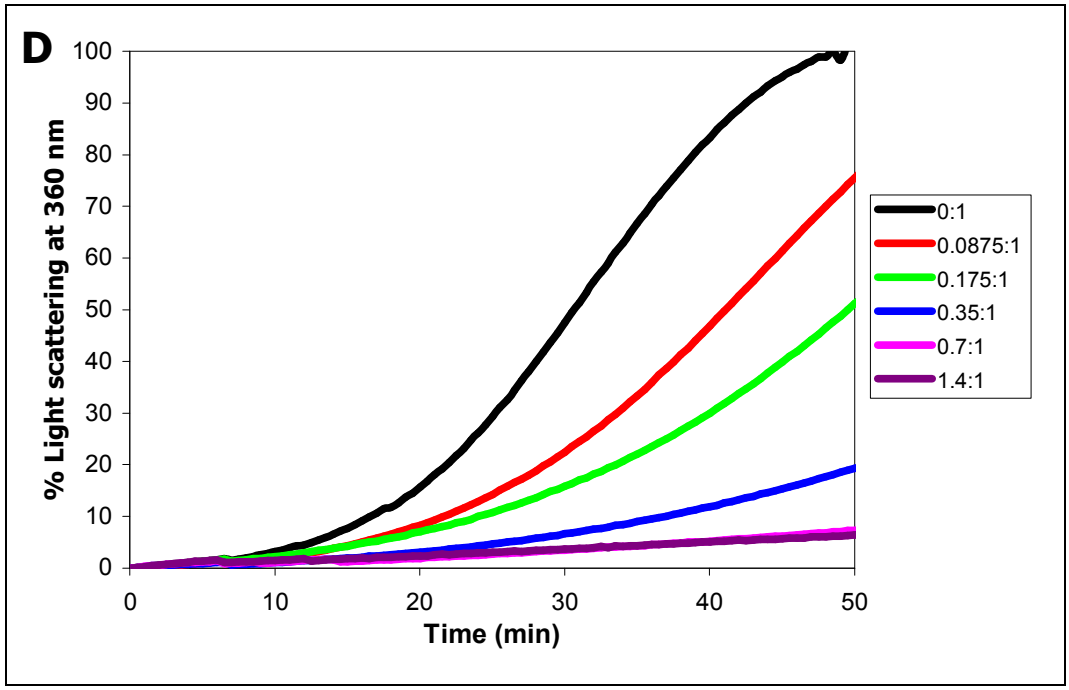
D
% Light scattering at 360 nm
Time (min)
0:1
0.0875:1
0.175:1
0.35:1
0.7:1
1.4:1

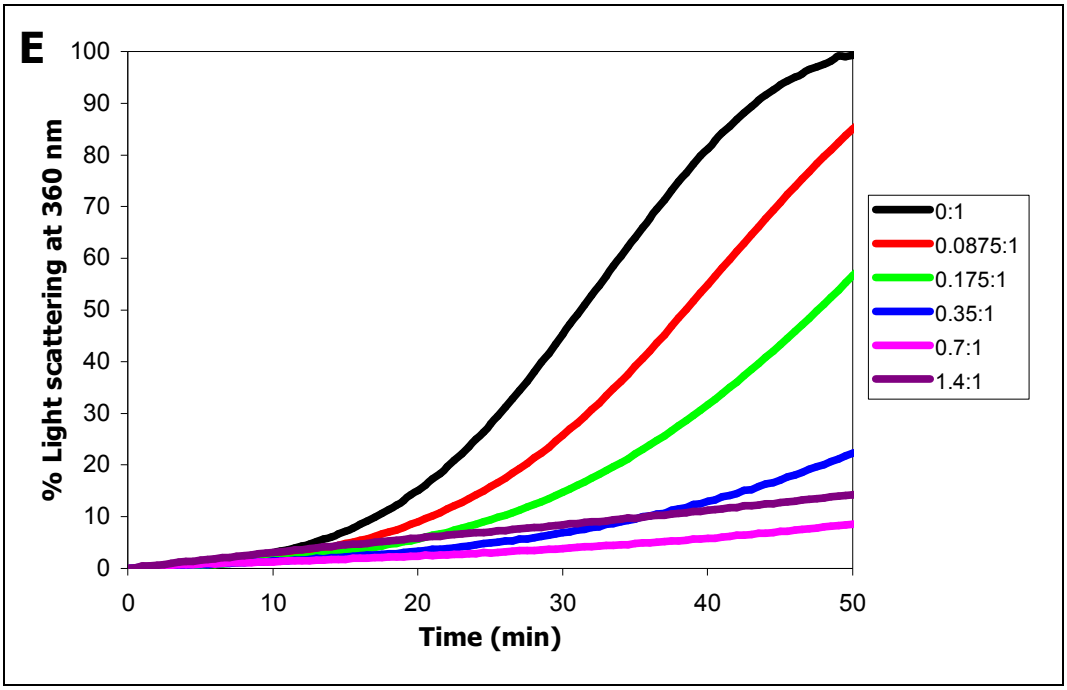
E
% Light scattering at 360 nm
Time (min)
0:1
0.0875:1
0.175:1
0.35:1
0.7:1
1.4:1

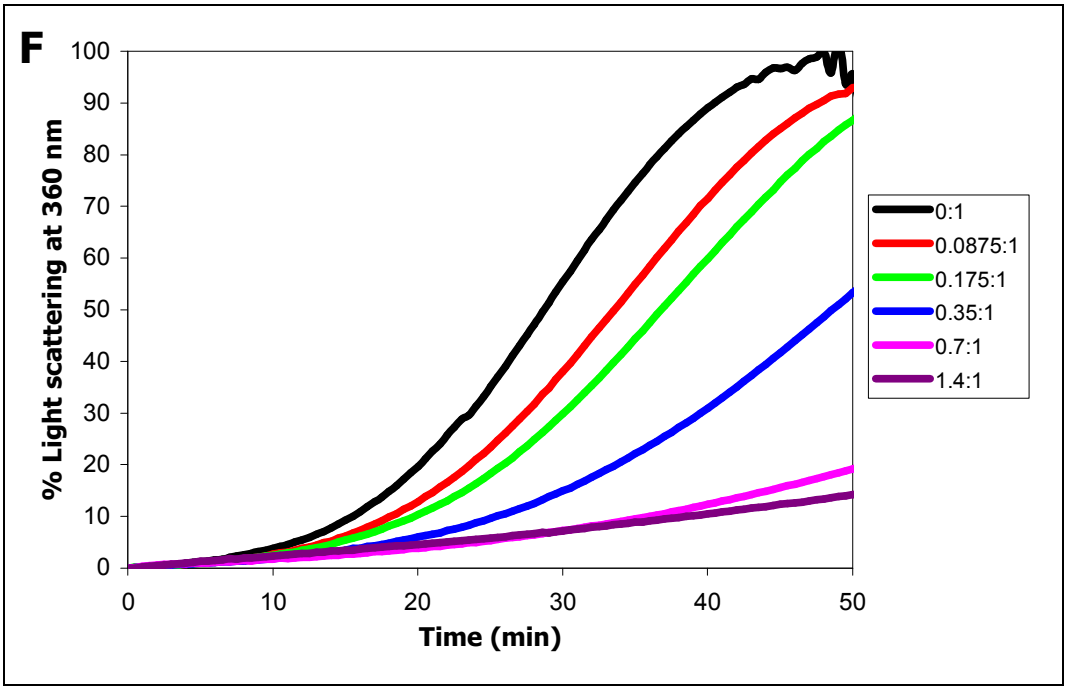
F
% Light scattering at 360 nm
Time (min)
0:1
0.0875:1
0.175:1
0.35:1
0.7:1
1.4:1

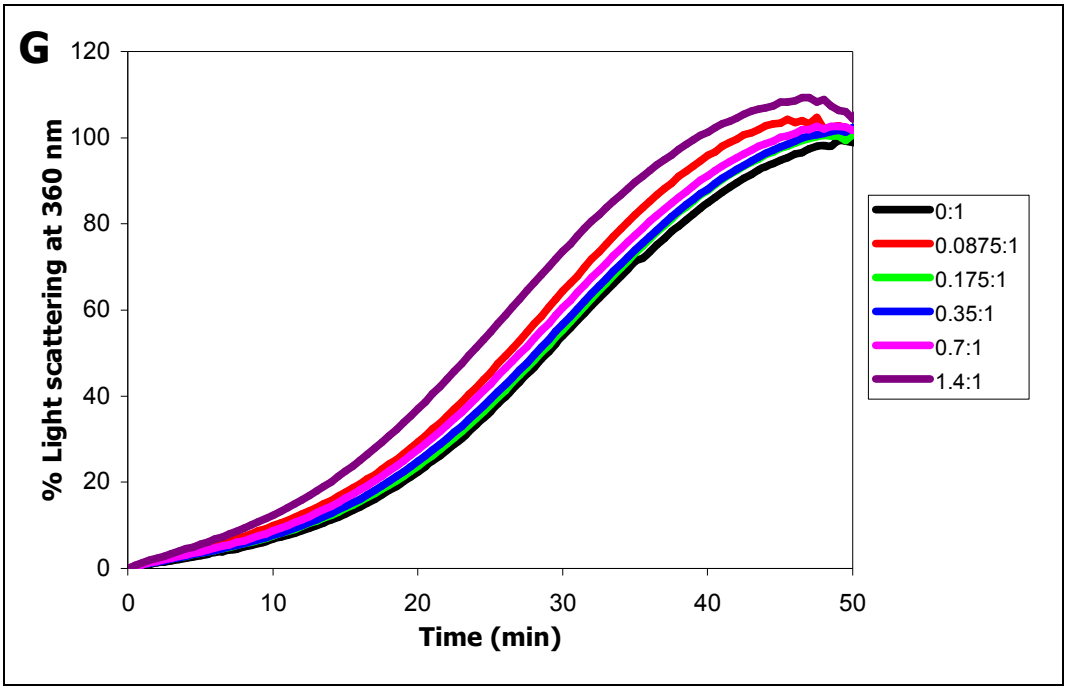
G
% Light scattering at 360 nm
Time (min)
0
20
40
60
80
100
120
0
10
20
30
40
50
0:1
0.0875:1
0.175:1
0.35:1
0.7:1
1.4:1

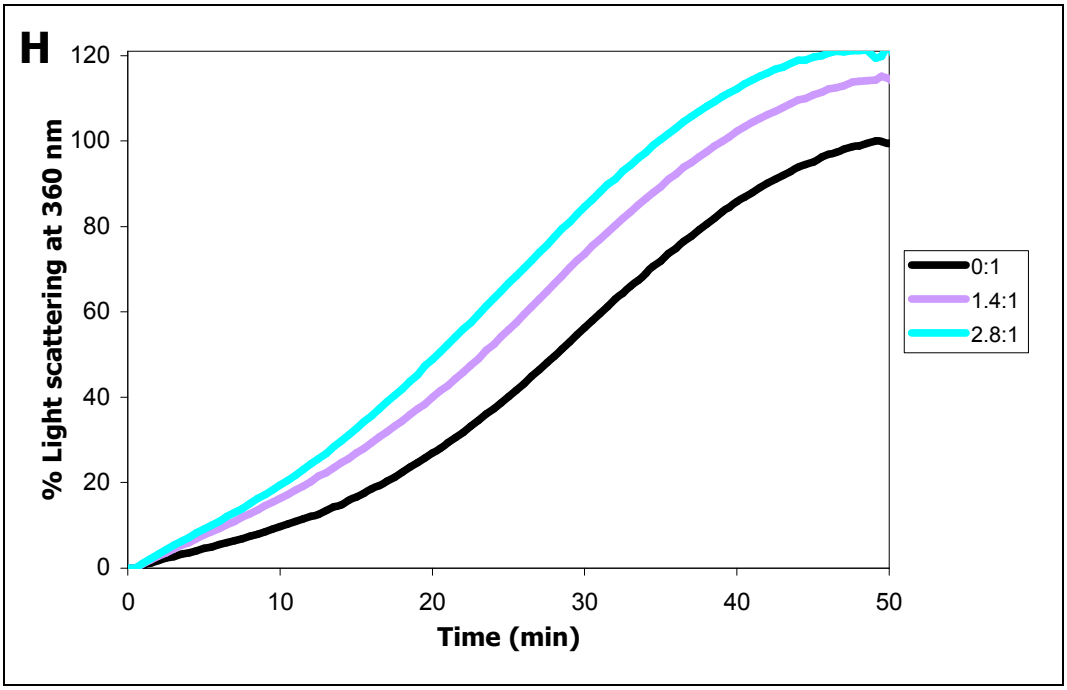
H
% Light scattering at 360 nm
Time (min)
0
20
40
60
80
100
120
0
10
20
30
40
50
0:1
1.4:1
2.8:1

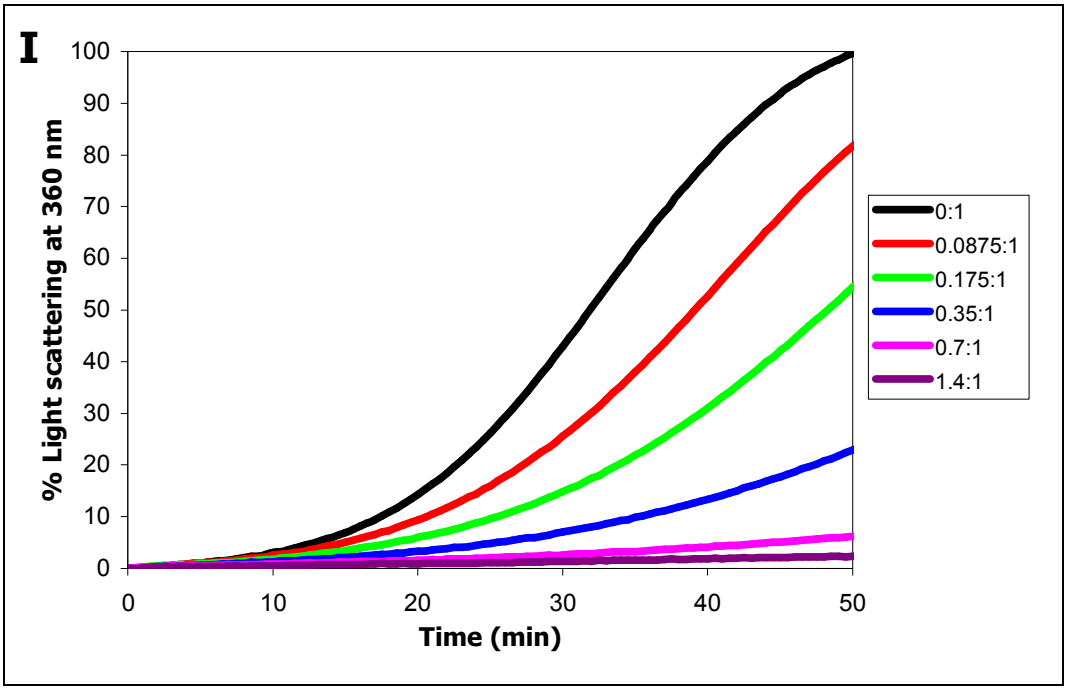

Figure 5.15: Chaperone activity of wildtype Hsp25 (A), Hsp25-E190A (B), Hsp25-R192A (C), Hsp25-Q194A (D), Hsp25-E199A (E), Hsp25-E204A (F), Hsp25-Q205A (G and H) and Hsp25-K209L (I) as measured by the suppression of aggregation of ADH under thermal stress. Assays were performed at 55°C in 50 mM sodium phosphate buffer (pH 7.3) containing 0.02% NaN_3. Ratios represent the molar concentration of Hsp25 monomers to ADH subunits. Traces are the average of duplicates.

The Q194A mutant exhibited comparable chaperone activity to wildtype Hsp25 whilst the R192A mutant displayed slightly better chaperone activity than the wildtype, with the latter protein showing full suppression of ADH precipitation at a ratio of 0.7:1. These observations are similar to those of the reduction stress assays for these mutants and parallel the results from the thermostability studies (section 5.6), suggesting that the same overall structural trends that affect the stability of Hsp25 also influence the effectiveness of chaperone activity.

Table 5.6: Suppression of precipitation [227] for ADH under thermal stress in the presence of Hsp25. Values are the relative suppression of precipitation at 40 min for the 0.175:1 ratio compared with the 0:1 ratio, which represented full precipitation.

Please see print copy for table

Interestingly, the K209L mutant displayed chaperone ability comparable to wildtype Hsp25 for the heat stress assay despite the presence of smaller oligomeric species and diminished activity in the reduction stress assay at 37°C. These observations suggest that the smaller species are not capable of chaperone activity under physiological temperatures but acquire function as a result of the increase in temperature.

It is not surprising that Hsp25-K209L displayed reduced chaperone activity at 37°C, given the decrease in surface hydrophobicity of this mutant observed at 25°C. Changes in sHsp structure occur with increases in temperature, with an accompanying enhancement of chaperone activity for αA- and αB-crystallin

[197,201,324]. In keeping with this observation, relative chaperone activity of the K209L mutant was significantly improved from 37 to 55°C. Additional hydrophobic exposure likely resulted in regions involved in association with the target protein that were obscured at lower temperatures becoming available.

As discussed previously (section 1.6), subunit exchange is a prerequisite for chaperone activity, with increases in temperature increasing the subunit exchange rate of sHsps (section 1.5.6). It is possible that the smaller K209L oligomers are ultimately capable of interacting with target proteins and subsequently assimilating into the large oligomer only at higher temperatures.

Whilst the R192A mutant has significant hydrophobic exposure at room temperature compared with the K209L mutant, these two mutants show the same pattern of increased chaperone activity with temperature. The temperature-induced structural changes therefore appear to facilitate the sequestration and binding of target proteins in both of these mutants, despite their overall structural differences at 25°C, again highlighting that caution must be used when linking the function of sHsps to the overall structure.

The C-terminal residue is proposed by some to act as a "hook" to bring the target proteins into the sHsp oligomer [151] However, substitution of the C-terminal lysine residue of Hsp25 did not significantly affect chaperone activity with ADH under thermal stress, suggesting that the C-terminal residue is not required for interactions between Hsp25 and target proteins. Previous studies have shown that sHsps lacking a C-terminal extension are able to prevent the

aggregation of target proteins to a significant degree at elevated temperatures [145,171,218,221]. This provides further evidence that the C-terminal extension is not vital for the chaperone activity of sHsps and any role it plays, if any, in the direct interaction with target proteins is minimal.

The chaperone activity of the E190A and E204A mutants with ADH under heat stress was significantly reduced whilst the E199A mutant showed comparable chaperone activity to wildtype Hsp25. This is surprising, given that all three glutamic acid residue mutants showed a decrease in chaperone activity under reduction stress conditions and similarities in overall structural changes and thermostability. It is therefore highly probable that the structure of regions important for the function of Hsp25 have been disrupted in all of the glutamic acid residue mutants under physiological conditions but that the increase in temperature induced structural changes that resulted in the E199A mutant being an effective chaperone at this elevated temperature.

Of the glutamic acid residue mutants, Hsp25-E204A showed the most pronounced reduction in chaperone activity under both reduction and heat stress when all ratios were considered. This mutant is the most structurally perturbed of the glutamic acids mutants overall, so it is intuitive that it would have the greatest functional impact. However, as mentioned previously, the overall structure must be linked to function with caution. The functional effects of the E204A mutant may therefore be at least partially attributed to the greater accessibility of this residue, with the reduction in polarity at this position

being more disruptive to important interactions than changes at the other locations. A similar substitution in Hsp30C in which the aspartic acid at the fifth residue from the C-terminus was replaced with a glycine also resulted in diminished chaperone activity, as measured by the protection of citrate synthase precipitation at 40°C and reactivation of luciferase at 42°C [226]. Thus, it appears that acidic residues in the C-terminal extension of sHsps are particularly important for proper functioning as chaperone proteins.

The Q205A mutant demonstrated inability to protect ADH under thermal stress (Figure 5.15G), with higher chaperone levels resulting in increased light scattering. This became more apparent with further increases in Hsp25-Q205A concentration (Figure 5.15H). Because maximum precipitation of the target protein occurs in the absence of chaperone, the increases in light scattering observed for all ratios in relation to the control is indicative of insolubilisation of the Q205A mutant as well as the target protein, i.e. co-precipitation [145].

The additional precipitation was not a result of interactions between Q205A oligomers as all Hsp25 mutants were stable in isolation at 55°C, as shown by thermostability studies (section 5.6). Precipitation of Hsp25-Q205A oligomers must therefore be a result of interactions with target proteins, with the formed complexes becoming unstable. This demonstrates that the Q205A mutant is capable of significant sequestration of target proteins despite a reduction in exposed hydrophobicity.

The insolubilisation of Hsp25-Q205A-target protein complexes indicates that target protein molecules associated with the sHsp oligomer retain a significant amount of hydrophobic exposure and are capable of interacting with each other [145]. This has also been observed for αB-crystallin in the presence of α-lactalbumin under reduction stress [152,256]. This is not simply a result of decreased overall exposed hydrophobicity, or the K209L mutant would have also co-precipitated with the target protein. It appears that the Q205A mutant is capable of effectively sequestering the target protein but not sufficiently shielding its hydrophobic regions. This is possibly a result of the target protein not fitting properly into the chaperone binding site due to structural perturbations in or around the binding site, leaving hydrophobic regions exposed. This would be exacerbated in the smaller oligomers, where steric hindrance would allow even less effective protection of the target protein.

As mentioned previously (section 1.6), target protein size can influence the efficiency of the chaperone action of sHsps. Smaller molecules, such as insulin, are able to fit more snugly into the proposed binding site in the grooves between sHsp monomers within the sHsp oligomer, whereas larger target proteins spill to the exterior of the complex. Larger target proteins are therefore able to interact with or block the C-terminal extension. This is shown by the loss of flexibility of the C-terminal extension of αB-crystallin for chaperone assays with α-lactalbumin and ovotransferrin (monomeric masses of 14 and 77 kDa, respectively) but the maintenance of flexibility when insulin is present as a target protein [216]. It is likely that the smaller Hsp25-Q205A

oligomeric species were unable to accommodate the larger ADH molecules due to steric restraints, whereas this was not a problem for the small insulin molecule.

In summary, wildtype Hsp25 and seven C-terminal extension mutants with reduced polarity in the flexible region were characterised by a variety of spectroscopic techniques. This study has found that, although polarity is an important feature of the C-terminal extension of sHsps, not every polar residue is important in Hsp25. The R192A and Q194A mutants showed only minor functional differences compared with the wildtype protein. The increased exposure of clustered hydrophobic regions and reduced flexibility in the vicinity of the tryptophan residues of these mutants were not sufficient to alter the oligomeric size or result in significant functional effects. It can be concluded that substitution of either the R192 or Q194 residues resulted in fully functional proteins with no detectable effect on the oligomeric structure.

Replacement of either the Q205 and K209 residues with alanine and leucine, respectively, produced proteins with significant reductions in exposed clustered hydrophobicity, which most likely contributed to the severely perturbed oligomeric structures observed. Both mutants were present as three distinct oligomeric species, although the sizes of the oligomers and relative distributions differed for the two proteins.

The predominant form of the K209L mutant was an oligomer corresponding in size to that of wildtype Hsp25, with the less abundant species both being

smaller than 250 kDa, the lower limit of the column used. This mutant was functionally deficient under reduction stress conditions but showed activity comparable to the wildtype protein in the heat stress assay, consistent with the smaller species being able to effectively sequester target proteins only after significant temperature-induced structural changes had taken place. The C-terminal lysine residue appears to be dispensable for function under some conditions but is required for the structural integrity of Hsp25.

Substitution of the Q205 residue resulted in a functionally defective protein with disrupted structure. None of the oligomeric sizes of the Q205A mutant corresponded to the wildtype Hsp25 oligomer and the most abundant species was the larger of the two forms with sizes less than 250 kDa, possibly a tetramer. This mutant was more susceptible to alterations in secondary and tertiary structures than the other mutants, with the polarity of the tryptophan environment being decreased. The reduction in thermostability of this mutant compared with wildtype Hsp25 is consistent with altered packing of the monomeric subunits. Comparable chaperone activity to the wildtype protein was observed under reduction stress conditions, indicating that all species were functional. However, the chaperone activity of this mutant was abolished under heat stress conditions, with the formation of unstable sHsp-target protein complexes resulting in co-precipitation. This is likely to be a result of incomplete protection of the hydrophobic regions on the target proteins as a result of the size of the target protein. NMR studies were performed to assess the flexibility of the C-terminal extension of the Q205A mutant in an attempt to

explain the unusual structure and chaperone behaviour of this mutant – these results are presented in Chapter 6.

Replacement of each of the glutamic acid residues in the C-terminal extension with alanines produced proteins with comparable and slightly smaller oligomeric sizes that were functionally deficient compared with wildtype Hsp25. These mutants displayed poor thermostability, consistent with the significant increases in exposed clustered hydrophobicity, and reduced chaperone activity under both reduction and heat stress. The presence of each of these residues is important for stabilisation of the entire protein, consistent with glutamic acid being vital for the formation of stabilising ion pairs in proteins from thermophilic organisms under extreme heat conditions [305,346,347]. From these studies, it is clear that each of the glutamic acid residues in the C-terminal extension of Hsp25 are required for the stability of Hsp25 at elevated temperatures and the ability of this sHsp to function effectively as a molecular chaperone.

Chapter 6

Nuclear Magnetic Resonance Spectroscopy of Wildtype and Mutant Hsp25

Because they exist under native conditions as large oligomeric species, sHsps would be expected to give rise to very broad NMR resonances which would not make them amenable to investigation by NMR spectroscopy. However, the protruding C-terminal extension is polar, highly mobile and relatively unstructured, making the investigation of the flexibility of residues in this region by NMR spectroscopy feasible [345].

NMR spectroscopy was performed on wildtype Hsp25 and a mutant protein in order to investigate the effects of the mutation on the flexibility of the C-terminal extension itself. The Q205A mutant was selected for investigation by NMR spectroscopy because it displayed some unusual structural and functional characteristics compared wildtype Hsp25 that were not observed for any of the other mutants investigated (Chapter 5). Hsp25-Q205A showed altered tertiary structure in the vicinity of the tryptophan residues in the N-terminal domain, disrupted oligomer formation and reduced thermostability. This mutant also became insoluble in the presence of unstable target proteins at high temperature. These observations indicate that the Q205 residue is particularly important for the formation of the native structure of Hsp25 and the chaperone activity of this sHsp under some conditions.

Wildtype Hsp25 and the Q205A mutant were uniformly labelled with the NMR-sensitive isotope ^{15}N for the purposes of 2D NMR studies to determine detailed and specific information about the relative flexibility of residues in this region of the protein.

6.1. Expression and Purification of ^{15}N-Labelled Wildtype Hsp25

^{15}N-Labelled Hsp25 proteins were expressed and purified in the same manner as unlabelled wildtype, except that bacteria were cultured in ^{15}N-M9 minimal media, in which the only source of nitrogen present was $^{15}NH_4Cl$. Bacterial growth of *E. coli* BL21(DE3) (pAK3038-Hsp25) in minimal media was considerably slower than in full nutrient media and a comparable level of overexpression was achieved by incubating for ~24 h after induction (data not shown).

The purity and labelling efficiency of Hsp25 and the Q205A mutant were assessed by mass spectrometry (Figure 6.1, Table 6.1 and Table 6.2). Both proteins existed mostly in the N-terminally excised form, consistent with purification of unlabelled Hsp25 (section 4.2.1). Modification of the cysteine residue was not observed for ^{15}N-labelled wildtype Hsp25, with the peak at 23,301.2 Da being within 1 Da of the expected mass for unmodified full-length ^{15}N-labelled Hsp25 and the predominant peak at 23,168.4 Da corresponding to this protein lacking the N-terminal methionine residue. ^{15}N-labelled Hsp25-Q205A, however, was found only in the modified form, with the peaks at 23,314.9 and 23,182.0 Da representing the full-length and N-terminally excised forms of the modified mutant protein, respectively. This is an unexpected result, as a significant proportion of unmodified proteins were present in

samples containing the modification for both unlabelled wildtype and mutant Hsp25. The reasons for these differences remain unclear.

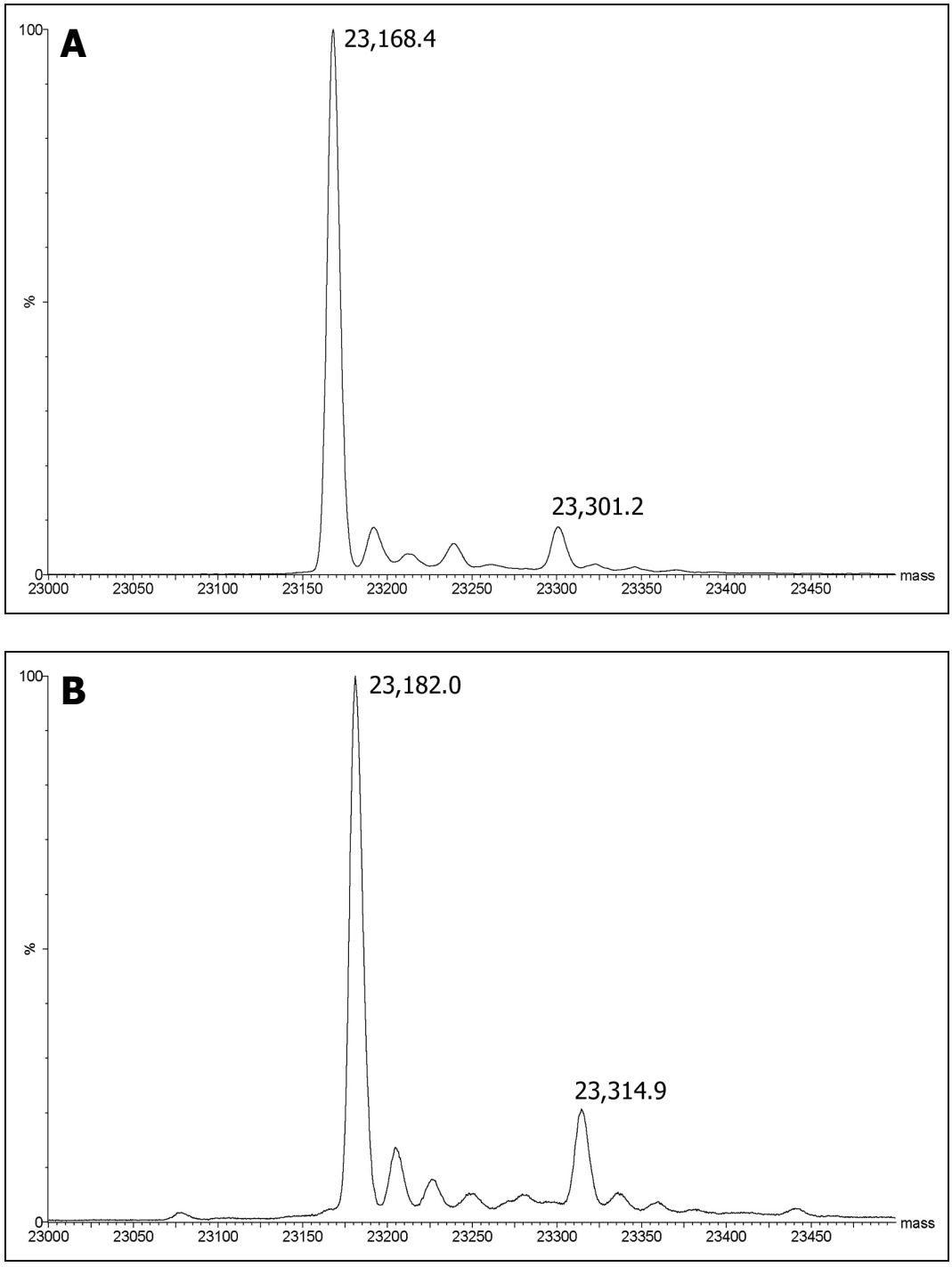

Figure 6.1: Mass spectra of purified ^{15}N-labelled wildtype Hsp25 (A) and ^{15}N-labelled Hsp25-Q205A (B) obtained by nanoscale electrospray ionisation mass spectrometry.

Table 6.1: Efficiency of uniform ^{15}N-labelling of wildtype Hsp25 as calculated from ESI-MS masses.

	Unmodified		With +71 Da adduct	
	full length	excised Met	full length	excised Met
Mass of unlabelled protein (Da)	23,014	22,883	23,085	22,954
Number of Nitrogens	288	287	288	287
Expected mass of labelled protein (Da)	23,302	23,170	23,373	23,241
Mass of labelled protein by ESI-MS (Da)	23,301.2	23,168.4	-	-
^{15}N-labelling efficiency	>99.9%	>99.9%	-	-

Table 6.2: Efficiency of uniform ^{15}N-labelling of Hsp25-Q205A as calculated from ESI-MS masses.

	Unmodified		With +71 Da adduct	
	full length	excised Met	full length	excised Met
Mass of unlabelled protein (Da)	22,957	22,826	23,028	22,897
Number of Nitrogens	287	286	287	286
Expected mass of labelled protein (Da)	23,244	23,112	23,315	23,183
Mass of labelled protein by ESI-MS (Da)	-	-	23,314.9	23,182.0
^{15}N-labelling efficiency	-	-	>99.9%	>99.9%

Purification of ^{15}N-labelled wildtype and mutant Hsp25 was successful, with minor contaminating peaks corresponding to sodium adducts on the various forms of this sHsp. Labelling efficiency was very high (>99.9%), as calculated by comparing the mass obtained by ESI-MS with the expected mass of each protein species (Table 6.1 and Table 6.2).

6.2. ^{1}H-^{1}H and ^{1}H-^{15}N Nuclear Magnetic Resonance Spectroscopy

Cross-peaks arising from residues in the C-terminal extension of wildtype Hsp25 and Hsp25-Q205A are shown in ^{1}H-^{15}N two-dimensional HSQC spectra (Figure 6.2 and Figure 6.3, respectively). The sequential assignment [352] of the majority of residues in the C-terminal extension was achieved by identification of residue type through intraresidue NH, αH, βH and occasionally γH couplings in the TOCSY spectra (Figure 6.4A and Figure 6.5A) and correlation to random coil values for amino acids followed by alanine or proline [353]. Residue sequence was confirmed through interresidue $NH_{i+1} \rightarrow \alpha CH_i$ correlations from NOEs observed in the NOESY spectra (Figure 6.4B and Figure 6.5B).

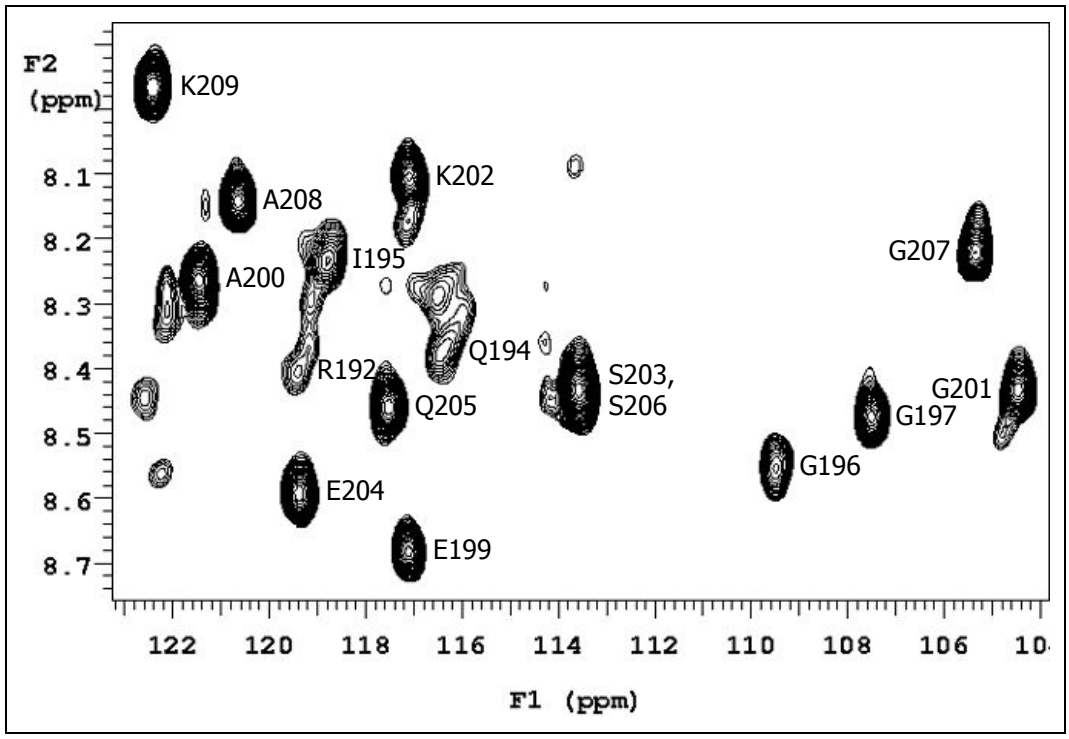

Figure 6.2: ^{15}N-^{1}H HSQC spectrum of ^{15}N-labelled wildtype Hsp25 in 10 mM phosphate buffer (pH 6.5) containing 0.02% NaN_3 at 25°C.

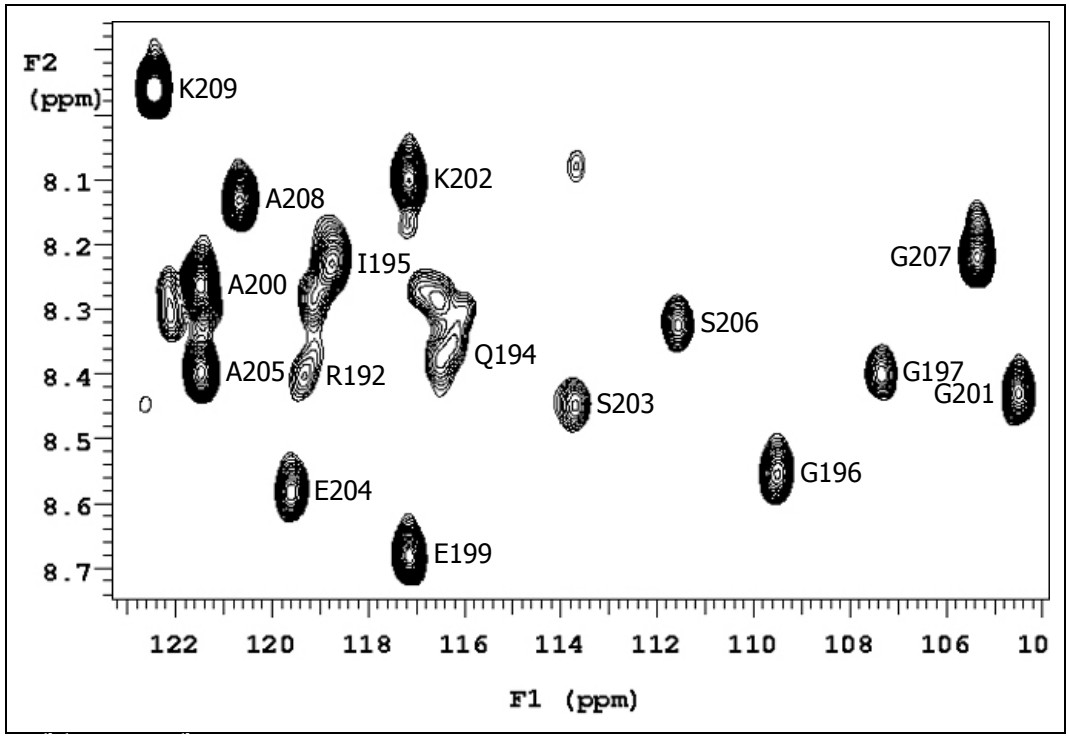

Figure 6.3: ^{15}N-^{1}H HSQC spectrum of ^{15}N-labelled Hsp25-Q205A in 10 mM phosphate buffer (pH 6.0) containing 0.02% NaN_3 at 25°C.

The chemical shifts of each of the identified residues in the C-terminal extension of wildtype Hsp25 and Hsp25-Q205A are given in Table 6.3 and Table 6.4, respectively, and compared with those of resonances from residues in a random coil conformation [353]. ^{1}H chemical shifts within $\pm$0.15 ppm of the expected values are considered to be representative of residues in regions that are flexible and unstructured [354]. Most of the residues in the C-terminal extension of both wildtype and mutant Hsp25 fall within this range. However, the residues in the I195-E199 region show greater differences compared with expected values for random coil regions. The presence of resonances arising from all of the residues in the C-terminal extension of Hsp25 in the NMR spectra demonstrate that they have little preferred conformation. The greater variation in chemical shift values of residues near the C-terminus compared with others in the C-terminal extension is consistent with a reduction in conformational flexibility towards the anchor point of the extension [345]. The K209 residue in both wildtype and mutant Hsp25 proteins is at the C-terminus, whereas expected random coil chemical shift values are based on residues followed by an alanine.

Table 6.3: ^{1}H chemical shifts for ^{15}N-labelled wildtype Hsp25. Expected values are random coil chemical shifts given by Wishart *et al.* (1995) [353]. *The G197 residue is followed by a proline residue.

Please see print copy for table

Table 6.4: ^{1}H chemical shifts for ^{15}N-labelled Hsp25-Q205A. Expected values are random coil chemical shifts given by Wishart *et al.* (1995) [353]. *The G197 residue is followed by a proline residue.

Please see print copy for table

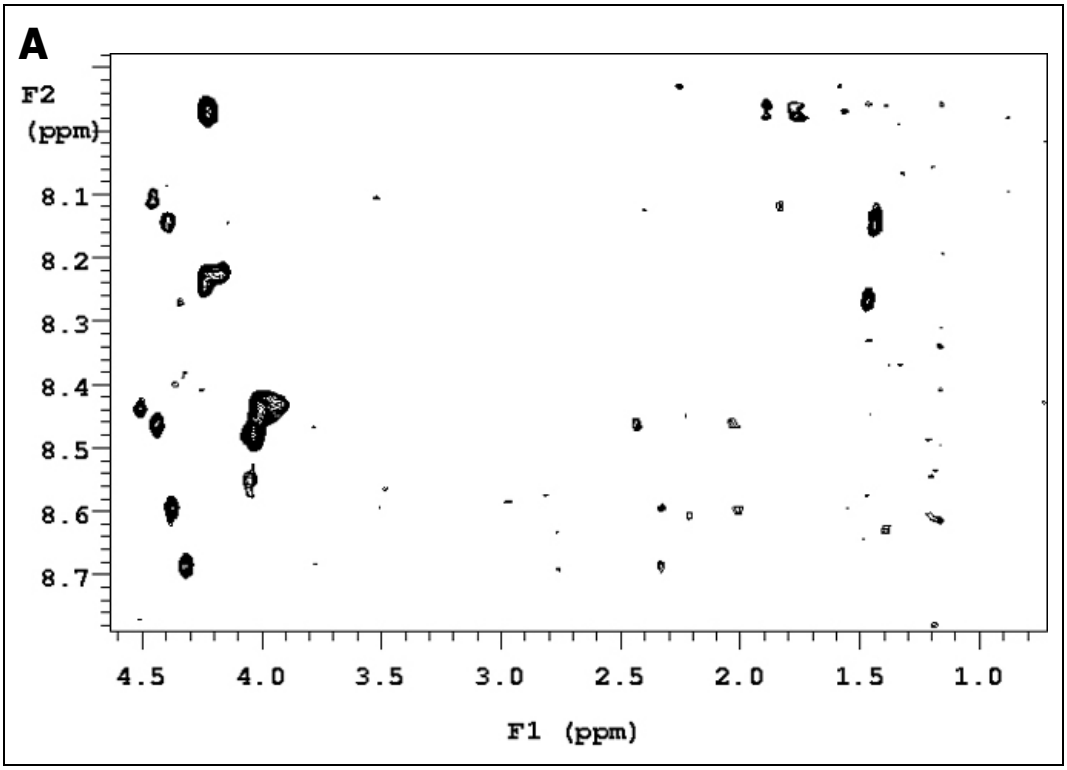

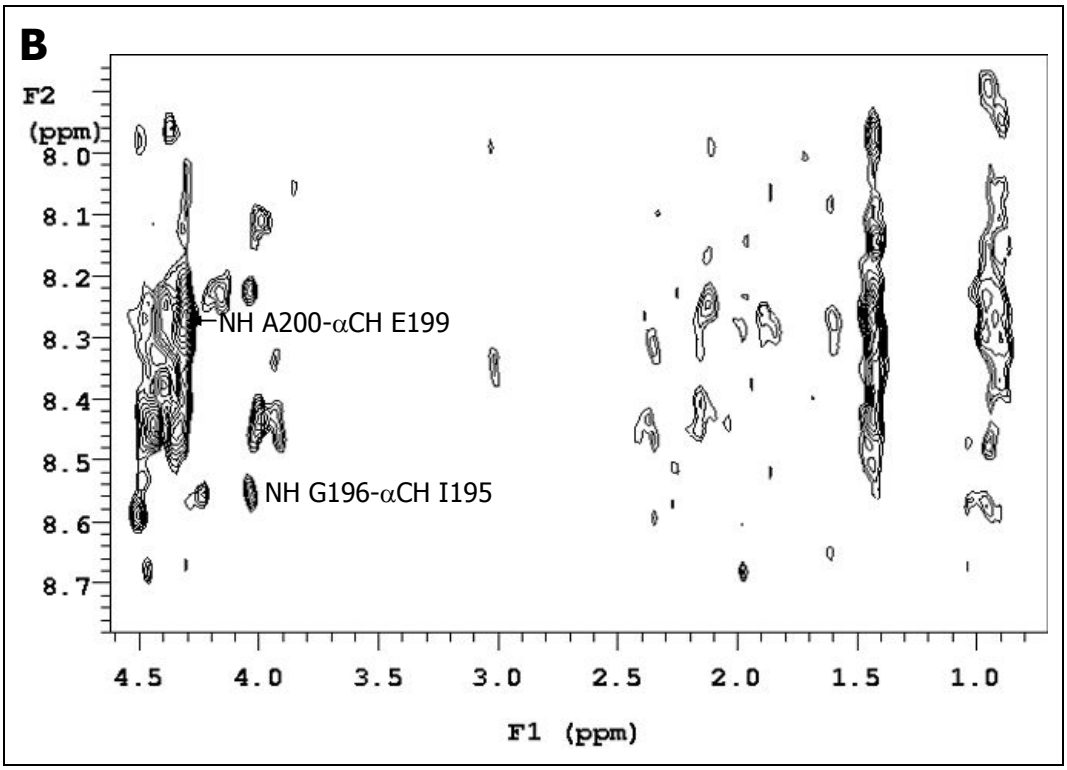

Figure 6.4: TOCSY (A) and NOESY (B) spectra of ^{15}N-labelled wildtype Hsp25 in 10 mM phosphate buffer (pH 6.5) containing 0.02% NaN_3 at 25°C. Representative NOEs between adjacent residues are indicated (B).

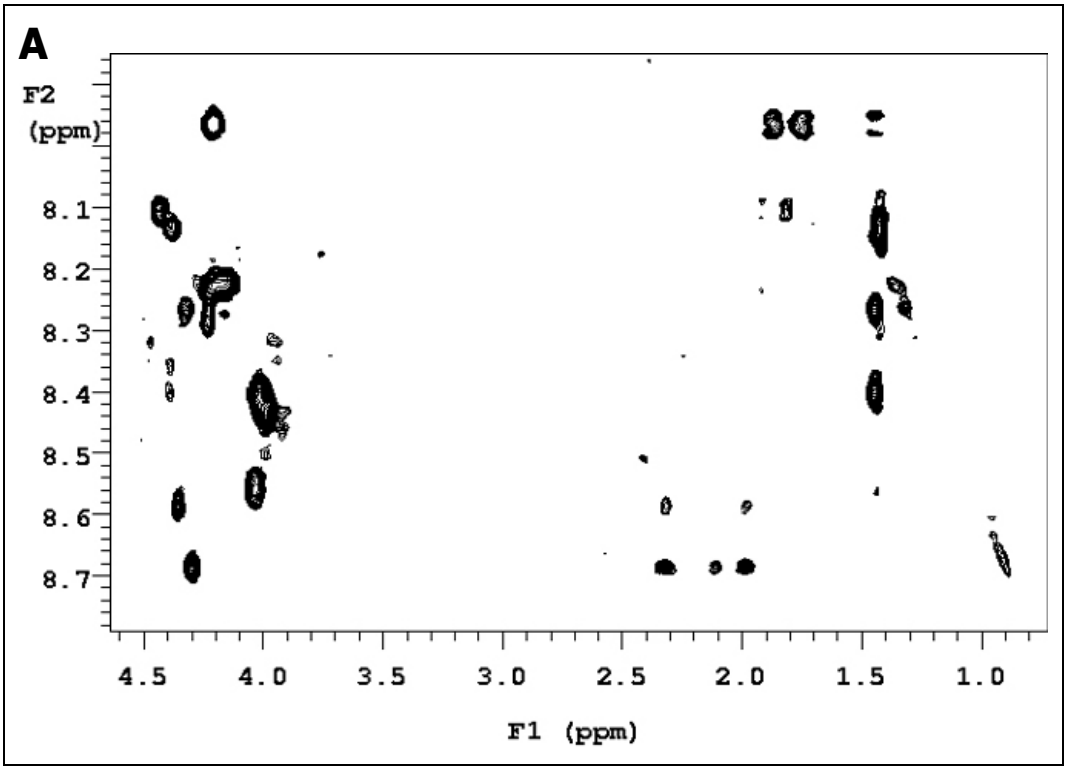

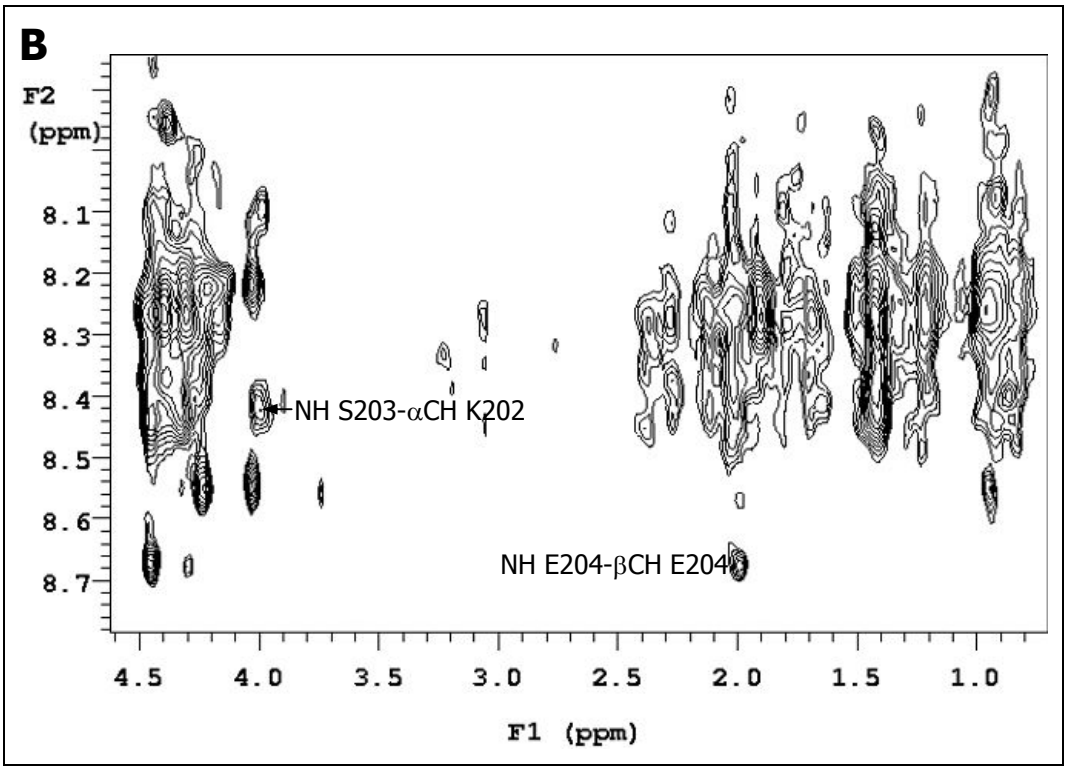

Figure 6.5: TOCSY (A) and NOESY (B) spectra of ^{15}N-labelled Hsp25-Q205A in 10 mM phosphate buffer (pH 6.0) containing 0.02% NaN_3 at 25°C. Representative NOEs between adjacent residues are indicated (B).

The ^{1}H NH chemical shifts are consistent between the two proteins, with the exception of G197 and S206, suggesting that the overall flexibility of the C-terminal extension is not significantly altered as a result of substitution of the glutamine residue at position 205 to non-polar alanine. The two serine residues overlap in the wildtype HSQC spectrum but are distinguishable in the Q205A spectrum, suggesting that the mutation of the Q205 residue has significant effects on the structure of the adjacent residue. Conversely, the preceding residue, E204, does not appear to be affected. This observation may be also be a result of localised alterations in the magnetic environment of the residues at positions 205 and 206 as a result of the mutation that slightly alters their chemical shifts.

Differences in the intensity of cross-peaks between wildtype Hsp25 and Hsp25-Q205A, particularly in the TOCSY and NOESY spectra, arise from minor differences in sample conditions between the two proteins. Preliminary spectra of wildtype Hsp25 were acquired using a sample that became unstable at pH 6.0 and some precipitate was observed. This was not seen for the mutant protein, which remained in solution at pH 6.0 for the duration of spectral acquisition. A second ^{15}N-labelled wildtype sample was used for the acquisition of the spectra presented here. In order to minimise the potential for precipitation of this sample, the pH was 6.5 rather than 6.0.

The structures of ^{15}N-labelled αA- and αB-crystallin, as determined by far- and near-UV CD and tryptophan fluorescence spectroscopy, have been shown to be

different to the corresponding unlabelled proteins, suggesting that the overall conformation of these proteins is affected by ^{15}N-labelling [221]. Such changes appear to have also occurred here, resulting in instability of ^{15}N-labelled wildtype Hsp25. The concentration of the wildtype protein was therefore lower than that of the Q205A mutant. These differences are not important for these studies, however, as the above spectra were used only for identification of the residues. The spectra presented in the remainder of this chapter were compared directly only to related spectra for the same sample and differences were therefore relative, not absolute, allowing comparisons between the samples under slightly different conditions to be made.

6.3. Longitudinal and Transverse ^{15}N Relaxation Studies

The measurement of ^{15}N longitudinal (T_1) and transverse (T_2) relaxation times gives valuable information on the dynamics of a protein over a wide time-scale [355]. The ^{15}N values measured give information on the peptide backbone, with T_1 values representing motion in the protein occurring in the time range of 10^8-10^{12} s^{-1} and T_2 values giving information on motion occurring within micro- or milliseconds.

A series of HSQC spectra were acquired with increasing delay times after the application of a 180° or 90° pulse for T_1 or T_2 measurements, respectively, and the peak integrals of each cross-peak were plotted against delay time (Figure 6.6). The peak integral typically decays exponentially with respect to the delay time and the exponent is the longitudinal or transverse relaxation time.

Experimental T_1 and T_2 relaxation time constants and T_1/T_2 ratios were determined for wildtype Hsp25 and Hsp25-Q205A (Figure 6.7 and Figure 6.8, respectively). Because of the overlapping locations of the serine residues in the HSQC spectra of wildtype Hsp25, the relaxation constants of these individual residues could not be determined. For each residue assigned in both proteins, the T_1 values were larger than the corresponding T_2 values, consistent with previous studies for other proteins [292]. The mean T_1 and T_2 values for wildtype Hsp25 were 0.41 ± 0.06 s and 0.16 ± 0.01 s, respectively, and mean T_1 and T_2 values for Hsp25-Q205A were 0.27 ± 0.04 s and 0.17 ± 0.01 s, respectively.

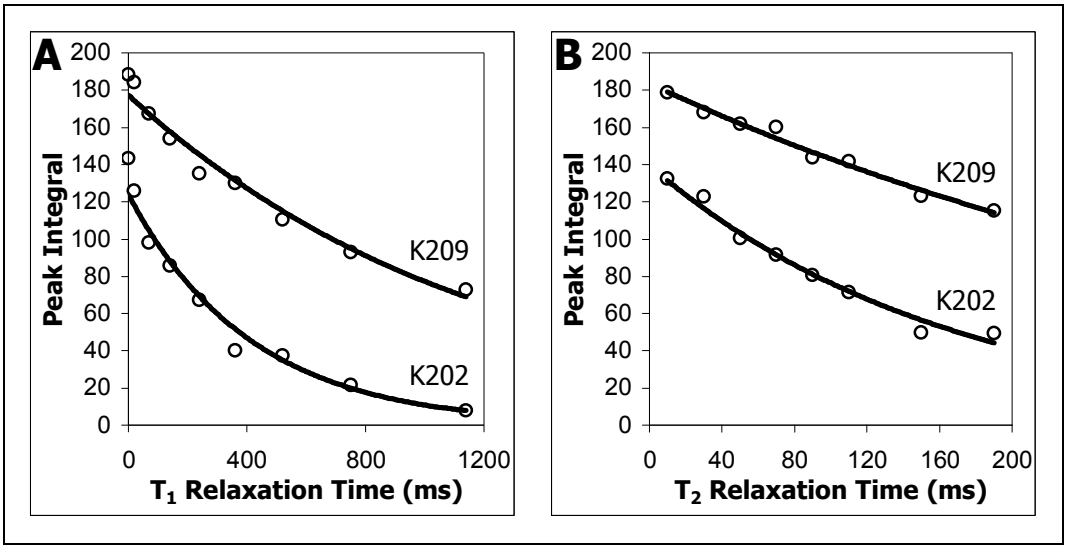

Figure 6.6: Representative exponential decay of peak volume of the cross-peak arising from the lysine residues in the C-terminal extension of wildtype Hsp25 with ^{15}N longitudinal relaxation time (T_1) (A) and ^{15}N transverse relaxation time (T_2) (B). R^2 values are 0.976 (K209 T_1), 0.978 (K202 T_1), 0.980 (K209 T_2) and 0.983 (K202 T_2) as calculated from single, two parameter exponential decay statistical regression in SigmaPlot.

Calculated T_1 and T_2 values were comparable for wildtype Hsp25 from I195 to A208, indicating relatively uniform flexibility in this region. Significant increases were observed for both relaxation times towards the C-terminus, representing a smaller correlation time, and thus greater flexibility, of the K209 residue in particular. Consistent with its location at the tethering point of the flexible region of the C-terminal extension, the R192 residue was found to be less flexible than the other, more C-terminal residues, as indicated by smaller T_1 and T_2 values. The cross-peaks corresponding to this residue were relatively weak as a result of the decreased flexibility.

Compared with the Q205 residue in the wildtype protein, the A205 residue in the mutant had a smaller T_1 value and thus reduced flexibility at this location. Unfortunately, information regarding the relative flexibility of the neighbouring S206 residue was unobtainable in wildtype Hsp25 as its cross-peak overlapped that of the S203 residue in the HSQC spectra. The significant upfield shift of the S206 residue in both ^{1}H and ^{15}N dimensions in the HSQC spectrum of Hsp25-Q205A compared with that of the wildtype protein is consistent with hydrogen bonding between the glutamine and serine residues in wildtype Hsp25 which is lost upon replacement of the glutamine residue with alanine in the mutant [356]. It is likely that such disruption to interactions between the neighbouring residues is at least a contributing factor in the localised variation in flexibility observed between the wildtype and mutant proteins.

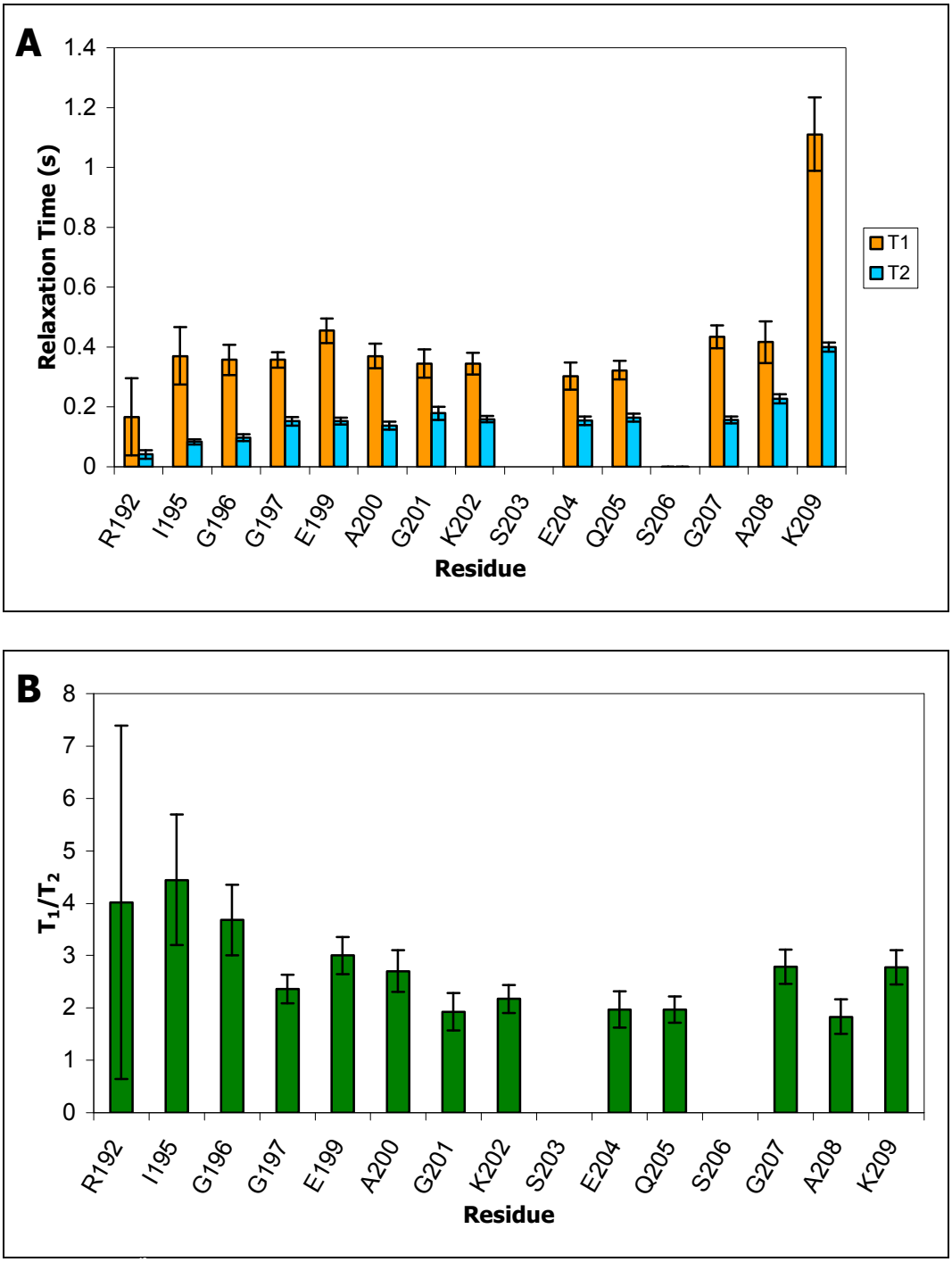

Figure 6.7: T_1 and T_2 analyses of ^{15}N-labelled wildtype Hsp25 showing T_1 and T_2 values (A) and T_1/T_2 ratios (B) for each identified residue in the C-terminal extension. Error bars represent standard errors of exponents given by non-linear statistical regression in SigmaPlot (A) and calculated standard error of a ratio (B).

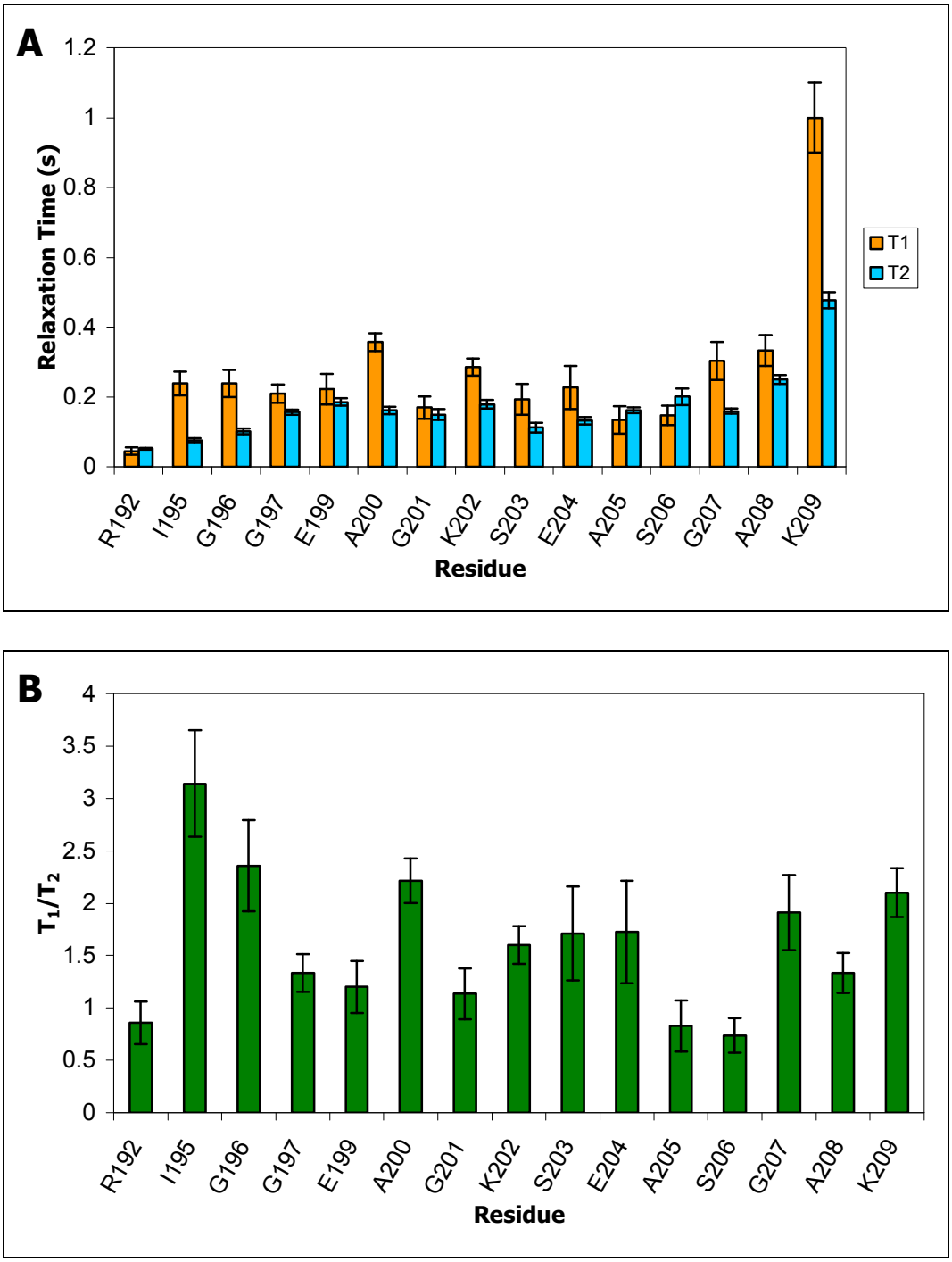

Figure 6.8: T1 and T2 analyses of ^{15}N-labelled Hsp25-Q205A showing T_1 and T_2 values (A) and T_1/T_2 ratios (B) for each identified residue in the C-terminal extension. Error bars represent standard errors of exponents given by non-linear statistical regression in SigmaPlot (A) and calculated standard error of a ratio (B).

Chapter 7

Interactions Between Hsp25 and αB-Crystallin

More than 90% of the dry weight of lens fibre cells is comprised of crystallin proteins [357]. Although significant amounts of other sHsps, notably Hsp27 and Hsp20, have been detected [120,358], α-crystallin is the main protein in the lens and constitutes 35-40% of the total protein content in human lenses and up to ~50% in some animal species [357,359,360]. Lens transparency is highly dependent on the short-range order of α-crystallin molecules [361,362] and the protection of other crystallins from aggregation [112].

As mentioned previously, α-crystallin in the lens exists as a hetero-oligomer of αA- and αB-crystallin subunits. At physiologically relevant temperatures, αB-crystallin is a more effective chaperone than αA-crystallin [148,227,309,324,363]. However, αB-crystallin is more susceptible to temperature-induced conformational changes than αA-crystallin and displays reduced thermostability at elevated temperatures [309,349]. *In vivo*, αB-crystallin forms mostly insoluble complexes in the lenses of αA-crystallin knockout mice [228]. The role of the αA-crystallin subunit as part of the α-crystallin oligomer therefore seems mainly to be to stabilise the more functionally efficient αB-crystallin subunit. The physiological ~3:1 ratio has been shown to be the most thermostable of a range of ratios *in vitro* and it is thought that this ratio is the result of a compromise between function and stability through a balance of charge and hydrophobicity [202].

αB-Crystallin is abundant in many tissues outside the lens [120,128,129,364] whilst αA-crystallin is found in only trace amounts in some non-lenticular

tissues, such as the spleen and thymus [365,366]. The stability of αB-crystallin in tissues outside the lens therefore cannot be strictly reliant on interactions with αA-crystallin. As mentioned previously (section 1.6.1), many of the human sHsps are expressed ubiquitously and can form mixed complexes in tissues in which they are co-localised. In particular, Hsp27 and αB-crystallin have been found to exist as hetero-oligomers *in vivo* [229,367,368]. In the presence of Hsp27, αB-crystallin incubated at 65°C has been found to be much more stable than αB-crystallin alone [369] and the formation of inclusion bodies of the insolubilisation-prone R120G mutant of αB-crystallin was reduced [370]. It has therefore been proposed that Hsp27 assumes the role of αB-crystallin stabilisation outside the lens [369].

Functional studies on the interaction between Hsp25, the murine homologue of Hsp27, and αB-crystallin were performed to further elucidate the role of Hsp27 in αB-crystallin-Hsp27 hetero-oligomers. The stoichiometry between Hsp27 and αB-crystallin in *in vivo* complexes is unknown. Ratios selected for this study were 1:1 Hsp25:αB-crystallin to investigate the effect of any interaction and 3:1 to correspond with the αA:αB-crystallin interaction in the human eye lens.

7.1. Thermostability Studies of Hsp25 and αB-Crystallin Mixtures

The thermostability of Hsp25, αB-crystallin and 1:1 and 3:1 Hsp25:αB-crystallin mixtures was assessed by measuring the light scattering of the samples with

increasing temperatures up to 100°C. Hsp25 showed only a slight increase in light scattering, consistent with limited aggregation as a result of temperature-induced structural changes, as discussed previously, whilst αB-crystallin showed significant precipitation commencing at ~68°C (Figure 7.1). The shape of the αB-crystallin profile is similar to some of the mutant Hsp25 proteins, with an increase in light scattering followed by a plateau region and then an accelerated increase in light scattering. How this relates to the structural changes involved was discussed in detail in section 5.6.

The 1:1 Hsp25:αB-crystallin sample showed reduced precipitation compared with αB-crystallin alone. The precipitate contained a significant amount of Hsp25 but was primarily comprised of αB-crystallin (Figure 7.2 lane 4). The increased amount of Hsp25 in the precipitate of this sample compared with the small amount for Hsp25 alone (Figure 7.2 lane 6) confirms that these two sHsps are indeed interacting with each other. That there is more αB-crystallin than Hsp25 in the precipitate suggests that the complexes that became insoluble were comprised primarily of αB-crystallin and thus subunit exchange did not result in complete equalisation of the two sHsp oligomer populations.

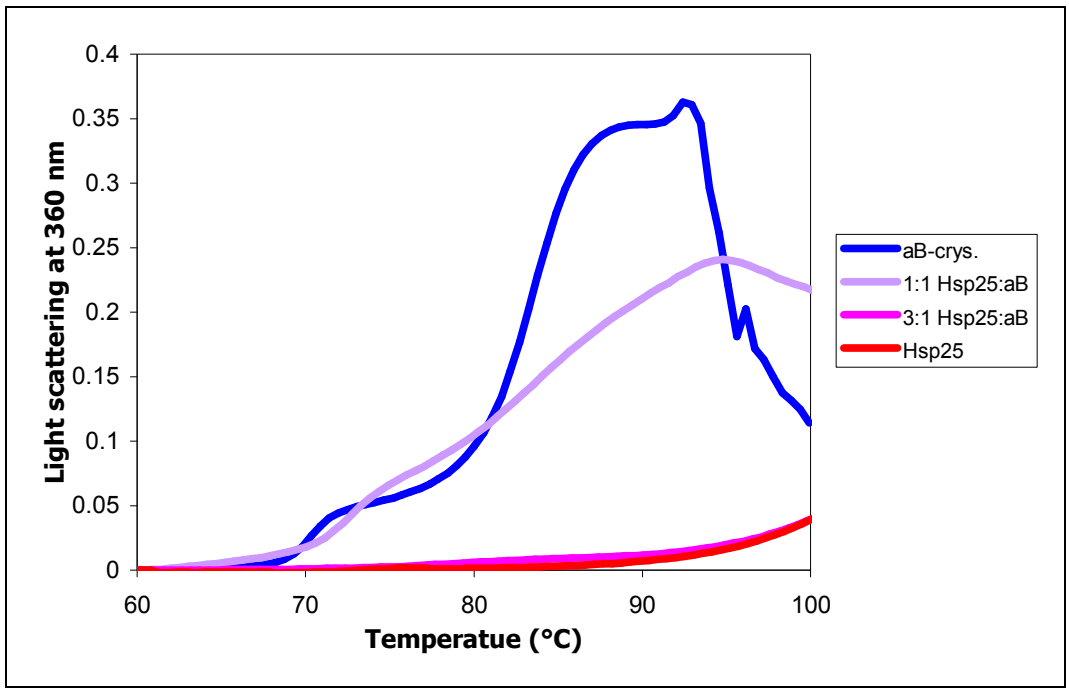

Figure 7.1: Thermostability profiles of Hsp25 and αB-crystallin mixtures. Samples were prepared in 50 mM sodium phosphate buffer (pH 7.3) containing 0.02% NaN_3 to a final protein concentration of 0.2 mg/mL. Temperature was increased at a rate of 1°C/min.

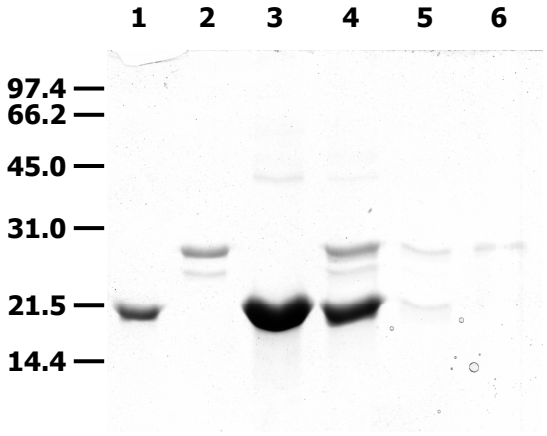

Figure 7.2: SDS-PAGE of precipitates from thermostability of Hsp25 and αB-crystallin showing αB-crystallin control (lane 1), Hsp25 control (lane 2) and resuspended pellets from the thermostability assays of αB-crystallin (lane 3), 1:1 Hsp25:αB-crystallin mixture (lane 4), 3:1 Hsp25:αB-crystallin mixture (lane 5) and Hsp25 (lane 6). Low range molecular weight standards are indicated, with masses given in kDa.

No precipitate was visually observed for the 3:1 Hsp25:αB-crystallin ratio but small amounts of both sHsps were detected in the pellet after centrifugation (Figure 7.2 lane 5). The higher concentration of Hsp25 relative to αB-crystallin appears to be capable of suppressing αB-crystallin precipitation almost completely. This parallels the scenario with αA-crystallin in the human lens.

7.2. Chaperone Activity Assays of Hsp25 and αB-Crystallin Mixtures

The chaperone activity of sHsp mixtures were compared to Hsp25 and αB-crystallin alone in assays similar to those used to compare Hsp25 mutants (section 5.7). The relative chaperone activity of Hsp25 and αB-crystallin differed depending on the ratio used (data not shown), making a series of ratios difficult to compare. Thus, a single ratio was selected for each chaperone assay.

7.2.1. Thermal Stress Assays

A ratio of 0.3:1 sHsp monomer:ADH subunit was selected for thermal stress assays of Hsp25 and αB-crystallin mixtures as this ratio gave intermediate suppression of precipitation for both homo-oligomers and resulted in the closest level of precipitation compared with similar ratios for homo-oligomers of these sHsps in preliminary experiments (data not shown). Despite using the same stock solutions for both preliminary and actual experiments, differences in the

level of precipitation for Hsp25 and αB-crystallin homo-oligomers were observed (Figure 7.3).

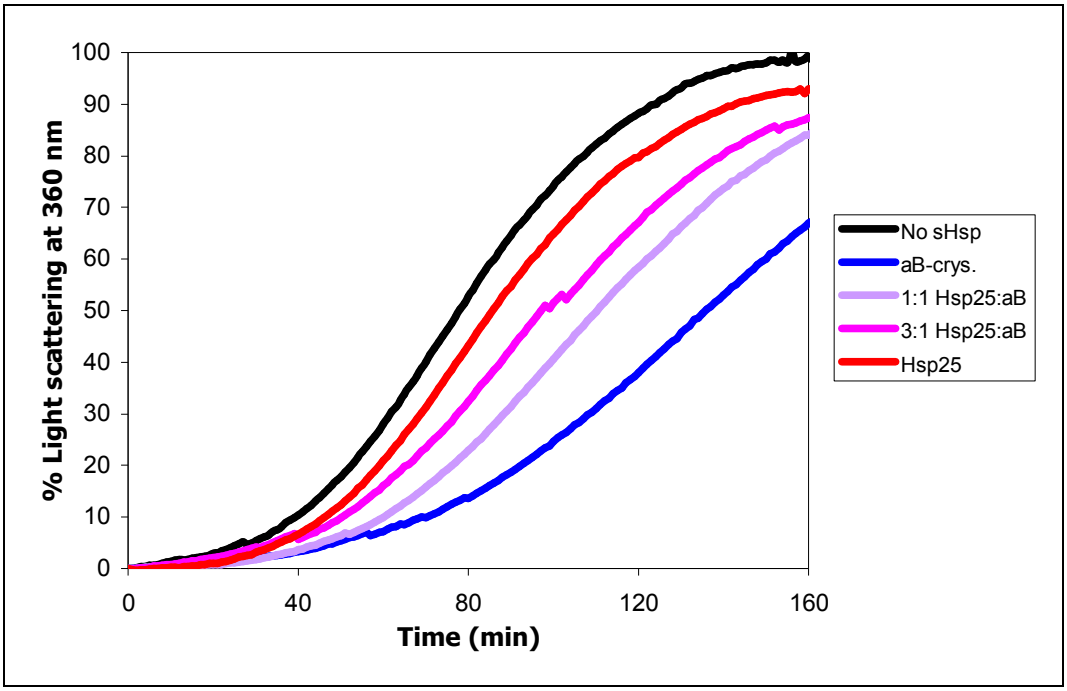

Figure 7.3: Chaperone activity of Hsp25 and αB-crystallin mixtures as measured by the suppression of aggregation of ADH under thermal stress. The total sHsp:ADH ratio for each assay was 0.3:1. Assays were performed at 55°C in 50 mM sodium phosphate buffer (pH 7.3) containing 0.02% NaN_3. Traces are the average of duplicates.

The efficiency of chaperone activity is dependent on the concentration of the sHsp, with different ratios giving rise to different comparable functional efficiencies. At the 0.3:1 ratio, αB-crystallin is a better chaperone than Hsp25. Mixtures of Hsp25 and αB-crystallin show intermediate levels of precipitation, with the 1:1 ratio being equidistant between the Hsp25 and αB-crystallin curves and the 3:1 ratio approaching the Hsp25 curve. Thus, it appears that the chaperone activity of Hsp25 and αB-crystallin mixtures as measured by the suppression of aggregation of ADH under thermal stress represents an average

chaperone activity of the two sHsps. No synergistic interactions which enhance the chaperone activity of either sHsp appear to be occurring.

7.2.2. Reduction Stress Assays

Selection of sHsp monomer:insulin ratios to assess the chaperone activity of Hsp25 and αB-crystallin towards insulin under reduction stress was undertaken with the same criteria as for the thermal stress assay, above. αB-Crystallin appears to be a more effective chaperone than Hsp25 under these conditions (Figure 7.4). The curves for the sHsp homo-oligomers show different patterns of precipitation, with αB-crystallin showing a gradual increase in precipitation and Hsp25 having an initial high precipitation rate followed by more gradual increases. This is advantageous as the precipitation rate of mixtures can be assessed in addition to the amount of precipitation occurring.

From the results of the thermostability and thermal stress assays, above, it would be expected that the 1:1 ratio would also give an average of the two homo-oligomers for the reduction stress assay. This was not the case, however, with both mixtures resulting in precipitation curves closely resembling that of Hsp25 in both level of precipitation and shape. All samples containing Hsp25 show the majority of insulin precipitation occurring relatively quickly. Hsp25 may preferentially interact with the target protein under these conditions.

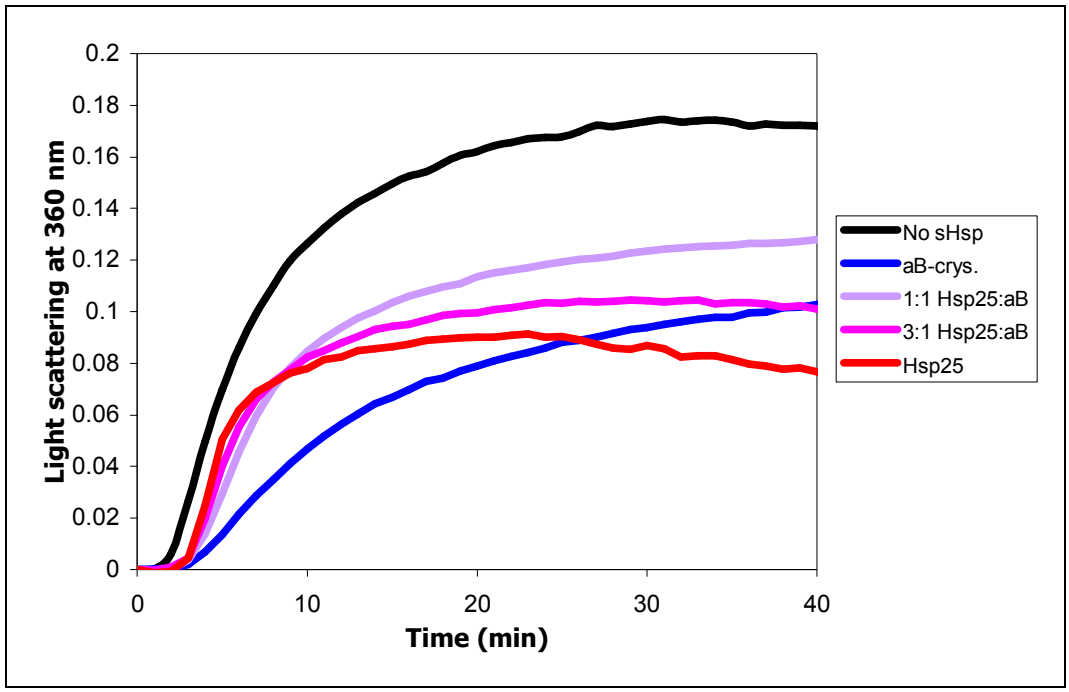

Figure 7.4: Chaperone activity of Hsp25 and αB-crystallin mixtures as measured by the suppression of aggregation of insulin under reduction stress. The total sHsp:insulin ratio for each assay was 0.1:1. Assays were performed at 37°C in 50 mM sodium phosphate buffer (pH 7.3) containing 0.02% NaN_3. The reduction of insulin was initiated by the addition of DTT to a final concentration of 20 mM. Traces are the average of quadruplicates.

Structural characterisation of mixtures of Hsp27 and αB-crystallin at elevated temperatures has previously been carried out by Fu and Liang (2003) [369]. Pre-incubation of these sHsps at 65°C resulted in the formation of high molecular weight aggregates for αB-crystallin but not Hsp27. This aggregation was reduced when both sHsps were heated together, highlighting the important stabilising role Hsp27 performs in the presence of αB-crystallin. Similarly, αB-crystallin alone showed perturbed tertiary structure at 65°C, as determined by near-UV CD, whilst a 1:1 mixture of Hsp27 and αB-crystallin resulted in only minor changes to the spectrum compared of an unheated sample of the

mixture. Interestingly, the CD spectral shape of both unheated and heated mixtures closely resemble that of the Hsp27 spectra. This correlates strongly with the functional studies, above, i.e. the presence of a significant amount of Hsp25 or Hsp27 in mixtures containing αB-crystallin results in hetero-oligomers with comparable structural and functional characteristics to Hsp25 or Hsp27 homo-oligomers. A similar trend has been observed for the oligomeric size of 1:1 mixtures of αA:αB-crystallin [371]. That this occurs when the sHsps are present in equal amounts indicates that αB-crystallin has little influence on the structural properties of the hetero-oligomer.

The chaperone activities of Hsp25 and αB-crystallin in co-complexes appears to be additive rather than synergistic, indicating that the formation of Hsp25:αB-crysatllin hetero-oligomers has no functional advantage over comparable levels of homo-oligomers. Rather, the decreased precipitation of αB-crystallin at high temperatures in the prescence of Hsp25 indicates that an important feature of the co-complexes is the stabilisation of αB-crysatllin. The ability of Hsp25 to protect αB-crystallin from heat-induced destabilisation demonstrates that αB-crystallin can indeed be stabilised by sHsps other than αA-crystallin. The complete suppression of precipitation of αB-crystallin in the presence of a three-fold excess of Hsp25 indicates that Hsp25 interacts with αB-crystallin in much the same way that αA-crystallin does. These data suggest that the co-complexes formed between Hsp25 or Hsp27 and αB-crystallin in non-lenticular tissues mirror the interactions that occur between αA- and αB-crystallin in the lens.

Chapter 8

Conclusions and Future Directions

Hsp25 is a member of the small heat shock protein family, the most efficient and strongly induced group of molecular chaperones under stress conditions. sHsps prevent the irreversible insolubilisation of intracellular proteins by recognising and interacting with unstable, partially-folded intermediate-state proteins. These target proteins are sequestered into large complexes and stabilised by interactions with the sHsp. The chaperone action of sHsps is independent of ATP, enabling sHsps to operate when cellular energy levels are low, as is the case under stress conditions. sHsps do not have the ability to refold captured target proteins. Rather, they serve as a "reservoir of folding intermediates" [118] that are able to be resurrected or degraded by other chaperone machinery when ATP levels return to normal.

Members of the sHsp family are closely associated with many disease conditions. sHsps are notably present in the characteristic insoluble brain deposits of neurodegenerative diseases such as Alzheimer's, Alexander's, Creutzfeld-Jakob and Parkinson's diseases. Elucidation of the role of sHsps in these diseases is hampered by the lack of structural information available on this family of molecular chaperones.

sHsps exist under physiological conditions as large oligomers, with the size and stoichiometry varying with the individual sHsp. Most sHsps, including all of those from mammals, are polydisperse aggregates capable of subunit exchange, features that are vital for the proper functioning of these proteins but inhibit the determination of their structure. Some features of lower order

structures have been elucidated but the variability in length and sequence of the N-terminal domain and C-terminal extension makes determination of a general structural model difficult.

The link between sHsps and various diseases make these proteins potential candidates for therapeutic applications. Research in this area is limited by the lack of detail with respect to how these proteins function as molecular chaperones. A much better understanding of the structural features of sHsps is required if the determination of a functional mechanism is to be achieved.

The aim of this study was to further our understanding of the structure and function of the mammalian sHsps using Hsp25, the murine equivalent of ubiquitous human Hsp27. A series of site-directed mutants were prepared in which various residues in the flexible region of the C-terminal extension were substituted. This short, unstructured and polar region is vital for sHsp solubility and is thought to counteract the large amount of exposed hydrophobicity associated with sHsp-target protein complexes. Mutants of Hsp25 produced included a truncation mutant (E190stop), three glutamic acid residue mutants (E190A, E199A and R204A), two glutamine mutants (Q194A and Q205A), an arginine mutant (R192A) and a C-terminal lysine mutant (K209L). The truncation mutant became insoluble after processing the cell lysate and was unable to be purified. This in itself demonstrates the importance of the C-terminal extension for sHsp stability. Spectroscopic studies on the sucessfully purified mutant Hsp25 proteins were valuable in identifying residues important

for chaperone activity. Substitution of the R192 and Q194 residues did not affect the structure or function of Hsp25 to any significant extent. Thus, these residues are dispensable for the correct functioning of this sHsp.

Each of the glutamic acid residues was found to be fundamental to the solubility of Hsp25 at elevated temperatures. The formation of stabilising ion pairs as a result of the increased abundance of charged and polar residues is a characteristic feature in proteins from thermophilic organisms. Glutamic acid and lysine residues are particularly implicated in such stabilisation. The abundance of glutamic acid and lysine residues in the C-terminal extensions of a wide range of sHsps strongly suggests that these proteins are stabilised at high temperatures in much the same way as proteins from thermophilic organisms. The replacement of each of the glutamic acid residues resulted in loss of a stabilisation mechanism important at elevated temperatures. The loss of solubilising power was exacerbated by the increased hydrophobic exposure of these mutants, which also resulted in the inefficient capture of target proteins and thus disrupted functional abilities.

The Q205 residue is vital for the formation of tertiary and quaternary structures. Mutation of this residue resulted in structural alterations involving the distant N-terminal domain and severely disrupted oligomer formation. Despite this, the Q205A mutant was functional under reducing conditions at physiological temperature. The importance of this residue is highlighted at elevated temperatures, with the Q205A mutant showing reduced

thermostability and insolubilisation in the presence of unstable target proteins. Because of this unusual observation, the Q205A mutant was selected for NMR studies to investigate the flexibility of the C-terminal extension. Uniform ^{15}N-labelling of this mutant was performed and ^{15}N relaxation (T_1 and T_2) data obtained on the residues in the C-terminal extension. The C-terminal extension of wildtype Hsp25 showed relatively uniform flexibility from I195 to A208, with the flexibility decreasing towards the anchor region and increasing towards the C-terminus. Replacement of the Q205 residue produced only localised effects, with the mutated residue becoming less flexible.

Oligomerisation of Hsp25 was shown to be partially dependent on the C-terminal lysine residue, with substitution of this residue resulting in the presence of smaller oligomeric species. The K209L mutant required structural changes associated with temperature increases to become fully functional, which is likely to be related to the smaller species acquiring chaperone ability at higher temperatures. Direct interaction between the K209 residue and target proteins seems unlikely as full chaperone activity of the K209L mutant was achievable.

In addition to identifying features of the C-terminal extension of Hsp25 vital for the formation of the correct structure of this sHsp and its proper functioning as a molecular chaperone, this study also enhances support for models of oligomeric structure and mechanism of chaperone action. The apparent lack of direct interaction between the C-terminus of Hsp25 and target proteins provides

further evidence that the C-terminal extension of sHsps remains unstructured and solvent-exposed, consistent with both the double annuli oligomeric model (section 1.5.5.1) and the model shown in Figure 1.6.

Interactions between Hsp25 and αB-crystallin were also investigated in this study. In the eye lens, the stability of αB-crystallin is dependent on the presence of αA-crystallin. However, αA-crystallin is found only in trace amounts in some non-lenticular tissues and thus αB-crystallin must be stabilised by alternative means outside the lens. Co-complexes between various sHsps have been observed in tissues in which more than one sHsp is distributed.

When present in a 3:1 ratio, the same ratio observed between αA- and αB-crystallin in the eye lens, Hsp25 was able to completely protect αB-crystallin from precipitating at elevated temperature and thus act much as αA-crystallin does towards αB-crystallin. Functionally, the 3:1 Hsp25:αB-crystallin mixture closely resembled the properties of the Hsp25 homo-oligomer. These findings parallel observations on the structure of hetero-oligomers between αB-crystallin and either Hsp27 or αA-crystallin. Thus, co-complexes formed between sHsps *in vivo* are capable of not only protection of target proteins but also stabilisation of the constituent sHsps.

Whilst this study has contributed to the wealth of knowledge available on the structure and function of sHsps, further experiments could be undertaken to compliment the results obtained. Near-UV CD spectroscopy of the mutants would help to understand the changes in tertiary structure, in particular in the

vicinity of the aromatic residues, as a result of the substitution of individual residues in the C-terminal extension of Hsp25. ^{15}N NOE data on the Q205A mutant needs to be obtained in order to fully assess changes in flexibility of the extension associated with substituting the Q205 residue. ^{15}N-labelling and NMR experiments could also be performed on at least one of the glutamic acid residue mutants, as replacement of each of the glutamic acid residues produced the most significant overall effect on the structure and function of the chaperone. Further attempts at purifying the truncation mutant should be made as it would be valuable to determine whether substitution of individual residues has the capacity to completely abolish chaperone action. Additional mutants could be produced, with substitutions to residues other than alanine or containing double or triple mutations to investigate cumulative effects, e.g. to determine if replacement of two glutamic acid residues produces different or more severe effects than a single substitution. The nature of the interaction between Hsp25 and αB-crystallin could be investigated further through the various spectroscopic techniques used on the mutant Hsp25 proteins.

sHsps have the potential to be very useful diagnostic and therapeutic tools but detailed knowledge is lacking, particularly with the secondary, tertiary and quaternary structures of mammalian sHsps still to be elucidated. This study has provided valuable insight into the role of the C-terminal extension in the determination of the structure of Hsp25 and its chaperone activity and in more general terms has contributed towards a greater understanding of how mammalian sHsps function as molecular chaperones.

Appendix A

Supplementary Information

A.1. List of sHsp Accession Numbers and Organisms

sHsp	Organism	Accession Number
Hsp27	*Homo sapiens* (human)	P04792
MKBP	*Homo sapiens* (human)	Q16082
HspB3	*Homo sapiens* (human)	Q12988
αA-crystallin	*Homo sapiens* (human)	P02489
αB-crystallin	*Homo sapiens* (human)	P02511
Hsp20	*Homo sapiens* (human)	O14558
HspB7	*Homo sapiens* (human)	Q9UBY9
Hsp22	*Homo sapiens* (human)	Q9UJY1
HspB9	*Homo sapiens* (human)	Q9BQS6
ODPF	*Homo sapiens* (human)	Q14990
Hsp25	*Mus musculus* (mouse)	P14602
αA-crystallin	*Mus musculus* (mouse)	P24622
αB-crystallin	*Mus musculus* (mouse)	P23927
αA-crystallin	*Bos taurus* (cow)	P02470
αB-crystallin	*Bos taurus* (cow)	P02510
Hsp30C	*Xenopus laevis* (frog)	P30218
Hsp26	*Drosophila melanogaster* (fruit fly)	P02517
Hsp27	*Drosophila melanogaster* (fruit fly)	P02518
Hsp12.6	*Brugia malayi* (parasitic nematode)	Q66M65
Hsp16-2	*Caenorhabditis elegans* (free-living nematode)	P06582

Hsp14	*Glycine max* (soybean)	P04794
Hsp21	*Glycine max* (soybean)	P05477
Hsp16.9	*Tritium aestivum* (wheat)	P12810
Hsp18.1	*Pisum sativum* (pea)	P19243
Hsp21	*Lycoperscon esculentum* (tomato)	Q95661
Hsp22	*Zea mays* (maize)	P24632
Hsp23	*Zea mays* (maize)	Q08275
Hsp26	*Saccharomyces cerevisae* (fungus (yeast))	P15992
Hsp42	*Saccharomyces cerevisae* (fungus (yeast))	Q12329
Hsp30	*Neurospora crassa* (fungus (mould))	P19752
Hsp16.5	*Methanococcus jannaschii* (archaeon)	Q57733
Hsp14	*Mycobacterium tuberculosis* (tuberculosis bacterium)	P0A5B7
Hsp18	*Mycobacterium leprae* (leprosy bacterium)	P12809
IbpA	*Escherichia coli* (bacterium)	P0C054
IbpB	*Escherichia coli* (bacterium)	P0C058
HspA	*Bradyrhizobium japonicum* (nitrogen-fixing bacterium)	P70917
HspB	*Bradyrhizobium japonicum* (nitrogen-fixing bacterium)	P70918

A.2. Amino Acid Properties

Amino Acid			Chemical	Polarity	Disorder/Order-Promoting [300]
Alanine	Ala	A	Aliphatic	Non-polar	disorder
Arginine	Arg	R	Basic	Charged (+)	disorder
Asparagine	Asn	N	Neutral	Polar	order
Aspartic acid	Asp	D	Acidic	Charged (–)	neither
Cysteine	Cys	C	S-containing	Polar	order
Glutamic acid	Glu	E	Acidic	Charged (–)	disorder
Glutamine	Gln	Q	Neutral	Polar	disorder
Glycine	Gly	G	Aliphatic	Non-polar	disorder
Histidine	His	H	Basic	Charged (+)	neither
Isoleucine	Ile	I	Aliphatic	Non-polar	order
Leucine	Leu	L	Aliphatic	Non-polar	order
Lysine	Lys	K	Basic	Charged (+)	disorder
Methionine	Met	M	S-containing	Non-polar	neither
Phenylalanine	Phe	F	Aromatic	Non-polar	order
Proline	Pro	P	Cyclic	Non-polar	disorder
Serine	Ser	S	Hydroxyl	Polar	disorder
Threonine	Thr	T	Hydroxyl	Polar	neither
Tryptophan	Trp	W	Aromatic	Non-polar	order
Tyrosine	Tyr	Y	Aromatic	Non-polar	order
Valine	Val	V	Aliphatic	Non-polar	order

A.3. Sequence Analysis of Representative Globular and Intrinsically-Disordered Proteins

Table A1: Frequency of residues in the representative globular proteins haemoglobin (accession number P69905), myoglobin (P02144) and insulin (P01315). Residues that promote disorder are shaded in blue and those that promote order are shown in brown [300]. Superscript text indicates the organism from which the proteins were derived: [H] human; [P] pig.

	L	A	G	V	P	E	K	T	S	Q	H	R	F	C	N	Y	D	M	W	I
Haem.[H]	18	21	7	13	7	4	11	9	11	1	10	3	7	1	4	3	8	3	1	
Myo.[H]	19	14	11	5	7	8	2	3	2	7	2	5	3	6	4	4		1	2	2
Ins.[P]	17	14	11	5	7	7	2	3	1	6	2	5	3	4	2	2		1	2	1
Total	*54*	*49*	*29*	*23*	*21*	*19*	*15*	*15*	*14*	*14*	*14*	*13*	*13*	*11*	*10*	*9*	*8*	*5*	*5*	*3*

Table A2: Frequency of residues in the representative intrinsically-disordered proteins p21[Waf1/Cip1/Sdi1] [372] (accession number Q64315), FlgM [373] (P0AEM4) and 4E-binding protein 1 [374] (Q13541). Residues that promote disorder are shaded in blue and those that promote order are shown in brown [300]. Superscript text indicates the organism from which the proteins were derived: [E] *E. coli*; ; [H] human; [R] rat.

	S	P	R	T	G	D	A	E	L	V	K	Q	I	N	M	C	F	H	Y	W
p21[R]	18	16	20	8	12	12	8	9	5	9	7	5	1	2	2	6	5	4	3	2
FlgM[E]	11	5	5	11	3	7	11	5	9	5	6	6	5	5	3					
4E-BP1[H]	15	15	9	12	12	7	4	7	6	5	3	4	5	2	4	2	3	1	2	
Total	*44*	*36*	*34*	*31*	*27*	*26*	*23*	*21*	*20*	*19*	*16*	*15*	*11*	*9*	*9*	*8*	*8*	*5*	*5*	*2*

Appendix B

Buffers and Solutions

Media

Z-Agar

Agar	1.5% (w/v)
Tryptone	1.0% (w/v)
NaCl	1.0% (w/v)
Yeast Extract	0.5% (w/v)
Glucose	0.1% (w/v)
$CaCl_2$	0.037% (w/v)

LB Medium

Tryptone	1.0% (w/v)
NaCl	1.0% (w/v)
Yeast Extract	0.5% (w/v)

SOC Medium

Tryptone	2% (w/v)
Yeast extract	0.5% (w/v)
NaCl	0.5% (w/v)
Glucose	22 mM
KCl	250 μM
$MgSO_4$	50 μM

NZY$^+$ Medium (pH 7.5)

NZ amine	1% (w/v)
Yeast extract	0.5% (w/v)
NaCl	0.5% (w/v)
Glucose	22 mM
$MgCl_2$	12.5 mM
$MgSO_4$	12.5 mM

M9 Minimal Medium Agar Plates

Agar	1.5% (w/v)
Na_2HPO_4	0.68% (w/v)
KH_2PO_4	0.3% (w/v)
NaCl	0.05% (w/v)
NH_4Cl	0.1% (w/v)
Glucose	22 mM
$MgSO_4$	2 mM
$CaCl_2$	100 μM

^{15}N-M9 Minimal Medium

Na_2HPO_4	0.68% (w/v)
KH_2PO_4	0.3% (w/v)
$^{15}NH_4Cl$	0.1% (w/v)
NaCl	0.05% (w/v)
Glucose	22 mM
$MgSO_4$	2 mM
$CaCl_2$	100 μM

SDS-PAGE

Reducing Buffer (2×)

DTT	200 mM
Tris-HCl (pH 6.8)	90 mM
Bromophenol blue	0.02% (w/v)
Glycerol	20% (v/v)
SDS	2% (w/v)

15% Resolving Gel

Acrylamide	15% (w/v)
Tris-HCl pH (8.8)	360 mM
SDS	0.1% (w/v)
APS	0.05% (w/v)
TEMED	0.5% (v/v)

4% Stacking Gel

Tris-HCl pH (6.8)	120 mM
Acrylamide	4% (w/v)
SDS	0.1% (w/v)
APS	0.05% (w/v)
TEMED	0.5% (v/v)

Running Buffer

Glycine	1.5% (w/v)
Tris base	0.3% (w/v)
SDS	0.1% (w/v)

Rapid Stain

Coomassie Blue	0.2% (w/v)
Methanol	40% (v/v)
Acetic acid	10% (v/v)

Rapid Destain

Methanol	40% (v/v)
Acetic acid	10% (v/v)

Final Destain

Acetic acid	10% (v/v)
Glycerol	4% (v/v)

Agarose Gel Electrophoresis

Loading Dye

Bromophenol blue	0.05% (w/v)
Glycerol	75% (v/v)
TE buffer	25% (v/v)

λ/Hind*III Markers*

λ DNA	50 μL
10× restriction enzyme buffer	20 μL
*Hind*III restriction enzyme	10 μL
dH_2O	120 μL

Digested at 37°C for 2 h.

TAE Buffer

Tris base	0.484% (w/v)
Acetic acid	0.1142% (v/v)
500 mM EDTA (pH 8.0)	0.2% (v/v)

Agarose Gel (0.85%)

Agarose	0.85% (w/v) in TAE buffer

Expression and Purification

Lysis Buffer (pH 8.0)

Tris-HCl	50 mM
NaCl	100 mM

Buffers

50 mM Phosphate Buffer (pH 7.3)

Sodium phosphate monobasic	0.168% (w/v)
Sodium phosphate dibasic	0.511% (w/v)
Sodium azide	0.02% (w/v)

10 mM Phosphate Buffer (pH 7.5)

Sodium phosphate monobasic	0.026% (w/v)
Sodium phosphate dibasic	0.218% (w/v)

10 mM Phosphate Buffer (pH 6.0)

Sodium phosphate monobasic	0.106% (w/v)
Sodium phosphate dibasic	0.017% (w/v)
Sodium azide	0.02% (w/v)

Appendix C

References

1 Anfinsen (1973) Principles that Govern the Folding of Protein Chains. *Science* 181(96): 223-230.

2 Hartl and Hayer-Hartl (2002) Molecular Chaperones in the Cytosol: from Nascent Chain to Folded Protein. *Science* 295: 1852-1858.

3 Horwich (2002) Protein aggregation in disease: a role for folding intermediates forming specific multimeric interactions. *J. Clin. Invest.* 110(9): 1221-1232.

4 Fink (1999) Chaperone-Mediated Protein Folding. *Physiol. Rev.* 79(2): 425-449.

5 Buchner (1996) Supervising the fold: functional principles of molecular chaperones. *FASEB J.* 10(1): 10-19.

6 Barral, Broadley, Schaffar and Hartl (2004) Roles of molecular chaperones in protein misfolding diseases. *Semin. Cell Dev. Biol.* 15: 17-29.

7 Ptitsyn, Pain, Semisotnov, Zerovnik and Razgulyaev (1990) Evidence for a molten globule state as a general intermediate in protein folding. *FEBS Lett.* 262(1): 20-24.

8 Brockwell, Smith and Radford (2000) Protein folding mechanisms: new methods and emerging ideas. *Curr. Opin. Struct. Biol.* 10(1): 16-25.

9 Fink (1995) Molten Globules. *Methods Mol. Biol.* 40 (Protein Stability and Folding: Theory and Practice): 343-360.

10 Ptitsyn (1991) How does protein synthesis give rise to the 3D-structure? *FEBS Lett.* 285(2): 176-181.

11 Ewbank and Creighton (1991) The molten globule protein conformation probed by disulphide bonds. *Nature* 350(6318): 518-820.

12 Gething and Sambrook (1992) Protein folding in the cell. *Nature* 355(6355): 33-45.

13 Jaenicke (1995) Folding and association versus misfolding and aggregation of proteins. *Phil. Trans. R. Soc. Lond. B* 348(1323): 97-105.

14 Jaenicke and Seckler (1999) Spontaneous Versus Assisted Protein Folding. *Molecular Chaperones and Folding Catalysts: Regulation, Cellular Function and Mechanisms*. Bukau, B. (Ed.) Harwood Academic, Amsterdam.

15 Dobson (2001) The structural basis of protein folding and its links with human disease. *Phil. Trans. R. Soc. Lond. B* 356(1406): 133-145.

16 Jaenicke (1991) Protein Folding: Local Structures, Domains, Subunits and Assemblies. *Biochemistry* 30(13): 3147-3161.

17 Feldman and Frydman (2000) Protein folding *in vivo*: the importance of molecular chaperones. *Curr. Opin. Struct. Biol.* 10(1): 26-33.

18 Carver, Lindner, Lyon, Canet, Hernandez, Dobson and Redfield (2002) The Interaction of the Molecular Chaperone α-Crystallin with Unfolding α-Lactalbumin: A Structural and Kinetic Spectroscopic Study. *J. Mol. Biol.* 318(3): 815-827.

19 Hagihara and Goto (1998) Folding of Monomeric Proteins In Vitro: Physiochemical and Biological Roles of the Intermediate States. *Molecular chaperones in the life cycle of proteins: structure, functions, and mode of action*. Fink, A. L. and Goto, Y. (Eds). Marcel Dekker, New York.

20 Schultz (2000) Illuminating folding intermediates. *Nat. Struct. Biol.* 7(1): 7-10.

21 Hartl (1996) Molecular chaperones in cellular protein folding. *Nature* 381(6583): 571-580.

22 Ellis and Hartl (1996) Protein folding in the cell: competing models of chaperonin function. *FASEB J.* 10(1): 20-26.

23 Scheibel and Buchner (2006) Protein Aggregation as a Cause for Disease. *Handb. Exp. Pharmacol.* 172 (Molecular Chaperones in Health and Disease): 199-219.

24 Peng, Wu, Schulman and Kim (1995) Does the molten globule have a native-like tertiary fold? *Phil. Trans. R. Soc. Lond. B* 348(1323): 43-47.

25 Lindner, Kapur and Carver (1997) The Interaction of the Molecular Chaperone, α-Crystallin, with Molten Globule States of Bovine α-Lactalbumin. *J. Biol. Chem.* 272(44): 27722-27729.

26 Ellis (1997) Molecular chaperones: Avoiding the crowd. *Curr. Biol.* 7(9): R531-R533.

27 Welch, Eggers, Hansen and Nagata (1999) Early Events in the Synthesis and Maturation of Polypeptides. *Molecular Chaperones and Folding Catalysts: Regulation, Cellular Function and Mechanisms*. Bukau, B. (Ed.) Harwood Academic, Amsterdam.

28 Zimmerman and Minton (1993) Macromolecular Crowding: Biochemical, Biophysical, and Physiological Consequences. *Annu. Rev. Biophys. Biomol. Struct.* 22: 27-65.

29 Ellis (2001) Macromolecular crowding: obvious but underappreciated. *TIBS* 26(10): 597-604.

30 Dobson and Karplus (1999) The fundamentals of protein folding: bringing together theory and experiment. *Curr. Opin. Struct. Biol.* 9(1): 92-101.

31 Minton (2000) Implications of macromolecular crowding for protein assembly. *Curr. Opin. Struct. Biol.* 10(1): 34-39.

32 Netzer and Hartl (1998) Protein folding in the cytosol: chaperonin-dependent and -independent mechanisms. *TIBS* 23(2): 68-73.

33 Ellis and Hartl (1999) Principles of protein folding in the cellular environment. *Curr. Opin. Struct. Biol.* 9(1): 102-110.

34 Martin and Hartl (1993) Protein folding in the cell: molecular chaperones pave the way. *Structure* 1(3): 161-164.

35 Ellisdon and Bottomley (2004) The Role of Protein Misfolding in the Pathogenesis of Human Diseases. *IUBMB Life* 56(3): 119-123.

36 Thomas, Qu and Pederson (1995) Defective protein folding as a basis of human disease. *TIBS* 20(11): 456-459.

37 Welch and Brown (1996) Influence of molecular and chemical chaperones on protein folding. *Cell Stress Chaperon.* 1(2): 109-115.

38 Dobson (2004) Principles of protein folding, misfolding and aggregation. *Semin. Cell Dev. Biol.* 15: 3-16.

39 Chaudhuri and Paul (2006) Protein-misfolding diseases and chaperone-based therapeutic approaches. *FEBS J.* 273(7): 1331-1349.

40 Carrell and Lomas (1997) Conformational disease. *Lancet* 350(9071): 134-138.

41 Selkoe (2003) Folding proteins in fatal ways. *Nature* 426(6968): 900-904.

42 Gregersen (2006) Protein misfolding disorders: Pathogenesis and intervention. *J. Inherit. Metab. Dis.* 29(2-3): 456-470.

43 Kerem, Rommens, Buchanan, Markiewicz, Cox, Chakravarti, Buchwald and Tsui (1989) Identification of the cystic fibrosis gene: genetic analysis. *Science* 245(4922): 1073-1080.

44 Yang, Janich, Cohn and Wilson (1990) The common variant of cystic fibrosis transmembrane conductance regulator is recognized by hsp70 and degraded in a pre-Golgi nonlysosomal compartment. *Proc. Natl. Acad. Sci. USA* 90(20): 9480-9484.

45 Quinton (1990) Cystic fibrosis: a disease in electrolyte transport. *FASEB J.* 4(10): 2709-2717.

46 Welch (2004) Role of quality control pathways in human diseases involving protein misfolding. *Semin. Cell Dev. Biol.* 15(1): 31-38.

47 Ellis (1987) Proteins as molecular chaperones. *Nature* 328(6129): 378-379.

48 Ellis and van der Vies (1991) Molecular Chaperones. *Annu. Rev. Biochem.* 60: 321-347.

49 Hartl (1995) Principles of chaperone-mediated protein folding. *Phil. Trans. R. Soc. Lond. B* 348(1323): 107-112.

50 Parsell and Lindquist (1993) The Function of Heat-Shock Proteins in Stress Tolerance: Degradation and Reactivation of Damaged Proteins. *Annu. Rev. Genet.* 27: 437-496.

51 Ritossa (1962) New puffing pattern induced by temperature shock and dinitrophenol in *Drosophila*. *Experientia* 18: 571-573.

52 Ritossa (1996) Discovery of the heat shock response. *Cell Stress Chaperon.* 1(2): 97-98.

53 Tissières, Mitchell and Tracy (1974) Protein Synthesis in Salivary Glands of *Drosophila melanogaster*: Relation to Chromosome Puffs. *J. Mol. Biol.* 84(3): 389-398.

54 Landry, Jordan, McMacken and Gierasch (1992) Different conformations for the same polypeptide bound to chaperones DnaK and GroEL. *Nature* 355(6359): 455-547.

55 Fourie, Sambrook and Gething (1994) Common and Divergent Peptide Binding Specificities of hsp70 Molecular Chaperones. *J. Biol. Chem.* 269(48): 30470-30478.

56 Rüdiger, Germeroth, Schneider-Mergener and Bukau (1997) Substrate specificity of the DnaK chaperone determined by screening cellulose-bound peptide libraries. *EMBO J.* 16(7): 1501-1507.

57 Hendrick and Hartl (1993) Molecular Chaperone Functions of Heat-Shock Proteins. *Annu. Rev. Biochem.* 62: 349-384.

58 Schirmer and Lindquist (1997) The HSP100 family - an overview. *Guidebook to the molecular chaperones and protein-folding catalysts*. Gething, M.-J. (Ed.) Oxford University Press, Oxford.

59 Bukau, Schmid and Buchner (1999) Assisted Protein Folding. *Molecular Chaperones and Folding Catalysts: Regulation, Cellular Function and Mechanisms*. Bukau, B. (Ed.) Harwood Academic, Amsterdam.

60 Jolly and Morimoto (2000) Role of the heat shock response and molecular chaperones in oncogenesis and cell death. *J. Natl Cancer Inst.* 92(19): 1564-1572.

61 Rüdiger, Schneider-Mergener and Bukau (2001) Its substrate specificity characterizes the DnaJ co-chaperone as a scanning factor for the DnaK chaperone. *EMBO J.* 20(5): 1042-1050.

62 Beckmann, Welch and Mizzen (1990) Interaction of Hsp 70 with newly synthesized proteins: implications for protein folding and assembly. *Science* 248(4957): 850-854.

63 Flynn, Chappell and Rothman (1989) Peptide binding and release by proteins implicated as catalysts of protein assembly. *Science* 245(4916): 385-390.

64 Langer, Lu, Echols, Flanagan, Hayer and Hartl (1992) Successive action of DnaK, DnaK and GroEL along the pathway of chaperone-mediated protein folding. *Nature* 356(6371): 683-689.

65 Thulasiraman, Yang and Frydman (1999) *In vivo* newly translated polypeptides are sequestered in a protected folding environment. *EMBO J.* 18(1): 85-95.

66 Ewalt, Hendrick, Houry and Hartl (1997) In Vivo Observation of Polypeptide Flux through the Bacterial Chaperonin System. *Cell* 90(3): 491-500.

67 Hendrix (1979) Purification and Properties of groE, a Host Protein Involved in Bacteriophage Assembly. *J. Mol. Biol.* 129(3): 375-392.

68 Hohn, Hohn, Engel and Wurtz (1979) Isolation and Characterization of the Host Protein groE Involved in Bacteriophage Lambda Assembly. *J. Mol. Biol.* 129(3): 359-373.

69 Laminet, Ziegelhoffer, Georgopoulos and Plückthun (1990) The *Escherichia coli* heat shock proteins GroEL and GroES modulate the folding of the β-lactamase precursor. *EMBO J.* 9(7):

70 Chen, Roseman, Hunter, Wood, Burston, Ranson, Clarke and Saibil (1994) Location of a folding protein and shape changes in GorEL-GroES complexes images by cryo-electron microscopy. *Nature* 71(6494): 261-264.

71 Martin, Langer, Boteva, Schramel, Horwich and Hartl (1991) Chaperonin-mediated protein folding at the surface of GroEL through a 'molten globule'-like intermediate. *Nature* 352(6330): 36-42.

72 Fenton, Kashi, Furtak and Horwich (1994) Residues in chaperonin GroEL required for polypeptide binding and release. *Nature* 371(3498): 614-619.

73 Ishii, Taguchi, Sasabe and Yoshida (1994) Folding Intermediate Binds to the Bottom of Bullet-shaped Holo-chaperonin and is Readily Accessible to Antibody. *J. Mol. Biol.* 236(3): 691-696.

74 Chandrasekhar, Tilly, Woolford, Hendrix and Georgopoulos (1986) Purification and Properties of the groES Morphogenetic Protein of Escherichia coli. *J. Biol. Chem.* 261(26): 12414-12419.

75 Langer, Pfeifer, Martin, Baumeister and Hartl (1992) Chaperonin-mediated protein folding: GroES binds to one end of the GroEL cylinder, which accommodates the protein substrate within its central cavity. *EMBO J.* 11(13): 4757-4765.

76 Braig, Simon, Furuya, Hainfeld and Horwich (1993) A polypeptide bound by the chaperonin groEL is localized within a central cavity. 90(9): 1978-3982.

77 Martin, Mayhew, Langer and Hartl (1993) The reaction cycle of GroEL and GroES in chaperonin-assisted protein folding. *Nature* 366(6452): 228-233.

78 Mayhew, da Silva, Martin, Erdjument-Bromage, Tempst and Hartl (1996) Protein folding in the central cavity of the GroEL-GroES chaperonin complex. *Nature* 379(6564): 420-426.

79 Mogk, Mayer and Deuerling (2002) Mechanisms of Protein Folding: Molecular Chaperones and Their Application in Biotechnology. *ChemBioChem* 3(9): 807-814.

80 Young, Agashe, Siegers and Hartl (2004) Pathways of Chaperone Mediated Protein Folding in the Cytosol. *Nat. Rev. Mol. Cell. Biol.* 5(10): 791-791.

81 Sanchez and Lindquist (1990) HSP104 Required for Induced Thermotolerance. *Science* 248(4959): 1112-1115.

82 Kessel, Maurizi, Kim, Kocsis, Trus, Singh and Steven (1995) Homology in Structural Organization Between *E. coli* ClpAP Protease and the Eukaryotic 26 S Proteasome. *J. Mol. Biol.* 250(5): 587-594.

83 Parsell, Kowal, Singer and Lindquist (1994) Protein disaggregation mediated by heat-shock protein Hsp104. *Nature* 372(6505): 475-478.

84 Glover and Lindquist (1998) Hsp104, Hsp70, and Hsp40: A Novel Chaperone System that Rescues Previously Aggregated Proteins. *Cell* 94(1): 73-82.

85 Goloubinoff, Mogk, Ben-Zvi, Tomoyasu and Bukau (1999) Sequential mechanism of solubilization and refolding of stable protein aggregates by a bichaperone network. *Proc. Natl. Acad. Sci. USA* 96(24): 13732.

86 Hwang, Park, Chung and Goldberg (1987) *Escherichia coli* contains a soluble ATP-dependent protease (Ti) distinct from protease La. *Proc. Natl. Acad. Sci. USA* 84(16): 5550-5554.

87 Katayama, Gottesman, Pumphrey, Rudikoff, Clark and Maurizi (1988) The Two-component, ATP-dependent Clp Protease of Escherichia coli: Purification, Cloning, and Mutational Analysis of the ATP-Binding Component. *J. Biol. Chem.* 263(29): 15226-15236.

88 Lindquist and Schirmer (1999) The Role of Hsp104 in Stress Tolerance and Prion Maintenance. *Molecular Chaperones and Folding Catalysts: Regulation, Cellular Function and Mechanisms*. Bukau, B. (Ed.) Harwood Academic, Amsterdam.

89 Neckers, Mimnaugh and Schulte (1999) The Hsp90 Chaperone Family. *Handb. Exp. Pharmacol.* 136 (Stress Proteins): 9-42.

90 Koyasu, Nishida, Kadowaki, Matsuzaki, Iida, Harada, Kasuga, Sakai and Yahara (1986) Two mammalian heat shock proteins, HSP90 and HSP100, are actin-binding proteins. *Proc. Natl. Acad. Sci. USA* 83(21): 8054-8058.

91 Minami, Kawasaki, Miyata, Suzuki and Yahara (1991) Analysis of Native Forms and Isoform Compositions of the Mouse 90-kDa Heat Shock Protein, HSP90. *J. Biol. Chem.* 266(16): 10099-10103.

92 Obermann, Sondermann, Russo, Pavletich and Hartl (1998) In Vivo Function of Hsp90 Is Dependent on ATP Binding and ATP Hydrolysis. *J. Cell. Biol.* 143(4): 901-910.

93 Richter and Buchner (2001) Hsp90: Chaperoning Signal Transduction. *J. Cell. Physiol.* 188(3): 188-281.

94 Pratt and Toft (2003) Regulation of Signaling Protein Function and Trafficking by the hsp90/hsp70-Based Chaperone Machinery. *Exp. Biol. Med.* 228(2): 111-133.

95 Picard, Khursheed, Garabedian, Fortin, Lindquist and Yamamoto (1990) Reduced levels of hsp90 compromise steroid receptor action *in vivo*. *Nature* 348(6297): 166-168.

96 Pearl and Prodromou (2002) Structure, Function, and Mechanism of the Hsp90 Molecular Chaperone. *Adv. Protein Chem.* 59 (Protein Folding in the Cell): 157-186.

97 Morishima, Murphy, Li, Sanchez and Pratt (2000) Stepwise Assembly of a Glucocorticoid Receptor·hsp90 Heterocomplex Resolves Two Sequential ATP-dependent Events Involving First hsp70 and Then hsp90 in Opening of the Steroid Binding Pocket. *J. Biol. Chem.* 275(24): 18054-18060.

98 Jakob and Buchner (1994) Assisting spontaneity: the role of Hsp90 and small Hsps as molecular chaperones. *TIBS* 19(5): 205-211.

99 Young, Moarefi and Hartl (2001) Hsp90: a specialized but essential protein-folding tool. *J. Cell. Biol.* 154(2): 267-273.

100 Arrigo and Landry (1994) Expression and Function of the Low-molecular-weight Heat Shock Proteins. *The Biology of Heat Shock Proteins and Molecular Chaperones*. Morimoto, R. I., Tissières, A. and Georgopoulos, C. (Eds). Cold Spring Harbor Laboratory Press, NY.

101 Narberhaus (2002) α-Crystallin-Type Heat Shock Proteins: Socializing Minichaperones in the Context of a Multichaperone Network. *Microbiol. Mol. Biol. R.* 66(1): 64-93.

102 Lindquist (1986) The Heat-Shock Response. *Annu. Rev. Biochem.* 55: 1151-1191.

103 Macario (1995) Heat-Shock Proteins and Molecular Chaperones: Implications for Pathogenesis, Diagnostics and Therapeutics. *Int. J. Clin. Lab. Res.* 25(2): 59-70.

104 Ehrnsperger, Buchner and Gaestel (1998) Structure and Function of Small Heat-Shock Proteins. *Molecular chaperones in the life cycle of proteins: structure, functions, and mode of action*. Fink, A. L. and Goto, Y. (Eds). Marcel Dekker, New York.

105 Bose, Ehrnsperger and Buchner (1999) Mechanisms of ATP-Independent vs ATP-Dependent Chaperones. *Molecular Chaperones and Folding Catalysts: Regulation, Cellular Function and Mechanisms*. Bukau, B. (Ed.) Harwood Academic, Amsterdam.

106 de Macario and Macario (2000) Stressors, Stress and Survival: Overview. *Front. Biosci.* 5: 780-786.

107 Richter-Landsberg and Goldbaum (2003) Stress proteins in neural cells: functional roles in health and disease. *Cell. Mol. Life Sci.* 60(2): 337-349.

108 Taylor and Benjamin (2005) Small heat shock proteins: a new classification scheme in mammals. *J. Mol. Cell Cardiol.* 38(3): 433-444.

109 de Jong, Caspers and Leunissen (1998) Genealogy of the α-crystallin–small heat-shock protein superfamily. *Int. J. Biol. Macromol.* 22(3-4): 151-162.

110 Gusev, Bogatcheva and Marston (2002) Structure and Properties of the Small Heat Shock Proteins (sHsp) and Their Interaction with Cytoskeleton Proteins. *Biochemistry (Mosc.)* 67(5): 511-519.

111 Haslbeck (2002) sHsps and their role in the chaperone network. *Cell. Mol. Life Sci.* 59(10): 1649-1657.

112 Horwitz (1992) α-Crystallin can function as a molecular chaperone. *Proc. Natl. Acad. Sci. USA* 89(21): 10449-10453.

113 Sun and MacRae (2005) The small heat shock proteins and their role in human disease. *FEBS J.* 271(11): 2613-2627.

114 Haslbeck, Franzmann, Weinfurtner and Buchner (2005) Some like it hot: the structure and function of small heat-shock proteins. *Nat. Struct. Mol. Biol.* 12(10): 842-846.

115 Waters, Lee and Vierling (1996) Evolution, structure and function of the small heat shock proteins in plants. *J. Exp. Bot.* 47(296): 325-338.

116 van Montfort, Slingsby and Vierling (2002) Structure and Function of the Small Heat Shock Protein/α-Crystallin Family of Molecular Chaperones. *Adv. Protein Chem.* 59 (Protein Folding in the Cell): 105-156.

117 Raman and Rao (1994) Chaperone-like Activity and Quaternary Structure of α-Crystallin. *J. Biol. Chem.* 269(44): 27264-27268.

118 Ehrnsperger, Gräber, Gaestel and Buchner (1997) Binding of non-native protein to Hsp25 during heat shock creates a reservoir of folding intermediates for reactivation. *EMBO J.* 16(2): 221-229.

119 Lee, Pokala and Vierling (1995) Structure and *in Vitro* Molecular Chaperone Activity of Cytosolic Small Heat Shock Proteins from Pea. *J. Biol. Chem.* 270(18): 10432-10438.

120 Klemenz, Andres, Fröhli, Schäfer and Aoyama (1993) Expression of the Murine Small Heat Shock Proteins hsp 25 and αB Crystallin in the Absence of Stress. *J. Cell. Biol.* 120(3): 639-645.

121 Kappé, Franck, Verschuure, Boelens, Leunissen and de Jong (2003) The human genome encodes 10 α-crystallin–related small heat shock proteins: HspB1–10. *Cell Stress Chaperon.* 8(1): 53-61.

122 Gastmann, Burfeind, Günther, Hameister, Szpirer and Hoyer-Fender (1993) Sequence, Expression, and Chromosomal Assignment of a Human Sperm Outer Dense Fiber Gene. *Mol. Reprod. Dev.* 36(4): 407-418.

123 Kappé, Verschuure, Philipsen, Staalduinen, Van de Boogaart, Boelens and De Jong (2001) Characterization of two novel human small heat shock proteins: protein kinase-related HspB8 and testis-specific HspB9. *Biochim. Biophys. Acta* 1520(1): 1-6.

124 van der Ouderaa, de Jong, Hilderink and Bloemendal (1974) The Amino-Acid Sequence of the αB_2 Chain of Bovine α-Crystallin. *Eur. J. Biochem.* 49(1): 157-168.

125 Horwitz (2000) The function of alpha-crystallin in vision. *Semin. Cell Dev. Biol.* 11: 53-60.

126 Velasco, Luka, Murthy, Duglas-Tabor, Garland and Lorand (1997) Hierarchy of Lens Proteins Requiring Protection Against Heat-Induced Precipitation by the α Crystallin Chaperone. *Exp. Eye Res.* 65(4): 497-505.

127 Tardieu (1998) α-Crystallin quaternary structure and interactive properties control eye lens transparency. *Int. J. Biol. Macromol.* 22(3-4): 211-217.

128 Dubin, Wawrousek and Piatigorsky (1989) Expression of the Murine αB-Crystallin Gene Is Not Restricted to the Lens. *Mol. Cell Biol.* 9(3): 1083-1091.

129 Iwaki, Kume-Iwaki and Goldman (1990) Cellular Distribution of αB-Crystallin in Non-lenticular Tissues. *J Histochem. Cytochem.* 38(1): 31-39.

130 Merck, Groenen, Voorter, de Haard-Hoekman, Horwitz, Bloemendal and de Jong (1993) Structural and Functional Similarities of Bovine α-Crystallin and Mouse Small Heat-shock Protein: a Family of Chaperones. *J. Biol. Chem.* 268(2): 1046-1052.

131 Plesofsky-Vig, Vig and Brambl (1992) Phylogeny of the α-Crystallin-Related Heat-Shock Proteins. *J. Mol. Evol.* 35(6): 537-545.

132 de Jong, Leunissen and Voorter (1993) Evolution of the α-Crystallin / Small Heat-Shock Protein Family. *Mol. Biol. Evol.* 10(1): 103-126.

133 Caspers, Leunissen and de Jong (1995) The Expanding Small Heat-Shock Protein Family, and Structure Predictions of the Conserved "α-Crystallin Domain". *J. Mol. Evol.* 40(3): 238-248.

134 Augusteyn (2004) α-crystallin: a review of its structure and function. *Clin. Exp. Optom.* 87(6): 356-366.

135 Quax-Jeuken, Quax, van Rens, Khan and Bloemendal (1985) Complete structure of the αB-crystallin gene: Conservation of the exon-intron distribution in the two nonlinked α-crystallin genes. *Proc. Natl. Acad. Sci. USA* 82(17): 5819-5823.

136 Kim, Kim and Kim (1998) Crystal structure of a small heat-shock protein. *Nature* 394(6693): 595-599.

137 Singh, Zewge, Groth-Vasselli and Farnsworth (1996) A comparison of structural relationships among α-crystallin, human Hsp27, γ-crystallins and βB2-crystallin. *Int. J. Biol. Macromol.* 19(4): 227-233.

138 Leroux, Ma, Batelier, Melki and Candido (1997) Unique Structural Features of a Novel Class of Small Heat Shock Proteins. *J. Biol. Chem.* 272(19): 12847-12853.

139 van Montfort, Basha, Friedrich, Slingsby and Vierling (2001) Crystal structure and assembly of a eukaryotic small heat shock protein. *Nat. Struct. Biol.* 8(12): 1025-1030.

140 Groenen, Merck, de Jong and Bloemendal (1994) Structure and modifications of the junior chaperone α-crystallin: From lens transparency to molecular pathology. *Eur. J. Biochem.* 225(1): 1-19.

141 Derham and Harding (1999) α-Crystallin as a Molecular Chaperone. *Prog. Retinal Eye Res.* 18(4): 463-509.

142 Koteiche and Mchaourab (1999) Folding Pattern of the α-Crystallin Domain in αA-Crystallin Determined by Site-Directed Spin Labeling. *J. Mol. Biol.* 294(2): 561-577.

143 Franck, Madsen, van Rheede, Richard, Huynen and de Jong (2004) Evolutionary Diversity of Vertebrate Small Heat Shock Proteins. *J. Mol. Evol.* 59(6): 792-805.

144 Farnsworth, Frauwirth, Groth-Vasselli and Singh (1998) Refinement of 3D structure of bovine lens αA-crystallin. *Int. J. Biol. Macromol.* 22(3-4): 175-185.

145 Lindner, Carver, Ehrnsperger, Buchner, Esposito, Behlke, Lutsch, Kotlyarov and Gaestel (2000) Mouse Hsp25, a small heat shock protein: The role of its C-terminal extension in oligomerization and chaperone action. *Eur. J. Biochem.* 267(7): 1923-1932.

146 Koretz, Doss and LaButti (1998) Environmental factors influencing the chaperone-like activity of α-crystallin. *Int. J. Biol. Macromol.* 22(3-4): 283-294.

147 Bloemendal, Toumadje and Johnson (1999) Bovine lens crystallins do contain helical structure: a circular dichroism study. *Biochim. Biophys. Acta* 1432(2): 234-238.

148 Sun, Das and Liang (1997) Conformational and Functional Differences between Recombinant Human Lens αA- and αB-Crystallin. *J. Biol. Chem.* 272(10): 6220-6225.

149 Shroff, Cherian-Shaw, Bera and Abraham (2000) Mutation of R116C Results in Highly Oligomerized αA-Crystallin with Modified Structure and Defective Chaperone-like Function. *Biochemistry* 39(6): 1420-1426.

150 Bera and Abraham (2002) The αA-Crystallin R116C Mutant Has a Higher Affinity for Forming Heteroaggregates with αB-crystallin. *Biochemistry* 41(1): 297-305.

151 Plater, Goode and Crabbe (1996) Effects of Site-directed Mutations on the Chaperone-like Activity of αB-Crystallin. *J. Biol. Chem.* 271(45): 28558-28566.

152 Bova, Yaron, Huang, Ding, Haley, Stewart and Horwitz (1999) Mutation R120G in αB-crystallin, which is linked to a desmin-related myopathy, results in an irregular structure and defective chaperone-like function. *Proc. Natl. Acad. Sci. USA* 96(11): 6137-6143.

153 Kelley and Abraham (2003) Thermally induced disintegration of the oligomeric structure of αB-crystallin mutant F28S is associated with diminished chaperone activity. *Mol. Cell. Biochem.* 252(1-2): 273-278.

154 Wistow (1985) Domain structure and evolution in α-crystallins and small heat-shock proteins. *FEBS Lett.* 181(1): 1-6.

155 Puri, Augusteyn, Owen and Siezen (1983) Immunochemical Properties of Vertebrate a-Crystallins. *Eur. J. Biochem.* 134(2): 321-326.

156 Carver, Aquilina and Truscott (1993) An investigation into the stability of α-crystallin by NMR spectroscopy; evidence for a two-domain structure. *Biochim. Biophys. Acta* 1164(1): 22-28.

157 Chang, Primm, Jakana, Lee, Seryshevai, Chiu, Gilbert and Quiocho (1996) *Mycobacterium tuberculosis* 16-kDa Antigen (Hsp16.3) Functions as an Oligomeric Structure *in Vitro* to Suppress Thermal Aggregation. *J. Biol. Chem.* 271(12): 7218-7223.

158 Sun and MacRae (2005) Small heat shock proteins: molecular structure and chaperone function. *Cell. Mol. Life Sci.* 62(21): 2460-2476.

159 Berengian, Bova and Mchaourab (1997) Structure and Function of the Conserved Domain in aA-Crystallin. Site-Directed Spin Labeling Identifies a β-Strand Located near a Subunit Interface. *Biochemistry* 36(33): 9951-9957.

160 Mchaourab, Berengian and Koteiche (1997) Site-Directed Spin-Labeling Study of the Structure and Subunit Interactions along a Conserved Sequence in the α-Crystallin Domain of Heat-Shock Protein 27. Evidence of a Conserved Subunit Interface. *Biochemistry* 36(48): 14627-14634.

161 Salerno, Eifert, Salerno and Koretz (2003) Structural diversity in the small heat shock protein superfamily: control of aggregation by the N-terminal region. *Protein Eng.* 16(11): 847-851.

162 Guruprasad and Kumari (2003) Three-dimensional models corresponding to the C-terminal domain of human αA- and αB-crystallins based on the crystal structure of the small heat-shock protein HSP16.9 from wheat. *Int. J. Biol. Macromol.* 33(1-3): 107-112.

163 Feil, Malfois, Hendel, van der Zandt and Svergun (2001) A Novel Quaternary Structure of the Dimeric a-Crystallin Domain with Chaperone-like Activity. *J. Biol. Chem.* 276(15): 12024-12029.

164 Bova, Ding, Horwitz and Fung (1997) Subunit Exchange of αA-Crystallin. *J. Biol. Chem.* 272(47): 29511-29517.

165 Leroux, Melki, Gordon, Batelier and Candido (1997) Structure-Function Studies on Small Heat Shock Protein Oligomeric Assembly and Interaction with Unfolded Polypeptides. *J. Biol. Chem.* 272(39): 24646-24656.

166 Boelens, Croes, de Ruwe, de Reu and de Jong (1998) Negative Charges in the C-terminal Domain Stabilize the αB-Crystallin Complex. *J. Biol. Chem.* 273(43): 28085-28090.

167 Bova, Mchaourab, Han and Fung (2000) Subunit Exchange of Small Heat Shock Proteins: Analysis of oligomer formation of aA-crystallin and Hsp27 by fluorescence resonance energy transfer and site-directed truncations. *J. Biol. Chem.* 275(2): 1035-1042.

168 Haslbeck, Ignatiou, Saibil, Helmich, Frenzl, Stromer and Buchner (2004) A Domain in the N-terminal Part of Hsp26 is Essential for Chaperone Function and Oligomerization. *J. Mol. Biol.* 343(2): 445-455.

169 Eifert, Burgio, Bennett, Salerno and Koretz (2005) N-terminal control of small heat shock protein oligomerization: Changes in aggregate size and chaperone-like function. *Biochim. Biophys. Acta* 1748(2): 146-156.

170 Studer, Obrist, Lentze and Narberhaus (2002) A critical motif for oligomerization and chaperone activity of bacterial α-heat shock proteins. *Eur. J. Biochem.* 269(14): 3578-3586.

171 Thampi and Abraham (2003) Influence of the C-Terminal Residues on Oligomerization of aA-Crystallin. *Biochemistry* 42(40): 11857-11863.

172 van de Klundert, Smulders, Gijsen, Lindner, Jaenicke, Carver and de Jong (1998) The mammalian small heat-shock protein Hsp20 forms dimers and is a poor chaperone. *Eur. J. Biochem.* 258(3): 1014-1021.

173 Haley, Bova, Huang, Mchaourab and Stewart (2000) Small Heat-Shock Protein Structures Reveal a Continuum from Symmetric to Variable Assemblies. *J. Mol. Biol.* 298(2): 261-272.

174 Haley, Horwitz and Stewart (1998) The Small Heat-shock Protein, aB-Crystallin, has a Variable Quaternary Structure. *J. Mol. Biol.* 277(1): 27-35.

175 Behlke, Lutsch, Gaestel and Bielka (1991) Supramolecular structure of the recombinant murine small heat shock protein hsp25. *FEBS Lett.* 288(1-2): 199-122.

176 Rogalla, Ehrnsperger, Preville, Kotlyarov, Lutsch, Ducasse, Paul, Wieske, Arrigo, Buchner and Gaestel (1999) Regulation of Hsp27 Oligomerization, Chaperone Function, and Protective Activity against Oxidative Stress/Tumor Necrosis Factor a by Phosphorylation. *J. Biol. Chem.* 274(27): 18947-18956.

177 MacRae (2000) Structure and function of small heat shock/a-crystallin proteins: established concepts and emerging ideas. *Cell. Mol. Life Sci.* 57(6): 899-913.

178 Augusteyn and Koretz (1987) A possible structure for α-crystallin. *FEBS Lett.* 222(1): 1-5.

179 Ehrnsperger, Lilie, Gaestel and Buchner (1999) The Dynamics of Hsp25 Quaternary Structure: Structure and Function of Different Oligomeric Species. *J. Biol. Chem.* 274(21): 14867-14874.

180 Smith, Liu and Smith (1996) Identification of Possible Regions of Chaperone Activity in Lens α-Crystallin. *Exp. Eye Res.* 63(1): 125-128.

181 Siezen and Hoenders (1979) The Quaternary Structure of Bovine α-Crystallin: Surface Probing by Limited Proteolysis *in vitro*. *Eur. J. Biochem.* 96(3): 431-440.

182 Thomson and Augusteyn (1984) On the Structure of α_m-Crystallin: The Reversibility of Urea Dissociation. *J. Biol. Chem.* 259(7): 339-4345.

183 Yoshida, Yumato, Tsukahara and Murochi (1986) The Degradation of a-Crystallin at Its Carboxyl-Terminal Portion by Calpain in Bovine Lens. *Invest. Ophthalmol. Vis. Sci.* 27(8): 1269-1273.

184 Groenen, van Dongen, Voorter, Bloemendal and de Jong (1993) Age-dependent deamidation of αB-crystallin. *FEBS Lett.* 322(1): 69-71.

185 Carver, Aquilina, Truscott and Ralston (1992) Identification by ^{1}H NMR spectroscopy of flexible C-terminal extensions in bovine lens a-crystallin. *FEBS Lett.* 311(2): 143-149.

186 Siezen, Bindels and Hoenders (1980) The Quaternary Structure of Bovine α-Crystallin: Effects of Variation in Alkaline pH, Ionic Strength, Temperature and Calcium Ion Concentration. *Eur. J. Biochem.* 111(2): 435-444.

187 Wistow (1993) Possible Tetramer-based Quaternary Structures for a-Crystallins and Small Heat Shock Proteins. *Exp. Eye Res.* 56(6): 729-732.

188 Groth-Vasselli, Kumosinki and Farnsworth (1995) Computer-Generated Model of the Quaternary Structure of Alpha Crystallin in the Lens. *Exp. Eye Res.* 61(2): 249-253.

189 Carver, Aquilina and Truscott (1994) A Possible Chaperone-like Quaternary Structure for α-crystallin. *Exp. Eye Res.* 59(2): 231-234.

190 Chiesa, Gawinowicz-Kolks, Kleiman and Spector (1988) Definition and Comparison of the Phosphorylation Sites of the A and B Chains of Bovine α-Crystallin. *Exp. Eye Res.* 46(1): 199-208.

191 Dudich, Zav'yalov, Pfeil, Gaestel, Zav'yalova, Denesyuk and Korpela (1995) Dimer structure as a minimum cooperative subunit of small heat-shock proteins. *Biochim. Biophys. Acta* 1253(2): 163-168.

192 Lambert, Charette, Bernier, Guimond and Landry (1999) HSP27 Multimerization Mediated by Phosphorylation-sensitive Intermolecular Interactions at the Amino Terminus. *J. Biol. Chem.* 274(14): 9378-9385.

193 Bova, Huang, Ding and Horwitz (2002) Subunit Exchange, Conformational Stability, and Chaperone-like Function of the Small Heat Shock Protein 16.5 from *Methanococcus jannaschii*. *J. Biol. Chem.* 277(41): 38468-38475.

194 Usui, Hatipoglu, Ishii and Yohda (2004) Role of the N-terminal region of the crenarchaeal sHsp, StHsp14.0, in thermal-induced disassembly of the complex and molecular chaperone activity. *Biochem. Biophys. Res. Commun.* 315(1): 113-118.

195 Aquilina, Benesch, Ding, Yaron, Horwitz and Robinson (2005) Subunit Exchange of Polydisperse Proteins: Mass Spectrometry Reveals Consequences of αA-Crystallin Truncation. *J. Biol. Chem.* 280(15): 14485-14491.

196 Das and Surewicz (1995) Temperature-induced exposure of hydrophobic surfaces and its effect on the chaperone activity of α-crystallin. *FEBS Lett.* 369(2-3): 321-325.

197 Raman, Ramakrishna and Rao (1995) Temperature dependent chaperone-like activity of alpha-crystallin. *FEBS Lett.* 365(2-3): 133-136.

198 Surewicz and Olesen (1995) On the Thermal Stability of α-Crystallin: A New Insight from Infrared Spectroscopy. *Biochemistry* 34(30): 9655-9660.

199 Farnsworth, Groth-Vasselli, Greenfield and Singh (1997) Effects of temperature and concentration on bovine lens α-crystallin secondary structure: a circular dichroism spectroscopic study. *Int. J. Biol. Macromol.* 20(4): 283-291.

200 Raman and Rao (1997) Chaperone-like Activity and Temperature-induced Structural Changes of α-Crystallin. *J. Biol. Chem.* 272(38): 23559-23564.

201 Das, Liang and Chakrabarti (1997) Heat-induced conformational change and increased chaperone activity of lens α-crystallin. *Curr. Eye Res.* 16(4): 303-309.

202 Sun and Liang (1998) Intermolecular Exchange and Stabilization of Recombinant Human αA- and αB-Crystallin. *J. Biol. Chem.* 273(1): 286-290.

203 Burgio, Jim, Dow and Koretz (2000) Correlation between the Chaperone-like Activity and Aggregate Size of α-Crystallin with Increasing Temperature. *Biochem. Biophys. Res. Commun.* 268(2): 426-432.

204 Burgio, Bennett and Koretz (2001) Heat-induced quaternary transitions in hetero- and homo-polymers of α-crystallin. *Mol. Vis.* 7: 228-233.

205 Liang and Fu (2002) Decreased subunit exchange of heat-treated lens αA-crystallin. *Biochem. Biophys. Res. Commun.* 293(1): 7-12.

206 Kim, Lee, Ha and Kim (2003) Activation mechanism of HSP16.5 from *Methanococcus jannaschii*. *Biochem. Biophys. Res. Commun.* 307(4): 991-998.

207 Putilina, Skouri-Panet, Prat, Lubsen and Tardieu (2003) Subunit Exchange Demonstrates a Differential Chaperone Activity of Calf α-Crystallin toward β_{LOW}- and Individual γ-Crystallins. *J. Biol. Chem.* 278(16): 13747-13756.

208 Fu and Chang (2004) Temperature-dependent subunit exchange and chaperone-like activities of Hsp16.3, a small heat shock protein from *Mycobacterium tuberculosis*. *Biochem. Biophys. Res. Commun.* 316(2): 291-299.

209 Lee, Roseman, Saibil and Vierling (1997) A small heat shock protein stably binds heat-denatured model substrates and can maintain a substrate in a folding-competent state. *EMBO J.* 16(3): 659-671.

210 Sharma, Kumar, Kumar and Quinn (2000) Synthesis and Characterization of a Peptide Identified as a Functional Element in αA-crystallin. *J. Biol. Chem.* 275(6): 3767-3771.

211 Ghosh, Shenoy and Clark (2006) N- and C-Terminal Motifs in Human αB Crystallin Play an Important Role in the Recognition, Selection, and Solubilization of Substrates. *Biochemistry* 45(46): 13847-13854.

212 Koteiche, Berengian and Mchaourab (1998) Identification of Protein Folding Patterns Using Site-Directed Spin Labeling. Structural Characterization of a b-Sheet and Putative Substrate Binding Regions in the Conserved Domain of αA-Crystallin. *Biochemistry* 37(37): 12681-12688.

213 Haslbeck and Buchner (2002) Chaperone Function of sHsps. *Prog. Mol. Subcell. Biol.* 28 (Small Stress Proteins): 37-59.

214 Carver, Guerreiro, Nicholls and Truscott (1995) On the interaction of α-crystallin with unfolded proteins. *Biochim. Biophys. Acta* 1252(2): 251-260.

215 Stromer, Ehrnsperger, Gaestel and Buchner (2003) Analysis of the Interaction of Small Heat Shock Proteins with Unfolding Proteins. *J. Biol. Chem.* 278(20): 18015-18021.

216 Lindner, Kapur, Mariani, Titmuss and Carver (1998) Structural alterations of α-crystallin during its chaperone action. *Eur. J. Biochem.* 258(1): 170-183.

217 Rao, Raman, Ramakrishna, Rajaraman, Ghosh, Datta, Trivedi and Sukhaswami (1998) Structural perturbation of α-crystallin and its chaperone-like activity. *Int. J. Biol. Macromol.* 22(3-4): 271-281.

218 Andley, Mathur, Griest and Petrash (1996) Cloning, Expression, and Chaperone-like Activity of Human αA-Crystallin. *J. Biol. Chem.* 271(50): 31973-31980.

219 Fernando and Heikkila (2000) Functional characterization of *Xenopus* small heat shock protein, Hsp30C: the carboxyl end is required for stability and chaperone activity. *Cell Stress Chaperon.* 5(2): 148-159.

220 Smulders, Carver, Lindner, van Boekel, Bloemendal and de Jong (1996) Immobilization of the C-terminal Extension of Bovine αA-Crystallin Reduces Chaperone-like Activity. *J. Biol. Chem.* 271(46): 29060-29066.

221 Treweek (2003) PhD Thesis: *Structure/function studies of the a-crystallin small heat-shock chaperone proteins*. University of Wollongong.

222 Groenen, Bloemendal and de Jong (1992) The carboxy-terminal lysine of αB-crystallin is an amine-donor substrate for tissue transglutaminase. *Eur. J. Biochem.* 205(2): 671-674.

223 Liao, Lee and Chiou (2002) C-terminal lysine truncation increases thermostability and enhances chaperone-like function of porcine αB-crystallin. *Biochem. Biophys. Res. Commun.* 297(2): 309-316.

224 Martin, Bluhm, He, Mestril and Dillmann (2002) Mutation of COOH-terminal lysines in overexpressed αB-crystallin abrogates ischemic protection in cardiomyocytes. *Am. J. Physiol. Heart Circ. Physiol.* 283(1): H85-H91.

225 Derham, van Boekel, Muchowski, Clark, Horwitz, Hepburne-Scott, de Jong, Crabbe and Harding (2001) Chaperone function of mutant versions of αA- and αB-crystallin prepared to pinpoint chaperone binding sites. *Eur. J. Biochem.* 268(3): 713-721.

226 Fernando, Abdulle, Mohindra, Guillemette and Heikkila (2002) Mutation or deletion of the C-terminal tail affects the function and structure of *Xenopus laevis* small heat shock protein, hsp30. *Comp. Biochem. Physiol. B* 133(1): 95-103.

227 Reddy, Das, Petrash and Surewicz (2000) Temperature-dependent Chaperone Activity and Structural Properties of Human αA- and αB-crystallins. *J. Biol. Chem.* 275(7): 4565-4570.

228 Brady, Garland, Duglas-Tabor, Robinson, Groome and Wawrousek (1997) Targeted disruption of the mouse αA-crystallin gene induces cataract and cytoplasmic inclusion bodies containing the small heat shock protein αB-crystallin *Proc. Natl. Acad. Sci. USA* 94(3): 884-889.

229 Zantema, Verlaan-De Vries, Maasdam, Bol and van der Eb (1992) Heat Shock Protein 27 and αB-Crystallin Can Form a Complex, Which Dissociates by Heat Shock. *J. Biol. Chem.* 267(18): 12936-12941.

230 Sugiyama, Suzuki, Kishikawa, Akutsu, Hirose, Waye, Tsui, Yoshida and Ohno (2000) Muscle Develops a Specific Form of Small Heat Shock Protein Complex Composed of MKBP/HSPB2 and HSPB3 during Myogenic Differentiation. *J. Biol. Chem.* 275(2): 1095-1104.

231 Fontaine, Sun, Benndorf and Welsh (2005) Interactions of HSP22 (HSPB8) with HSP20, αB-crystallin, and HSPB3. *Biochem. Biophys. Res. Commun.* 337(3): 1006-1011.

232 Selkoe (1996) Amyloid β-Protein and the Genetics of Alzheimer's Disease. *J. Biol. Chem.* 271(31): 18295-18298.

233 Skovronsky, Lee and Trojanowski (2006) Neurodegenerative Diseases: New Concepts of Pathogenesis and Their Therapeutic Implications. *Annu. Rev. Pathol. Mech. Dis.* 1: 151-170.

234 Arrigo and Préville (1999) Role of Hsp27 and Related Proteins. *Handb. Exp. Pharmacol.* 136 (Stress Proteins): 101-132.

235 Renkawek, Stege and Bosman (1999) Dementia, gliosis and expression of the small heat shock proteins hsp27 and αB-crystallin in Parkinson's disease. *NeuroReport* 10(11): 2273-2276.

236 van Rijk and Bloemendal (2000) Alpha-B-crystallin in neuropathology. *Ophthalmologica* 214(1): 7-12.

237 Crowther (2002) Familial Conformational Diseases and Dementias. *Hum Mutat.* 20(1): 1-14.

238 Agorogiannis, Agorogiannis, Papadimitriou and Hadjigeorgiou (2004) Protein misfolding in neurodegenerative diseases. *Neuropath. Appl. Neuro.* 30(3): 215-224.

239 Soto (2001) Protein misfolding and disease; protein refolding and therapy. *FEBS Lett.* 498(2-3): 204-207.

240 Ganea (2001) Chaperone-like Activity of α-Crystallin and Other Small Heat Shock Proteins. *Curr. Protein Pept. Sc.* 2(3): 205-225.

241 Söti and Csermely (2002) Chaperones and aging: role in neurodegeneration and in other civilizational diseases. *Neurochem. Int.* 41(6): 383-389.

242 Howlett (2003) Protein Misfolding in Disease: Cause or Response? *Curr. Med. Chem. - Immun., Endoc. & Metab. Agents* 3(4): 371-383.

243 Muchowski (2002) Protein Misfolding, Amyloid Formation, and Neurodegeneration: A Critical Role for Molecular Chaperones? *Neuron* 35(1): 9-12.

244 Yoo, Kim, Cairns, Fountoulakis and Lubec (2001) Deranged Expression of Molecular Chaperones in Brains of Patients with Alzheimer's Disease. *Biochem. Biophys. Res. Commun.* 280(1): 249-258.

245 Ferns, Shams and Shafi (2006) Heat shock protein 27: its potential role in vascular disease. *Int. J. Exp. Path.* 87(4): 253-274.

246 de Wit, Verschuure, Kappé, King, de Jong, van Muijena and Boelens (2004) Testis-specific human small heat shock protein HSPB9 is a cancer/testis antigen, and potentially interacts with the dynein subunit TCTEL1. *Eur. J. Cell Biol.* 83(7): 337-345.

247 Graw (1997) The crystallins: Genes, proteins and diseases. *Biol. Chem.* 378(11): 1331-1348.

248 Bloemendal, de Jong, Jaenicke, Lubsen, Slingsby and Tardieu (2004) Ageing and vision: structure, stability and function of lens crystallins. *Prog. Biophys. Mol. Bio.* 86(3): 407-485.

249 Litt, Kramer, LaMorticella, Murphey, Lovrien and Weleber (1998) Autosomal dominant congenital cataract associated with a missense mutation in the human alpha crystallin gene CRYAA. *Hum. Mol. Gen.* 7(3): 471-474.

250 Vicart, Caron, Guicheney, Li, Prévost, Faure, Chateau, Chapon, Tomé, Dupret, Paulin and Fardeau (1998) A missense mutation in the αB-crystallin chaperone gene causes a desmin-related myopathy. *Nat. Genet.* 20(1): 92-95.

251 Kumar, Ramakrishna and Rao (1999) Structural and Functional Consequences of the Mutation of a Conserved Arginine Residue in αA and αB Crystallins. *J. Biol. Chem.* 274(34): 24137-24141.

252 van den IJssel and Norman (1999) Molecular chaperones: Small heat shock proteins in the limelight. *Curr. Biol.* 9(3): R103-105.

253 Goebel (1995) Desmin-Related Neuromuscular Disorders. *Muscle & Nerve* 18(11): 1306-1320.

254 Perng, Cairns, van den IJssel, Prescott and Hutcheson (1999) Intermediate filament interactions can be altered by HSP27 and αB-crystallin. *J. Cell Sci.* 112(13): 2099-2112.

255 Wang, Klevitsky, Huang, Glasford, Li and Robbins (2003) αB-Crystallin Modulates Protein Aggregation of Abnormal Desmin. *Circ. Res.* 93(14): 998-1005.

256 Treweek, Rekas, Lindner, Walker, Aquilina, Robinson, Horwitz, Perng, Quinlan and Carver (2005) R120G αB-crystallin promotes the unfolding of reduced a-lactalbumin and is inherently unstable. *FEBS J.* 272(3): 711-724.

257 Perng, Muchowski, van den IJssel, Wu, Hutcheson, Clark and Quinlan (1999) The Cardiomyopathy and Lens Cataract Mutation in αB-crystallin Alters Its Protein Structure, Chaperone Activity, and Interaction with Intermediate Filaments in Vitro. *J. Biol. Chem.* 274(47): 33235-33243.

258 Evgrafov, Mersiyanova, Irobi, Van Den Bosch, Dierick, Leung, Schagina, Verpoorten, Van Impe, Fedotov, Dadali, Auer-Grumbach, Windpassinger, Wagner, Mitrovic, Hilton-Jones, Talbot, Martin, Vasserman, Tverskaya, Polyakov, Liem, Gettemans, Robberecht, De Jonghe and Timmerman (2004) Mutant small heat-shock protein 27 causes axonal Charcot-Marie-Tooth disease and distal hereditary motor neuropathy. *Nat. Genet.* 36(6): 602-606.

259 Ackerly, James, Kalli, French, Davies and Talbot (2006) A mutation in the small heat-shock protein HSPB1 leading to distal hereditary motor neuronopathy disrupts neurofilament assembly and the axonal transport of specific cellular cargoes. *Hum. Mol. Gen.* 15(2): 347-354.

260 Berengian, Parfenova and Mchaourab (1999) Site-directed Spin Labelling Study of Subunit Interactions in the α-Crystallin Domain of Small Heat-Shock Proteins: Comparison of the Oligomer Symmetry in αA-Crystallin, HSP 27, and HSP 16.3. *J. Biol. Chem.* 274(10): 6305-6314.

261 Irobi, Van Impe, Seeman, Jordanova, Dierick, Verpoorten, Michalik, De Vriendt, Jacobs, Van Gerwen, Vennekens, Mazanec, Tournev, Hilton-Jones, Talbot, Kremensky, Van Den Bosch, Robberecht, Vandekerckhove, Van Broeckhoven, Gettemans, De Jonghe and Timmerman (2004) Hot-spot residue in small heat-shock protein 22 causes distal motor neuropathy. *Nat. Genet.* 36(6): 597-601.

262 Tang, Zhao, Luo, Xia, Cai, Pan, Zhang, Zhang, Liu, Chen, Zhang, Shen, Jiang, Long and Dai (2005) Small heat-shock protein 22 mutated in autosomal dominant Charcot-Marie-Tooth disease type 2L. *Hum. Genet.* (3): 222-224.

263 Xiao and Benjamin (1999) Stress-Response Proteins in Cardiovascular Disease. *Am. J. Hum. Genet.* 64(3): 685-690.

264 Treweek, Morris and Carver (2003) Intracelluler Protein Unfolding and Aggregation: The Role of Small Heat-Shock Chaperone Proteins. *Aust. J. Chem.* 56(5): 357-367.

265 Mehlen, Preville, Chareyron, Briolay, Klemenz and Arrigo (1995) Constitutive Expression of Human hsp27, *Drosophila* hsp27, or Human αB-Crystallin Confers Resistance to TNF- and Oxidative Stress-Induced Cytotoxicity in Stably Transfected Murine 1929 Fibroblasts. *J. Immunol.* 154(1): 363-374.

266 Bush, Goldberg and Nigam (1997) Proteasome Inhibition Leads to a Heat-shock Response, Induction of Endoplasmic Reticulum Chaperones, and Thermotolerance. *J. Biol. Chem.* 272(14): 9086-9092.

267 Gaestel, Gotthardt and Müller (1993) Structure and organisation of a murine gene encoding small heat-shock protein Hsp25. *Gene* 128(2): 279-283.

268 Studier and Moffatt (1986) Use of Bacteriophage T7 RNA Polymerase to Direct Selective High-level Expression of Cloned Genes. *J. Mol. Biol.* 189(1): 113-130.

269 Rosenberg, Lade, Chui, Lin, Dunn and Studier (1987) Vectors for selective expression of cloned DNAs by T7 RNA polymerase. *Gene* 56(1): 125-135.

270 Gaestel, Gross, Benndorf, Strauss, Schunk, Kraft, Otto, Böhm, Stahl, Drabsch and Bielka (1989) Molecular cloning, sequencing and expression of *Escherichia coli* of the 25-kDa growth-related protein of Ehrlich ascites tumor and its homology to mammalian stress proteins. *Eur. J. Biochem.* 179(1): 209-213.

271 Jakob, Gaestel, Engel and Buchner (1993) Small Heat Shock Proteins Are Molecular Chaperones. *J. Biol. Chem.* 268(3): 1517-1520.

272 Buchner, Ehrnsperger, Gaestel and Walke (1998) Purification and Characterization of Small Heat Shock Proteins. *Method. Enzymol.* 290 (Molecular Chaperones): 339-349.

273 Horwitz, Huang, Ding and Bova (1998) Lens α-Crystallin: Chaperone-Like Properties. *Method. Enzymol.* 290 (Molecular Chaperones): 365-383.

274 Zavialov, Benndorf, Ehrnsperger, Zav'yalov, Dudich, Buchner and Gaestel (1998) The effect of the intersubunit disulfide bond on the structural and functional properties of the small heat shock protein Hsp25. *Int. J. Biol. Macromol.* 22(3-4): 163-173.

275 Schmid (1989) Spectral methods of characterizing protein conformation and conformational changes. *Protein structure: a practical approach*. Creighton, T. E. (Ed.) IRL Press, Oxford.

276 Compton and Johnson (1986) Analysis of Protein Circular Dichroism Spectra for Secondary Structure Using a Simple Matrix Multiplication. *Anal. Biochem.* 155(1): 155-167.

277 Manavalan and Johnson (1987) Variable Selection Method Improves the Prediction of Protein Secondary Structure from Circular Dichroism Spectra. *Anal. Biochem.* 167(1): 76-85.

278 Johnson (1999) Analyzing Protein Circular Dichroism Spectra for Accurate Secondary Structures. *Proteins* 35(3): 307-312.

279 Sreermar and Woody (2000) Estimation of Protein Secondary Structure from Circular Dichroism Spectra: Comparison of CONTIN, SELCON, and CDSSTR Methods with an Expanded Reference Set. *Anal. Biochem.* 287(2): 252-260.

280 Lobley, Whitmore and Wallace (2002) DICHROWEB: an interactive website for the analysis of protein secondary structure from circular dichroism spectra. *Bioinformatics* 18(1): 211-212.

281 Whitmore and Wallace (2004) DICHROWEB, an online server for protein secondary structure analyses from circular dichroism spectroscopic data. *Nucleic Acids Res.* 32(Web Server issue): W668-W673.

282 Bühner and Sund (1969) Yeast Alcohol Dehydrogenase: -SH Groups, Disulfide Groups, Quaternary Structure, and Reactivation by Reductive Cleavage of Disulfide Groups. *Eur. J. Biochem.* 11(1): 73-79.

283 Weil, Seibles and Herskovits (1965) Phooxidation of Bovine Insulin Sensitized by Methylene Blue. *Arch. Biochem. Biophys.* 111(2): 308-320.

284 Piotto, Saudek and Sklenář (1992) Gradient-tailored excitation for single-quantum NMR spectroscopy of aqueous solutions. *J. Biomol. NMR* 2(6): 661-665.

285 Jeener, Meier, Bachmann and Ernst (1979) Investigation of exchange processes by two-dimensional NMR spectroscopy. *J. Chem. Phys.* 71(11): 4546-4553.

286 States, Haberkorn and Ruben (1982) A Two-Dimensional Nuclear Overhauser Experiment with Pure Absorption Phase in Four Quadrants. *J. Magn. Reson.* 48(2): 286-292.

287 Shaka, Barker and Freeman (1985) Computer-Optimized Decoupling Scheme for Wideband Applications and Low-Level Operation. *J. Magn. Reson.* 64(3): 547-552.

288 Smallcombe, Patt and Keifer (1995) WET Solvent Suppression and Its Applications to LC NMR and High-Resolution NMR Spectroscopy. *J. Magn. Res., Ser. A* 117(2): 295-303.

289 Kay, Keifer and Saarinen (1992) Pure Absorption Gradient Enhanced Heteronuclear Single Quantum Correlation Spectroscopy with Improved Sensitivity. *J. Am. Chem. Soc.* 144(26): 10663-10665.

290 Boyd, Hommel and Campbell (1990) Influence of cross-correlation between dipolar and anisotropic chemical shift relaxation mechanisms upon longitudinal relaxation rates of ^{15}N macromolecules. *Chem. Phys. Lett.* 175(5): 477-482.

291 Palmer, Skelton, Chazin, Wright and Rance (1992) Suppression of the effects of cross-correlation between dipolar and anisotropic chemical shift relaxation mechanisms in the measurement of spin-spin relaxation rates. *Mol. Phys.* 75(3): 699-711.

292 Farrow, Muhandiram, Singer, Pascal, Kay, Gish, Shoelson, Pawson, Forman-Kay and Kay (1994) Backbone Dynamics of a Free and a Phosphopeptide-Complexed Src Homology 2 Domain Studied by ^{15}N NMR Relaxation. *Biochemistry* 33(19): 5984-6003.

293 Dunker, Garner, Guilliot, Romero, Albrecht, Hart and Obradovic (1998) Protein Disorder and the Evolution of Molecular Recognition: Theory, Predictions and Observations. *Pac. Smp. Biocomput.* 3: 473-484.

294 Wright and Dyson (1999) Intrinsically Unstructured Proteins: Re-assessing the Protein Structure-Function Paradigm. *J. Mol. Biol.* 293(2): 321-331.

295 Fink (2005) Natively unfolded proteins. *Curr. Opin. Struct. Biol.* 15(1): 34-41.

296 Romero, Obradović, Kissinger, Villafranca and Dunker (1997) Identifying Disordered Regions in Proteins from Amino Acid Sequence NEW. *IEEE Int. Conf. Neural Netw.* 1: 90-95.

297 Williams, Obradović, Mathura, Braun, Garner, Young, Takayama, Brown and Dunker (2001) The Protein Non-Folding Problem: Amino Acid Determinants of Intrinsic Order and Disorder. *Pac. Smp. Biocomput.* 6: 89-100.

298 Lu and Hansen (2004) Identification of Specific Functional Subdomains within the Linker Histone H1^0 C-terminal Domain. *J. Biol. Chem.* 279(10): 8701-8707.

299 Carver and Lindner (1998) NMR Spectroscopy of α-crystallin. Insights into the structure, interactions and chaperone action of small heat-shock proteins. *Int. J. Biol. Macromol.* 22(3-4): 197-209.

300 Dunker, Lawson, Brown, Williams, Campen, Ratliff, Hipps, Ausio, Nissen, Reeves, Kang, Kissinger, Bailey, Griswold, Chiu, Garner and Obradovic (2001) Intrinsically disordered protein. *J. Mol. Graph. Model.* 19(1): 26-59.

301 Schlessinger and Rost (2005) Protein Flexibility and Rigidity Predicted From Sequence. *Proteins* 61(1): 115-126.

302 Romero, Obradovic, Li, Garner, Brown and Dunker (2001) Sequence Complexity of Disordered Protein. *Proteins* 42(1): 38-48.

303 Radivojac, Obradovic, Smith, Zhu, Vucetic, Brown, Lawson and Dunker (2004) Protein flexibility and intrinsic disorder. *Prot. Sci.* 13(1): 71-80.

304 Spassov, Karshikoff and Ladenstein (1995) The optimization of protein-solvent interactions: Thermostability and the role of hydrophobic and electrostatic interactions. *Prot. Sci.* 4(8): 1516-1527.

305 Karshikoff and Ladenstein (1998) Proteins from thermophilic and mesophilic organisms essentially do not differ in packing. *Protein Eng.* 11(10): 867-872.

306 Cambillau and Claverie (2000) Structural and Genomic Correlates of Hyperthermostability. *J. Biol. Chem.* 275(42): 32383-32386.

307 Szilágyi and Závodszky (2000) Structural differences between mesophilic, moderately thermophilic and extremely thermophilic protein subunits: results of a comprehensive survey. *Structure* 8(5): 493-504.

308 Cheung, Lam, Chu, Allen, Bycroft and Wong (2005) Crystal Structure of a Hyperthermophilic Archaeal Acylphosphatase from Pyrococcus horikoshii–Structural Insights into Enzymatic Catalysis, Thermostability, and Dimerization. *Biochemistry* 44(12): 4601-4611.

309 Liao, Lee and Chiou (2002) Distinct roles of αA- and αB-crystallins under thermal and UV stresses. *Biochem. Biophys. Res. Commun.* 295(4): 854-861.

310 Kumarevel, Gromiha and Ponnuswamy (1998) Analysis of hydrophobic and charged patches and influence of medium- and long-range interactions in molecular chaperones. *Biophys. Chem.* 75(2): 105-113.

311 Hirel, Schmitter, Dessen, Fayat and Blanquet (1989) Extent of N-terminal methionine excision from *Escherichia coli* proteins is governed by the side-chain length of the penultimate amino acid. *Proc. Natl. Acad. Sci. USA* 86(21): 8247-8251.

312 Dalbøge, Bayne and Pederson (1990) In vivo processing of N-terminal methionine in *E. coli*. *FEBS Lett.* 266(1-2): 1-3.

313 Flinta, Persson, Jörnvall and von Heijnr (1986) Sequence determinants of cytosolic N-terminal protein processing. *Eur. J. Biochem.* 154(1): 193-196.

314 Giglione, Boularot and Meinnel (2004) Protein N-terminal methionine excision. *Cell. Mol. Life Sci.* 61(12): 1455-1474.

315 Muchowski, Bassuk, Lubsen and Clark (1997) Human αB-Crystallin: Small heat shock protein and molecular chaperone. *J. Biol. Chem.* 272(4): 2578-2582.

316 Guo and Cooper (2000) An N-Terminal 33-Amino-Acid-Deletion Variant of hsp25 Retains Oligomerization and Functional Properties. *Biochem. Biophys. Res. Commun.* 270(1): 183-189.

317 Ehrnsperger, Gaestel and Buchner (2000) Analysis of Chaperone Properties of Small Hsp's. *Methods Mol. Biol.* 99 (Stress Response: Methods and Protocols): 421-429.

318 Avilov, Bode, Tolgyesi, Klymchenko, Fidy and Demchenko (2005) Temperature effects on α-crystallin structure probed by 6-bromophenyl-2-(2-furanyl)-3-hydroxychromone, an environmentally sensitive two-wavelength fluorescent dye covalently attached to the single Cys residue. *Int. J. Biol. Macromol.* 36(5): 290-298.

319 Dinner, Šali, Smith, Dobson and Karplus (2000) Understanding protein folding via free-energy surfaces from theory and experiment. *TIBS* 25(7): 331-339.

320 Manavalan and Johnson (1983) Sensitivity of circular dichroism to protein tertiary structure class. *Nature* 305(5937): 831-832.

321 Shearstone and Baneyx (1999) Biochemical Characterization of the Small Heat Shock Protein IbpB from *Escherichia coli*. *J. Biol. Chem.* 274(15): 9937-9945.

322 Aquilina, Benesch, Ding, Yaron, Horwitz and Robinson (2004) Phosphorylation of αB-Crystallin Alters Chaperone Function through Loss of Dimeric Substructure. *J. Biol. Chem.* 279(27): 28675-28680.

323 Walsh, Sen and Chakrabarti (1991) Micellar Subunit Assembly in a Three-layer Model of Oligomeric α-Crystallin. *J. Biol. Chem.* 266(30): 20079-20084.

324 Datta and Rao (1999) Differential Temperature-dependent Chaperone-like Activity of αA- and αB-crystallin Homoaggregates. *J. Biol. Chem.* 274(49): 34773-34778.

325 Muchowski, Wu, Liang, Adman and Clark (1999) Site-directed mutations within the core "alpha-crystallin" domain of the small heat-shock protein, human alpha B-crystallin, decrease molecular chaperone functions. *J. Mol. Biol.* 289(2): 397-411.

326 Pasta, Raman, Ramakrishna and Rao (2002) Role of the C-terminal Extensions of α-Crystallins: Swapping the C-Terminal Extension of αA-Crystallin to αB-Crystallin Results in Enhanced Chaperone Activity. *J. Biol. Chem.* 277(48): 45821–45828.

327 Chang, Li and Rao (2004) A preliminary study on functional domains of small heat shock protein Hsp16.3. *Prog. Nat. Sci.* 14(1): 21-25.

328 Maiti, Kono and Chakrabarti (1988) Heat-induced changes in the conformation of α- and β-crystallins: unique thermal stability of α-crystallin. *FEBS Lett.* 236(1): 109-114.

329 Jiao, Qian, Li, Zhao and Chang (2005) The Essential Role of the Flexible Termini in the Temperature-responsiveness of the Oligomeric State and Chaperone-like Activity for the Polydisperse Small Heat Shock Protein IbpB from *Escherichia coli*. *J. Mol. Biol.* 347(4): 871-884.

330 Freifelder (1982) *Physical Biochemistry: Applications to Biochemistry and Molecular Biology*. W.H. Freeman and Company, San Fransisco.

331 Burstein, Vedenkina and Ivkova (1973) Fluorescence and the Location of Tryptophan Residues in Protein Molecules. *Photochem. Photobiol.* 18(4): 263-279.

332 Smulders, van Geel, Gerards, Bloemendal and de Jong (1995) Reduced Chaperone-like Activity of αA^{ins}-crystallin, an Alternative Splicing Product Containing a Large Insert Peptide. *J. Biol. Chem.* 270(23): 13916-13924.

333 Das, Petrash and Surewicz (1996) Conformational Properties of Substrate Proteins Bound to a Molecular Chaperone α-Crystallin. *J. Biol. Chem.* 271(18): 10449-10452.

334 Smulders, Merck, Aendekerk, Horwitz, Takemoto, Slingsby, Bloemendal and de Jong (1995) The mutation Asp69$\rightarrow$Ser affects the chaperone-like activity of αA-crystallin. *Eur. J. Biochem.* 232(3): 834-838.

335 Campbell and Dwek (1984) *Biological Spectroscopy*. The Benjamin/Cummings Publishing Company, Inc, Menlo Park, California.

336 Cardamone and Puri (1992) Spectrofluorimetric assessment of the surface hydrophobicity of proteins. *Biochem. J.* 282(2): 589-593.

337 Randall (1992) Peptide Binding by Chaperone SecB: Implications for Recognition of Nonnative Structure. *Science* 257(5067): 241-245.

338 Semisotnov, Rodionova, Razgulyaev, Uversky, Gripas' and Gilmanshin (1991) Study of the "Molten Globule" Intermediate State in Protein Folding by a Hydrophobic Fluorescent Probe. *Biopolymers* 31(1): 119-128.

339 Shroff, Bera, Cherian-Shaw and Abraham (2001) Substituted hydrophobic and hydrophilic residues at methionine-68 influence the chaperone-like function of αB-crystallin. *Mol. Cell. Biochem.* 220(1-2): 127-133.

340 Sreelakshmi, Santhoshkumar, Bhattacharyya and Sharma (2004) αA-Crystallin Interacting Regions in the Small Heat Shock Protein, αB-Crystallin. *Biochemistry* 43(50): 15785-15795.

341 Santhoshkumar and Sharma (2001) Phe^{71} Is Essential for Chaperone-like Function in αA-crystallin. *J. Biol. Chem.* 276(20): 47094-47099.

342 Dai, Mao, Yang, Huang and Chang (2000) Probing the Roles of the Only Universally Conserved Leucine Residue (Leu122) in the Oligomerization and Chaperone-like Activity of *Mycobacterium tuberculosis* Small Heat Shock Protein Hsp16.3. *J. Protein Chem.* 19(4): 319-326.

343 Carver, Esposito, Schwedersky and Gaestel (1995) ^{1}H-NMR Spectroscopy reveals that mouse Hsp25 has a flexible C-terminal extension of 18 amino acids. *FEBS Lett.* 369(2-3): 305-310.

344 Clark and Huang (1996) Modulation of the chaperone-like activity of bovine α-crystallin. *Proc. Natl. Acad. Sci. USA* 93(26): 15185-15189.

345 Esposito, Viglino, Fogolari, Gaestel and Carver (1998) Selective NMR Experiments on Macromolecules: Implementation and Analysis of QUIET-NOESY. *J. Magn. Reson.* 132(2): 204-213.

346 Karshikoff and Ladenstein (2001) Ion pairs and the thermotolerance of proteins from hyperthermophiles: a 'traffic rule' for hot roads. *TIBS* 26(9): 550-556.

347 Kreil and Ouzounis (2001) Identification of thermophilic species by the amino acid compositions deduced from their genomes. *Nucleic Acids Res.* 29(7): 1608-1615.

348 Kumar, Kapoor, Sinha and Reddy (2005) Insights into Hydrophobicity and the Chaperone-like Function of αA- and αB-crystallins: An Isothermal Titration Calorimetric Study. *J. Biol. Chem.* 280(23): 21726-21730.

349 Liang, Sun and Akhtar (2000) Heat-induced conformational change of human lens recombinant αA- and αB-crystallins. *Mol. Vis.* 6: 10-14.

350 Fu, Zhang, Zhang, Cao, Jiao, Liu, Song, Abulimiti and Chang (2005) A Dual Role for the N-terminal Region of *Mycobacterium tuberculosis* Hsp16.3 in Self-oligomerization and Binding Denaturing Substrate Proteins. *J. Biol. Chem.* 280(8): 6337-6348.

351 Vallee and Hoch (1955) Zinc, A Component of Yeast Alcohol Dehydrogenase. *Proc. Natl. Acad. Sci. USA* 41(6): 327-338.

352 Wüthrich (1986) *NMR of Proteins and Nucleic Acids*. John Wiley & Sons Inc., New York.

353 Wishart, Bigam, Holm, Hodges and Sykes (1995) ^{1}H, ^{13}C and ^{15}N random coil NMR chemical shifts of the common amino acids. I. Investigations of nearest-neighbor effects. *J. Biomol. NMR* 5(1): 67-81.

354 Wishart, Sykes and Richards (1991) Relationship between Nuclear Magnetic Resonance Chemical Shift and Protein Secondary Structure. *J. Mol. Biol.* 222(2): 311-333.

355 Kay, Torchia and Bax (1989) Backbone Dynamics of Proteins As Studied by ^{15}N Inverse Detected Heteronuclear NMR Spectroscopy: Application to Staphylococcal Nuclease. *Biochemistry* 28(23): 8972-8979.

356 Ash, Sudmeier, Day, Vincent, Torchilin, Haddad, Bradshaw, Sanford and Bachovin (2000) Unusual ^{1}H NMR chemical shifts support (His) $C^{\varepsilon 1}$—O•••H═C H-bond: Proposal for reaction-driven ring flip mechanism in serine protease catalysis. *Proc. Natl. Acad. Sci. USA* 97(19): 10371-10376.

357 Bloemendal (1977) The Vertebrate Eye Lens: A useful system for the study of fundamental biological processes on a molecular level. *Science* 197(4299): 127-138.

358 Verschuure, Tatard, Boelens, Grongnet and David (2003) Expression of small heat shock proteins HspB2, HspB8, Hsp20 and cvHsp in different tissues of the perinatal developing pig. *Eur. J. Cell Biol.* 82(10): 523-530.

359 de Jong (1981) Evolution of Lens and Crystallins. *Molecular and Cellular Biology of the Eye Lens*. Bloemendal, H. (Ed.) John Wiley & Sons, Inc., New York.

360 Boelens and de Jong (1995) α-Crystallins, versatile stress-proteins. *Mol. Biol. Rep.* 21(2): 75-80.

361 Delaye and Tardieu (1983) Short-range order of crystallin proteins accounts for eye lens transparency. *Nature* 302(5907): 415-417.

362 Andries and Clauwaert (1985) Photon Correlation Spectroscopy and Light Scattering of Eye Lens Proteins at High Concentrations. *Biophys. J.* 47(5): 591-605.

363 Rajaraman, Raman, Ramakrishna and Rao (2001) Interaction of human recombinant αA- and αB-crystallins with early and late unfolding intermediates of citrate synthase on its thermal denaturation. *FEBS Lett.* 497(2): 118-123.

364 Bhat and Nagineni (1989) αB subunit of lens-specific protein α-crystallin is present in other ocular and non-ocular tissues. *Biochem. Biophys. Res. Commun.* 158(1): 319-325.

365 Kato, Shinohara, Kurobe, Goto, Inaguma and Ohshima (1991) Immunoreactive αA crystallin in rat non-lenticular tissues detected with a sensitive immunoassay method. *Biochim. Biophys. Acta* 1080(2): 173-180.

366 Krausz, Augusteyn, Quinlan, Reddan, Russell, Sax and Graw (1996) Expression of *Crystallins*, *Pax6*, *Filensin*, *CP49*, *MIP*, and *MP20* in Lens-Derived Cell Lines. *Invest. Ophthalmol. Vis. Sci.* 37(10): 2120-2128.

367 Zantema, de Jong, Lardenoije and van der Eb (1989) The Expression of Heat Shock Protein hsp27 and a Complexed 22-Kilodalton Protein Is Inversely Correlated with Oncogenicity of Adenovirus-Transformed Cells. *J. Virol.* 63(8): 3368-3375.

368 Kato, Shinohara, Goto, Inaguma, Morishita and Asano (1992) Copurification of Small Heat Shock Protein with αB Crystallin from Human Skeletal Muscle. *J. Biol. Chem.* 387(11): 7718-7725.

369 Fu and Liang (2003) Enhanced stability of αB-crystallin in the presence of small heat shock protein Hsp27. *Biochem. Biophys. Res. Commun.* 302(4): 710-714.

370 Ito, Kamei, Iwamoto, Inaguma, Tsuzuki, Kishikawa, Shimada, Hosokawa and Kato (2003) Hsp27 suppresses the formation of inclusion bodies induced by expression of R120GαB-crystallin, a cause of desmin-related myopathy. *Cell. Mol. Life Sci.* 60(6): 1217-1223.

371 Datta and Rao (2000) Packing-induced Conformational and Functional Changes in the Subunits of α-Crystallin. *J. Biol. Chem.* 275(52): 41004-41010.

372 Kriwacki, Hengst, Tennant, Reed and Wright (1996) Structural studies of $p21^{Waf1/Clp1/Sdi1}$ in the free and Cdk2-bound state: Conformational disorder mediates binding diversity. *Proc. Natl. Acad. Sci. USA* 93(21): 11504-11509.

373 Daughdrill, Chadsey, Karlinsey, Hughes and Dahlquist (1997) The C-terminal half of the anti-sigma factor, FlgM, becomes unstructured when bound to its target, σ^{28}. *Nat. Struct. Biol.* 4(4): 285-291.

374 Fletcher and Wagner (1998) The interaction of eIF4E with 4E-BP1 is an induced fit to a completely disordered protein. *Prot. Sci.* 7(7): 1639-1642.